INDIAN NATIONAL COMMITTEE ON SURFACE WATER (INCSW-CWC)

UID	**UK-2012-111**
Type (State whether final or draft report)	**Final Report**
Name of R&D Scheme	**EXPERIMENTAL VERIFICATION OF SCS RUNOFF CURVE NUMBERS FOR SELECTED SOILS AND LAND USES**
Name of PI & Co-PI	**Dr. S.K. Mishra, Professor & PI** **Dept. of Water Resources Development and Management** **Indian Institute of Technology Roorkee** **Roorkee-247 667 (Uttarakhand)** **&** **Dr. Ashish Pandey, Associate Professor & Co-PI** **Dept. of Water Resources Development and Management** **Indian Institute of Technology Roorkee** **Roorkee-247 667 (Uttarakhand)** **&** **Dr. R.P. Pandey, Scientist G & Co-PI** **NIH Roorkee-247667, Roorkee (Uttarakhand)** **&** **Mohan Lal, Assistant Professor & Co-PI,** **GB Pant University of Ag. & Technology** **Pantnagar, Uttarakhand**
Institute Address	**Indian Institute of Technology Roorkee** **Roorkee-247 667 (Uttarakhand)** **https://www.iitr.ac.in/**
Circulation (State whether Open for public or not)	**Open for Public**
Month & Year of Report Submission	**October 2019**

IITR PROJECT NO. MOW-627-WRD **Final Report**

R & D PROJECT

EXPERIMENTAL VERIFICATION OF SCS RUNOFF CURVE NUMBERS FOR SELECTED SOILS AND LAND USES

Sponsor: Indian National Committee for Surface Water (INCSW), Ministry of Water Resources, River Development and Ganga Rejuvenation, Government of India, New Delhi

Submitted By

Dr. S.K. Mishra, Professor & Principal Investigator.

Dr. Ashish Pandey, Associate Professor & Investigator

Dr. R.P. Pandey, Scientist F & Investigator, NIH, Roorkee

Er. Mohan Lal, Assistant Professor & Investigator, Pantnagar

Department of Water Resources Development and Management

INDIAN INSTITUTE OF TECHNOLOGY ROORKEE

Roorkee (Uttarakhand) 247 667, India

October, 2019

RESEARCH TEAM

The following Ph.D. and M.Tech scholars of the Department of Water Resources Development and Management, Indian Institute of Technology, Roorkee contributed to the project:

1) Shailendra Kumre, Ph.D.
2) Anubhav Chaudhary, M. Tech
3) Raj Kaji Shrestha, M. Tech
4) Ranjit Kumar Jha, M. Tech
5) Binaya Paudel, M. Tech
6) Dinesh Poudel, M. Tech
7) Lekh Nath Subedi, M. Tech
8) Rajendra Prasad Deo, M. Tech
9) Santosh Kumar Chaudhary, M. Tech
10) Arun Lal Karn, M. Tech
11) Shree Prasad Sah, M. Tech
12) Lek Nath Subedi, M. Tech
13) Ajit Kumar Shreevastava, M. Tech
14) Srinivasulu Pasila, M. Tech
15) Mohit Tomar, M. Tech

ACKNOWLEDGEMENT

The investigators of the project owe to the sponsoring agency the Indian National Committee on Surface Water (INCSW) (former Indian National Committee on Hydrology (INCOH)), Ministry of Water Resources, Govt. of India, New Delhi, for their financial support. The project could be successfully completed with availability of funds and the support of the INCSW personnel/staff at its Head Quarter, New Delhi. The project was fully facilitated by the DEAN (SRIC) and his office staff at the institute level and by Professor & Head, Dept. of Water Resources Development and Management (WRDM), faculty colleagues, and staff of the Dept. of WRDM.

In addition, the project could be successfully completed only because of the whole-hearted support and dedication of the project staff and other Research/M.Tech scholars. The appreciation of the referees/reviewers of the project report was remarkable and it is gratefully acknowledged.

S.K. Mishra, Principal Investigator

Ashish Pandey, Investigator

R.P. Pandey, Investigator

Mohan Lal, Investigator

REVIEWER'S COMMENTS

Highlights of the study

The present study evaluates the curve number (CN) values by experimentally monitoring rainfall- runoff-sediment yield for varying slopes, land uses and soils in agricultural plots of 20mx5m located nearby Roorkee (Uttarakhand). Runoff generated at the outlet of each plot as a result of both natural and artificial rainfall events was collected in runoff collection chambers of size 1mx1mx1m connected with a mild sloped conveyance channel of 3m length fitted with a screen to check the debris flow into the chambers. The rainfall-runoff data were collected for a period of 5 years (i.e. 2013 — 2018). The study was carried out by employing of SCS-CN methodology and accurate runoff measures were evaluated through precisely designed experimentation procedure. The study investigates the applicability of NEH-4 CN pertaining to Indian scenarios as well as to determine the climatic parameter initial abstraction ratio (λ) tor the study region. The study also focuses on the effect of various factors such as slope, soil type and land cover type on runoff, sediment yield and CN values.

Comments on the study

1. The study presents an interesting concept based methodology for evaluating the runoff-sediment yield by employing the modified SGS-CN method and demonstrated an enhanced insight of the approach that finds a significant contribution to the field of water resources planning, management and development,
2. The framed objectives of the project were accomplished through setting up of experimentation plots and execution of rigorous field experiments and precise measurement of target variables.
3. Most importantly, the study identified and recommended the appropriate value of λ for field applications, especially for Indian watersheds for estimating runoff generation more accurately and a SCS-CN based sediment yield has also been proposed and suggested. Results are well presented and study findings suggest high potentiality to various academic, State irrigation departments and other institutions working on soil and water conservation programs.
4. The subject area concerned demands more focused research towards development of simplified rainfall-runoff simulation models involving fewer numbers of input variables.
5. Moreover, the study came forth with a total of 15 publications in the journals of international and national repute as well as conferences of national and international levels, thereby, corroborating to the effectiveness of the modified SCS-CN based approach. Further commendable achievements of the study emerged through successful completion of 2 doctoral theses and 14 M-Tech dissertations.

Overall, this is a prospective study compounded with exhaustive field investigations and should be of great interest to the researchers working in the similar domain.

Dr. Saif Said,
Aligarh Muslim University (AMU),
Aligarh (India)

CONTENTS

Descriptions	Page No.
RESEARCH TEAM	I
ACKNOWLEDGEMENT	Ii
REVIEWER'S COMMENTS	iii
CONTENTS	iv-viii
LIST OF FIGURES	ix-xii
LIST OF TABLES	xiii-xiv
LIST OF ABBREVIATIONS AND SYMBOLS	xv-xviii
CHAPTER 1 INTRODUCTION	1
1.1 OBJECTIVES OF THE STUDY	1
1.2 ORGANIZATION OF THE PROJECT REPORT	3
CHAPTER 2 STUDY AREA AND EXPERIMENTAL SETUP	4
2.1 STUDY AREA	4
2.1.1 Climate	4
2.1.2 Soil type and land use	4
2.2 DESIGN AND LAYOUT PLAN OF THE EXPERIMENTAL FARM	6
2.2.1 Construction of experimental plots during phase 1	6
2.2.2 Infrastructures established during phase 1	7
(a) Raingauge installation	8
(b) Runoff Collection Chamber construction	8
(c) Land Preparation and Cultivation	9
(d) Safety, drain, repair, and construction of Shelter/Control Room	13
(e) Construction of plot boundary and approach channel	15
2.2.3 Construction of experimental plots during phase 2	16
2.2.4 Infrastructures established during phase 2	17
(a) Raingauge installation	17
(b) Preparation of Plots	17
(c) Construction of runoff collection tanks	18
(d) Crop cultivation	19
(e) Safety, drain and repair	20
CHAPTER 3 DATA COLLECTION	21

3.1 RAINFALL MEASUREMENT	21
3.2 RUNOFF MEASUREMENT	29
3.3 ANTECEDENT SOIL MOISTURE MEASUREMENT	30
3.4 INFILTRATION CAPACITY OF THE SOIL	32
CHAPTER 4 SCS-CN METHODOLOGY	35
4.1 INTRODUCTION	35
4.2 EXISTING SCS–CN METHOD	35
4.3 FACTORS AFFECTING CURVE NUMBER	37
4.3.1 Soli type:	37
4.3.2 Land use:	38
4.3.3 Hydrologic Condition:	39
4.3.4 Agricultural management practice:	39
4.3.5 Antecedent moisture condition (AMC):	40
4.3.6 Initial abstraction and climate:	40
4.3.7 Rainfall intensity and duration, Turbidity:	41
4.4 STATISTICAL ANALYSIS FOR GOODNESS OF FIT	41
CHAPTER 5 DETERMINATION OF CURVE NUMBER	44
5.1 DETERMINATION OF CURVE NUMBER FROM OBSERVED P-Q DATA	44
5.1.1 Storm event method	44
5.1.2 Least square fit method	44
5.1.3 Geometric mean method	44
5.1.4 Log-normal frequency method	45
5.1.5 NEH-4 median method	45
5.1.6 Rank-Order method	45
5.1.7 S-probability method	45
5.2 COMPARISON OF CN VALUES ESTIMATED FROM P-Q DATA	46
5.3 PERFORMANCE EVALUATION OF M1-M8 METHOD IN RUNOFF ESTIMATION	48
5.4 COMPARISON BETWEEN NEH-4 TABLE'S AND OBSERVED P–Q DATA-BASED CURVE NUMBERS	52
5.5 RELATIONSHIP BETWEEN ORDERED (i.e. CN_{LSMO}) AND NATURAL (i.e. CN_{LSMN}) DATA CNS	66

CHAPTER 6 EVALUATION OF INITIAL ABSTRACTION COEFFICIENT	68
6.1 DERIVATION OF λ VALUES FROM OBSERVED P-Q DATA	68
6.2 PROPOSED MODEL BASED ON OPTIMIZED λ VALUES	72
6.2.1 Performance evaluation of the Proposed λ-based Model	72
6.3 SENSITIVITY OF λ TO CN AND RUNOFF	75
6.4 EMPIRICAL EQUATION FOR CONVERSION OF $CN_{0.2}$ INTO $CN_{0.03}$	78
CHAPTER 7 EFFECT OF LAND USE, SOIL, AND SLOPE ON CURVE NUMBER	83
7.1 EFFECT OF LAND USE, INFILTRATION CAPACITY (OR SOIL TYPE), AND PLOT SLOPE ON Q AND CN	83
7.1.1 Utilizing P-Q data monitored during phase 1	83
7.1.2 Utilizing P-Q data monitored during phase 2	87
(a) Effect of plot Slope on Runoff and Curve Number	87
(b) Effect of land use on Curve Number	96
(c) Relation between Curve Number (CN) and AMC (θ_0%)	97
7.2 EVALUATION OF EXISTING SLOPE-BASED CN FORMULAE	98
7.2.1 Existing Slope-adjusted CN ($CN_{II\alpha}$) Models	98
(a) Ajmal et al. Model:	98
(b) Sharpley and Williams Model	98
(c) Huang et al. Model	98
7.2.2 Development of slope and Ia-Based CN ($CN_{II\alpha}$) Models	99
7.2.2.1 Parameterization of the Proposed Models:	99
(a) Model No.1 (M1):	99
(b) Model No.2 (M2):	99
(c) Model No.3 (M3):	99
7.2.3 Application of $CNII_{(\alpha,\lambda)}$ Models for runoff Estimation Using NRCS-CN Method	100
7.2.4 Comparison Between Observed CNII and Computed CNIIα/CNII(α,λ)	116
7.3 RELATIONSHIP BETWEEN CN AND ANTECEDENT WETNESS CONDITION	119
CHAPTER 8 COMPARISON OF SCS-CN INSPIRED MODELS	122
8.1 EVALUATION AND COMPARISON OF SCS-CN INSPIRED MODELS	122

8.1.1 Model description and its parameterization	122
(a) Original SCS-CN method	122
(b) Woodward et al. (2004) model	122
(c) Ajmal et al. (2015a) model	122
(d) Mishra and Singh (2002)	122
(e) Mishra and Singh Model (2003)	123
(f) Mishra et al. (2006b) model	123
(g) Jain et al. (2006) model	123
8.1.2 Model parameter description	124
8.1.3 Model parameter estimation	126
8.2 EVALUATION AND COMPARISON OF SCS-CN INSPIRED MODELS	129
8.2.1 Analysis based on individual plot datasets	129
8.2.2 Performance based on the results of all watersheds data	133
CHAPTER 9 EVALUATION OF CURVE NUMBER-BASED SEDIMENT YIELD MODELS	134
9.1 EVALUATION OF SCS-CN BASED SEDIMENT YIELD MODEL	134
9.1.1 description of model	134
9.1.2 Parameter estimation (or optimization)	135
9.2 MODEL PERFORMANCE EVALUATION USING PLOT DATA	135
9.3 PERFORMANCE EVALUATION FOR OVERALL PLOTS DATASET	138
9.4 DEVELOPMENT OF SEDIMENT-DISCHARGE RELATIONSHIPS	141
CHAPTER 10 SUMMARY AND CONCLUSSIONS	147
10.1 RAINFALL−RUNOFF BEHAVIOR STUDY	147
10.2 CN-DETERMINATION METHODS	148
10.3 INVESTIGATION FOR INITIAL ABSTRACTION RATIO (λ)	149
10.4 INVESTIGATION FOR ANTECEDENT MOISTURE CONDITION (AMC)	149
10.5 COMPARATIVE EVALUATION OF SCS-CN-INSPIRED MODELS	150
10.6 EFFECT OF SLOPE ON CURVE NUMBER (CN)	150
10.7 CN-BASED SEDIMENT YIELD MODELLING	151
CHAPTER 11 RESEARCH ACCOMPLISHMENTS AND ACHIEVEMENTS	152
11.1 ACCOMPLISHMENT OF THE RESEARCH OBJECTIVES	152

11.2 RESEARCH ACHIEVEMENTS	153
11.2.1 Research Publications	152
11.2.2 Ph.D and M.Tech Degrees Awarded	155
REFERENCES	156
APPENDIX A	162
APPENDIX B	173
APPENDIX C	180
APPENDIX D	189

LIST OF FIGURES

Figure No.	Description	Page No.
2.1	Location of the experimental farm	5
2.2	Design and layout plan of the experimental farm during phase 1	7
2.3a	Setup of Ordinary Raingauge (ORG) and Self – Recording Raingauge (SRRG)	8
2.3b	Finished ORG and SRRG ready for rainfall observation.	8
2.4	Runoff collection chamber constructed at outlet of maize plot	9
2.5	Conveyance Channel with Screen and Multi-Slot Divisor	9
2.6	Addition and mixing of Sandy Soil to the Existing Soil	10
2.7	Ploughing by Tractor for mixing of soil	10
2.8	Slope fixing and demarking of plot after mixing of sandy soil	11
2.9	Seed bed preparation for sugarcane planting	12
2.10	Manual row to row planting of sugarcane	12
2.11	Manual line sowing of maize	13
2.12	Fencing column and tank repairing	13
2.13	Construction of bund at farm for preventing the flooding at plots	14
2.14	Construction of Pond/Ditch	14
2.15	Figure showing the construction of room	15
2.16	Construction of plot boundary	15
2.17	Construction of Approach Channel	15
2.18	Design layout of the experimental plots constructed during phase 2	16
2.19	Raingauge installation during phase 2 of research project	17
2.20	Preparation of plots of required size and grade	18
2.21	Snapshots of Masonary work for plot having Slopes16%.	18
2.22	Construction of runoff collection tanks at the outlet of each plot	19
2.23	manual sowing of maize crop	19
2.24	Snapshots showing the growth of Crops in monsoon season	20
2.25	Construction of unlined small drain for preventing the flooding at plots.	20
3.1	Rainfall measurement using non recording type raingauge	29
3.2	Runoff depth measurement by metallic measuring scale	30
3.3a	Figure showing the measurement of soil Moisture Content in sugarcane	31

	plot during phase 1	
3.3b	Measurement of soil Moisture Content (θ_o) in maize plot during phase 2	31
3.4	Time domain reflectometry TDR 300 manufactured by "Field Scout" with probe 20 cm.	32
3.5a	Installation of double ring infiltrometer during phase 1 & Phase 2	35
3.5b	Measuring the water level in double ring infiltrometer while conducting infiltration test during phase1	35
4.1	Proportionality concept of the existing SCS-CN method	36
5.1	Box plot showing the CN estimated by methods M1-M8.	46
5.2	Box and whisker plot showing the RMSE obtained by methods M1-M8	49
5.3	Box and whisker plot showing the bias (e) obtained by methods M1-M8	49
5.4	Box and whisker plot showing the d obtained by methods M1-M8	50
5.5	Box and whisker plot showing the E obtained by methods M1-M8	50
5.6	Box and whisker plot showing the comparison among tabulated and observed P-Q data based CNs	55
5.7	CN Plot for comparison between CN_m and CN_{HT}	59
5.8	CN Plot for comparison between CN_{LSn} and CN_{HT}	59
5.9	CN Plot for comparison between CN_{LSo} and CN_{HT}	60
5.10	CN comparison plot for CN_{LSMn} vs CN_{HT}	61
5.11	CN comparison plot for CN_{LSMo} vs CN_{HT}	61
5.12	CN comparison plot for CN_{LS} vs CN_m	62
5.13a	CN comparison plot of CN_{LSM} vs CN_m for natural datasets	62
5.13b	CN comparison plot of CN_{LSM} vs CN_m for ordered datasets	63
5.14	CN plot for CN_{LSMo} vs CN_{LSMn}	67
6.1	Cumulative frequency distribution of model fitted λ-values for 27 plot-datasets	70
6.2	Relationship between I_a and S for 27 plots natural occurred P-Q datasets	71
6.3	Relationship between I_a and S for 27 plots ordered P-Q datasets	71
6.4	The cumulative frequency distribution of improvement in NSE using r^2 criteria	75
6.5	Variation in CNs (AMC-2) with λ for 5 plot-data	76
6.6	Variation in E with λ	77
6.7	Relationship between relative increase in estimated runoff (%) vs relative	77

	decrease in λ (%)	
6.8	Plot of fitting between $S_{0.2}$ and $S_{0.03}$ for 27 agricultural plots data	78
6.9	plot of ratio of $S_{0.03}$ to $S_{0.2}$ (i.e. $S_{0.03}/S_{0.2}$) vs Rc_m	79
6.10	The cumulative frequency distribution of improvement in NSE using r^2 criteria	82
7.1	Relationship of mean runoff depth (Q_m) with Infiltration capacity (fc) of soil for all 27 agricultural plots data.	84
7.2	Relationship of mean runoff coefficient (Rc_m) with Infiltration capacity (fc) of soil for all 27 agricultural plots data.	84
7.3	Relationship of Curve Number (CN) with Infiltration capacity (fc) of soil for all 27 agricultural plots data	85
7.4	Rainfall vs runoff graph for Maize crop	92
7.5	Rainfall vs runoff graph for Finger millet crop	92
7.6	Rainfall vs runoff graph for Fallow land	93
7.7	Effect of slope on Curve Number	93
7.8	Effect of slope on Curve number at AMC condition of Maize	95
7.9	Effect of slope on Curve number at AMC condition of Finger millet	95
7.10	Effect of slope on Curve number at AMC condition of the Fallow land	96
7.11	Effect of land use on Curve Number	96
7.12	Relation between Curve number and AMC Maize Crops	97
7.13	Relation between Curve Number and AMC Finger millet Crop	97
7.14	Relation between Curve Number and AMC fallow land	98
7.15	Comparison between Observed versus Computed runoff for Fallow land	106
7.16	Comparison between Observed versus Computed runoff for Maize	107
7.17	Comparison between Observed versus Computed runoff for Raagi	108
7.18	Inter-comparison of Models M1-M3 for a constant value of λ = 0.3 for Fallow land	109
7.19	Inter-comparison of Models M1-M3 for a constant value of λ = 0.3 for Maize	110
7.20	Inter-comparison of Models M1-M3 for a constant value of λ = 0.3 for Raagi	111
7.21	Inter-comparison of Models M1-M3 for varying λ for 8% watershed slope for Fallow Land	112

7.22	Inter-comparison of Models M1-M3 for varying λ for 8% watershed slope for Maize Land	113
7.23	Inter-comparison of Models M1-M3 for varying λ for 8% watershed slope for Raagi	114
7.24	Observed CNII variation with varying slope and landuse for λ = 0.3	115
7.25	Comparison of CNII versus $CNII_{\alpha}/CNII_{(\alpha, \lambda)}$ for Fallow land with λ=0.3	117
7.26	Comparison of CNII versus $CNII_{\alpha}/CNII_{(\alpha, \lambda)}$ for Raagi with λ=0.3	118
7.27	Comparison of CNII versus $CNII_{\alpha}/CNII_{(\alpha, \lambda)}$ for Maize with λ=0.3	119
8.1	Observed runoff versus calculated runoff for models M1 to M8 in Hemawati watershed.	132
9.1	Relationship between CNs derived from sediment yield model and existing SCS-CN model (using rainfall-runoff data)	138
9.2	Comparison between observed and computed sediment yield using model S1	139
9.3	Comparison between observed and computed sediment yield using model S2	140
9.4	Comparison between observed and computed sediment yield using model S4	140
9.5	Sediment rating curve of Maize Crops 8% slope (Plot 12)	144
9.6	Sediment rating curve of Maize Crops 12% slope (Plot 11)	144
9.7	Sediment rating curve of Maize Crops 16% slope (Plot 10)	144
9.8	Sediment rating curve of Finger Millet 8% slope (Plot 15)	145
9.9	Sediment rating curve of Finger Millet 12% slope (Plot 14)	145
9.10	Sediment rating curve of Finger Millet 16% slope (Plot 13)	145
9.11	Sediment rating curve of Fallow land 8% slope (Plot 18)	146
9.12	Sediment rating curve of Fallow land 12% slope (Plot 17)	146
9.13	Sediment rating curve of Fallow land 16% slope (Plot 16)	146

LIST OF TABLES

Table No.	Description	Page No.
3.1	Characteristics of plots used for P-Q data monitoring during phase 1 of the research project	22
3.2	Characteristics of plots used for P-Q data monitoring during phase 2 of the research project	26
3.3	Rainfall characteristics during the phase 1 (August 2012–April 2015)	29
3.4	Rainfall characteristics during the phase 2	29
3.5	Hydrologic soil group (HSG) based on soil texture and minimum infiltration rate	34
4.1	Classification of native pasture or range (Source: SCS, 1971)	39
4.2	Antecedent Soil Moisture Conditions (AMC)	40
5.1	Estimated curve numbers using the eight different methods for the 36 agricultural plots of various characteristics.	47
5.2	Comparison of CN determination methods based on the Kruskal–Wallis test	48
5.3	Comparison of runoff estimation using eight different curve number determination methods for 24 plots datasets.	51
5.4	Performance evaluation of models based on ranks (scores)	53
5.5	Summary of runoff plot characteristics and CN values derived using NEH-4 median, Least-Squares fit method (LSM) and Handbook tables (Used partial dataset excluding P<15 mm)	56
5.6a	Performance statistic for runoff estimation using CN_{HT} and CN_m	64
5.6b	Performance statistic for runoff estimation using CN_{LSn} and CN_{LSo}	65
6.1	Optimized λ values from observed P-Q data	69
6.2	Performance statistic for runoff estimation using Equation 4.5 with λ = 0.2 (model $M_{0.2}$) and λ = 0.03 (model $M_{0.03}$) (Used all runoff producing events)	73
6.3	Performance statistic for runoff estimation using CN_{HT} associated to λ=0.20 ($CN_{HT0.20}$) and λ=0.03 ($CN_{HT0.03}$)	80
7.1	Mean event runoff coefficient (Rc) and CNs for the groups of different land uses, HSGs and slopes	86

7.2	Coefficients of determination (R^2) of daily runoff (Q) (mm) and runoff coefficients (Rc) with previous day soil moisture (θ) (%), along with mean runoff coefficient (Rc_m) for each plot	88
7.3	Computation of CN for plot nos. 10-12 of phase 2.	89
7.4	Computation of CN for plot nos. 13-15 of phase 2.	90
7.5	Computation of CN for plot nos. 16-18 of phase 2.	91
7.6	Different AMCs CN calculation following Hjelmfelt et al. (1981) criterion	94
7.7	Proposed Models (M1-M3) with Optimized parameters	100
7.8	Performance Evaluation of the Six Models for Slope 16%, λ= 0.3 and 3 land uses (Fallow, Raagi and Maize)	101
7.9	Performance Evaluation of the Six Models for Slope 8%, λ= 0.3 and 3 land uses (Fallow, Raagi and Maize)	101
7.10	Performance Evaluation of the Six Models for Slope 16%, λ= 0.2 and 3 land uses (Fallow, Raagi and Maize)	101
7.11	Performance Evaluation of the Six Models for Slope 12%, λ= 0.2 and 3 land uses (Fallow, Raagi and Maize)	102
7.12	Performance Evaluation of the Six Models for Slope 8%, λ= 0.2 and 3 land uses (Fallow, Raagi and Maize)	102
7.13	Performance Evaluation of the Six Models for Slope 16%, λ= 0.1 and 3 land uses (Fallow, Raagi and Maize)	102
7.14	Performance Evaluation of the Six Models for Slope 12%, λ= 0.1 and 3 land uses (Fallow, Raagi and Maize)	103
7.15	Performance Evaluation of the Six Models for Slope 8%, λ= 0.1 and 3 land uses (Fallow, Raagi and Maize)	103
7.16	Performance Evaluation of the Six Models for Slope 16%, λ= 0.05 and 3 land uses (Fallow, Raagi and Maize)	103
7.17	Performance Evaluation of the Six Models for Slope 12%, λ= 0.05 and 3 land uses (Fallow, Raagi and Maize)	104
7.18	Performance Evaluation of Six Models for Slope 8%, λ= 0.05 and 3 land uses (Fallow, Raagi and Maize)	104
7.19	Performance of various relations between CN and AWC indices	121
7.20	Performance statistic for runoff estimation using CN relationship with θ_{o1} and P_5	120

8.1	Characteristics of study plots and watersheds used in evaluation of SCS inspired models	125
8.2	SCS inspired models and their parameter description.	126
8.3	SCS inspired models estimated parameters	127
8.4	Comparison of RMSE (mm) in all watersheds.	129
8.5	Comparison of n (t) in all watersheds.	130
8.6	Comparison of E (%) in all watersheds.	131
8.7	Performance evaluation of models based on cumulative means values and rank score.	133
9.1	Different forms of SCS-CN based sediment yield model	135
9.2	Results of application of sediment yield model (S2) for plot wise data sets	136
9.3	CN values derived from runoff model and sediment yield model (S2)	137
9.4	Comparison of runoff computation using S value from Sediment yield model	138
9.5	Results of various model applications to data sets of overall plots	140
9.6	Observed runoff and sediment yield for Maize crop (or plot nos. 10-12)	141
9.7	Observed runoff and sediment yield for Finger millet (or plot nos. 13-15)	142
9.8	Observed runoff and sediment yield for Fallow land (or plot nos. 16-18)	143

LIST OF ABBREVIATIONS AND SYMBOLS

Abbreviation	Definition
P	Rainfall depth (mm)
Q	Runoff depth (mm)
NEH	National engineering Handbook
NEH-4	National engineering Handbook chapter-4
HSG	Hydrologic soil group
CN	Curve number
AMC	Antecedent moisture condition
CN_1	Curve number for dry condition or AMC-1
CN_2	Curve number for average condition or AMC-2
CN_3	Curve number for wet condition or AMC-3
AMC-1	Dry antecedent moisture condition
AMC-2	Average antecedent moisture condition
AMC-3	Wet antecedent moisture condition
CN_{HT}	Curve number derived from NEH-4 table
CN_m	Median curve number derived from P-Q data set
CN_{LSM}	Curve number derived from P-Q data set using least square method for $\lambda = 0.2$ (i.e. single way fitting CN)
CN_{LS}	Curve number derived from P-Q data set using least square method for optimized λ (i.e. double way fitting CN)
CN_{LSn}	Curve number derived from P–Q data set using least square method (optimized λ) for natural data series
CN_{LSo}	Curve number derived from P–Q data set using least square method (optimized λ) for ordered data series
CN_{LSMn}	Curve number derived from P–Q data set using least square method ($\lambda = 0.2$) for natural data series
CN_{LSMo}	Curve number derived from P–Q data set using least square method ($\lambda = 0.2$) for ordered data series
$CN_{HT0.20}$	NEH-4 tables CN associated with λ=0.20
$CN_{HT0.03}$	NEH-4 tables CN associated with λ=0.03

$CN_{0.2}$	Curve number associated with $\lambda = 0.2$
$CN_{0.03}$	Curve number associated with $\lambda = 0.03$
S	Maximum potential retention (mm)
$S_{0.2}$	Maximum potential retention (mm)associated with $\lambda = 0.2$
$S_{0.03}$	Maximum potential retention (mm) associated with $\lambda = 0.03$
θ_{o1}	1-day antecedent soil moisture (%)
θ_{o3}	3-day average antecedent soil moisture (%)
θ_{o5}	5-day average antecedent soil moisture (%)
Θ	Previous day soil moisture (%)
P_5	5-day antecedent rainfall (mm)
°C	Degree Celsius
N	number of rainfall events
Ln	natural logarithm operator
POE	probability of exceedance
GM	geometric mean
TDR	Time domain reflectometry
AWC	Antecedent wetness condition
LSM	Least square method
PRA	Public road administration
I_a	Initial abstraction (mm)
I	Rainfall threshold for runoff generation
Rc_m	Mean runoff coefficient of plot
Rc	Event runoff coefficient
Fc	Infiltration capacity (mm/hr)
F	cumulative infiltration
AFM	asymptotic fitting method
HEC-HMS	Hydrologic Engineering Center Hydrologic Modeling System
SWAT	Soil and Water Assessment Tool
ANSWERS	Areal Non-point Source Watershed Environment Response Simulation
AGNPS	Agricultural Non-point Source Model

EPIC	Erosion Productivity Impact Calculator
HEC-1	Hydrologic Engineering Center-1
APEX	Agricultural Policy/Environmental eXtender
GLEAMS	Groundwater Loading Effect of Agricultural Management Systems
CREAMS	Chemicals, Runoff, and Erosion from Agricultural Management Systems
USLE	universal soil loss equation
SCS	Soil conservation services
SE	Standard error
E	Nash-Sutcliffe efficiency coefficient
R^2	coefficient of determination
D	index of agreement
RMSE	root mean square error (mm)
PBIAS	Percent bias (%)
Re	Relative error
E	Bias
K-W	Kruskal–Wallis
ANOVA	one-way analysis of variance
LSD	least significant difference
SPSS	Statistical Package for the Social Sciences

CHAPTER 1
INTRODUCTION

The Soil Conservation Service Curve Number (SCS-CN) method was developed in 1954. It is documented in Section 4 of the National Engineering Handbook (NEH-4) published by the Soil Conservation Service (now called the Natural Resources Conservation Service), U.S. Department of Agriculture in 1956. The document has since been revised several times. The SCS-CN method is the result of exhaustive field investigations carried out during 1930s and 1940s. The method has since then witnessed myriad applications world over. It is one of the most popular methods for computing the surface runoff for a given rainfall event from small agricultural, forest, and urban watersheds. It is simple, easy to understand and apply, stable, and useful for ungauged watersheds. The primary reason for its wide applicability and acceptability lies in the fact that it accounts for most runoff producing watershed characteristics: soil type, land use/treatment, surface condition, and antecedent moisture condition. The only parameter of this methodology, i.e. the Curve Number (CN), is crucial for accurate runoff prediction. Based on exhaustive field investigations carried out in the United States, curve numbers were derived for different land uses, soil types, hydrologic condition, and management practices and these are reported in NEH-4. These numbers have seldom been verified for Indian watersheds.

In present study, CN values have been derived from experimentally monitored rainfall-runoff-sediment yield for varying slopes, land uses, and soils situated at single climatic condition. In addition, the effect of slope on CNs as well as, the link between CN (or potential maximum retention) and potential maximum erosion in the experimental plot was also investigated. Such a development would help refine the CN values for more accurate runoff prediction. The need for such investigations has been realized since long.

1.1 OBJECTIVES OF THE STUDY

The objectives of the present project report, as envisaged at the stage of proposal formulation, were as follows:

a) Finding answers to as yet un-answered questions.
   - What is the physical significance of curve number?
   - Are the NEH-4 curve numbers applicable universally?

b) Development of a new computational procedure.

CNs derived experimentally for varying watershed slopes will be used for investigating the effect of slope on CN. Such a development would help refine the CN values for more accurate runoff prediction.

c) Development of a new software/application.

Guidelines will be provided for the application of the results derived from experimental study.

d) Development of a new field technique.

The present research envisages experimental verification of the available CN values for different soil types and land uses. The effect of watershed slope on CN is also planned to be investigated. In addition, since the sediment yield is also planned to be measured during rain storms, the existence of a link between CN (or potential maximum retention) and the potential maximum erosion will be investigated.

e) Design and/or develop a new device.

The experimental study envisages exploration of improving the existing SCS-CN methodology and developing an SCS-CN-based rainfall-runoff-sediment yield model.

f) Investigation of the behaviour of a natural process.

The SCS-CN method deals with runoff estimation from given rainfall magnitude and this runoff is directly related with sediment erosion and transport. Thus, the proposed experimental study is primarily an investigation of the natural rainfall-runoff-sediment yield process, which is planned to be investigated in terms of the runoff curve number used in the available SCS-CN-based sediment yield model.

In an attempt to fulfill the above objectives, the following works were carried out, and accordingly, the objectives were re-framed for better organization of the studied work as follows:

- To investigate the applicability of NEH-4 curve numbers to Indian Watersheds.
- To determine the climatic parameter initial abstraction ratio (λ) value for study region.
- To study the effects of various watershed slopes, land use and soil type on runoff and CN for different land uses and soils.
- To investigate the effect of slope on sediment yield for different land uses and soils.
- To propose an improved version of the existing SCS-CN methodology and an SCS-CN based rainfall – runoff – sediment yield model.
- To provide guidelines for the application of the results derived from the experimental study.

1.2 ORGANIZATION OF THE PROJECT REPORT

CHAPTER 1 introduces the project work, sets the objectives, and presents the organization of the project report.

CHAPTER 2 describes the study area and experimental setup for monitoring the data to fulfil the proposed research objectives.

CHAPTER 3 describes about the data collected of which the proposed methodology was employed for experimental verification of SCS runoff curve numbers for different soils and sugarcane, maize, blackgram, fallow, maduwa and ragi landuses.

CHAPTER 4 explains the basics of SCS-CN methodology.

CHAPTER 5 describes different curve number methods employed to estimate CN from observed P-Q data. Further these observed P-Q data based CNs were compared with NEH-4 CN values for agricultural plots in Indian conditions.

CHAPTER 6 describes the initial abstraction coefficient (λ) calculation along with the performance evaluation of the λ-based proposed model, sensitivity of λ on CN and runoff, conversion of CNs associated with one λ into another.

CHAPTER 7 deals with study of interaction among different hydrological parameters like rainfall, runoff, runoff coefficient and soil moisture; and effect of experimental plot characteristics such as soil type, land use and slope on runoff and curve number. The existence of a relationship between CN (or S) and antecedent wetness condition were also explored in this section using in-situ observed soil moisture.

CHAPTER 8 deals with comparative evaluation of the SCS-CN inspired models in Indian climatic condition.

CHAPTER 9 evaluates the performance of SCS-CN based sediment yield models using observed data from the experimental plots which will help decide the applicability of these models to predicting the event-based sediment yield for the given climatic condition and watershed characteristics.

CHAPTER 2
STUDY AREA AND EXPERIMENTAL SETUP

2.1 STUDY AREA

As mentioned at the stage of research project proposal formulation, this study is conducted in an experimental field located at 29°08' N and 77°09' E, in Roorkee, district Haridwar, Uttarakhand (India) (Figure 1.1). The study area is a part of the Solani River catchment, which is a sub watershed of Ganga River-the largest river basin in India. In terms of topography, Solani watershed has three major zones: hills, piedmont and plains, and emerges from Shivalik range of great Himalayas. The average elevation of the experimental site is about 266m above mean sea level (amsl) and situated within the Solani watershed at about 30-60 km south of the foothills of the Himalayas.

2.1.1 Climate

The climate at the experimental site is sub-tropical type characterized by hot summers and cold winters, along with three pronounced seasons; viz., summer, monsoon and winter. In the summer period the minimum and maximum monthly temperature values, on average, are 20°C and 45°C respectively, whereas in winter period these are 10°C and 27°C respectively. The relative humidity varies from 30% to 99%, and average annual PET of the order of 1340 mm. The annual precipitation varies from 1120 to 1500 mm with most of the rainfall (around 70-80%) occuring during monsoon season (June-October).

2.1.2 Soil type and land use

The type of soil in the study area is loam (US Bureau of Soil and PRA Classification) with an average proportion of 50–55 % of sand, 35–42 % silt and 8-15 % clay (Kumar et al., 2012). The upper hilly area of Solani watershed is mainly consisting of sandy loam whereas lower flat terrain (experimental site) is dominated by loam and loamy sand (Garg et al., 2013). The study area constitutes three major land cover classes: Forest land, bare soil and vegetated land. A significant portion of the vegetated land is agricultural with more than 35% of the area coverage, and fallow land account for 17% to the total area whereas forest covers around 30% of the total area, especially in hilly part of the basin. Sugarcane is the perennial crop in the area whereas wheat, maize, and pulses grown as seasonal crops (Garg et al., 2013).

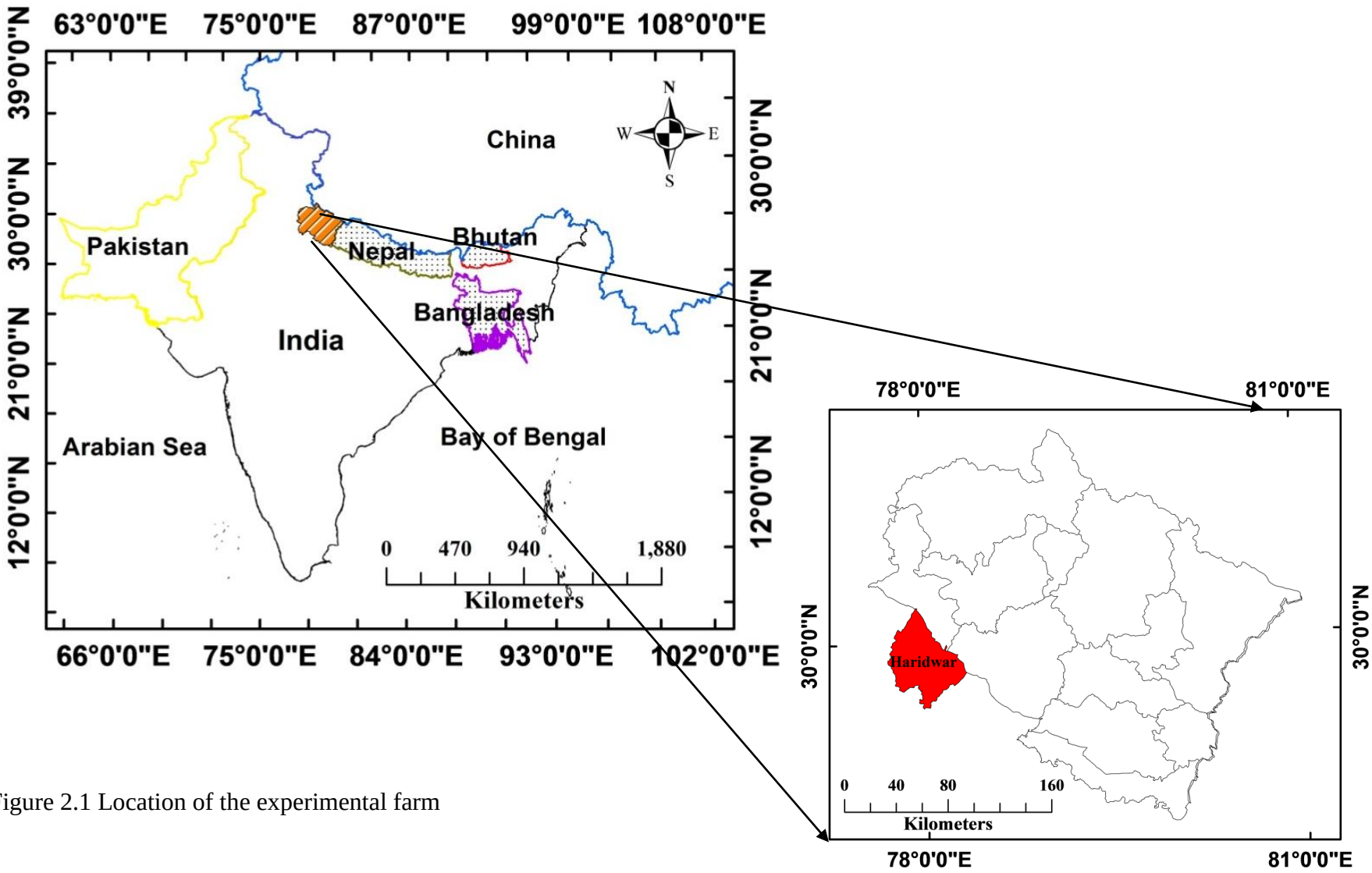

Figure 2.1 Location of the experimental farm

2.2 DESIGN AND LAYOUT PLAN OF THE EXPERIMENTAL FARM

The experimental farm having size of 70m × 50m, originally plain agricultural land, was taken on lease in 2012. The research project was completed in two phases (hereafter termed as phase 1 and phase 2).

2.2.1 Construction of experimental plots during phase 1

In phase 1, selected agricultural field for experimental work was divided into plots of 22m length and 5m width with three independent variables: soils, land use, and slope/gradient. Pegs and strings with white chalk were used for marking the plots with its level, which guided the tractor to pile up the soil accordingly. The frequent movement of tractors on the deposited soil compacted the plots enough requiring no further compaction. The layout of the experimental plots is shown in Figure 2.2. In this phase, experimental work was conducted for three years (i.e. August 2012 – April 2015) in which experimental plots included four types of vegetative cover: sugarcane, maize, blackgram, and fallow land with slopes of 1%, 3%, and 5%. During the first year of study (i.e. August 2012 – May 2013), rainfall and runoff were measured for six plots with land use of sugarcane and Maize, and slopes of 1%, 3%, and 5%. However, to change the soil property during the second year (i.e. June 2013 – May 2014) of experimental work, sand was added to the existing soil, and rainfall (P) and runoff (Q) (hereafter termed as "P-Q data) were monitored in twelve plots having four different land use covers: sugarcane, maize, blackgram, and fallow land with slopes of 1%, 3% and 5%. Similarly, for the third year (i.e. June 2014 – April 2015), sand was again added to the previous year soil, and P-Q data were monitored on the twelve plots having four different land use covers: sugarcane, blackgram, maize, and fallow land with slopes of 1%, 3% and 5%. In phase 1, P-Q data were monitored on total 30 plots. It is worth emphasizing that the normal agricultural practices of mixing of soil, seed selection etc. were followed for cultivation of crops throughout the study period, and all the necessary infrastructure was created as described later in this chapter.

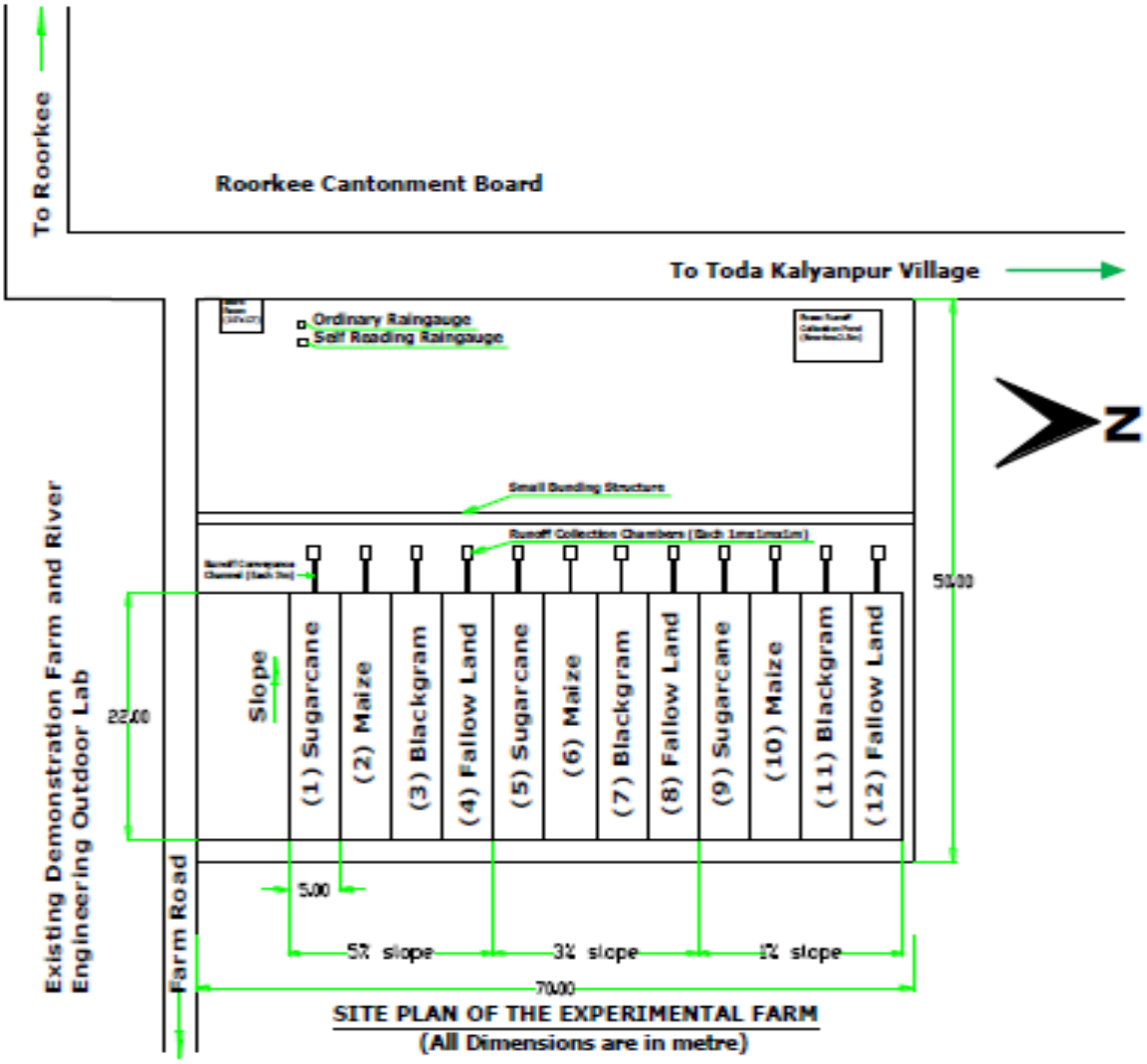

Figure 2.2 Design and layout plan of the experimental farm during phase 1

2.2.2 Infrastructures established during phase 1

(a) Raingauge installation

For the measurement of rainfall, both the types of raingauges (ordinary and self-recording) as shown in Figure 2.3a,b have been installed on the farm in open space considering no obstruction in collecting the rainfall. Self-recording raingauge was equipped with a data logger. Data logger is an electronic instrument designed to read and store information and the data can be transferred to computer. Event wise rainfall details as well as rainfall intensity can be obtained from self-recording raingauge. The ordinary type (non-recording type) raingauge gives amount of rainfall by collecting rain water over a period of time.

Figure 2.3a Setup of Ordinary Raingauge (ORG) and Self – Recording Raingauge (SRRG)

Figure 2.3b Finished ORG and SRRG ready for rainfall observation.

(b) Runoff Collection Chamber construction

To measure the runoff discharge and sediment yield as well as to collect the samples, runoff collection chambers of size 1m × 1m × 1m as shown in Figure 2.4 have been constructed at the end of each plot and later the depth of the chambers was increased as required. Each chamber was connected to the respective plot by a mild sloped conveyance channel of 3m length having a screen to check unwanted materials and multi-slots divisor (5 equal slots) at the exit of the channel as shown in Figure 2.5 so that the runoff passes equally through all the slots without creating turbulence flow.

Of the 5 slots, the runoff is discharged out of the chamber from 4 slots and only one slot is directed to the chamber so that the runoff volume can be measured 5 times more than the capacity of the chamber.

Figure 2.4 Runoff collection chamber constructed at outlet of maize plot

Figure 2.5 Conveyance Channel with Screen and Multi-Slot Divisor

(c) Land Preparation and Cultivation

The experimental farm was designed and developed as per our requirements. The design included three independent variables: soil type, land use and slope. Sandy soil was mixed with the existing soil to change the type and properties of the soil while preparing the land as shown in Figure 2.6 and then it was ploughed by tractor (Figure 2.7). Figure 2.8 shows the fixing of slope of plot after mixing of sandy soil. Dumpy level was used in demarking the slope of plots.

Figure 2.6 Addition and mixing of Sandy Soil to the Existing Soil

Figure 2.7 Ploughing by Tractor for mixing of soil

Figure 2.8 Slope fixing and demarking of plot after mixing of sandy soil

After ploughing, levelling and providing desired slope, all 12 plots were cultivated with three crops viz. sugarcane, maize, black gram (Urd) and one plot was left as fallow land (Note: these cropping patterns were followed during second and third year). Figures 2.9 and 2.10 show the planting the sugarcane in 5% slope plot. Similarly, figure 2.11 shows the manual line sowing of maize crop. Here, it is worth noting that these practices were followed each year to grow the crops in experimental plots.

Figure 2.9 Seed bed preparation for sugarcane planting

Figure 2.10 Manual row to row planting of sugarcane

Figure 2.11 Manual line sowing of maize

(d) Safety, drain, repair, and construction of Shelter/Control Room

The farm was open from all the four sides. Therefore, all the four sides were protected by fencing and nailed wire was grilled to check the entry of animals as well as unauthorized persons minimizing the damage to the farm (figure 2.12). A drain beside the storage chamber was constructed so that water emptied from the tanks as well as additional rainwater might be discharged safely without any damage to the farm. To prevent runoff collection tank from over flooding, a bund was also constructed. Water collecting tanks were also repaired regularly to prevent the seepage during the rainfall. The glimpse of these works is shown below in Figure 2.13.

Figure 2.12 Fencing column and tank repairing

Figure 2.13 Construction of bund at farm for preventing the flooding at plots

A pond of size about 8.0 m × 4.0 m × 2.5 m was constructed with the help of excavator to catch the runoff water from the farm since there is no drainage facility available. The water collected during rains was pumped out as per requirement. The figure 2.14 shows the construction of water storage tank of pond.

Figure 2.14 Construction of Pond/Ditch

A shelter/control room (size 12’ x 10’) at the site of Experimental Farm was constructed, also for storing tools and equipment. This room is also being used for the watchman who has been appointed for security and taking care of the farm. The photograph of the room is shown in figure 2.15.

Figure 2.15 Figure showing the construction of room

(e) Construction of plot boundary and approach channel

To collect the runoff discharge from the plots, boundary was constructed along the plot boundary at its downstream end. This helped in flowing the runoff discharge as well as sediment yield towards the measuring chamber. A lateral slope of 1:100 in the plot was provided and the width of channel boundary was kept as 25 cm. The glimpse of plot boundary construction is shown in figure 2.16.

Figure 2.16 Construction of plot boundary

Figure 2.17 Construction of Approach Channel

Similarly approach channels were constructed to convey the collected runoff as well the sediment yield from the plot to the measuring chamber as shown in Figure 2.17.

2.2.3 Construction of experimental plots during phase 2

Similar to phase 1, an experimental farm adjacent to the previous phase-1 located in the same Village of Toda Kalyanpur (Latitude: 29^0 50' 9" N, Longitude: 77^0 55' 21" E) in Roorkee in Haridwar District of Uttarakhand State, India was developed, and experimental plots constructed. In this phase, the plots consisted of three soil types, viz., land use (Maize, Mandua and Fallow land) and slopes/grades (8%, 12% and 16%). Figure 2.18 shows the design layout of these experimental plots. The experimental work during this phase was also conducted for three years (i.e. April 2016 to November 2018). During the first year of study (i.e. April, 2016) nine plots of size 12.0 m × 3.0 m having different slopes and land uses were constructed. Further, to change the soil property during the second year (i.e. 2017) of experimental work, fine sand was mixed up to 20 cm depth with the previous year soil. To avoid the damage of experimental setup, mixing was done manually. During the second year of study nine plots of size 12.0 m × 3.0 m having different slopes and land uses were constructed. Similarly, fine sand was again added in third year (i.e. 2018) and nine plots of size 12.0 m × 3.0 m having different slopes and land uses were constructed.

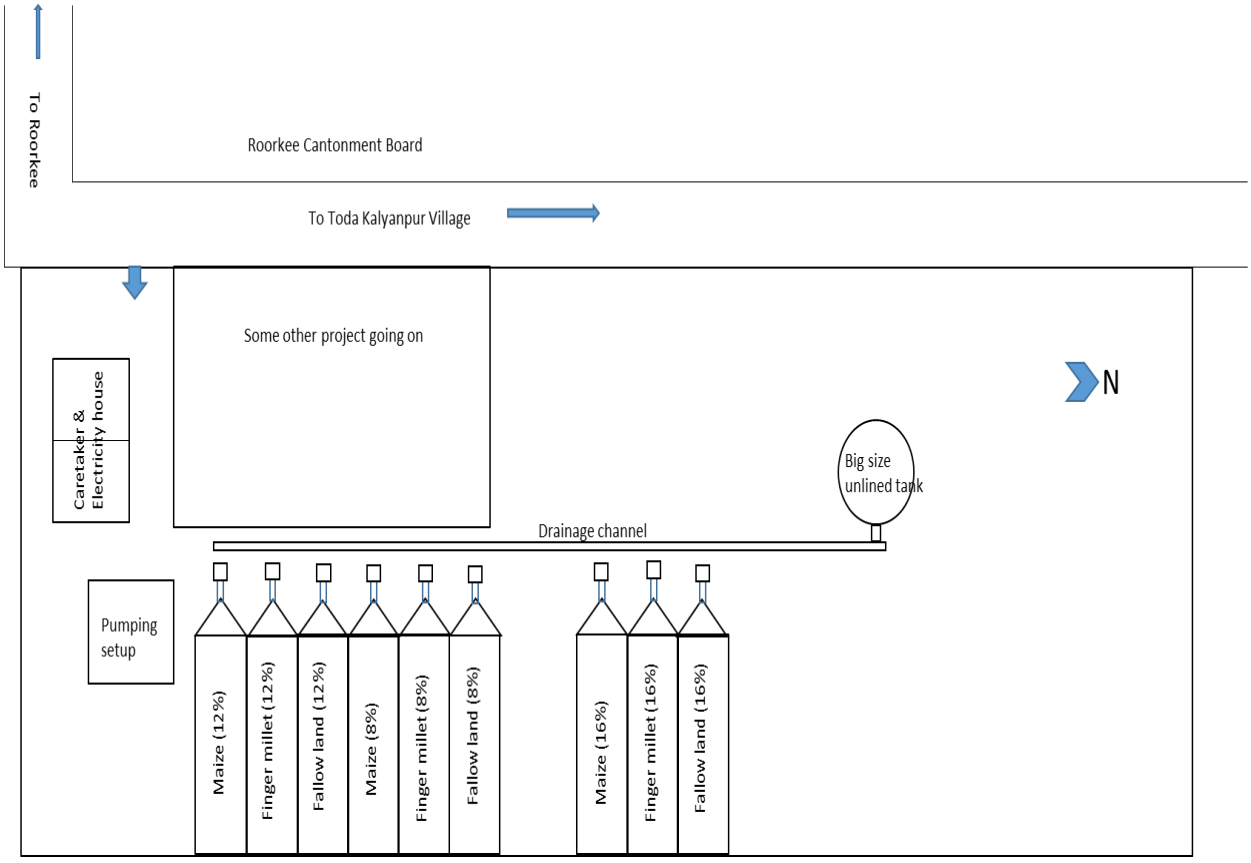

Figure 2.18 Design layout of the experimental plots constructed during phase 2

2.2.4 Infrastructures established during phase 2

(a) Raingauge installation

Similar to phase 1, Ordinary Raingauge (ORG) and Self – Recording Raingauge (SRRG) were installed at study site (figure 2.19).

Figure 2.19 Raingauge installation during phase 2 of research project

(b) Preparation of Plots

Initially, the field was having plain topography. The required 8%, 12% and 16% slopes of the land were prepared using JCB machine, and tractor trolley was used for filling. Each plot was made of size 70 m × 50 m, which is then sub divided into three small plots of size 20 m x 9.0 m in each grade of plots (viz., 8%, 12% and 16%). Each slope group plots were further sub divided into 3 plots of size 20 m × 3.0 m. Pegs and strings with white chalk were used for marking the plots with its level, which guided the tractor to pile up the soil accordingly. The frequent movement of JCB and tractor trolley on the deposited soil compacted the plots sufficiently enough. The steps involving the work are shown in Figures 2.20 and 2.21.

Figure 2.20 Preparation of plots of required size and grade

Figure 2.21 Snapshots of Masonary work for plot having Slopes16%.

(c) Construction of runoff collection tanks

Runoff generated for each rainfall event from each plot was collected in a chamber of size 1.5m × 1.5m × 1.5m. Multi-slot divisor was arranged in the approach channel leading from plot to chamber. Multi-slot divisor had five equal numbers of slots and runoff was collected in the chamber coming only through middle slot and that of other slots was diverted outside the chamber so that size of the chamber and the ultimate cost of work could be minimized. The depth of runoff volume in the chamber was measured with steel tape (Figure 2.22). Since collecting chamber and conveyance channel were open to sky, volume due to direct rainfall contribution was also deducted for accuracy in runoff calculation.

Figure 2.22 Construction of runoff collection tanks at the outlet of each plot

(d) Crop cultivation

After making the desired slope, plots delineated in each slope grades were cultivated with different crops viz. maize, mandua and one plot is left as fallow land during monsoon season. Normal cultivation practices for seed selection, application of fertilizer, application of herbicides and pesticides, application of irrigation and weeding is adopted as per requirement. The steps involving in growing different crops are shown in figures 2.23 and 2.24 given below:

Figure 2.23 manual sowing of maize crop

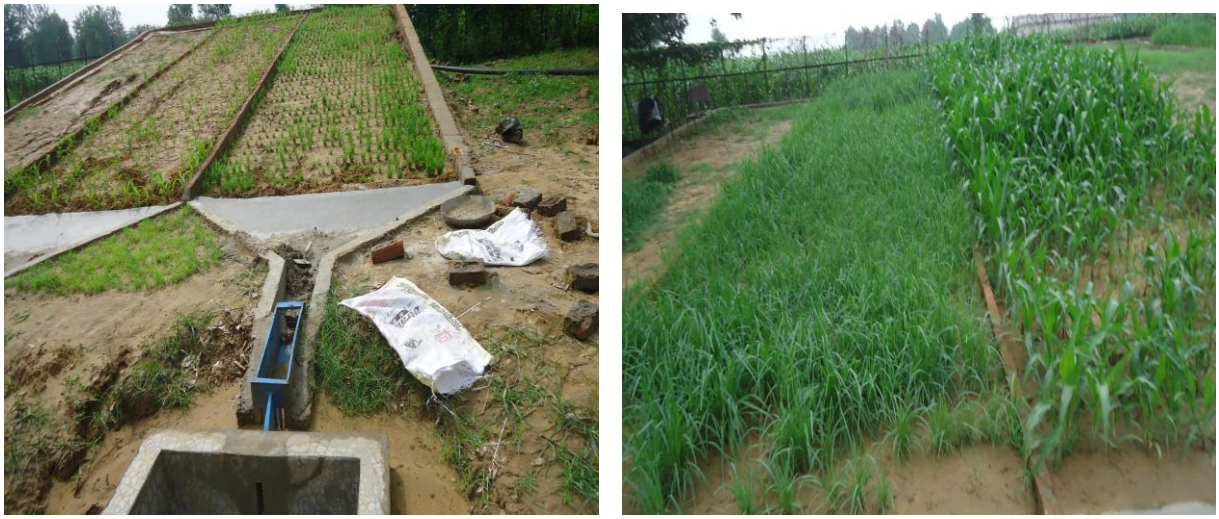

Figure 2.24 Snapshots showing the growth of Crops in monsoon season

(e) Safety, drain and repair

In addition to the existing fencing, the remaining two sides were protected by fencing and nailed wire was grilled to check the entry of animals as well as unauthorized persons minimizing the damage to the farm (Figure 2.25). A drain beside the storage chamber was constructed so that water emptied from the tanks as well as additional rainwater might be discharged safely without any damage to the farm. Water collection tanks were also repaired to prevent the seepage during the rainfall.

Figure 2.25 Construction of unlined small drain for preventing the flooding at plots.

CHAPTER 3
DATA COLLECTION

The characteristics of experimental runoff plots used for monitoring of P-Q data are given in Table 3.1 and Table 3.2 for phase 1 and phase 2, respectively. The main data observed and collected from the experimental farm and laboratory during the study period are given below:

i) Rainfall (P)

ii) Surface runoff (Q)

iii) Antecedent soil moisture (θ_0)

iv) Infiltration capacity of the soil (*f*c)

3.1 Rainfall measurement

Rainfall (P) data were collected using both the raingauges (self-recording type and ordinary type). Event wise rainfall details as well as rainfall intensity were recorded from self-recording raingauge and total (24 hours) amount of rainfall in mm were observed from ordinary type (non-recording type) raingauge as shown in Figure 3.1 for the verification of data as well. The distribution of rainfall measured during study period is shown in Tables 3.3 and Table 3.4 for Phase 1 and phase 2 respectively. As seen from table 3.3, during phase 1, a total number of 101 rainfall events were captured with rainfall amount varying from 0.5 mm to 93.8 mm and only 42 events produced significant amount of runoff for measurement. A total of 11, 18, and 13 runoff producing events were captured during the first, second, and third years of phase 1, respectively. Similarly, during phase 2, a total of 84 rainfall events were captured, and only 55 events produced significant amount of runoff for measurement.

Table 3.1 Characteristics of plots used for P-Q data monitoring during phase 1 of the research project

Watershed/ Plot No.	n	Land use	Slope (%)	*'fc'* (mm/hr)	HSG	Area (km^2)	Rainfall (mm)	Altitude (m)	Climate type	Study location
1	15	Sugarcane	5	7.36	B	110×10^{-6}	1120-1500	266	humid sub–tropical	Solani river catchment (India)
2	15	Sugarcane	3	8.77	A	110×10^{-6}	1120-1500	266	humid sub–tropical	Solani river catchment (India)
3	15	Sugarcane	1	6.51	B	110×10^{-6}	1120-1500	266	humid sub–tropical	Solani river catchment (India)
4	10	Fallow	5	12.1	A	110×10^{-6}	1120-1500	266	humid sub–tropical	Solani river catchment (India)
5	10	Fallow	3	6.15	B	110×10^{-6}	1120-1500	266	humid sub–tropical	Solani river catchment (India)
6	10	Fallow	1	10.28	A	110×10^{-6}	1120-1500	266	humid sub–tropical	Solani river catchment (India)
7	10	Maize	5	4.24	B	110×10^{-6}	1120-1500	266	humid sub–tropical	Solani river catchment (India)
8	10	Maize	3	5.52	B	110×10^{-6}	1120-1500	266	humid sub–tropical	Solani river catchment (India)
9	10	Maize	1	2.82	C	110×10^{-6}	1120-1500	266	humid sub–tropical	Solani river catchment (India)

Table 1 (continued)

Watershed/ Plot No.	n	Land use	Slope (%)	*'fc'* (mm/hr)	HSG	Area (km^2)	Rainfall (mm)	Altitude (m)	Climate type	Study location
10	10	Blackgram	5	15.22	A	110×10^{-6}	1120-1500	266	humid sub–tropical	Solani river catchment (India)
11	10	Blackgram	3	13.82	A	110×10^{-6}	1120-1500	266	humid sub–tropical	Solani river catchment (India)
12	10	Blackgram	1	5.66	B	110×10^{-6}	1120-1500	266	humid sub–tropical	Solani river catchment (India)
13	13	Sugarcane	5	25.5	A	110×10^{-6}	1120-1500	266	humid sub–tropical	Solani river catchment (India)
14	13	Sugarcane	3	10.18	A	110×10^{-6}	1120-1500	266	humid sub–tropical	Solani river catchment (India)
15	13	Sugarcane	1	14.9	A	110×10^{-6}	1120-1500	266	humid sub–tropical	Solani river catchment (India)
16	11	Maize	5	10.25	A	110×10^{-6}	1120-1500	266	humid sub–tropical	Solani river catchment (India)
17	11	Maize	3	26.9	A	110×10^{-6}	1120-1500	266	humid sub–tropical	Solani river catchment (India)
18	11	Maize	1	22.05	A	110×10^{-6}	1120-1500	266	humid sub–tropical	Solani river catchment (India)

Table 3.1 (continued)

Watershed/ Plot No.	n	Land use	Slope (%)	*'fc'* (mm/hr)	HSG	Area (m^2)	Rainfall (mm)	Altitude (m)	Climate type	Study location
19	11	Blackgram	5	21.5	A	110	1120-1500	266	humid sub–tropical	Solani river catchment (India)
20	11	Blackgram	3	19.4	A	110	1120-1500	266	humid sub–tropical	Solani river catchment (India)
21	11	Blackgram	1	18.5	A	110	1120-1500	266	humid sub–tropical	Solani river catchment (India)
22	13	Fallow	5	22.92	A	110	1120-1500	266	humid sub–tropical	Solani river catchment (India)
23	11	Fallow	3	7.9	A	110	1120-1500	266	humid sub–tropical	Solani river catchment (India)
24	13	Fallow	1	19.8	A	110	1120-1500	266	humid sub–tropical	Solani river catchment (India)
25	10	Sugarcane	5	2.68	C	110	1120-1500	266	humid sub–tropical	Solani river catchment (India)
26	10	Sugarcane	3	3.5	C	110	1120-1500	266	humid sub–tropical	Solani river catchment (India)
27	10	Sugarcane	1	3.1	C	110	1120-1500	266	humid sub–tropical	Solani river catchment (India)

Table 3.1 (continued)

Watershed/ Plot No.	n	Land use	Slope (%)	'*f*c' (mm/hr)	HSG	Area (m^2)	Rainfall (mm)	Altitude (m)	Climate type	Study location
28	4	Maize	5	2.67	C	110	1120-1500	266	humid sub–tropical	Solani river catchment (India)
29	4	Maize	3	3.96	C	110	1120-1500	266	humid sub–tropical	Solani river catchment (India)
30	4	Maize	1	3.45	C	110	1120-1500	266	humid sub–tropical	Solani river catchment (India)
31	5	Lentil	5	4.24	B	110	1120-1500	266	humid sub–tropical	Solani river catchment (India)
32	5	Lentil	3	5.52	B	110	1120-1500	266	humid sub–tropical	Solani river catchment (India)
33	5	Chana	5	15.22	A	110	1120-1500	266	humid sub–tropical	Solani river catchment (India)
34	5	Chana	3	13.82	A	110	1120-1500	266	humid sub–tropical	Solani river catchment (India)
35	5	Chana	1	5.66	B	110	1120-1500	266	humid sub–tropical	Solani river catchment (India)

n = number of rainfall events; *f*c = infiltration rate mm/hr; HSG = hydrologic soil group

Table 3.2 Characteristics of plots used for P-Q data monitoring during phase 2 of the research project

Watershed/ Plot No.	n	Land use	Slope (%)	*'fc'* (mm/hr)	HSG	Area (m^2)	Rainfall (mm)	Altitude (m)	Climate type	Study location
1	17	Maize	16	26	A	36	1120-1500	266	humid sub–tropical	Solani river catchment (India)
2	17	Maize	12	30	A	36	1120-1500	266	humid sub–tropical	Solani river catchment (India)
3	17	Maize	8	20	A	36	1120-1500	266	humid sub–tropical	Solani river catchment (India)
4	17	Finger millet	16	9	A	36	1120-1500	266	humid sub–tropical	Solani river catchment (India)
5	17	Finger millet	12	23	A	36	1120-1500	266	humid sub–tropical	Solani river catchment (India)
6	17	Finger millet	8	15	A	36	1120-1500	266	humid sub–tropical	Solani river catchment (India)
7	17	Fallow	16	30	A	36	1120-1500	266	humid sub–tropical	Solani river catchment (India)
8	17	Fallow	12	12	A	36	1120-1500	266	humid sub–tropical	Solani river catchment (India)
9	17	Fallow	8	18	A	36	1120-1500	266	humid sub–tropical	Solani river catchment (India)

10	21	Maize	16	22	A	36	1120-1500	266	humid sub–tropical	Solani river catchment (India)
11	21	Maize	12	22	A	36	1120-1500	266	humid sub–tropical	Solani river catchment (India)
12	21	Maize	8	30	A	36	1120-1500	266	humid sub–tropical	Solani river catchment (India)
13	21	Finger millet	16	60	A	36	1120-1500	266	humid sub–tropical	Solani river catchment (India)
14	21	Finger millet	12	26	A	36	1120-1500	266	humid sub–tropical	Solani river catchment (India)
15	21	Finger millet	8	40	A	36	1120-1500	266	humid sub–tropical	Solani river catchment (India)
16	21	Fallow	16	20	A	36	1120-1500	266	humid sub–tropical	Solani river catchment (India)
17	21	Fallow	12	20	A	36	1120-1500	266	humid sub–tropical	Solani river catchment (India)
18	21	Fallow	8	28	A	36	1120-1500	266	humid sub–tropical	Solani river catchment (India)
19	19	Maize	16	6	B	36	1120-1500	266	humid sub–tropical	Solani river catchment (India)

20	19	Maize	12	15	A	36	1120-1500	266	humid sub–tropical	Solani river catchment (India)
21	19	Maize	8	51	A	36	1120-1500	266	humid sub–tropical	Solani river catchment (India)
22	19	Finger millet	16	33	A	36	1120-1500	266	humid sub–tropical	Solani river catchment (India)
23	19	Finger millet	12	10	A	36	1120-1500	266	humid sub–tropical	Solani river catchment (India)
24	19	Finger millet	8	15	A	36	1120-1500	266	humid sub–tropical	Solani river catchment (India)
25	19	Fallow	16	62	A	36	1120-1500	266	humid sub–tropical	Solani river catchment (India)
26	19	Fallow	12	34	A	36	1120-1500	266	humid sub–tropical	Solani river catchment (India)
27	19	Fallow	8	7	A	36	1120-1500	266	humid sub–tropical	Solani river catchment (India)

n = number of rainfall events; *f*c = infiltration rate mm/hr; HSG = hydrologic soil group

Figure 3.1 Rainfall measurement using non recording type raingauge

Table 3.3 Rainfall characteristics during the phase 1 (August 2012–April 2015)

Rainfall depth (mm)	0-10	10-20	20-30	30-40	40-50	50-60	60-70	70-80	>80
No. of events	59	8	13	5	6	4	2	3	0
No. of events generated runoff	5	4	13	5	6	4	2	3	0

Table 3.4 Rainfall characteristics during the phase 2

Rainfall depth (mm)	0-10	10-20	20-30	30-40	40-50	50-60	60-70	70-80	>80
No. of events	31	15	15	8	6	3	3	0	3
No. of events generated runoff	2	15	15	8	6	3	3	0	3

3.2 Runoff measurement

The surface runoff (Q) generated from each plot was collected in the collection chambers. From multi-slot divisor, having 5 numbers of slots, runoff was collected through only one central slot. The remaining runoff through other slots diverted out of the collection chamber. As the collection chamber and conveyance channel are not covered from the top surface, the amount of rainfall collected from the open spaces were deducted from the total runoff

collected. Then, the collected runoff from one slot (after deduction) was multiplied by 5 to get the net total (actual) runoff from the respective plots. For the measurement of the collected runoff, the depth of surface runoff generated by one day (24 hours) natural rainfall event was measured in cm by using steel scale as shown in Figure 3.2 and converted to meter. Then the depth (m) of rainfall of each collection chamber was multiplied by surface area (Phase 1: 1m × 1m; Phase 2: 1.5m × 1.5m) to get volume in cubic meter. The rainfall and runoff depths measured during phase 1 for different plots are shown in appendix A. Similarly, rainfall and runoff depths measured during phase 2 for different plots are shown in appendix B.

Figure 3.2 Runoff depth measurement by metallic measuring scale

3.3 Antecedent soil moisture measurement

The antecedent soil moisture (θ_0) of each plot was measured using soil moisture tester (Fieldscout time domain reflectometry (TDR) 300, having probes of length 20cm) as shown in Figure 3.3a,b. The TDR-300 instrument used in measuring the moisture is shown in Figure 3.4. These observations were taken on daily basis.

Figure 3.3a Figure showing the measurement of soil Moisture Content in sugarcane plot during phase 1

Figure 3.3b Measurement of soil Moisture Content (θ_o) in maize plot during phase 2

Figure 3.4 Time domain reflectometer (TDR- 300) manufactured by "Field Scout" with probe 20 cm.

TDR directly yields volumetric water content (VWC) in percentage. The average value of in-situ moisture content measured in three points as upstream, middle and downstream side of each plot was adopted as antecedent soil moisture content as percentage in terms of volumetric water content. The measurement of soil moisture was proceeded for whole rainy season and remained continued for as and when required after the monsoon. It was necessarily observed the moisture content of the soil before every rainfall event. The previous data soil moisture data for each plot prior to rainfall events is shown in Appendices A and B for phase 1 and phase 2, respectively.

3.4 Infiltration Capacity of the Soil

The infiltration capacity (*f*c) of the soil for each sub-plot was found out by conducting the infiltration test by using double ring infiltrometer as shown in Figure 3.5a,b. The two rings were inserted into the ground maintaining the level and water was applied into both the rings to maintain a constant depth during the observation period. Two concentric rings of 30cm and 45cm diameters and 30cm height were drove into the soil such that about 10 cm was left above the ground. The measurement of the water volume to maintain the constant depth was done on the inner ring only and the respective elapsed time period was measured. The minimum infiltration rate in terms of mm/hr for each case was determined by plotting the infiltration curve. The hydrologic soil group of each plot was then described according to the range of the

minimum infiltration rates. The minimum infiltration rate of each plot with corresponding hydrologic soil is given in the Tables 3.1 and 3.2 for phase 1 and phase 2, respectively.

Figure 3.5a Installation of double ring infiltrometer during phase 1 & Phase 2

Figure 3.5b measuring the water level in double ring infiltrometer while conducting infiltration test during phase1

The infiltration test data measured during phase 1 and phase 2 for different plots are shown in appendix C and D, respectively. Further, to calculate the hydrologic soil group (HSG), the

infiltration capacity (*f*c) values were utilized following criteria given below in Table 3.5 (Hawkins et al. 2009). The HSGs based on *f*c for each plot is shown in Tables 3.1 and 3.2.

Table 3.5 Hydrologic soil group (HSG) based on soil texture and minimum infiltration rate

HSG	Texture	minimum infiltration rate (mm/hr)
A	Sand, Loamy Sand, Sandy Loam	> 7.62
B	Silt Loam or loam	3.81-7.62
C	Sandy clay loam	0.127-3.81
D	Clay loam, Silty clay loam, sandy clay, silty clay or clay	0-0.127

CHAPTER 4
SCS-CN METHODOLOGY

4.1 INTRODUCTION

The Soil Conservation Service Curve Number (SCS-CN) method is one of the most popular method for computing the volume of surface runoff for a given rainfall event from small watersheds. It was developed in 1954 and documented in Section 4 of the National Engineering Handbook (NEH-4) published by the Soil Conservation Service (now called the Natural Resources Conservation Service or NRCS), United State Department of Agriculture (USDA) in 1956. The document has since been revised in 1964, 1965, 1971, 1972, and 1993.

The SCS model is based on a non-linear rainfall-runoff relation that includes a third variable (curve parameter) called the runoff curve number (CN). The curve number is a function of the hydrologic soil type, land use and treatment, ground surface condition and antecedent moisture condition. Of these, the determination of land use and land cover is one of the most important tasks for the estimation of runoff curve number.

The SCS-CN method is well established in hydrologic engineering and environmental impact analysis. The main reason the method has been adopted by most engineers and hydrologists is because of its simplicity and applicability to those watersheds with minimum of hydrologic information: soil type, land use and treatment, ground surface condition, and antecedent moisture condition, incorporating them in a single CN parameter. Since the conventional method was developed for agricultural sites, it works best on these sites, fairly on range sites, and poorly on forest sites.

4.2 EXISTING SCS–CN METHOD

The SCS–CN method was developed based on the water balance equation (Equation 4.1) incorporating two fundamental hypotheses (Equations 4.2 and 4.3).

$$P = Q + F + I_a \tag{4.1}$$

In Equation 4.1, P is the rainfall (mm), Q is the direct surface runoff (mm), I_a is the initial abstraction (mm), and F is the cumulative infiltration (mm).

The first hypothesis equates the ratio of actual amount of direct surface runoff (Q) to the total rainfall (P) (or maximum potential surface runoff) to the ratio of actual infiltration (F) to the amount of the potential maximum retention (S) (Figure 4.1).

$$\frac{Q}{(P - I_a)} = \frac{F}{S} \tag{4.2}$$

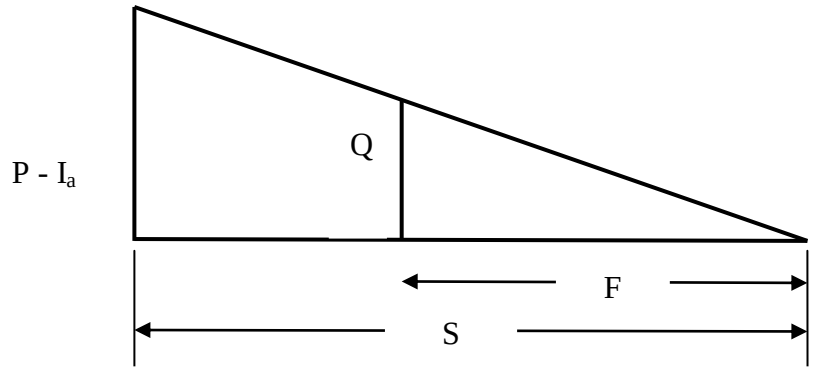

Figure 4.1 Proportionality concept of the existing SCS-CN method

The second hypothesis relates the initial abstraction (I_a) to the potential maximum retention (S).

$$I_a = \lambda S \tag{4.3}$$

In above Equation, S is the potential maximum retention (mm) and λ is the initial abstraction coefficient.

The combination of Equations 4.1 and 4.2 leads to the general form of the SCS–CN method as given below (SCS, 1972):

$$Q = \begin{cases} \dfrac{(P-I_a)^2}{(P+S-I_a)}, & P > I_a \\ 0 & P \le I_a \end{cases} \tag{4.4}$$

The existing version of the SCS–CN method recommended a standard value of λ=0.20 in field applications (SCS 1972, 1985). The research community however pointed out that the standard value of λ = 0.20 is vague and a value of about 0.05 or less is more practical for various parts of world (Baltas et al. 2007; D'Asaro et al. 2014; Fu et al. 2011; Lal et al. 2015; Menberu et al. 2015; Zhou and Lei 2011). For Indian conditions, Central Unit of Soil Conservation Ministry of Agriculture, Government of India (1972) suggested I_a – S relations as: I_a = 0.1S for black soil region with AMC-2 and AMC-3, I_a = 0.2S for black soil region with AMC-1 (watershed soils are dry), and I_a = 0.3S for all other soils.

The use of $I_a = \lambda S$ in Equation 4.4 amplifies it as:

$$Q = \frac{(P-\lambda S)^2}{(P+S-\lambda S)} \text{ for } P > \lambda S\text{; otherwise } Q = 0 \tag{4.5}$$

For λ=0.2, Equation 4.5 reduces to

$$Q = \frac{(P-0.2S)^2}{(P+0.8S)} \text{ for } P > 0.2S\text{; otherwise } Q = 0 \tag{4.6}$$

For a given observed rainfall (P)–runoff (Q) data, S can be calculated by solving Equation 4.5, as follows (Hawkins 1973; Hawkins 1993):

$$S = \frac{\left(\{2\lambda P + (1-\lambda)Q\} - \sqrt{\{2\lambda P + (1-\lambda)Q\}^2 - 4(\lambda P)^2 + 4\lambda^2 QP} \right)}{2\lambda^2} \text{ for } 0 < Q < P \qquad (4.7)$$

Further, for λ=0.2, Equation 4.6 reduces to

$$S = 5[(P + 2Q) - (4Q^2 + 5PQ)^{1/2}] \qquad (4.8)$$

Here, S can vary in the range of $0 \leq S \leq \infty$. Therefore, it can be transformed into CN varying in a more appealing range, $0 \leq CN \leq 100$, and vice versa:

$$CN = \frac{25400}{S + 254} \qquad (4.9)$$

In Equation 4.9, S is in mm and CN is the dimensionless entity.

4.3 FACTORS AFFECTING CURVE NUMBER

The existing SCS-CN method as given in equation 4.6 is a one-parameter model for computing surface runoff from daily storm rainfall. To determine the unknown parameter S, in the above Equation 4.9, a dimensionless curve number (CN) was introduced. Following are the major watershed characteristics that affect the SCS-CN parameter S or curve number (CN).

- Soil type
- Land use/ treatment
- Agricultural management practice
- Hydrologic condition
- Antecedent moisture condition
- Initial abstraction and Climate
- Rainfall intensity and duration, Turbidity etc.

The combination of soil type, vegetation cover and land use/ treatment is referred to as soil-vegetation-land use (SVL) complex (Miller and Cronshey, 1989). These characteristics primarily affect the infiltration potential of a watershed. For a given rainfall amount, the magnitude of Q depends on S or the infiltration potential.

4.3.1 Soli type:

The soil type of a watershed significantly affects the runoff potential of the watershed. Soils are broadly classified as sand, silt and clay on the basis of the grain size. The size of pores in soil mass, depends on the grain sizes, which affects the surface tension and therefore affects infiltration. Other major factors in this category include soil texture, structure, hydraulic conductivity and initial moisture content. Loose conductive sandy soil will have larger

infiltration rate than the tightly packed soil. In the same way, a dry soil will exhibit larger infiltration rate than the wet soil.

The Soil Conservation Service identified four hydrologic groups of soils A, B, C and D, based on their infiltration and transmission rates. The former is measured by the infiltration capacity of the soil whereas the latter refers to the hydraulic conductivity of the soil. The characteristics of various soil groups classified above have been described by Mishra and Singh (2003) as below. The runoff potential increases (and hence curve number increases) as the soil type changes from Group A to Group D.

Group A: The soils falling in Group A exhibit high infiltration rates even when they are thoroughly wetted, high rate of water transmission, and low runoff potential. Such soil include primarily deep, well to excessively drained sand or gravels.

Group B: The soils falling in Group B have moderate infiltration rates when thoroughly wetted and consist primarily of moderately deep to deep, moderately well to well drained soils with fine, moderately fine to moderately coarse textures, for example, shallow loess and sandy loam. These soils exhibit moderate rates of water transmission.

Group C: The soils falling in Group C have low infiltration rates when thoroughly wetted. These soils primarily contain a layer that impedes downward movement of water. Such soils are of moderately fine to fine texture as, for example, clay loams, shallow sandy loam, and soils low in organic content. These soils exhibit a slow rate of water transmission.

Group D: The soils falling in Group D have very low rates of infiltration when they are thoroughly wetted. Such soils are primarily clay soils of high swelling potential, soils with a permanent high water table, soils with a claypan or clay layer at or near the surface, and shallow soils over nearly impervious material. These soils exhibit a very slow rate of water transmission.

This classification is based on the fact that the soils that are similar in depth, organic matter content, structure, and the degree of swelling when saturated will respond in an essentially similar fashion during a storm of excessively high rainfall intensities. The classification based on the minimum infiltration rates is given in the Table 3.5.

4.3.2 Land use:

The land use characterizes the uppermost surface of the soil system and has a definite bearing on infiltration. It describes the watershed cover and includes every kind of vegetation, litter and mulch, and fallow as well as nonagricultural uses, such as water surfaces, roads, roofs, etc.

It affects infiltration. A forest soil, rich in organic matter, allows greater infiltration than a paved one in urban areas. On agriculture land or a land surface with loose soil whose particles

are easily detached by the impact of rainfall, infiltration is affected by the process of rearrangement of these particles in the upper layers such that the pores are clogged leading to reduction in the infiltration rate. The land use and treatment classes can be broadly classified into urban land, cultivated land, and woods and forest. Urban land refers to the areas of low or insignificant permeability. It includes residential areas, paved parking lots, streets and roads, commercial and industrial areas, developing areas, open spaces including lawns, parks etc.

The agriculture land uses are classified as fallow land, row crops, small grain crops, close-seeded legumes or rotation meadow, pasture or range and meadow. Fallow refers to bare agricultural land having the highest runoff potential. Planting the crops in rows on contours increases infiltration and hence decreases runoff.

Woods are usually small isolated grooves of trees raised for farm use. Forest generally covers a considerable part of watershed. Humus increases with age of forest. Because of porous nature, it increases infiltration and hence decreases runoff.

4.3.3 Hydrologic Condition:

The hydrologic condition of an agriculture watershed is defined to be Poor, Fair, and Good on the basis of percent area of grass cover, as shown in the following table. A watershed having larger area of grass cover allows more infiltration and less runoff and this situation of watershed is said to be in good hydrologic condition because it favors the protection of watershed from soil erosion. Similarly, a watershed having lesser area of grass cover can be defined as poor hydrologic condition. The curve number will be the highest for poor, average for fair, and lowest for good hydrologic condition.

Table 4.1 Classification of native pasture or range (Source: SCS, 1971)

S. No.	Vegetation condition	Hydrologic condition
1	Heavily grazed and no mulch or plant cover less than ½ of the area.	Poor
2	Not heavily grazed and plant cover less than ½ to ¾ of the area.	Fair
3	Lightly grazed and plant cover on more than ¾ of the area.	Good

4.3.4 Agricultural management practice:

Agricultural management systems involve different types of tillage (moldboard plough, chisel plough), vegetation, and surface cover. Brakensiek and Rawls (1988) reported that moldboard plough increases soil porosity by 10-20%, depending on the soil texture and increases infiltration rates. It is shown (Rawls, 1983) that an increase in organic matter in the soil lowers

bulk density or increase porosity, and hence increases infiltration and decreases the runoff potential.

4.3.5 Antecedent moisture condition (AMC):

The Soil Conservation Service defines antecedent moisture condition (AMC) as an index of the watershed wetness (Hjelmfelt, 1991). Mishra et al. (2003a, 2004a) defined the AMC as the initial moisture condition of the soil prior to occurrence of rainstorm. If the soil is fully saturated, the whole amount of rainfall is directly converted to runoff without infiltration losses and if the soil is fully dry, it is possible that the rainfall amount is absorbed by the soil, leading to no surface runoff. Thus, the AMC affects the process of rainfall-runoff significantly.

The National Engineering Handbook (SCS, 1971) uses the antecedent 5-days antecedent rainfall for for defining AMC and is generally used in practice. AMC is categorized into three levels: AMC I (dry), AMC II (normal), and AMC III (wet). Where, the AMC I have the lowest runoff potential; AMC II have the average runoff potential; and AMC III have the highest runoff potential. In other words, higher the antecedent moisture, higher will be the CN and the runoff potential of the watershed and vice versa. These dry, wet, and normal conditions of the watershed statistically correspond to respective 90%, 10%, and 50% cumulative probability of exceedance of runoff depth for a given rainfall (Hjelmfelt et al., 1982)

Table 4.2 Antecedent Soil Moisture Conditions (AMC)

AMC	Total 5-days antecedent rainfall (cm)	
	Dormant season	Growing season
I	Less than 1.3	Less than 3.6
II	1.3 to 2.8	3.6 to 5.3
III	More than 2.8	More than 5.3

4.3.6 Initial abstraction and climate:

The initial abstraction consists of interception, surface detention, evaporation, and infiltration. The water held by interception, surface detention, and infiltration at the beginning of a storm finally goes back to atmosphere through evaporation. Thus, the initial abstraction depends on evaporation and since S includes the initial abstraction; S is also affected by evaporation. Evaporation is primarily governed by metrological factors, such as radiation, temperature, humidity, wind, sun-shine hours etc., which describe the climate. Thus, the effect of the climatic condition of the watershed is accounted for the existing SCS-CN method in terms of the initial abstraction. The initial abstraction reduces the runoff potential of the watershed and hence reduces the curve number. The temperature also affects the viscosity of water and affects to the infiltration rate.

4.3.7 Rainfall intensity and duration, Turbidity:

For a given rainfall amount, the runoff will be more in high rainfall intensity and vice versa. It is because if the rainfall amount is constant, the greater the rainfall intensity, the lesser will be the time duration and vice versa. Hence, a greater intensity rainfall yields lesser time for rain water to stay over the land surface, leading to a lesser amount of infiltration and consequently, a greater amount of runoff. Similarly, a longer duration of rainfall will result in a greater amount of infiltration for a given rainfall amount than otherwise.

In reality, a high intensity rainfall breaks down the soil structure to make soil fines move into the soil surface and forms a layer of fine soils which obstruct infiltration, i.e. decreases S or increases CN. This is the reason that a fallow land exposed to raindrop produces higher runoff than does the covered land.

The term turbidity refers to impurities of water that affect infiltration by clogging of soil pores. The contaminated water with dissolved minerals, such as salts, affects the soil structure and consequently, infiltration.

4.4 STATISTICAL ANALYSIS FOR GOODNESS OF FIT

The goodness of fit between observed and predicted variables was evaluated using coefficient of determination (R^2), Nash-Sutcliffe efficiency coefficient (E) (Nash and Sutcliffe 1970), index of agreement (d) (Legates and McCabe 1999) and root mean square error (RMSE), number of times n_t that the observed variability is greater than the mean error (Ritter and Mu˜noz-Carpena 2013), Percent bias (PBIAS), Relative error (Re), and the Bias (e).

The R^2 expressed as:

$$R^2 = \left(\frac{\sum_{i=1}^{n} \left(X_i - \overline{X}\right)\left(Y_i - \overline{Y}\right)}{\left[\sum_{i=1}^{n} \left(X_i - \overline{X}\right)^2 \sum_{i=1}^{n} \left(Y_i - \overline{Y}\right)^2\right]^{0.5}} \right)^2 \qquad (4.10)$$

where $\overline{X}$ (mm) is the average of observed runoff for all storm events Xi, $\overline{Y}$ (mm) is the average of predicted runoff for all storm events Yi, and n is the total number of storm events. The R^2 ranges from 0 to 1 and a value close to 1 signify the better degree of association between the observed and estimated runoff. $R^2 > 0.6$ is considered as acceptable for satisfactory agreement between observed and predicted variables (Moriasi et al. 2007).

The E has been widely used to evaluation of hydrological model (Ajmal et al. 2015a,b,c; Sahu et al. 2007; Yuan et al. 2014). It is expressed as follows:

$$E = \left(1 - \frac{\sum_{i=1}^{n} (X_i - Y_i)^2}{\sum_{i=1}^{n} (X_i - \overline{X})^2} \right) \tag{4.11}$$

The E ranges from -∞ to 1 and a value close to 1 indicates a perfect agreement between the observed and estimated runoff. Its decreasing values indicate poor agreement. The negative value of E can also occur for biased estimate indicating that the mean observed runoff is a better estimate than predicted. According to Motovilov et al. (1999), Moriasi et al. (2007), Parajuli et al. (2007, 2009), 0.75 □ E ≤ 1.0, Very good; 0.65 □ E ≤ 0.75, Good; 0.50 □ E ≤ 0.65, Satisfactory; E ≤ 0.50 indicates an unsatisfactory fit.

The d is expressed as:

$$d = \left(1 - \frac{\sum_{i=1}^{n} (X_i - Y_i)^2}{\sum_{i=1}^{n} \left(|Y_i - \overline{X}| + |X_i - \overline{X}| \right)^2} \right) \tag{4.12}$$

Similar to the interpretation of R^2, d also varies from 0 to 1, with higher values indicating better agreement, and vice versa.

RMSE (Ajmal et al. 2015c; Jain et al. 2006b; Sahu et al. 2007) is defined as:

$$RMSE = \left(\frac{1}{n} \sum_{i=1}^{n} (X_i - Y_i)^2 \right)^{0.5} \tag{4.13}$$

RMSE ranges from 0 to ∞ and a value close to zero indicates perfect fit.

The n_t is expressed as (Ritter and Mu˜noz-Carpena 2013):

$$n_t = \frac{SD}{RMSE} - 1 \tag{4.14}$$

where SD is the standard deviation. $n_t \geq 2.2$ indicates Very Good agreement; $1.2 \leq n_t < 2.2$ implies Good; $0.7 \leq n_t < 1.2$ shows Satisfactory; and $n_t < 0.7$ indicates an unsatisfactory fit.

The PBIAS measures average tendency of the estimated data to be larger or smaller than their observed data (Ajmal et al. 2015c; Moriasi et al. 2007). It is expressed as:

$$PBIAS = \left[\frac{\sum_{i=1}^{n} (X_i - Y_i) \times 100}{\sum_{i=1}^{n} X_i} \right] \tag{4.15}$$

PBIAS indicates the method to be consistently over-predicting or under-predicting. Its positive values indicate model underestimation, and negative values overestimation (Moriasi et al. 2007; Yuan et al. 2014). For perfect agreement, PBIAS = 0. According to Moriasi et al. 2007, PBIAS < ±10% indicates Very Good fit; ±10% ≤ PBIAS < ±15%, Good; ±15% ≤ PBIAS < ±25%, Satisfactory; and PBIAS ≥ ±25%, unsatisfactory.

The Re is used to measure the average difference between observations and model simulations of variable Q.

$$\text{Re}=\left|\frac{\sum_{i=1}^{n}(X_i - Y_i)}{\sum_{i=1}^{n} X_i}\right| \tag{4.16}$$

The e is a measure of the systematic error and is calculated as the average difference between the predicted and measured values of a random variable as follows:

$$\text{e} = \frac{\sum_{i=1}^{n}(Y_i - X_i)}{n} \tag{4.17}$$

The bias indicates the amount that a method consistently over predicts or under predicts the Q-value.

This study compares various versions of the same kind of formulae, and therefore, to evaluate the improvement in performance efficiency of the modified model (or best model) over the other one, the r^2–statistic as given in Equation 4.18 is used. It was recommended by Nash and Sutcliffe (1970) and used by Ajmal et al. 2015d; Ajmal et al. 2016; Lal et al. (2017) and Senbeta et al. (1999) in their researches.

$$r^2 = \frac{E_2 - E_1}{1 - E_1} \times 100 \tag{4.18}$$

where E_1 and E_2 are respectively the efficiencies due to the existing and the proposed formulae. r^2 > 10% indicates the significant improvement of the proposed relations over the existing one (Senbeta et al. 1999).

CHAPTER 5

DETERMINATION OF CURVE NUMBER

The eight different Curve Number (CN) estimation methods from available P–Q data have been used for comparison and these are detailed below.

5.1 DETERMINATION OF CURVE NUMBER FROM OBSERVED P-Q DATA

5.1.1 Storm event method

In this method, natural P-Q data set is used to derive event wise CN using standard Equations 4.8 and 4.9. The mean of all event wise CNs was considered as representative CN correspond to the average antecedent moisture condition (AMC-2) of the plot (Bonta 1997). In the present study, representative mean CN method is designated as M1.

5.1.2 Least square fit method

Based on the observed P–Q data, the only parameter S (or CN) was estimated using least square fit minimizing the sum of squares of residuals (Equation 5.1) (Hawkins et al. 2002) employing Microsoft Excel (solver):

$$\sum_{i}^{n}(Q_i - Q_{ci})^2 = \sum\left\{Q_i - \left[\frac{(P-0.2S)^2}{(P+0.8S)}\right]\right\}^2 \Rightarrow \text{Minimum} \tag{5.1}$$

where Q_{ci} (mm) and Q_i (mm) are the respectively predicted and observed runoff for rainfall event i, n is the total number of rainfall events. Here, the least square fit CN method is designated as M2.

5.1.3 Geometric mean method

The step wise procedure for deriving the CN (AMC-2) using geometric mean method is given below (Hawkins et al. 2009; Tedla et al. 2012):

i. Derive the event wise S using standard Equation 4.8.
ii. Take the Logarithm of the events S (i.e. log S).
iii. Find the arithmetic mean of the log S series.
iv. Estimate the geometric mean (GM) of the S (S_{GM}) by taking the antilogarithm of the mean of log S (i.e. $S_{GM} = 10^{\log S}$).
v. Calculate the geometric mean CN as given below:
   $CN_{GM} = 25400/(254 + 10^{\log S})$.

The Geometric mean CN method is designated as M3.

5.1.4 Log-normal frequency method

In this method, the logarithms of each set of natural P and Q pair were computed individually. The value of S was then calculated by employing Equation 4.8 using mean log P and log Q values (Schneider and McCuen, 2005). Finally, the representative CN (AMC-2) value for plot was computed using Equation 4.9. Here, this method is designated as M4.

5.1.5 NEH-4 median method

This method is traditionally recommended by SCS (SCS 1972; Hawkins et al. 2009), in which the median of event wise CN derived using standard Equations 4.8 and 4.9 was considered as representative CN of plot. Here, the median CN method is designated as M5.

5.1.6 Rank-Order method

This method requires ordered series of P–Q pairs (Hawkins et al. 2009). The naturally measured P and Q values were sorted separately and then realigned by common rank order basis to form a new set of P–Q pairs of the equal return period, in which runoff Q is not necessarily matched with the original rainfall P (D'Asaro and Grillone 2012; Hawkins et al. 2009; Soulis and Valiantzas 2013). For each ordered P–Q pair, S and CN were determined employing Equations 4.8 and 4.9, respectively. The representative CN (AMC-2) of the plot is mean or median of the event wise CNs series computed with the ranked P–Q pairs. Here, mean and median are designated as method M6 and M7, respectively.

In method M1 to M7, the AMC was decided based on the 5-day antecedent rainfall (P5). In order to determine AMC of a rainfall event used in runoff prediction, P_5 was used as follows: AMC-1 if $P_5 < 35.56$ mm in growing season or $P_5 < 12.7$ mm in dormant season, AMC-2 if $35.56 \leq P_5 \leq 53.34$ mm in growing season or $12.70 \leq P_5 \leq 27.94$ mm in dormant season, and AMC-3 if $P_5 > 53.34$ mm in growing season or $P_5 > 27.94$ mm in dormant season (Ajmal et al. 2015a,b,c; Mays 2005).

For wet (CN_3) and dry (CN_1) conditions curve number, the CN_2 (AMC-2) values were adjusted using Equations 5.2 and 5.3, respectively, as given by Hawkins et al. (1985).

$$CN_3 = \frac{CN_2}{0.427 + 0.00573 CN_2} \tag{5.2}$$

$$CN_1 = \frac{CN_2}{2.281 - 0.01281 CN_2} \tag{5.3}$$

5.1.7 S-probability method

For each set of natural P–Q pair, the value of S (or CN) is determined using Equations 4.8 and 4.9. The Weibull's plotting position was then used to derive the lognormal probability distribution for the calculated values of S. The S values corresponding to 90, 50 and 10%

probability levels were used to estimate the representative CN values for AMC-3, AMC-2 and AMC-1, respectively (Hjelmfelt 1980; Hjelmfelt 1991; Ali and Sharda 2008). Here, this method is designated as M8.

5.2 COMPARISON OF CN VALUES ESTIMATED FROM P-Q DATA

The results of estimated CNs using eight different methods are shown in Table 5.1. The box plot showing the CN estimated by methods M1-M8 is given in Figure 5.1. As seen, the CNs estimated by least squares fit (M2) method range from 45.12 (plot 35) to 95.30 (plot 28). The CNs estimated by traditionally recommended NEH-4 median (M5) method range from 72.26 (plot 34) to 95.55 (plot 28). In general, the CNs estimated by geometric-mean (M3) method are usually larger (17 of 36 plots) followed by S-probability (M8) (15 of 36 plots). Based on overall mean (mean of representative CNs of 36 plot), M2 was found to estimate the lowest CNs among all methods. In contrast, M8 method estimated larger CNs. The multiple comparison results of CNs estimated by all the eight methods is shown in Table 5.2. Based on the Kruskal–Wallis test analysis, mix results were obtained. There was no single method which has produced significantly higher (or lower) CNs than other. Method M3 produced significantly ($p < 0.05$) higher CNs than M2 and M4, but it was statistically insignificant with others (i.e. M1, M5, M6, M7, M8). Similarly, M2 produced significantly lower CNs than other methods except M4. The CNs estimated by M1, M3, M5, M6, M7 and M8 were statistically insignificant among each other.

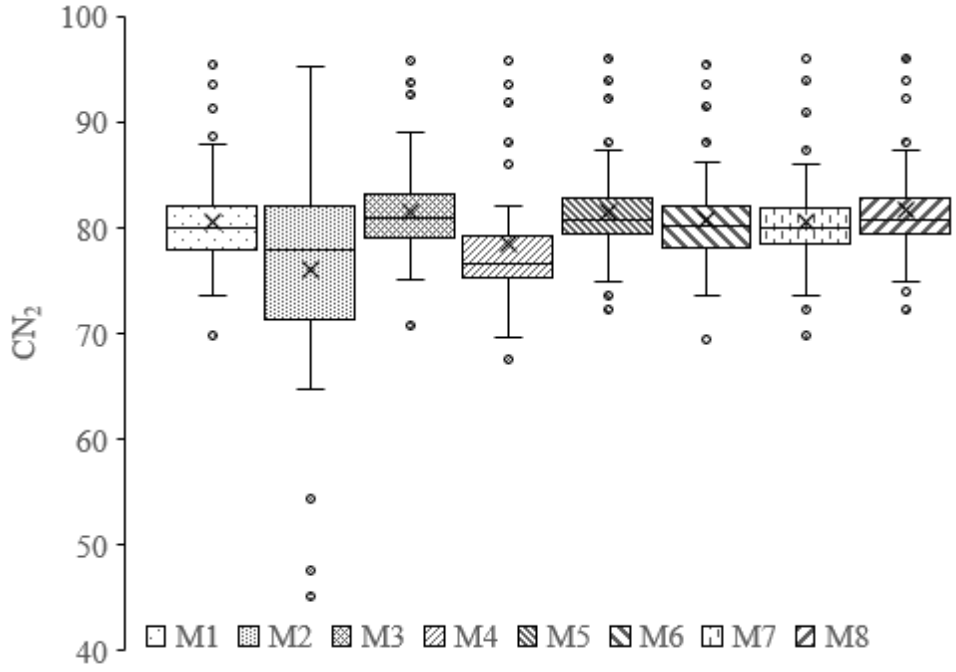

Figure 5.1 Box plot showing the CN estimated by methods M1-M8.

Table 5.1 Estimated curve numbers using eight different methods for 36 agricultural plots of varying characteristics. n = No. of events.

Plot No.	n	Curve Number (AMC-2) estimation method							
		M1	M2	M3	M4	M5	M6	M7	M8
1	15	80.61	79.93	81.42	77.77	81.24	80.79	81.24	81.24
2	15	79.47	80.09	80.75	76.00	79.88	79.74	79.71	79.88
3	15	81.27	81.51	82.69	76.39	81.09	81.60	81.37	81.09
4	10	78.49	75.05	79.15	75.97	78.08	78.58	79.06	78.08
5	10	80.10	75.52	81.13	75.24	79.21	80.19	79.07	79.21
6	10	74.64	70.87	75.22	72.24	77.75	74.64	73.60	77.75
7	10	82.10	82.19	82.73	76.10	80.88	82.18	81.86	80.88
8	10	80.31	80.24	80.61	75.62	79.77	80.33	79.22	79.77
9	10	83.46	84.81	84.14	77.95	81.49	82.44	84.13	81.49
10	10	81.12	82.06	81.92	76.65	79.77	81.30	81.65	79.77
11	10	78.87	78.38	79.59	75.23	79.16	79.02	79.72	79.16
12	10	79.26	78.95	80.49	75.36	80.28	79.47	80.28	80.28
13	13	79.38	74.49	80.18	79.05	79.83	79.46	80.10	79.83
14	13	82.71	78.50	84.27	82.13	83.65	82.96	83.76	83.65
15	13	81.10	76.05	82.21	80.88	84.48	81.25	80.88	84.48
16	11	80.17	77.97	81.14	78.01	81.52	80.21	79.88	81.52
17	11	78.79	75.49	79.53	76.35	80.02	78.87	78.47	80.02
18	11	81.92	82.26	83.34	79.00	82.47	82.04	81.50	82.47
19	11	76.53	64.73	77.59	76.15	79.44	80.98	79.65	79.44
20	11	80.06	73.07	81.17	79.44	81.72	80.20	80.94	81.72
21	11	80.78	77.88	82.41	78.76	79.65	80.98	79.65	79.65
22	13	77.89	69.61	79.15	77.76	83.07	78.01	80.01	83.07
23	11	77.94	68.90	79.64	74.19	81.66	73.81	72.75	81.66
24	13	78.34	70.59	79.62	78.10	81.42	78.45	78.64	81.42
25	10	91.36	90.33	92.60	91.92	92.35	91.55	91.02	92.35
26	10	87.99	86.84	88.75	88.11	88.10	88.17	87.97	88.10
27	10	85.95	84.62	86.83	85.97	86.29	86.20	86.00	86.29
28	4	95.55	95.30	95.81	95.76	95.95	95.55	95.96	95.95

Table 5.1 (Continued)

Plot No.	n	Curve Number (AMC-2) estimation method							
		M1	M2	M3	M4	M5	M6	M7	M8
29	4	93.60	93.49	93.81	93.56	93.95	93.59	93.95	93.95
30	4	88.63	88.89	89.01	88.23	87.44	88.63	87.44	87.44
31	5	77.96	66.70	79.11	76.61	79.80	78.12	77.22	79.80
32	5	74.25	73.57	75.37	69.62	75.28	74.38	73.82	75.28
33	5	74.44	47.61	75.41	74.05	75.00	74.48	75.00	75.00
34	5	69.79	54.35	70.70	67.58	72.26	69.46	69.91	72.26
35	5	73.68	45.13	75.04	70.11	80.55	73.55	72.23	80.55
36	40	74.05	72.87	75.09	72.23	73.69	74.15	73.90	73.90

Table 5.2 Comparison of CN determination methods based on the Kruskal–Wallis test. n = No. of events.

Method	CN	n
M1	80.63 a	36
M2	76.08 b	36
M3	81.60 a	36
M4	78.45 c, b	36
M5	81.62 a	36
M6	80.70 a	36
M7	80.60 a	36
M8	81.62 a	36

Note: variables with no letter (alphabet, a, b, c) in common have been significantly different CN at 0.05 significance level (based on the Kruskal–Wallis test), (n is the number of rainfall events).

5.3 PERFORMANCE EVALUATION OF M1-M8 METHOD IN RUNOFF ESTIMATION

In order to judge the runoff estimation accuracy of CNs estimated by various methods used in this study, the runoff was estimated for the 1-24 plots' datasets. The plots 25-36 were excluded from the analysis due to unavailability of P_5 data. The standard SCS-CN procedure was followed to estimate the runoff. The Box and Whisker plots for plot wise E, RMSE, e and d are shown in Figures 5.2-5.5, respectively.

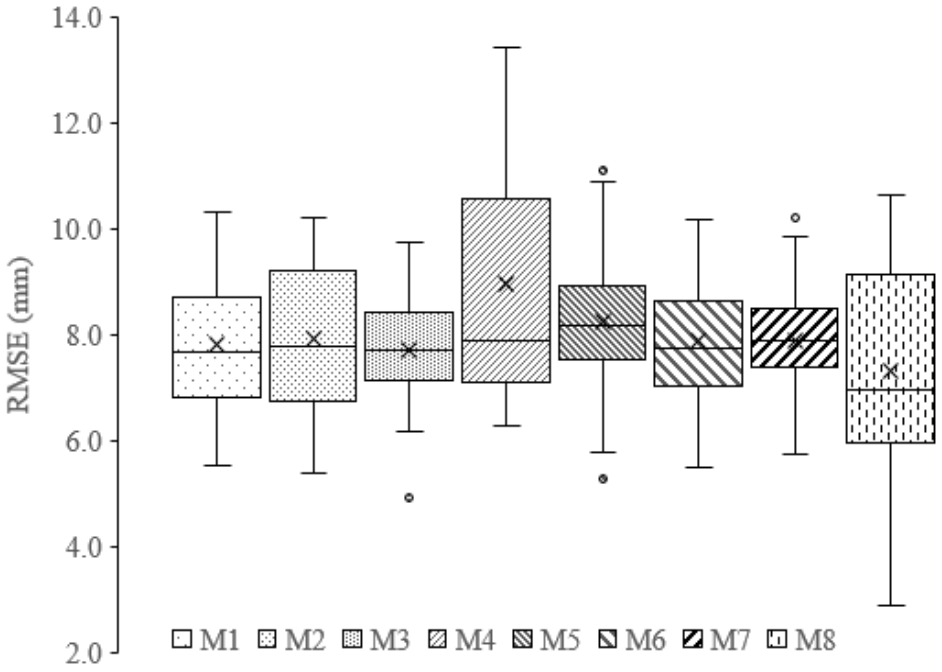

Figure 5.2 Box and Whisker plot showing the RMSE obtained by methods M1-M8

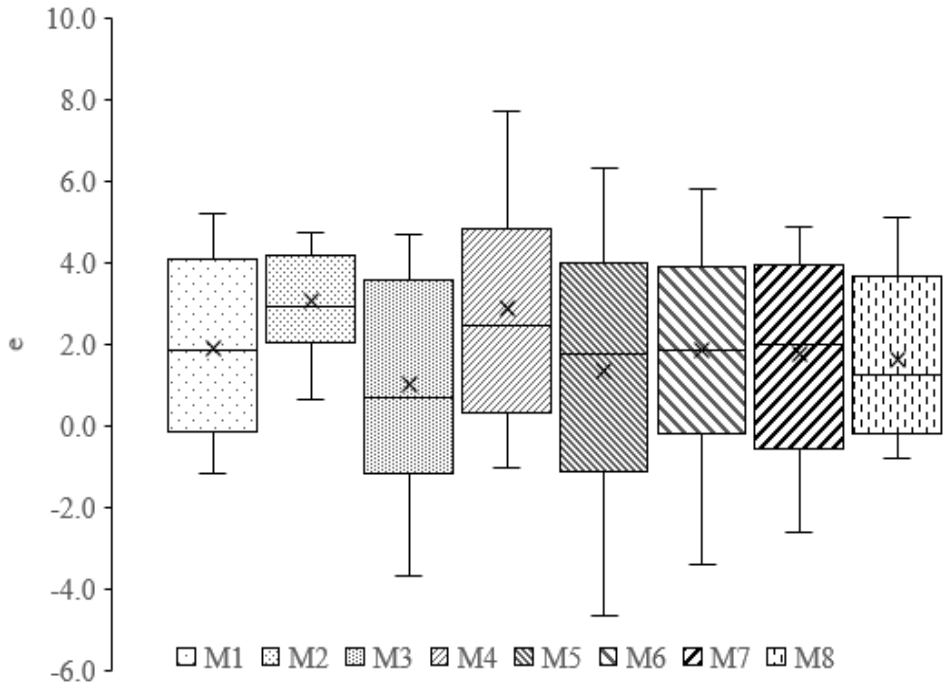

Figure 5.3 Box and Whisker plot showing the bias (e) obtained by methods M1-M8

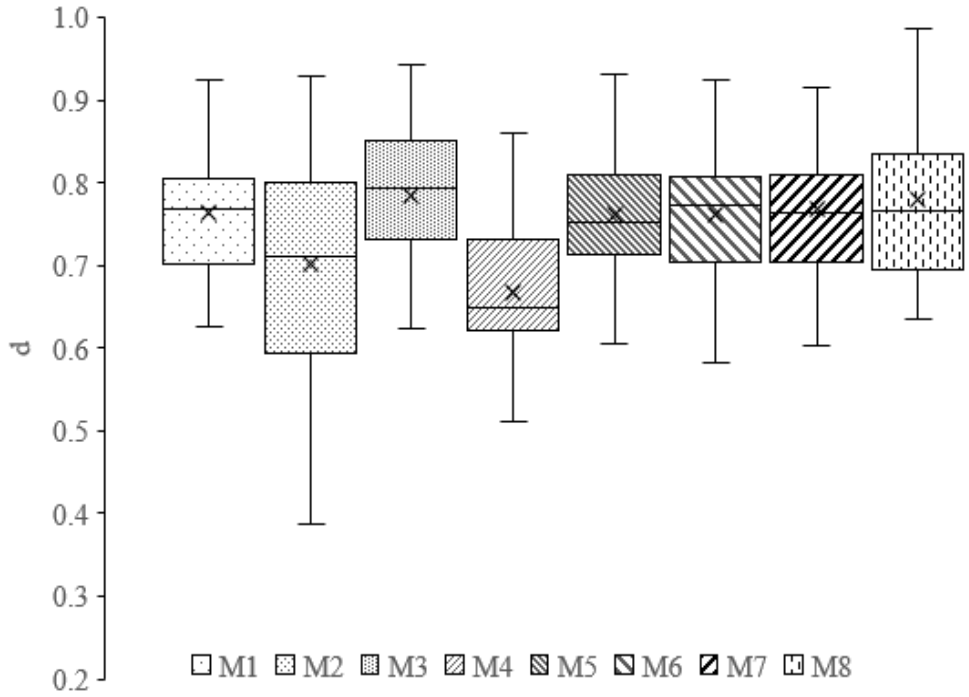

Figure 5.4 Box and Whisker plot showing the d obtained by methods M1-M8

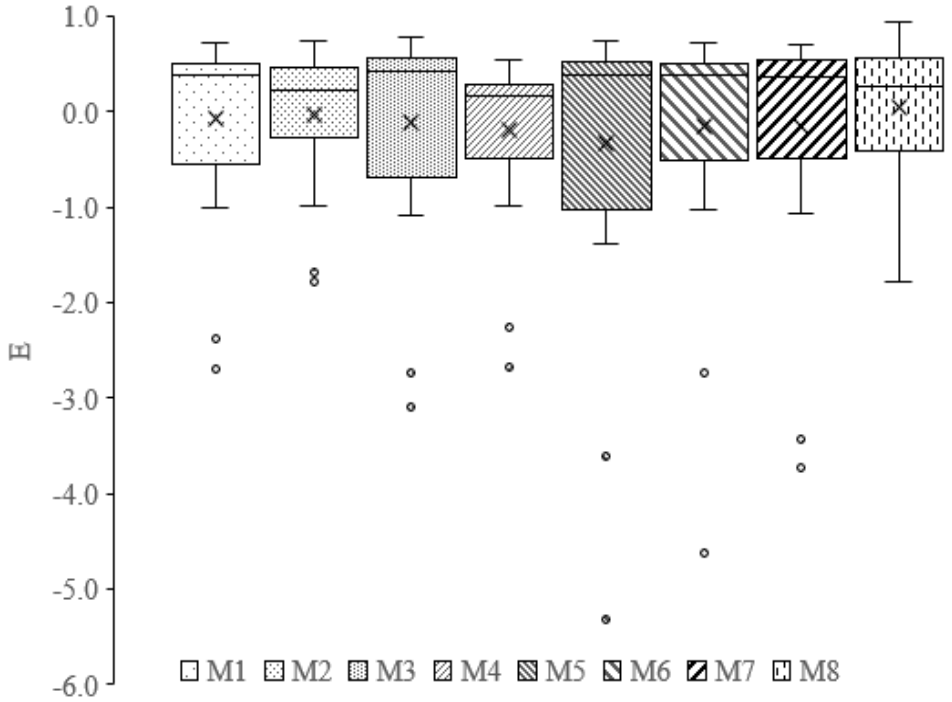

Figure 5.5 Box and Whisker plot showing the E obtained by methods M1-M8

Table 5.3 shows the mean values of E, RMSE, e and d from all the 24 plots for the runoff estimation using the CNs estimated by M1-M8 methods. Considering the cumulative mean value of RMSE as a yardstick of evaluation, the performance of eight method was as follows:

M8 > M3 > M1 > M7 > M6 > M2 > M5 > M4.

For further analyses based on the mean values of d, the M3 was found to perform superior followed by M8. Similarly, based on mean values of E, M8 performance was good whereas M5 performed poorest. The model performance based on E was as follows:

M8 > M2 > M1 > M3 > M7 > M6 > M4 > M5.

Table 5.4 Comparison of runoff estimation using eight different curve number determination methods for 24 plots datasets.

	M1	M2	M3	M4	M5	M6	M7	M8
	RMSE (mm)							
Maximum	10.303	10.211	9.746	13.429	11.106	10.189	10.200	10.631
Mean	7.834	7.915	7.716	8.953	8.247	7.909	7.895	7.307
Minimum	5.545	5.377	4.911	6.269	5.276	5.483	5.759	2.880
	Index of agreement (d)							
Maximum	0.923	0.929	0.944	0.860	0.932	0.925	0.916	0.986
Mean	0.764	0.703	0.784	0.667	0.761	0.762	0.761	0.779
Minimum	0.626	0.387	0.623	0.512	0.606	0.582	0.603	0.635
	Bias (mm)							
Maximum	5.186	4.733	4.713	7.727	6.333	5.813	4.897	5.130
Mean	1.896	3.043	1.041	2.873	1.328	1.856	1.783	1.617
Minimum	-1.162	0.666	-3.674	-1.021	-4.643	-3.387	-2.606	-0.779
	E							
Maximum	0.724	0.741	0.784	0.545	0.750	0.730	0.703	0.950
Mean	-0.068	-0.024	-0.111	-0.195	-0.324	-0.159	-0.158	0.052
Minimum	-2.705	-1.791	-3.094	-2.671	-5.319	-4.628	-3.726	-1.791

As shown in Table 5.3, the variation in the mean bias values by different methods was varies from 1.041 mm (for M3) to 3.043 (for M2). The performance of different methods based on Bias criteria can be described as:

M3 > M5 > M8 > M7 > M6 > M1 > M4 > M2.

The results from the present analysis show that there is no single method which could perform well based on all the above four goodness of fit criteria. However, either M3 or M8 can be considered as good among all based on individual goodness of fit criteria.

For evaluating the overall performance, the methods were ranked based on the mean statistics viz. d, RMSE, Bias and E. To this end, a rank of 1-8 was assigned to show the RMSE, Bias from lowest to highest, and d and E from highest to lowest. After assigning of ranks, corresponding marks of 8 to 1 are given to each index. For example, a method having the minimum RMSE, Bias, and maximum d, E will be ranked 1. The method corresponding to rank 1 will be achieved to score 8 marks. The overall performance of method was judged based on the total marks gained by method using all four statistics. The first rank will be given to the method scoring highest marks whereas last rank (i.e. eight) will be given to method scoring lowest marks. Table 5.4 shows the ranks and marks achieved by all methods for their respective performance indices. As seen from this table, M8 performed best followed by M3. Based on overall score the methods performance can be described as follows:

M8 > M3 > M1 > M7 > M6 > M2 > M5 > M4

5.4 COMPARISON BETWEEN NEH-4 TABLE'S AND OBSERVED P–Q DATA-BASED CURVE NUMBERS

One of the aims of the present study was to investigate the applicability of NEH-4 CN values to Indian watersheds, which are otherwise based on a large P-Q dataset of a number of small US watersheds. Therefore, in order to check the suitability of NEH–4 tables CN (CN_{HT}) for agricultural plots of study region, the P–Q data based CNs determined by NEH–4 median and least square fit methods were compared with CN_{HT}. The NEH–4 median CNs (CN_m) were estimated using the procedures given in previous section 5.1.5 for method M5. Further, the least square fit CNs were also estimated by two different approaches. In the first approach (i.e. single way fitting), the only parameter S (or CN) was estimated using least square fit minimizing the sum of squares of residuals as given in Equation 5.1. Notably, each P:Q dataset yields only one value of S, i.e. only one representative value of S (or CN) for a plot. This CN value of a plot is designated as CN_{LSM}. In the second approach (i.e. double way fitting), the parameter S is determined by iterative least squares fitting (or best fit) procedure for both λ and S of the SCS-CN equation (Equation 5.4), consistent with the work of Hawkins et al. (2002).

Table 5.4 Performance evaluation of models based on ranks (scores)

Performance indices and their ranks (scores)										
Method	RMSE (mm)	Rank (score)	d	Rank (score)	Bias (mm)	Rank (score)	NSE	Rank (score)	Total score	Overall Rank
M1	7.834	3 (6)	0.764	3 (6)	1.896	6 (3)	-0.068	3 (6)	21	3
M2	7.915	6 (3)	0.702	7 (2)	3.043	8 (1)	-0.024	2 (7)	13	6
M3	**7.716**	**2 (7)**	**0.784**	**1(8)**	**1.041**	**1 (8)**	**-0.111**	**4 (5)**	**28**	**2**
M4	8.953	8 (1)	0.667	8 (1)	2.873	7 (2)	-0.195	7 (2)	6	8
M5	8.247	7 (2)	0.761	6 (3)	1.328	2 (7)	-0.324	8 (1)	13	7
M6	7.909	5 (4)	0.761	4 (5)	1.856	5 (4)	-0.159	6 (3)	16	5
M7	7.895	4 (5)	0.761	5 (4)	1.783	4 (5)	-0.158	5 (4)	18	4
M8	**7.307**	**1 (8)**	**0.779**	**2 (7)**	**1.617**	**3 (6)**	**0.052**	**1 (8)**	**29**	**1**

The objective of the fitting is to find the values of λ and S such that the following is a minimum:

$$\Sigma_{i=1}^{n}(X_i - Y_i)^2 = \Sigma\left\{X_i - \left[\frac{(P-\lambda S)^2}{(P+(1-\lambda)S)}\right]\right\}^2 \Rightarrow \text{Minimum} \quad (5.4)$$

where Y_i (mm) and X_i (mm) are respectively the predicted and observed runoff for storm event i, and n is the total number of storm events. Here also, each P:Q dataset yields only one value of S, i.e. only one representative value of S (or CN) for a plot. This CN value of a plot is designated as CN_{LS}.

In two of the above least square fit approaches, both natural and ordered data series were used to fit the CNs. For approach first (i.e. single way fitting), these CN values of a plot are designated as CN_{LSMn} and CN_{LSMo} for natural and ordered datasets, respectively. On the other hand, CN values of a plot are designated as CN_{LSn} and CN_{LSo} for natural and ordered datasets, respectively for approach two (i.e. double way fitting). The natural P–Q data consists of the actually observed dataset. In ordered data series, the observed P and Q values were first sorted separately and then realigned by common rank-order basis to form a new set of P–Q pairs of equal return period, in which runoff Q is not necessarily matched with that due to original rainfall P (Ajmal et al. 2015a; D'Asaro and Grillone 2012; Hawkins 1993; Hawkins et al. 2009; Lal et al. 2015; Soulis and Valiantzas 2013). Here, it is noted that only large storm events with P >10 mm were used to avoid the biasing effects of small storms towards high CNs. For statistical analysis, only plots having more than 10 rainfall–runoff events were considered for λ and CN calculation.

The CN values (CN_{HT}, CN_m, CN_{LSMn}, CN_{LSMo}, CN_{LSn}, and CN_{LSo}) thus estimated are taken to correspond to the average antecedent moisture condition (AMC-2) of the plot. For wet (CN_3) and dry (CN_1) conditions curve number, the CN_2 (AMC-2) values were adjusted using Equations 5.2 and 5.3, respectively.

The CN_{HT} and P-Q based CNs i.e. CN_m, CN_{LSn}, CN_{LSo}, CN_{LSMn}, CN_{LSMo} estimated for 27 plots are shown in Table 5.5. As seen, CN_{HT} ranged from 58 (plots 19, 20, and 21) to 88 (plots 25, 26, and 27). The optimized values of CN_{LSMn} ranged respectively from 64.73 (plot 19) to 90.33 (plot 25), and CN_{LSMo} from 67.47 to 90.59 for ordered dataset. Whereas the optimized values of CN_{LSn} ranged respectively from 38.72 (plot 19) to 85.36 (plot 25), and CN_{LSo} from 42.16 to 87.12 (plot 10) for ordered dataset. Similarly, CN_m were ranged from 77.75 to 92.35. The box plot of these CNs is shown in Figure 5.6. As seen from this figure, the CN_{LSMn}, CN_{LSMo} and CN_m values were higher than CN_{HT}.

The Comparison of CN_{HT} with CN_m, CN_{LSn}, CN_{LSo}, CN_{LSMn}, CN_{LSMo} are shown in Figures 5.7-5.11 respectively. From Figure 5.7, it is seen that the comparison between CN_{HT} and CN_m is less than satisfactory. Furthermore, CN_m obtained by traditional median method assume high values compared to CN_{HT} and the discrepancy increases for CNs below 75. Most of the CN_m values (24 out of 27) were greater than the CN_{HT} values, consistent with those reported in literature (D'Asaro et al. 2014; Hawkins and Ward 1998). The group of CN_{HT} lower than 80 was found to observed high amount of bias (e = -11.38 CN) as compare to (e =0.89 CN) group of CN_{HT} higher than 80.

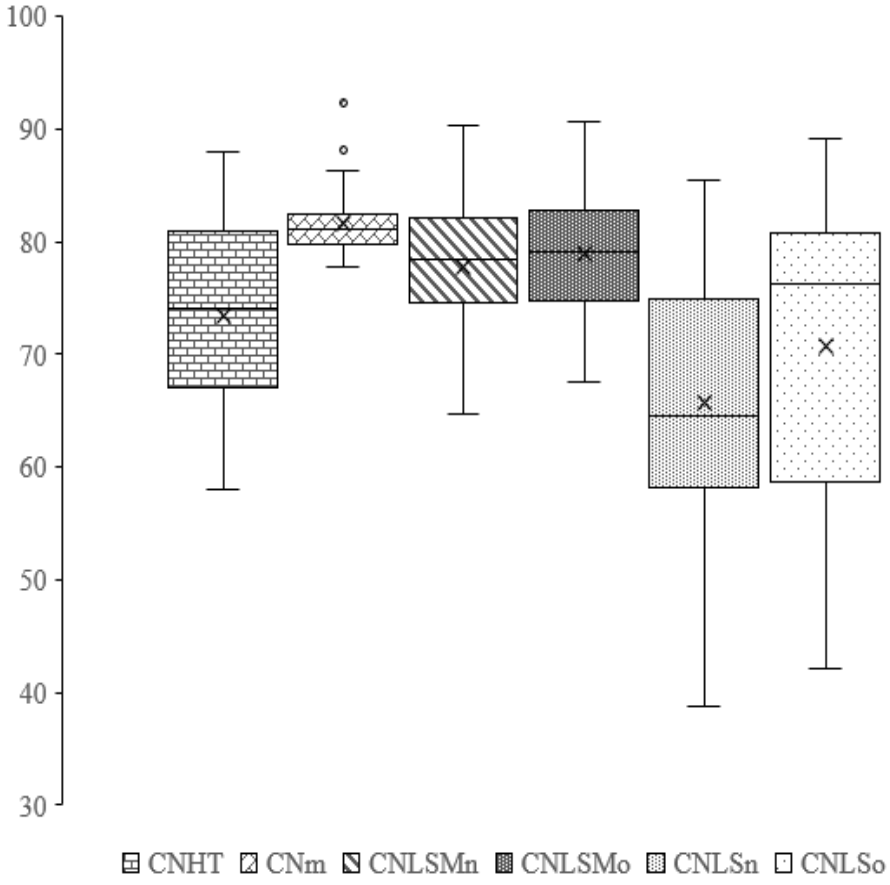

Figure 5.6 Box and Whisker plot showing the comparison among tabulated and observed P-Q data based CNs

Table 5.5 Summary of runoff plot characteristics and CN values derived using NEH-4 median, Least-Squares fit method (LSM) and Handbook tables (Used partial dataset excluding P<15 mm)

Plot No.	Land use	n	NEH-4 Table	NEH-4 method (natural data, λ=0.20)	LSM (λ=0.20)		LSM (Optimized λ)			
					Natural	Ordered	Natural data		Ordered data	
			CN_{HT}	CN_m	CN_{LSMn}	CN_{LSMo}	CN_{LSn}	λ	CN_{LSo}	λ
1	Sugarcane	15	81	81.24	79.93	81.01	70.79	0.0334	81.87	0.2276
2	Sugarcane	15	72	79.88	80.09	81.41	77.00	0.1244	89.17	0.6590
3	Sugarcane	15	81	81.09	81.51	82.75	70.30	0.0002	80.23	0.1267
4	Fallow	10	76	78.08	75.05	76.16	62.61	0.0204	80.74	0.3513
5	Fallow	10	85	79.21	75.52	76.99	59.91	0.000	66.61	0.0245
6	Fallow	10	76	77.75	70.87	71.94	60.86	0.0631	76.63	0.3174
7	Maize	10	78	80.88	82.19	82.46	74.91	0.0314	76.17	0.0455
8	Maize	10	78	79.77	80.24	80.39	80.49	0.2079	80.98	0.2192
9	Maize	10	85	81.49	84.81	85.04	81.89	0.0999	83.60	0.1443
10	Blackgram	10	66	79.77	82.06	82.83	79.07	0.1141	87.13	0.4213
11	Blackgram	10	66	79.16	78.38	79.16	73.13	0.0879	79.09	0.1966
12	Blackgram	10	77	80.28	78.95	80.01	69.93	0.0328	77.81	0.1412

Table 5.5 (Continued)

Plot No.	Land use	n	NEH-4 Table	NEH-4 method (natural data, λ=0.20)	LSM (λ=0.20)		LSM (Optimized λ)			
					Natural	Ordered	Natural data		Ordered data	
			CN_{HT}	CN_m	CN_{LSMn}	CN_{LSMo}	CN_{LSn}	λ	CN_{LSo}	λ
13	Sugarcane	13	67	79.83	74.49	74.74	56.94	0.0003	57.21	0.0000
14	Sugarcane	13	67	83.65	78.5	79.72	64.47	0.0000	67.69	0.0000
15	Sugarcane	13	67	84.48	76.05	77.10	61.23	0.0002	62.22	0.0000
16	Maize	11	67	81.52	77.97	78.59	62.39	0.0000	64.06	0.0000
17	Maize	11	67	80.02	75.49	75.94	58.13	0.0001	58.65	0.0001
18	Maize	11	67	82.47	82.26	82.92	70.93	0.0000	75.77	0.0415
19	Blackgram	11	58	79.44	64.73	67.47	38.72	0.0000	42.16	0.0000
20	Blackgram	11	58	81.72	73.07	74.79	55.95	0.0000	56.11	0.0000
21	Blackgram	11	58	79.65	77.88	78.96	61.92	0.0000	64.30	0.0000
22	Fallow	13	74	83.07	69.61	71.43	46.21	0.0000	51.12	0.0001
23	Fallow	11	74	81.66	68.90	72.23	45.80	0.0000	55.11	0.0001
24	Fallow	13	74	81.42	70.59	73.76	51.79	0.0000	54.66	0.0001
25	Sugarcane	10	88	92.35	90.33	90.59	85.36	0.0000	85.97	0.0000
26	Sugarcane	10	88	88.10	86.84	87.19	79.03	0.0000	79.88	0.0000

Table 5.5 (Continued)

Plot No.	Land use	n	NEH-4 Table	NEH-4 method (natural data, λ=0.20)	LSM (λ=0.20)		LSM (Optimized λ)			
					Natural	Ordered	Natural data		Ordered data	
			CN_{HT}	CN_m	CN_{LSMn}	CN_{LSMo}	CN_{LSn}	λ	CN_{LSo}	λ
27	Sugarcane	10	88	86.29	84.62	85.27	74.56	0.0000	76.17	0.0000
	Statistics									
	Mean		73.44	81.64	77.83	78.92	65.72	0.0302	70.78	0.1080
	Median		74.00	81.09	78.38	79.16	64.47	0.0001	76.17	0.0001
	Standard deviation		9.12	3.17	5.85	5.27	11.93	0.0527	12.68	0.1665
	Maximum		88.00	92.35	90.33	90.59	85.39	0.2079	89.17	0.6590
	Minimum		58.00	77.75	64.73	67.47	38.72	0.0000	42.16	0.0000
	Skewness		0.00	1.90	-0.15	0.00	-0.41	2.0189	-0.51	1.8609

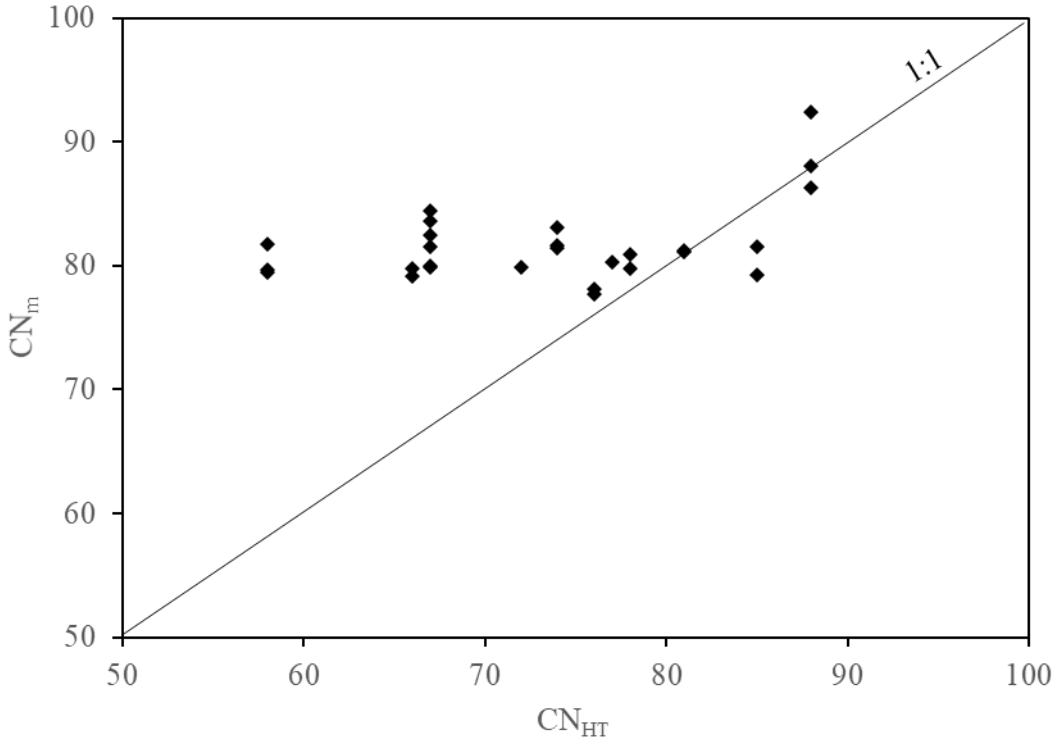

Figure 5.7 CN Plot for comparison between CN_m and CN_{HT}

As shown in Figures 5.8 and 5.9, the comparison between CN_{HT} and CN_{LS} is also poor for both natural and ordered datasets. In general, CN_{HT} values are higher than CN_{LS} and the difference is larger for CN values varying from 68-78.

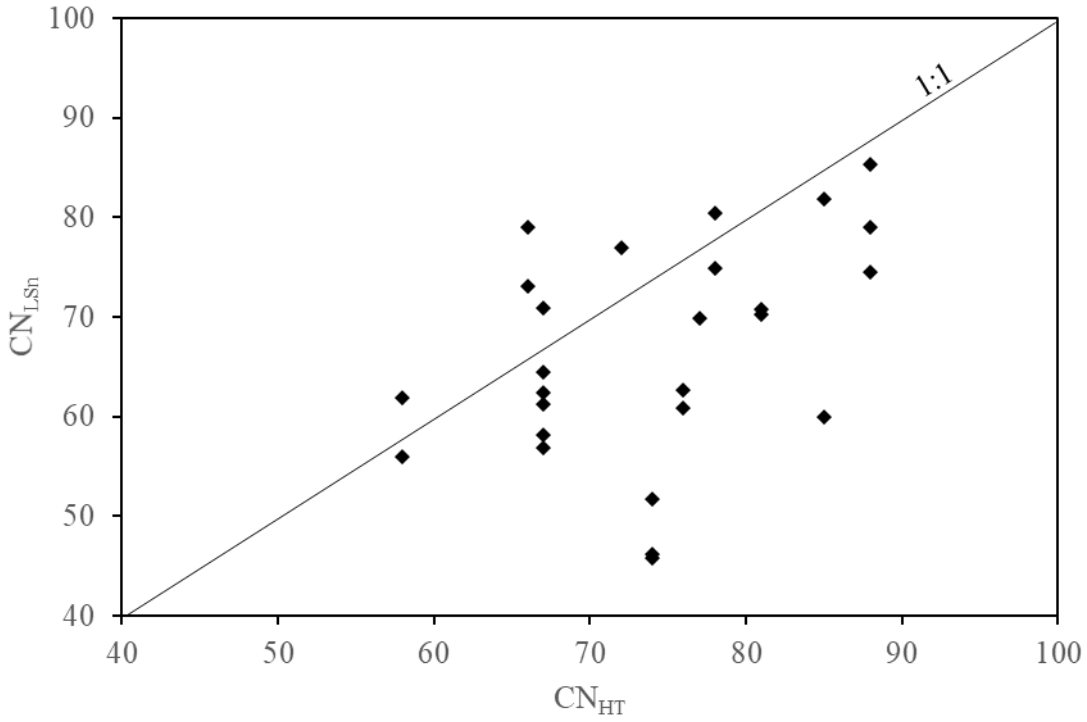

Figure 5.8 CN Plot for comparison between CN_{LSn} and CN_{HT}

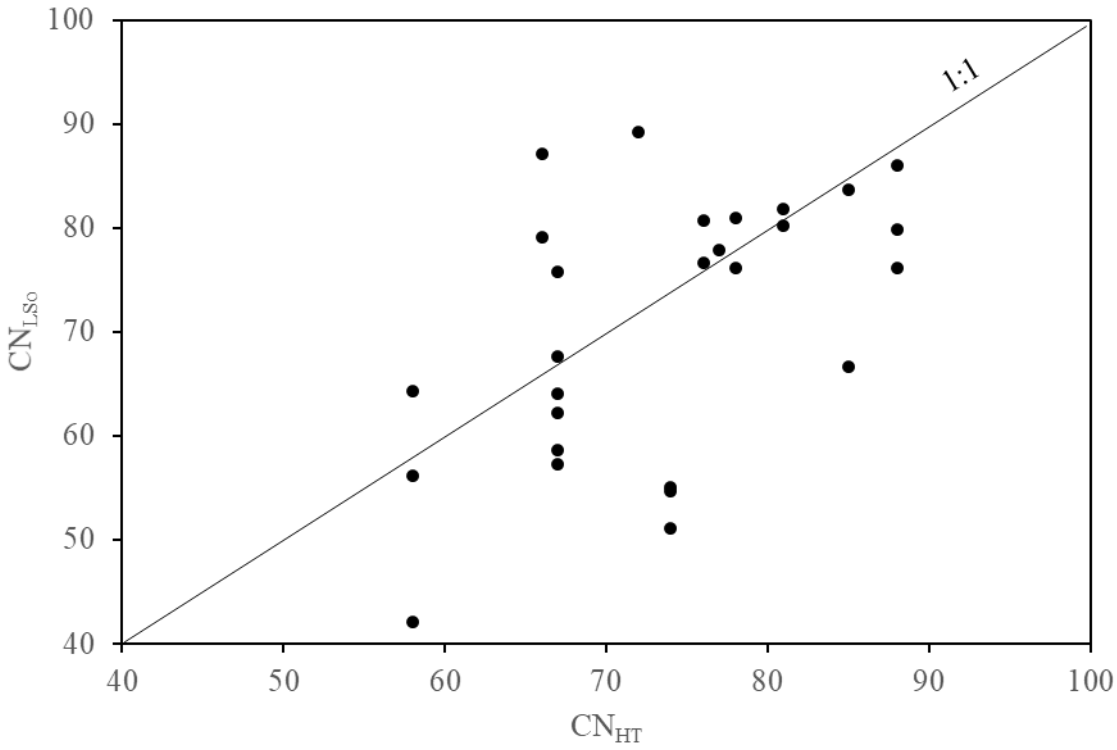

Figure 5.9 CN Plot for comparison between CN_{LSo} and CN_{HT}

The comparison of CN_{HT} with CN_{LSMn} and CN_{LSMo} are given in Figures 5.10 and 5.11 respectively. As in Figure 5.10, CN_{HT} and CN_{LSMn} do not compare well, for 17 out of 27 CN_{LSMn}–values are higher than CN_{HT}; both exhibiting greater difference for values lower than 75. However, the difference diminishes with increasing values. The group of CN_{HT} lower than 75 shows a higher PBIAS (= -12.84%) than the group of CN_{HT} higher than 75 (=1.03%). Overall, pair–wise comparison showed a significant difference ($p<0.05$) to exist between CN_{HT} and CN_{LSMn} means. Such an inference is consistent with the general notion that the existing SCS–CN method performs better for high P–Q (or CN) events.

From Figure 5.11, CN_{HT} with CN_{LSMo} compare similarly as in Figure 5.10. However, PBIAS of the group of CN_{HT} lower than 75 is -14.87% compared to 0.12% for the group higher than 75.

Figures 5.12 and 5.13a & 5.13b show a plot of CN_m with CN_{LS} and CN_{LSM} for both natural and ordered P-Q datasets. The difference is noticeable between CN_m and CN_{LSM} (or CN_{LS}) for lower CN values. As shown in Table 5.5 and Figures 5.12 and 5.13, CN_m are higher than that of both CN_{LSM} and CN_{LS}, consistent with those reported in literature (D'Asaro and Grillone 2012; D'Asaro et al. 2014; Stewart et al. 2012).

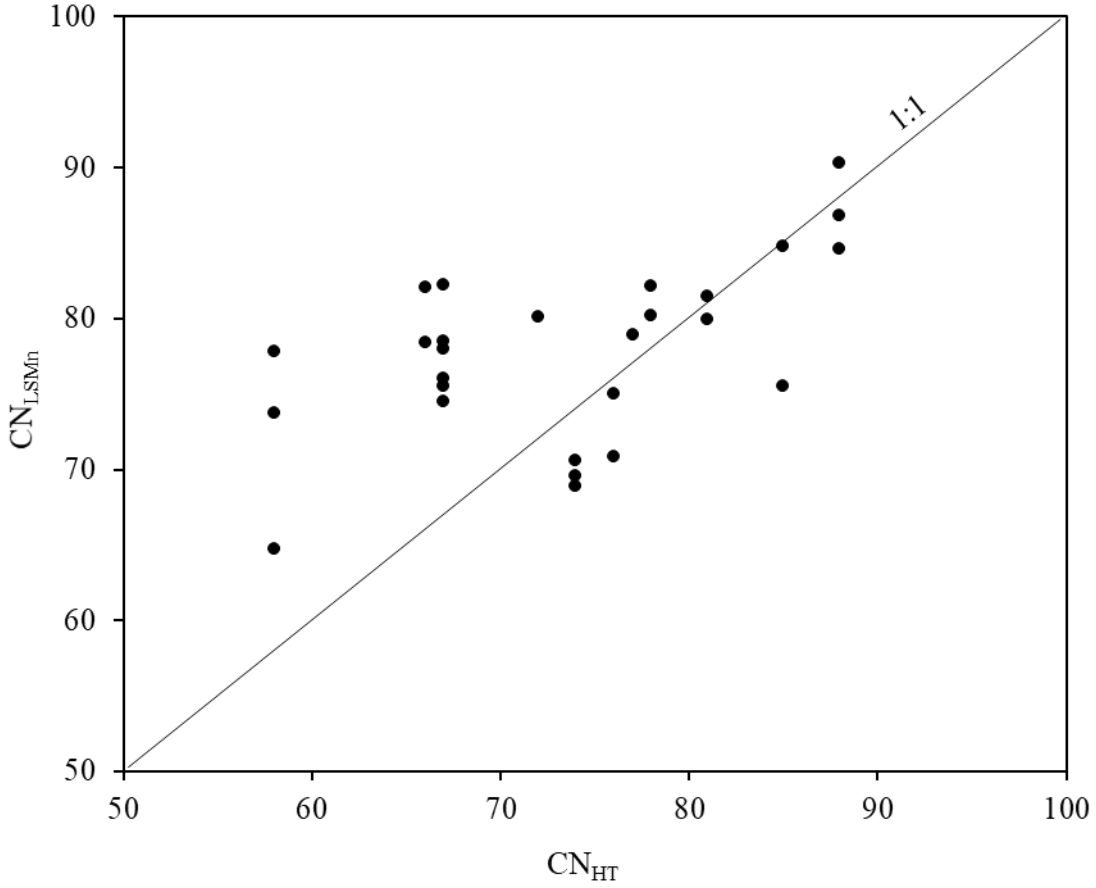

Figure 5.10 CN comparison plot for CN_{LSMn} vs CN_{HT}

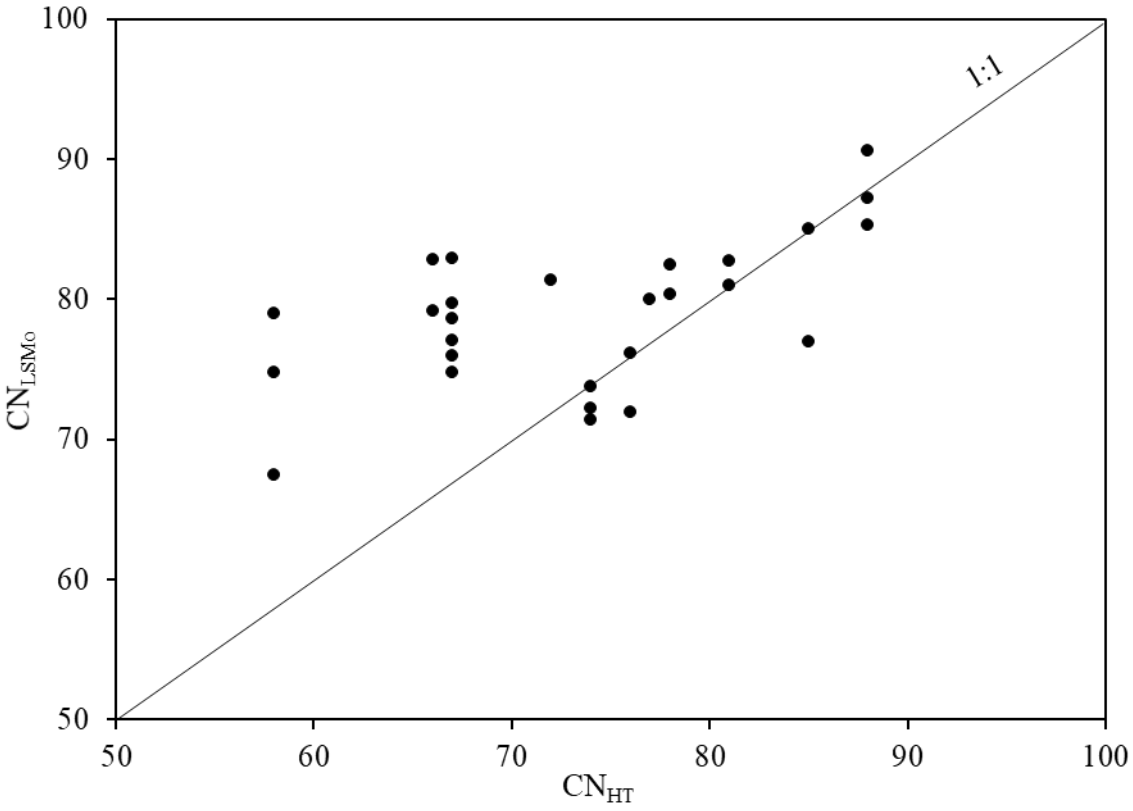

Figure 5.11 CN comparison plot for CN_{LSMo} vs CN_{HT}

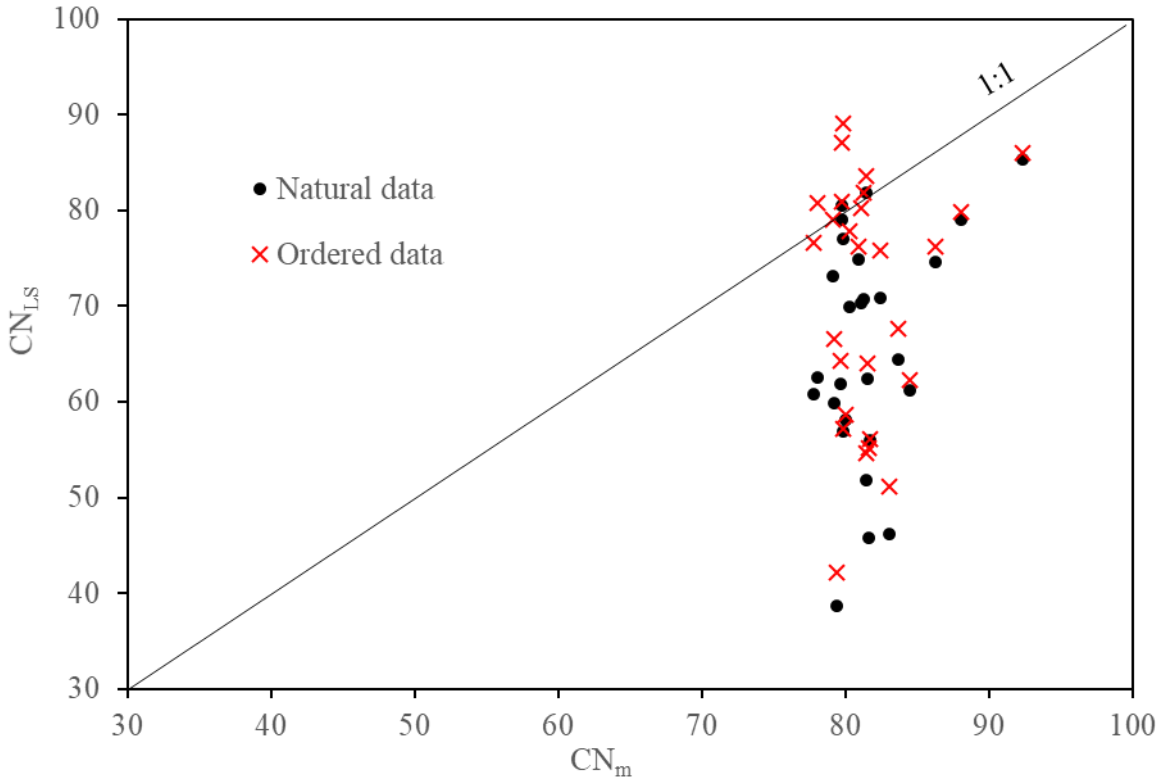

Figure 5.12 CN comparison plot for CN_{LS} vs CN_m

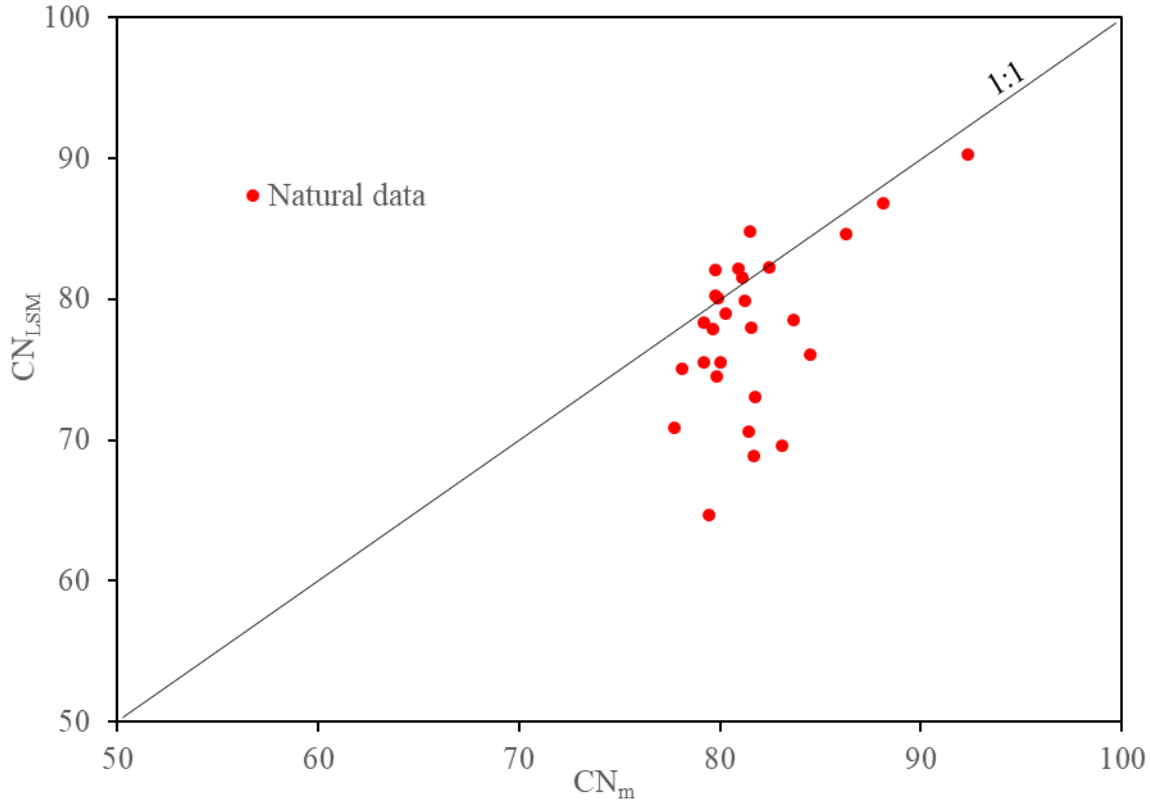

Figure 5.13a CN comparison plot of CN_{LSM} vs CN_m for natural datasets

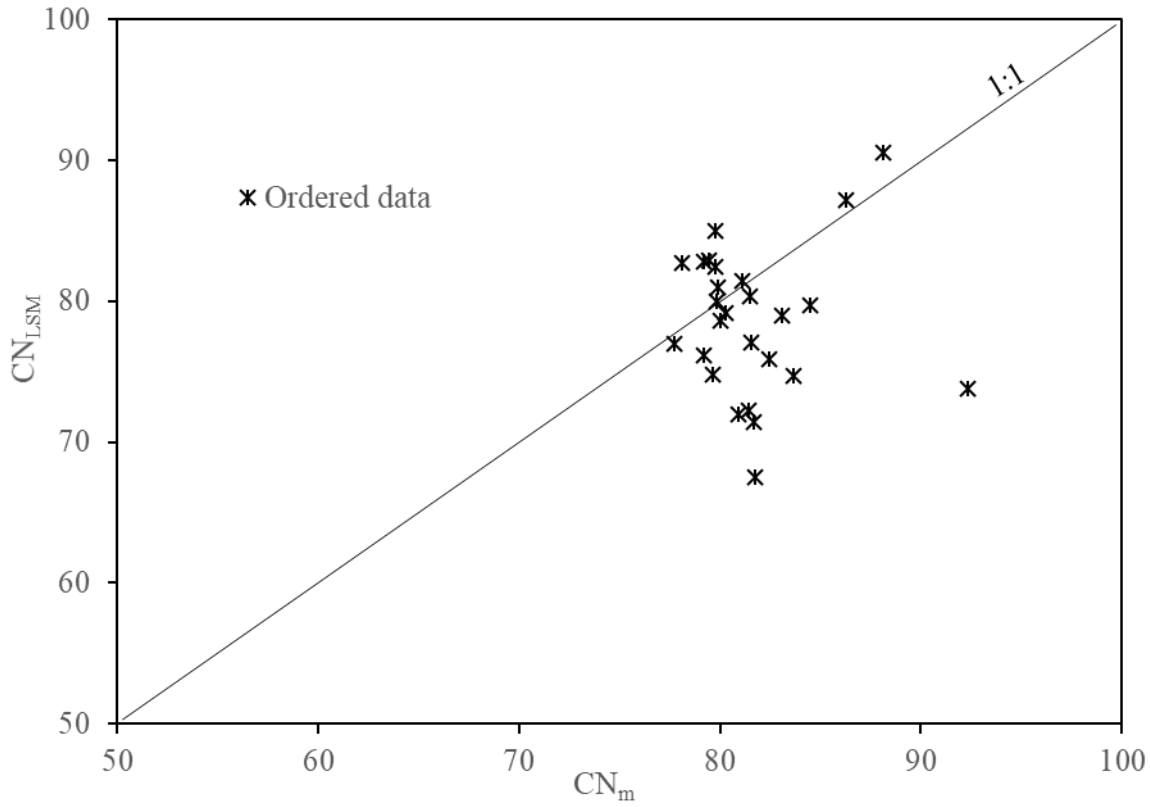

Figure 5.13b CN comparison plot of CN_{LSM} vs CN_m for ordered datasets

To check the accuracy of CNs in estimation of runoff from the studied agricultural plots, runoff was estimated by using all the four sets of CNs, viz., CN_{HT}, CN_m, CN_{LSMn} and CN_{LSMo} for the data of 24 plots (plots 1–24 of Table 5.5). In order to estimate the runoff, it is required to correct the AMC of CNs based on P_5 values. Therefore, plot nos. 25–27 were excluded from comparison due to unavailability of their corresponding P_5 data. The AMC correction formulae as given in Equations 5.2 & 5.3 have been used for estimating the CN_1 and CN_3 from CN_{HT}, CN_m, CN_{LSMn} and CN_{LSMo}. Here notable point is that CN_{LSn} and CN_{LSo} were excluded from this analysis because there are no formulae available for estimating the CN_1 and CN_3 from CN_2 for λ value other than 0.2.

Tables 5.6a and 5.6b show the performance statistic along with the resulting RMSE, R^2 and E values, used to test the accuracy of all four sets of CNs in runoff estimation. As seen from this table, CN_{HT} values derived from plot characteristics do not estimate the runoff from these plots as accurately as do the other CNs. As seen from these tables, both E and R^2 show the estimated runoff based on all four CNs to be poorly matching (except for a few plots) the observed runoff. In general, CN_{LSMo} performed the best of all, and CN_m better than CN_{HT}. The reason for CN_{HT} to have performed most poorly is that these are the generalized values derived from

Table 5.6a Performance statistic for runoff estimation using CN_{HT} and CN_m

Plot No.	NEH-4 Table (λ=0.20)				NEH-4 method (natural data, λ=0.20)		
	CN_{HT}	R^2	E	RMSE (mm)	CN_m	E	RMSE (mm)
1	81	0.543	0.451	8.631	79.93	0.465	8.518
2	72	0.154	-0.042	13.029	80.09	0.371	10.126
3	81	0.505	0.365	9.708	81.51	0.373	9.649
4	76	0.597	0.357	8.875	75.05	0.439	8.290
5	85	0.601	0.551	7.429	75.52	0.387	8.679
6	76	0.641	0.496	6.454	70.87	0.596	5.780
7	78	0.805	0.321	10.935	82.19	0.544	8.966
8	78	0.921	0.474	9.307	80.24	0.606	8.062
9	85	0.884	0.751	7.680	84.81	0.499	10.909
10	66	0.025	-0.264	16.483	82.06	0.426	11.106
11	66	0.013	-0.231	13.397	78.38	0.530	8.276
12	77	0.660	0.305	10.284	78.95	0.526	8.499
13	67	0.001	-1.296	8.240	74.49	-1.047	7.779
14	67	0.092	-1.120	9.828	78.5	-0.195	7.377
15	67	0.030	-1.157	8.710	76.05	-1.193	8.784
16	67	0.056	-0.349	9.536	77.97	0.421	6.157
17	67	0.023	-0.504	8.204	75.49	0.011	6.553
18	67	0.134	-0.263	12.027	82.26	0.750	5.276
19	58	0.040	-1.376	5.484	64.73	-3.604	7.448
20	58	0.001	-1.160	8.189	73.07	-1.054	7.802
21	58	0.000	-0.752	10.503	77.88	0.015	7.740
22	74	0.135	-2.033	6.990	69.61	-3.319	10.089
23	74	0.290	-0.146	6.340	68.9	-0.929	8.100
24	74	0.390	-0.305	5.879	70.59	-1.390	7.956
Mean		0.314	-0.289	9.256		-0.241	8.247

Table 5.6b Performance statistic for runoff estimation using CN_{LSMn} and CN_{LSMo}

Plot No.	LSM (Natural data, λ=0.20)				LSM (Ordered data, λ=0.20)			
	CN_{LSMn}	R^2	E	RMSE (mm)	CN_{LSMo}	R^2	E	RMSE (mm)
1	79.93	0.514	0.387	9.123	81.01	0.543	0.452	8.625
2	80.09	0.470	0.382	10.035	81.41	0.518	0.451	9.456
3	81.51	0.520	0.400	9.442	82.75	0.550	0.474	8.837
4	75.05	0.564	0.296	9.283	76.16	0.602	0.367	8.805
5	75.52	0.414	0.172	10.081	76.99	0.638	0.560	7.355
6	70.87	0.313	0.152	8.372	71.94	0.437	0.226	7.999
7	82.19	0.868	0.643	7.925	82.46	0.872	0.663	7.700
8	80.24	0.943	0.640	7.706	80.39	0.943	0.651	7.589
9	84.81	0.883	0.739	7.869	85.04	0.884	0.754	7.637
10	82.06	0.759	0.573	9.578	82.83	0.766	0.622	9.040
11	78.38	0.767	0.477	8.728	79.16	0.778	0.530	8.275
12	78.95	0.701	0.437	9.256	80.01	0.718	0.508	8.658
13	74.49	0.141	-0.984	7.659	74.74	0.316	-0.577	6.829
14	78.5	0.451	-0.181	7.336	79.72	0.481	-0.121	7.145
15	76.05	0.274	-0.598	7.498	77.10	0.304	-0.557	7.401
16	77.97	0.490	0.336	6.688	78.59	0.612	0.598	4.252
17	75.49	0.313	-0.038	6.816	75.94	0.331	-0.019	6.754
18	82.26	0.779	0.748	5.377	82.92	0.795	0.775	5.077
19	64.73	0.000	-1.548	5.680	67.47	0.060	-1.356	5.461
20	73.07	0.110	-0.813	7.503	74.79	0.165	-0.743	7.357
21	77.88	0.310	-0.032	8.061	78.96	0.346	0.021	7.851
22	69.61	0.047	-1.791	6.705	71.43	0.081	-1.848	6.773
23	68.9	0.154	-0.224	6.553	72.23	0.177	-0.378	6.953
24	70.59	0.315	-0.288	5.839	73.76	0.386	-0.386	5.860
mean		0.463	-0.005	7.880	-	0.513	0.069	7.404

small watersheds of United States for high magnitude P-Q events (or high CN values). As seen from Tables 5.6a and 5.6b, for 15 out of 24 plots, a simple mean of the observed runoff was a better estimate (due to negative E values) than that due to CN_{HT}. CN_{HT} estimates reasonably correlated (E > 0.50) with observed runoff for only two plots. Similarly, the mean of observed runoff series was a better estimate for 8 out of 24 plots than that due to CN_{LSn} or CN_{LSMo}. The runoff estimated by CN_{LSMn} and CN_{LSMo} was reasonably close (E > 0.50) to the observed for 5 and 9 plots, respectively.

From Figures 5.7 & 5.10–5.11, and Tables 5.6a & 5.6b, it is evident that the general agreement between CN_{HT} and CN_m, CN_{LSMn} or CN_{LSMo} is poor, consistent with that reported elsewhere (D'Asaro et al. 2014; Fennessey 2000; Feyereisen et al. 2008; Hawkins 1984; Hawkins and Ward 1998; Stewart et al. 2012; Titmarsh et al. 1989, 1995, 1996; Tedela et al. 2008; Taguas et al. 2015). As an alternative to CN_{HT}, the best CN-values based on the highest R^2, E (or lowest RMSE) as given in Tables 5.6a & 5.6b are suggested for each of 24 plots. As seen, CN_{LSMo} ranked first for 20 out of 24 plots whereas each of CN_{HT} and CN_{LSMn} ranked first on only 2 plots. Therefore, CN_{LSMo} are suggested as a preference over CN_{HT} for use in areas with similar plot characteristics and climatic conditions.

5.5 RELATIONSHIP BETWEEN ORDERED (i.e. CN_{LSMO}) AND NATURAL (i.e. CN_{LSMN}) DATA CNS

The graphical representation between ordered CNs (i.e. CN_{LSMo}) and natural data CNs (i.e. CN_{LSMn}) is given in Figure 5.14. As expected, CN values derived from ordered data (CN_{LSMo}) are higher than CN values derived from natural data (CN_{LSMn}). From this figure, CN_{LSMo} values are seen to be higher than CN_{LSMn}, consistent with that reported elsewhere (Ajmal et al. 2015a; D'Asaro and Grillone 2012; D'Asaro et al. 2014; Hawkins et al. 2009; Stewart et al. 2012). It is for the obvious reason that the former CN values derived from frequency matched P and Q data will always be higher than the latter ones derived from natural data as Q corresponding to a P of certain frequency will always be higher than or equal to the observed Q. CN values derived for individual plots using ordered dataset differ from 0.15 to 3.22 CN compared with those derived from natural data. The trend between CN_{LSMo} and CN_{LSMn} allow a conversion as given in Equation 5.5:

$$CN_{LSMo} = 0.005 (CN_{LSMn})^2 + 0.182\ CN_{LSMn} + 36.83;\ R^2 = 0.990;\ SE = 0.552\ CN \quad (5.5)$$

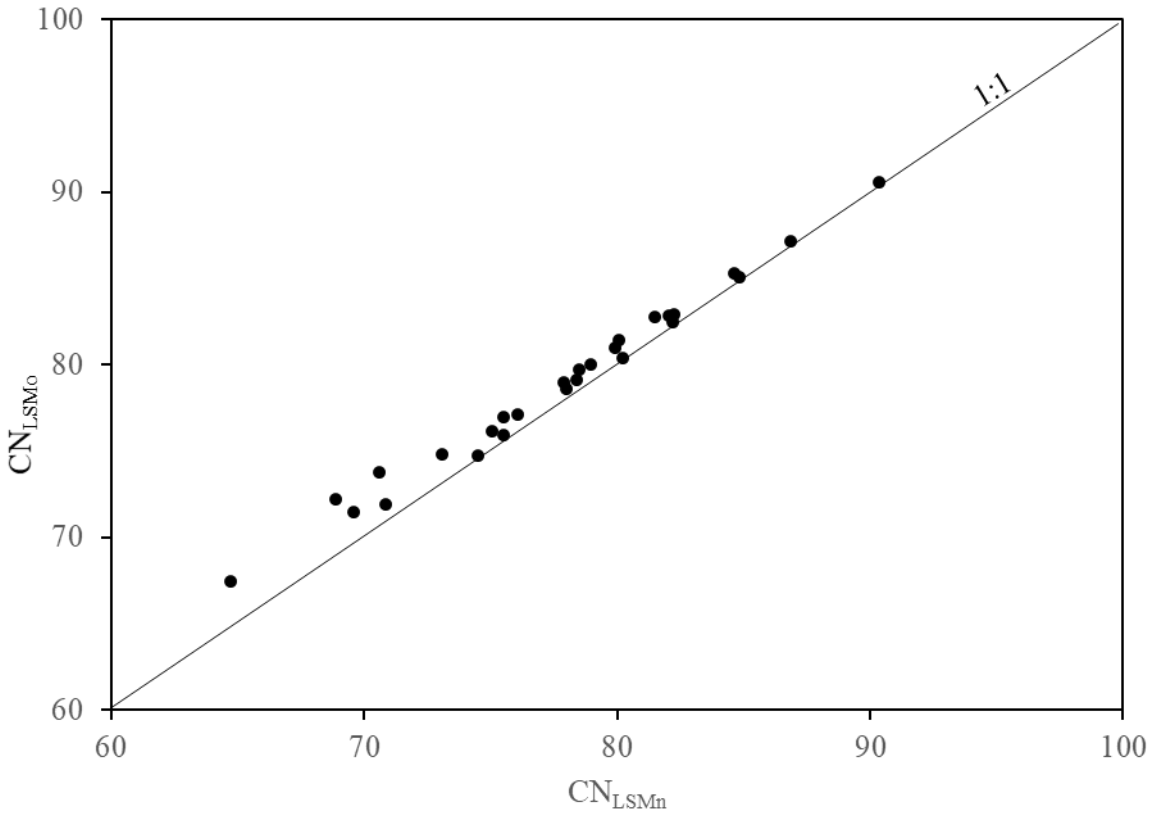

Figure 5.14 CN plot for CN_{LSMo} vs CN_{LSMn}

CHAPTER 6

EVALUATION OF INITIAL ABSTRACTION COEFFICIENT

6.1 DERIVATION OF λ VALUES FROM OBSERVED P-Q DATA

To derive λ values, both S and λ were optimized by iterative least squares fitting (or best fit) procedure of the general SCS-CN Equation 6.1, consistent with the work of Hawkins et al. (2002). Similar to the CNs, model fitting yields only one value of λ from all P–Q events of plot, i.e. only one representative value of λ for a plot. Also, both natural and ordered datasets consisting of only large storm events with (arbitrary) P >15 mm criterion to avoid biasing effect, but to retain sufficient number of P–Q data for analysis were used. Only plots having at least 10 observed rainfall–runoff events were considered for optimization study.

$$\Sigma_{i=1}^{n}(X_i - Y_i)^2 = \Sigma\left\{X_i - \left[\frac{(P-\lambda S)^2}{(P+(1-\lambda)S)}\right]\right\}^2 \Rightarrow \text{Minimum} \qquad (6.1)$$

The results of optimized λ-values derived for different P-Q (both ordered and natural) data sets observed at 27 runoff plots are shown in Table 6.1. As seen, the optimized λ–values derived for both natural (ranging from 0 to 0.208) and ordered (ranging from 0 to 0.659) P–Q datasets are seen to vary widely from plot to plot with 0 as the most frequent value. The cumulative frequency distribution of λ-values for both datasets given in Figure 6.1 shows that λ values are larger for ordered data, the distribution is skewed, and most λ-values (out of 27, 26 for natural and 21 for ordered P–Q datasets) are less than the standard λ=0.2 value. The mean and median λ-values are 0.030 & 0 for natural, and 0.108 & 0 for ordered data, quite different from standard λ = 0.20, but consistent with the results of other studies carried out elsewhere (Ajmal et al. 2015a; Baltas et al. 2007; D'Asaro and Grillone 2012; D'Asaro et al. 2014; Elhakeem and Papanicolaou 2009; Fu et al. 2011; Hawkins et al. 2002; Menberu et al. 2015; Shi et al. 2009; Yuan et al. 2014; Zhou and Lei 2011).

In addition, the existence of I_a-S relationship for different plots was also investigated using the whole data of 27 plots. In contrast to the existing notion, I_a when plotted against S (Figures 6.2 and 6.3) exhibited no correlation for both natural and ordered datasets, consistent with the findings of Jiang (2001).

Table 6.1 Optimized λ values from observed P-Q data

Plot No.	Land use	n	LSM (Optimized λ)			
			Natural data		Ordered data	
			CN_{LSn}	λ	CN_{LSo}	λ
1	Sugarcane	15	70.79	0.0334	81.87	0.2276
2	Sugarcane	15	77.00	0.1244	89.17	0.6590
3	Sugarcane	15	70.30	0.0002	80.23	0.1267
4	Fallow	10	62.61	0.0204	80.74	0.3513
5	Fallow	10	59.91	0.000	66.61	0.0245
6	Fallow	10	60.86	0.0631	76.63	0.3174
7	Maize	10	74.91	0.0314	76.17	0.0455
8	Maize	10	80.49	0.2079	80.98	0.2192
9	Maize	10	81.89	0.0999	83.60	0.1443
10	Blackgram	10	79.07	0.1141	87.13	0.4213
11	Blackgram	10	73.13	0.0879	79.09	0.1966
12	Blackgram	10	69.93	0.0328	77.81	0.1412
13	Sugarcane	13	56.94	0.0003	57.21	0.0000
14	Sugarcane	13	64.47	0.0000	67.69	0.0000
15	Sugarcane	13	61.23	0.0002	62.22	0.0000
16	Maize	11	62.39	0.0000	64.06	0.0000
17	Maize	11	58.13	0.0001	58.65	0.0001
18	Maize	11	70.93	0.0000	75.77	0.0415
19	Blackgram	11	38.72	0.0000	42.16	0.0000
20	Blackgram	11	55.95	0.0000	56.11	0.0000
21	Blackgram	11	61.92	0.0000	64.30	0.0000
22	Fallow	13	46.21	0.0000	51.12	0.0001
23	Fallow	11	45.80	0.0000	55.11	0.0001
24	Fallow	13	51.79	0.0000	54.66	0.0001
25	Sugarcane	10	85.36	0.0000	85.97	0.0000
26	Sugarcane	10	79.03	0.0000	79.88	0.0000

Table 6.1 (Continued)

Plot No.	Land use	n	LSM (Optimized λ)			
			Natural data		Ordered data	
			CN_{LSn}	λ	CN_{LSo}	λ
27	Sugarcane	10	74.56	0.0000	76.17	0.0000
	Statistics					
	Mean		65.72	0.0302	70.78	0.1080
	Median		64.47	0.0001	76.17	0.0001
	Standard deviation		11.93	0.0527	12.68	0.1665
	Maximum		85.39	0.2079	89.17	0.6590
	Minimum		38.72	0.0000	42.16	0.0000
	Skewness		-0.41	2.0189	-0.51	1.8609

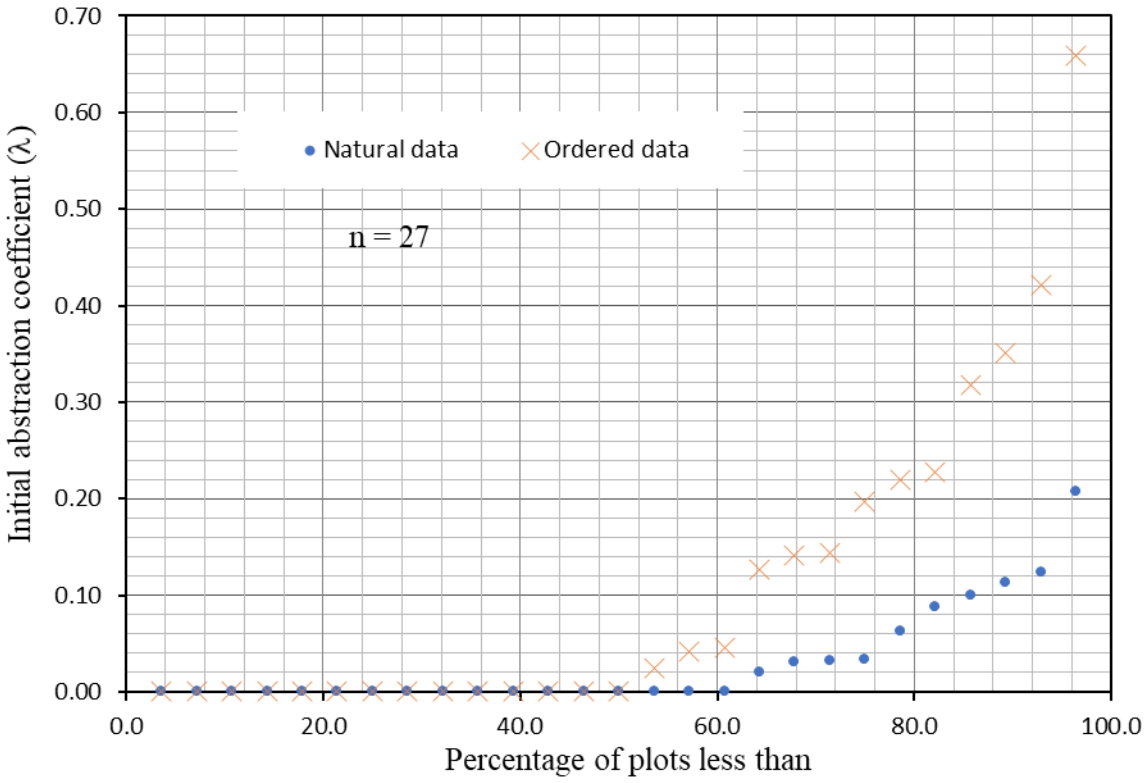

Figure 6.1 Cumulative frequency distribution of model fitted λ-values for 27 plot-datasets

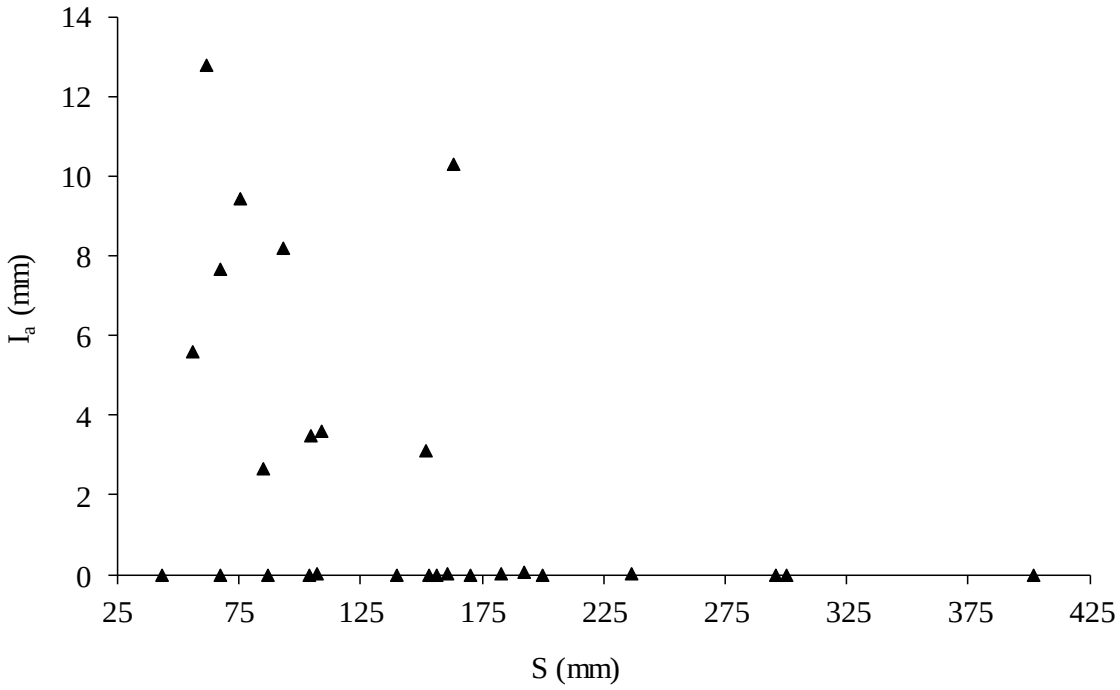

Figure 6.2 Relationship between I_a and S for 27 plots natural occurred P-Q datasets

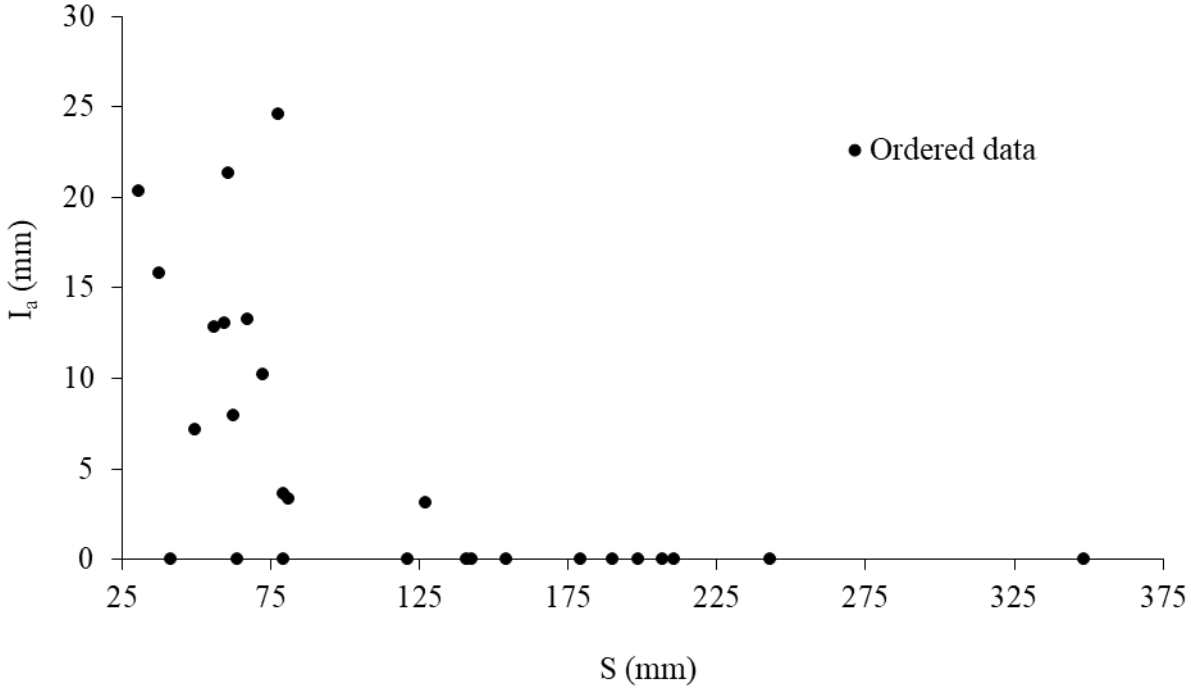

Figure 6.3 Relationship between I_a and S for 27 plots ordered P-Q datasets

6.2 PROPOSED MODEL BASED ON OPTIMIZED λ VALUES

Performance of the existing SCS-CN model (Equation 4.5) with traditional $\lambda = 0.2$ was compared with that employing an average $\lambda = 0.03$ value derived from 27 natural P–Q plot-dataset. The average is considered instead of median as the former yielded the smallest standard error (Fu et al. 2011). Here, it is notable that all runoff producing rainfall events only were used in this analysis.

6.2.1 Performance evaluation of the Proposed λ-based Model

Table 6.2 shows the performance indices (viz., R^2, E, RMSE, n_t and PBIAS) for fitting of Equation 4.5 with $\lambda = 0.2$ (existing SCS-CN method i.e. $M_{0.2}$) and $\lambda = 0.03$ (proposed method i.e. $M_{0.03}$). As seen from the table, the runoff estimates with $\lambda=0.03$ ($M_{0.03}$) provides larger E and lower RMSE for 26 out of 27 plots than those due to $\lambda=0.2$ ($M_{0.2}$). Based on E, performance of the existing SCS–CN method ($M_{\lambda=0.2}$) is seen to be unsatisfactory, satisfactory, good, and very good on the data of 12, 5, 3, and 7 plots out of 27 plots, respectively. On the other hand, the performance of the proposed method ($M_{0.03}$) is unsatisfactory, satisfactory, good, and very good on 8, 5, 5 and 9 plots out of 27 plots, respectively. Based on the mean values of E, $M_{0.03}$ performed satisfactorily (E = 0.565) compared to $M_{0.2}$ (E = 0.392).

The positive PBIAS values resulting for both the methods indicate that the existing SCS–CN method (i.e. $M_{0.2}$) underestimated the average runoff. However, these values for $M_{0.03}$ were much lower than those due to $M_{0.2}$, indicating an improvement in model performance. $M_{\lambda=0.2}$ performance was unsatisfactory, satisfactory, good, and very good on the data of 6, 10, 1, and 9 plots out of 27 plots, respectively. On the other hand, $M_{0.03}$ performance was unsatisfactory, satisfactory, good, and very good on 4, 4, 6 and 13 plots out of 27 plots, respectively.

Thus, based on the mean PBIAS values, $M_{0.03}$ performed good (=10.78) whereas M1 performed satisfactorily (=16.90). For further analysis based on nt, $M_{0.2}$ exhibited satisfactory or good performance on 11 plots out of 27 plots. The performance improved to 16 plots when used $M_{0.03}$. The improved $M_{0.03}$ model performance is also supported by the higher r^2-value. As shown in Figure 6.4, the significant improvement in E (or r^2) using $M_{0.03}$ model was observed in 26 out of the 27 study plots. On the contrary, the runoff predictions by $M_{0.03}$ model were debased ($r^2 \leq 0$) in only one plot. Overall, as seen from Table 6.2 and Figure 6.4, $M_{0.03}$ performed better than $M_{\lambda=0.2}$.

Table 6.2 Performance statistic for runoff estimation using Equation 3.5 with $\lambda = 0.2$ (model $M_{0.2}$) and $\lambda = 0.03$ (model $M_{0.03}$) (Used all runoff producing events)

Plot No.	n	Existing SCS-CN method (λ=0.20) (model $M_{0.2}$)						Proposed method (λ=0.03) (model $M_{0.03}$)						r^2 (%)
		CN	R^2	E	n_t	PBIAS (%)	RMSE (mm)	CN	R^2	E	n_t	PBIAS (%)	RMSE (mm)	
1	18	76.16	0.701	0.626	0.69	20.04	4.71	63.65	0.739	0.726	0.03	10.22	4.04	26.74
2	18	75.24	0.695	0.657	0.76	17.17	4.62	62.29	0.721	0.718	0.97	6.16	4.19	17.78
3	18	78.91	0.634	0.556	0.55	18.78	6.05	68.03	0.666	0.648	0.94	10.68	5.38	20.72
4	12	68.01	0.899	0.875	1.97	-0.78	2.00	51.67	0.985	0.979	0.74	11.52	0.83	83.20
5	12	67.09	0.507	0.341	0.29	23.46	4.44	51.13	0.731	0.627	6.16	33.18	3.34	43.40
6	12	65.25	0.941	0.890	2.17	-41.82	1.59	45.58	0.966	0.966	0.72	2.11	0.89	69.09
7	13	82.84	0.925	0.918	2.65	7.48	3.52	75.46	0.928	0.928	4.69	-1.47	3.29	12.20
8	13	80.84	0.969	0.969	4.97	1.20	2.10	72.66	0.960	0.952	2.91	-10.80	2.64	-54.84
9	13	82.80	0.936	0.928	2.88	8.55	3.27	75.41	0.941	0.941	3.76	-0.33	2.93	18.06
10	13	77.11	0.890	0.875	1.95	11.59	3.33	66.42	0.909	0.910	3.33	1.65	2.83	28.00
11	13	74.93	0.856	0.849	1.69	8.64	3.43	62.95	0.873	0.873	2.48	-0.73	3.14	15.89
12	13	74.91	0.766	0.738	1.04	17.17	4.48	63.00	0.792	0.788	1.93	8.37	4.03	19.08
13	13	74.49	0.808	0.509	0.49	21.91	3.81	60.85	0.810	0.724	1.27	11.09	2.86	43.79
14	13	78.50	0.407	-0.217	-0.06	23.26	7.45	67.44	0.419	0.096	0.98	17.33	6.42	25.72

Table 6.2 (continued)

Plot No.	n	Existing SCS-CN method (λ=0.20) (model $M_{0.2}$)						Proposed method (λ=0.03) (model $M_{0.03}$)						r^2 (%)
		CN	R^2	E	n_t	PBIAS (%)	RMSE (mm)	CN	R^2	E	n_t	PBIAS (%)	RMSE (mm)	
15	13	76.05	0.518	-0.015	0.03	24.58	5.98	63.41	0.532	0.299	0.09	16.08	4.97	30.94
16	11	77.97	0.612	0.468	0.46	16.72	5.80	66.46	0.624	0.598	0.24	7.63	5.13	24.44
17	11	75.49	0.804	0.679	0.85	18.97	3.73	62.45	0.812	0.796	0.65	6.47	2.98	36.45
18	11	82.26	0.657	0.608	0.68	8.48	6.61	73.69	0.661	0.655	1.32	2.93	6.20	11.99
19	11	67.48	0.415	-0.390	-0.11	45.43	4.44	50.26	0.480	0.136	0.79	25.33	3.50	37.84
20	11	73.70	0.489	-0.089	0.00	33.27	5.68	59.67	0.517	0.282	0.13	20.13	4.61	34.07
21	11	77.80	0.440	0.152	0.14	23.24	7.18	66.13	0.456	0.347	0.24	14.85	6.30	23.00
22	13	69.61	0.330	-0.718	-0.21	39.32	5.26	53.13	0.362	-0.151	0.30	24.22	4.31	33.00
23	11	69.63	0.127	-0.554	-0.16	46.94	7.11	53.76	0.161	-0.178	-0.03	29.67	6.19	24.20
24	13	70.59	0.155	-0.676	-0.20	38.47	6.66	54.49	0.189	-0.228	-0.03	25.20	5.70	26.73
25	11	90.36	0.675	0.484	0.46	7.84	6.57	86.50	0.678	0.554	-0.06	7.41	6.11	13.57
26	11	86.84	0.716	0.622	0.71	7.38	5.08	80.88	0.731	0.690	0.57	5.54	4.61	17.99
27	11	84.62	0.606	0.499	0.48	8.98	5.42	77.05	0.628	0.584	0.88	6.54	4.94	16.97
Mean		76.28	0.647	0.392	0.93	16.90	4.83	64.24	0.677	0.565	1.36	10.78	4.16	28.45

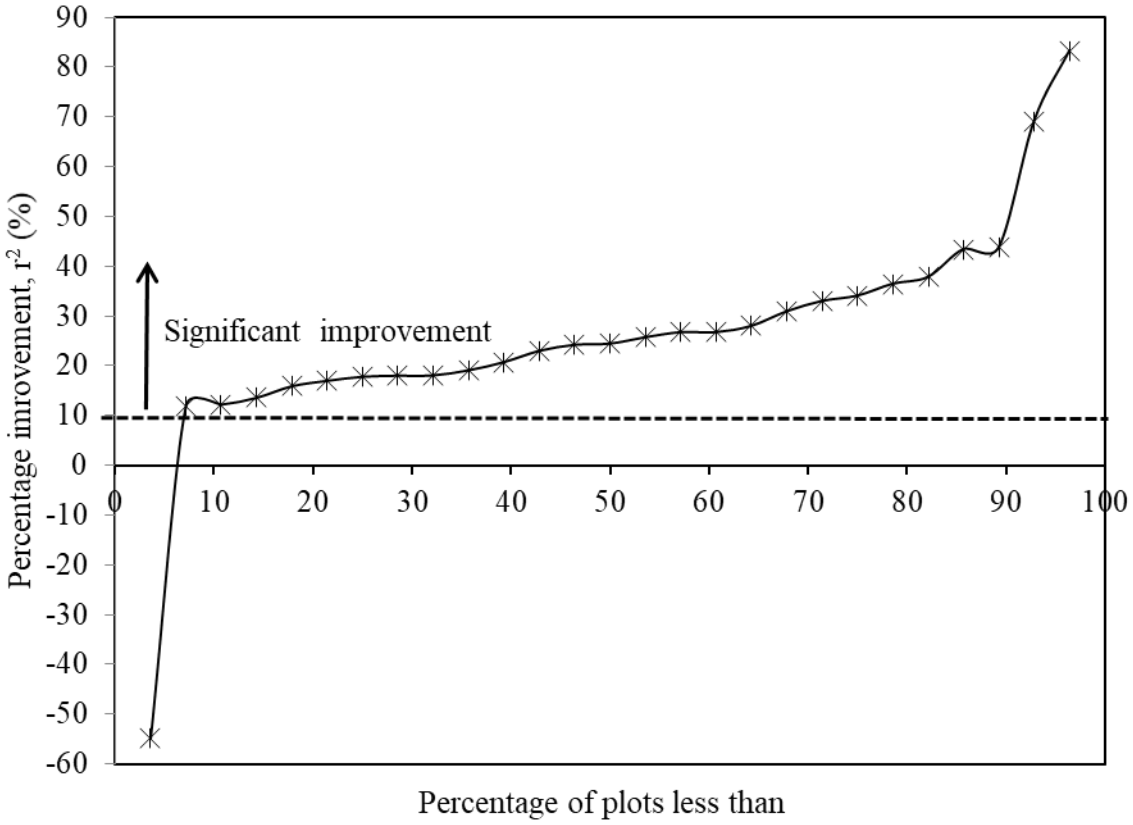

Figure 6.4 The cumulative frequency distribution of improvement in E using r^2 criteria

6.3 SENSITIVITY OF λ TO CN AND RUNOFF

The effect of variation in λ on CNs (or runoff) has been evaluated using the randomly selected 5 plot-data. In addition, the relative change in estimated runoff with progressive changes in λ-value was also analysed as follows:

$$\Delta Q_i = \frac{(Q_i - Q_a)}{Q_a} \times 100 \qquad (6.2)$$

Where ΔQ_i is the relative change of runoff at step i, and Q_i and Q_a are respectively the estimated runoff at step i and step a. Initially, λ = 0.2 was fixed for step a and then reduced by 10% at each step down to 0.02, and runoff was estimated at each step using Equation 4.5 consistent with the work of Yuan et al. (2014). The average CN_{LSo} (=78.92) was estimated from event-based CNs of the 27-plot data and was used for S-computation in Equation 3.9. P = 30 mm was used in Equation 4.5 due to its highest frequency of occurrence.

This sensitivity analysis was carried out using the data of only 5 plots. To this end, as shown in Figure 6.5, for a plot dataset and a given λ-value, S (or CN) was optimised using Equation 4.5. As seen, the rising trends are similar to each plot. In general, CN is seen to increase with λ. It is for the reason that for a given P-Q data, an increase in λ would require an

increase in CN (or decrease in S) to obtain the same Q-value for a given P. Furthermore, variation in CN narrows down with increasing λ-values. Another alternative interpretation of such variation could be that the SCS-CN model is actually a two-parameter model. The two parameters are Ia and S and both are independent of each other. Since Ia is taken as a function of S for simplicity reasons, an increase or decrease in λ-value necessitates S to decrease or increase (or CN to increase or decrease) to maintain Ia.

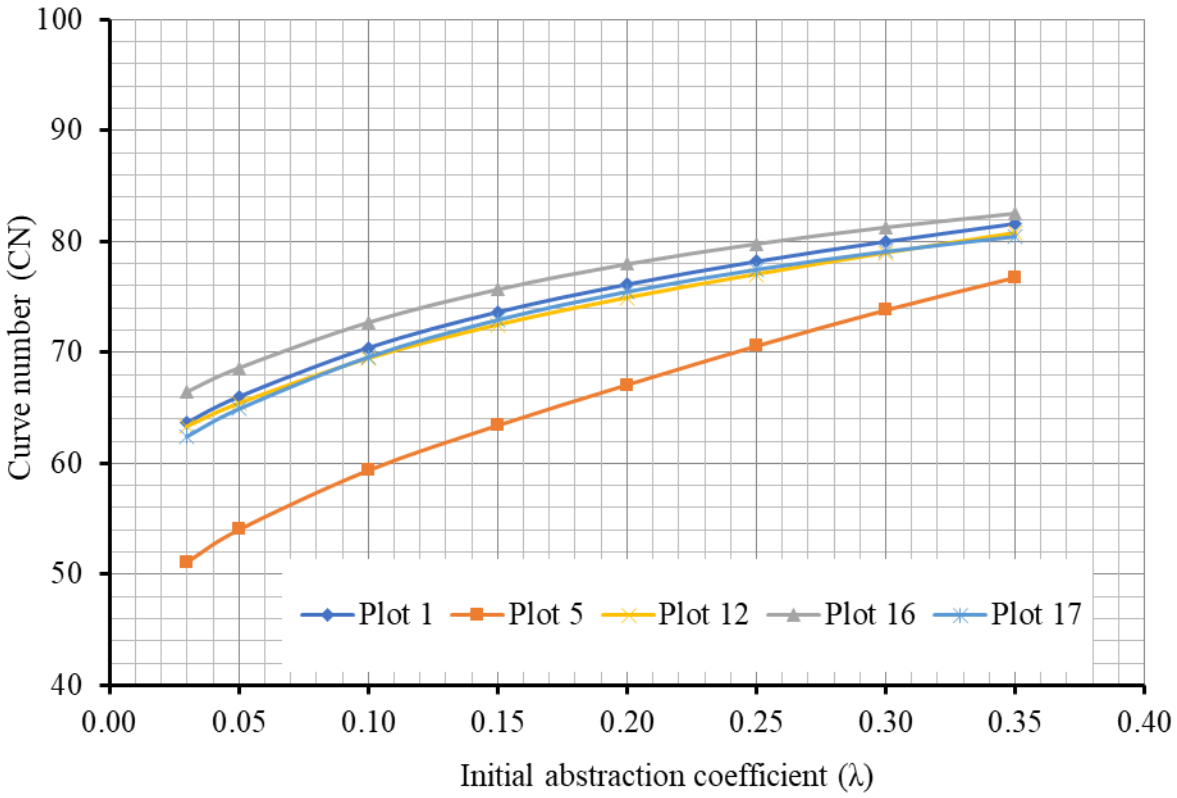

Figure 6.5 Variation in CNs (AMC-II) with λ for 5 plot-data

To indicate the most appropriate λ-value, variation of E with λ was plotted as shown in Figure 6.6. In general, E showed a decreasing trend with λ for all 5 plots, consistent with the findings of Woodward et al. (2004) and Yuan et al. (2014). It implies that low λ-value provides a better prediction of runoff, and vice versa. To show the sensitivity of λ to runoff (employing Equation 3.15), for a given CN=78.92 and P=30 mm, the estimated runoff increased by 165% when λ decreased from 0.2 to 0.02, i.e. by 90%, consistent with the findings of Yuan et al. (2014) (Figure 6.7).

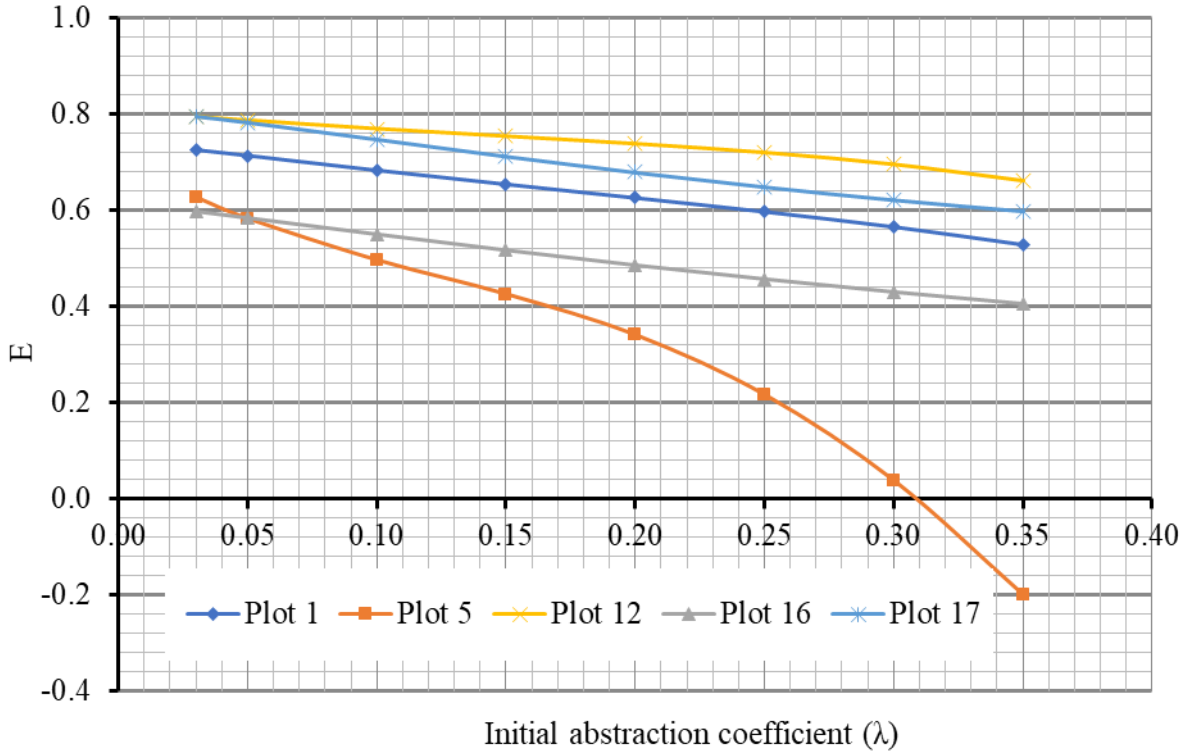

Figure 6.6 Variation in E with λ

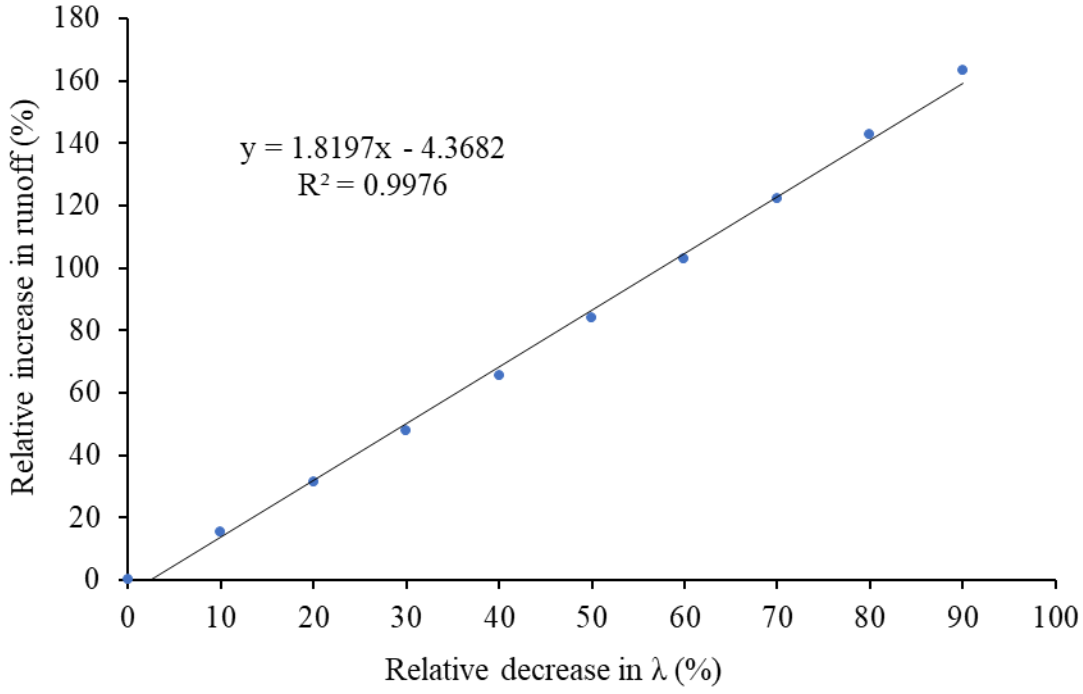

Figure 6.7 Relationship between relative increase in estimated runoff (%) vs relative decrease in λ (%)

6.4 EMPIRICAL EQUATION FOR CONVERSION OF $CN_{0.2}$ INTO $CN_{0.03}$

Similar to Hawkins et al. (2002) and Jiang (2001), Yuan et al. (2014), a conjugate CN empirical conversion equation for converting CNs associated with $\lambda = 0.2$ ($CN_{0.2}$) to $\lambda = 0.03$ ($CN_{0.03}$) is proposed based on direct least squares fitting of Equation 6.1 using 27 plots natural P-Q data sets.

It is of common experience that the existing NEH-4 CNs are based on λ value equal to 0.2. Therefore, a transformation of CNs from $\lambda = 0.2$ to $\lambda = 0.03$ is imperative before using $\lambda = 0.03$ in runoff modeling. To this end, an empirical conversion equation based on direct least squares fitting of 27 plots natural data sets for converting CNs associated with $\lambda = 0.2$ ($CN_{0.2}$) to $\lambda = 0.03$ ($CN_{0.03}$) is proposed as follows (Figure 6.8):

$$S_{0.03} = 0.614\ (S_{0.2})^{1.248};\ R^2 = 0.9948;\ SE = 0.035\ mm \qquad (6.3)$$

In Equation 6.3, maximum potential retention (S) is in mm and $S_{0.03} = S_{0.2}$ at 7.148 mm or $CN_{0.2}$ = 97.268. The plot of graphical representation of ratio of $S_{0.03}$ to $S_{0.2}$ (i.e. $S_{0.03}/S_{0.2}$) with mean ratio of Q to P (i.e. Rc_m) is given in Figure 6.9. From this figure, the $S_{0.03}/S_{0.2}$ ratio was seen to be inversely related to Rc_m.

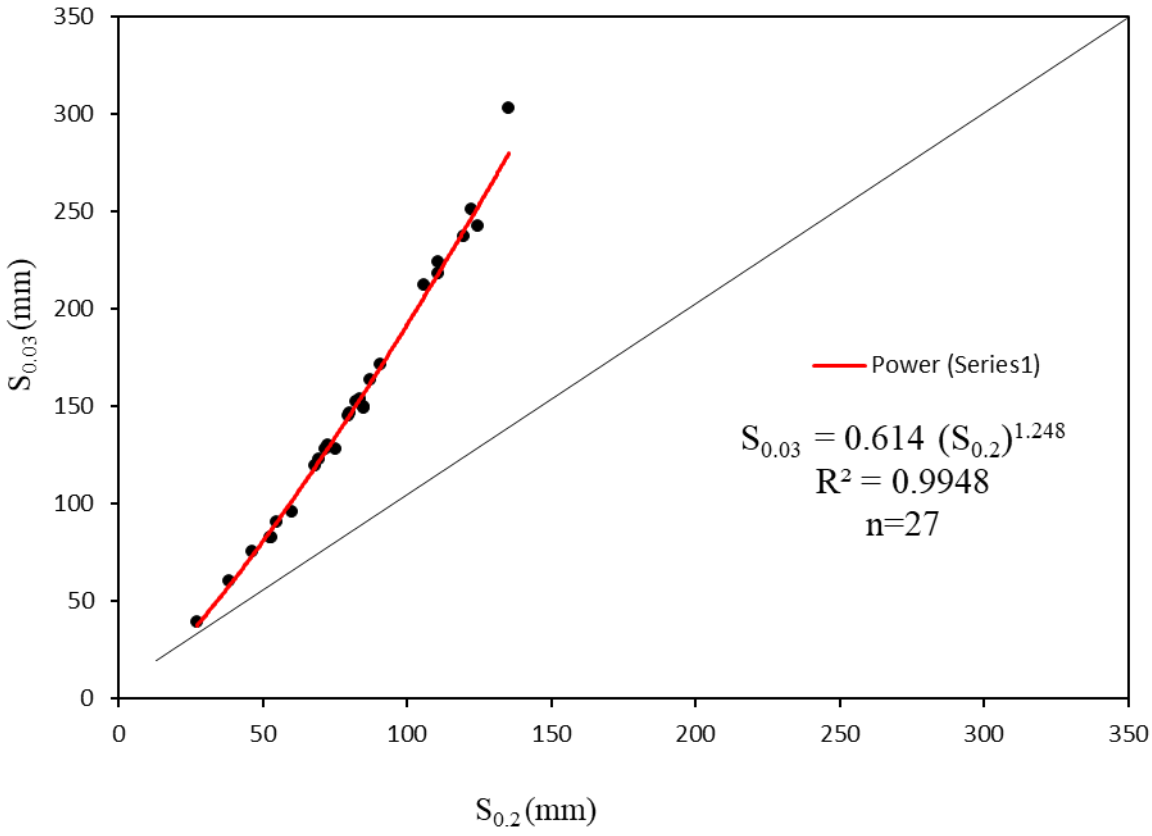

Figure 6.8 Plot of fitting between $S_{0.2}$ and $S_{0.03}$ for 27 agricultural plots data

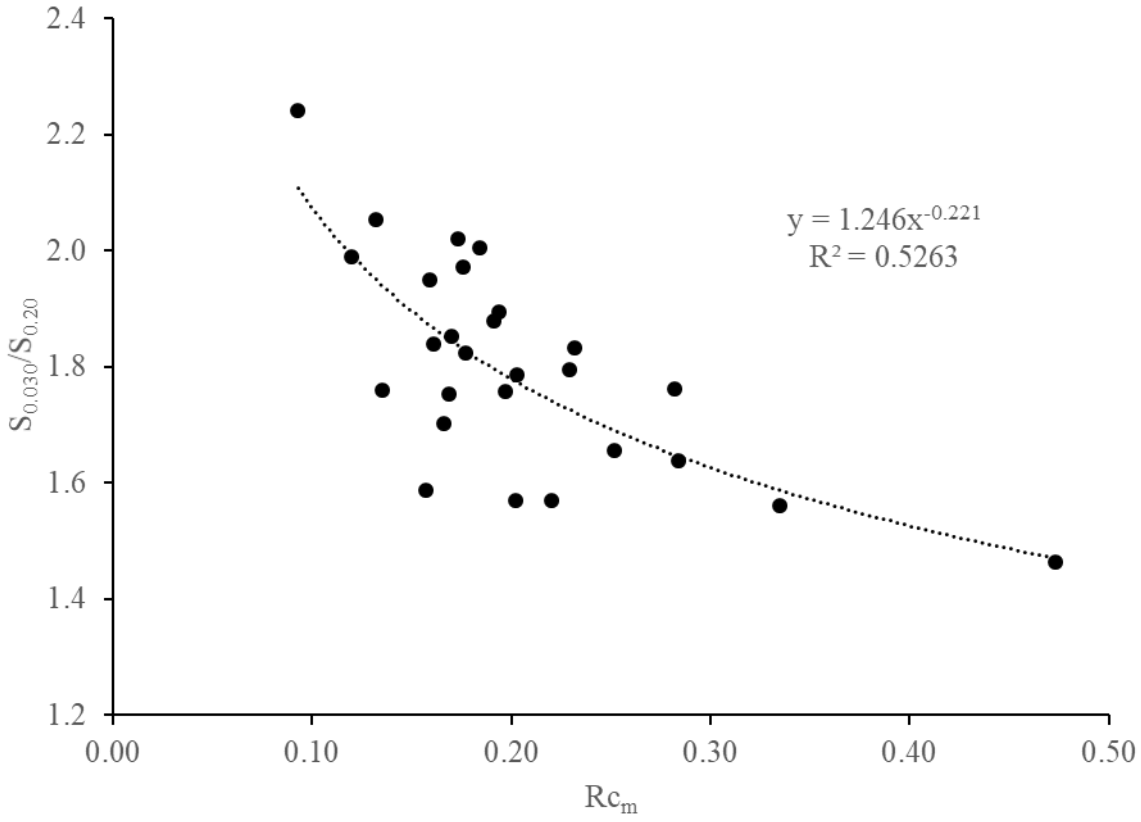

Figure 6.9 plot of ratio of $S_{0.03}$ to $S_{0.2}$ (i.e. $S_{0.03}/S_{0.2}$) vs Rc_m

The substitution of Equation 6.3 into definition of CN yields

$$CN_{0.03} = \frac{25400}{\left[254 + 0.614\left(\frac{25400}{CN_{0.2}} - 254\right)^{1.248}\right]} \tag{6.4}$$

Lastly, the applicability of Equation 6.4 in prediction of runoff using NEH-4 tables Curve number (CN_{HT}) is also investigated. To this end, the estimated NEH-4 CNs (or $CN_{HT0.20}$) based on plot characteristics for all 27 plots were first converted to $CN_{HT0.03}$, and then employed for runoff estimation as shown in Table 6.3 along with R^2, E, and RMSE. As seen, $CN_{HT0.03}$ from Equation 6.4 estimates the runoff more accurately than did $CN_{HT0.20}$. Besides, the r^2-statistic (Figure 6.10) also shows the use of Equation 6.4 to have significantly improved E in 22 out of 24 study plots.

Table 6.3 Performance statistic for runoff estimation using CN_{HT} associated to λ=0.20 ($CN_{HT0.20}$) and λ=0.03 ($CN_{HT0.03}$)

Plot No.	CN_{HT} associated to λ=0.20				CN_{HT} associated to λ=0.03				r^2 (%)
	$CN_{HT0.20}$	R^2	E	RMSE (mm)	$CN_{HT0.03}$	R^2	E	RMSE (mm)	
1	81	0.543	0.451	8.631	71.59	0.602	0.514	8.121	11.48
2	72	0.154	-0.042	13.029	57.28	0.465	0.143	11.187	17.75
3	81	0.505	0.365	9.708	71.59	0.579	0.448	9.054	13.07
4	76	0.597	0.357	8.875	63.48	0.706	0.476	8.010	18.51
5	85	0.601	0.551	7.429	78.23	0.623	0.615	6.880	14.25
6	76	0.641	0.496	6.454	63.48	0.710	0.595	5.783	19.64
7	78	0.805	0.321	10.935	66.69	0.895	0.424	10.075	15.17
8	78	0.921	0.474	9.307	66.69	0.958	0.545	8.663	13.50
9	85	0.884	0.751	7.680	78.23	0.902	0.759	7.569	3.21
10	66	0.025	-0.264	16.483	48.56	0.730	-0.041	14.957	17.64
11	66	0.013	-0.231	13.397	48.56	0.785	0.043	11.812	22.26
12	77	0.660	0.305	10.284	65.08	0.758	0.419	9.408	16.40
13	67	0.001	-1.296	8.240	49.96	0.207	-0.497	6.653	34.80
14	67	0.092	-1.120	9.828	49.96	0.413	-0.747	8.922	17.59
15	67	0.030	-1.157	8.710	49.96	0.304	-0.589	7.476	26.33
16	67	0.056	-0.349	9.536	49.96	0.441	0.034	8.071	28.39

Table 6.3 (continued)

Plot No.	CN_{HT} associated to λ=0.20				CN_{HT} associated to λ=0.03				r^2 (%)
	$CN_{HT0.20}$	R^2	E	RMSE (mm)	$CN_{HT0.03}$	R^2	E	RMSE (mm)	
17	67	0.023	-0.504	8.204	49.96	0.351	0.030	6.588	35.51
18	67	0.134	-0.263	12.027	49.96	0.591	-0.023	10.822	19.00
19	58	0.040	-1.376	5.484	38.16	0.300	-0.513	4.377	36.32
20	58	0.001	-1.160	8.189	38.16	0.135	-0.932	7.743	10.56
21	58	0.000	-0.752	10.503	38.16	0.170	-0.699	10.343	3.03
22	74	0.135	-2.033	6.990	60.35	0.256	-0.905	5.539	37.19
23	74	0.290	-0.146	6.340	60.35	0.367	0.158	5.434	26.53
24	74	0.390	-0.305	5.879	60.35	0.447	0.156	4.729	35.33
Mean		0.314	-0.289	9.256	-	0.529	0.017	8.259	23.74

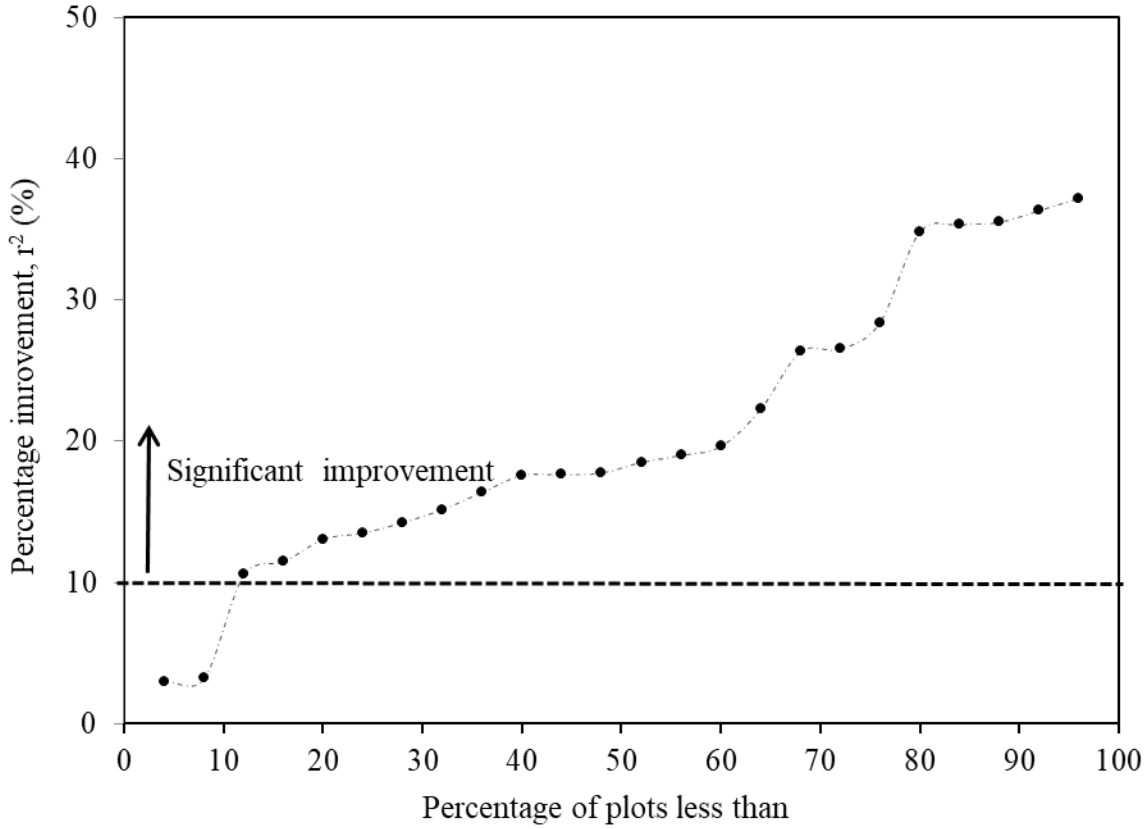

Figure 6.10 The cumulative frequency distribution of improvement in NSE using r^2 criteria

CHAPTER 7

EFFECT OF LAND USE, SOIL, AND SLOPE ON CURVE NUMBER

7.1 EFFECT OF LAND USE, INFILTRATION CAPACITY (OR SOIL TYPE), AND PLOT SLOPE ON Q AND CN

7.1.1 Utilizing P-Q data monitored during phase 1

The effect of land use, infiltration capacity, and slope on Q (or Rc) was also tested individually for their significance. To this end, plots (1-27 of Table 3.1) located in the same land use, HSG, and slope were grouped separately for checking their significance among studied variables. Since the data distribution fails to pass the normality test for the entire three individual groups (i.e. land use, HSG, and slope), non-parametric Kruskal–Wallis test was used to test significance level and the results are shown in Table 7.1. The test revealed that land uses did not show any significant difference in Rc except sugarcane which produced significantly ($p < 0.05$) higher Rc than blackgram and fallow land uses. In case of HSGs, however, HSG C had significantly higher Rc than did B and A, but the last ones did not differ from each other. In addition, slope did not show any effect on Rc as all three groups of slopes were insignificantly different from each other. Thus, Rc (or Q) is more significantly influenced by infiltration capacity (*f*c) of soil rather than land uses or slopes. The graphical representation of relationship between mean runoff (Q_m) of the plot against corresponding *f*c is shown in Figure 7.1. As seen from this figure, Q_m produced at the study plots significantly ($R^2=0.269$; $p < 0.01$) influenced by soil permeability described by plots soil *f*c. With an increase in *f*c, Q_m decreased logarithmically, and vice versa. Similarly, graphical representation of relationship between mean runoff coefficient (Rc_m) of the plot against corresponding *f*c is shown in Figure 7.2. Similar to the Figure 7.1, the correlation ($R^2=0.214$; $p < 0.05$) between Rc_m and *f*c is also significant; and with an increase in *f*c, Rc_m also decreased logarithmically, and vice versa

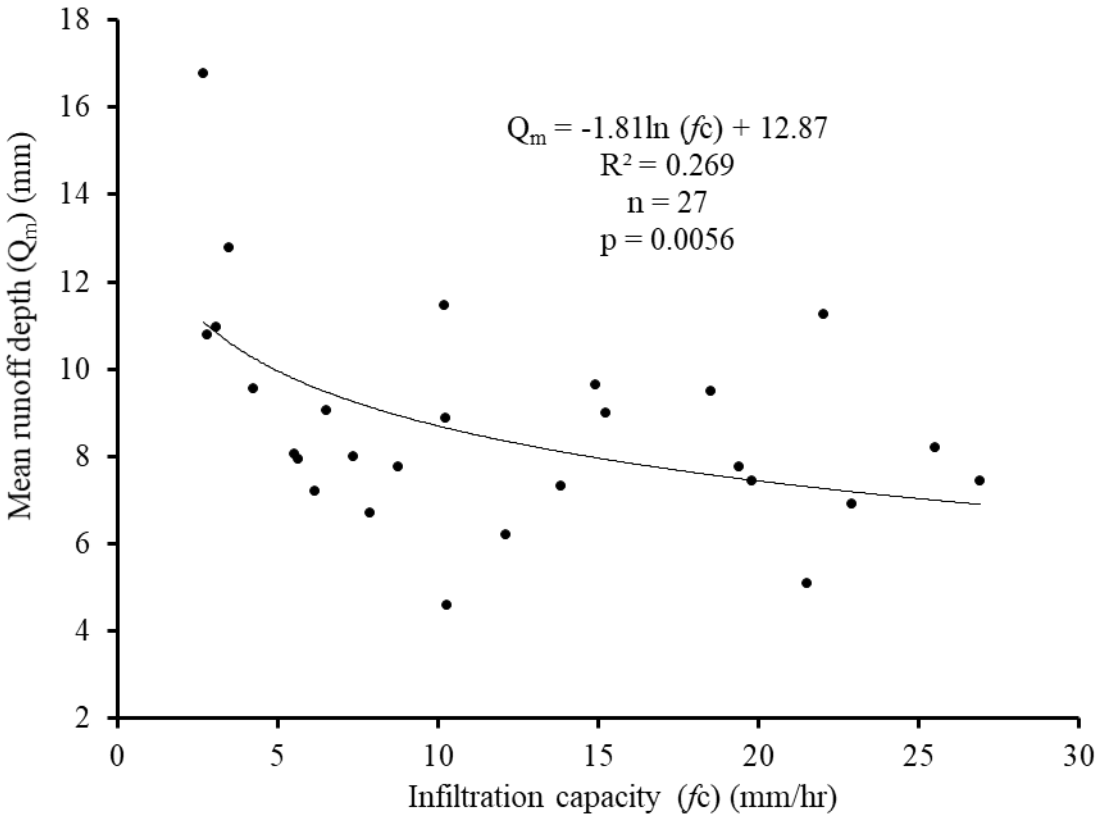

Figure 7.1 Relationship of mean runoff depth (Q_m) with Infiltration capacity (*f*c) of soil for all 27 agricultural plots data (i.e. plots 1-27 of Table 3.1).

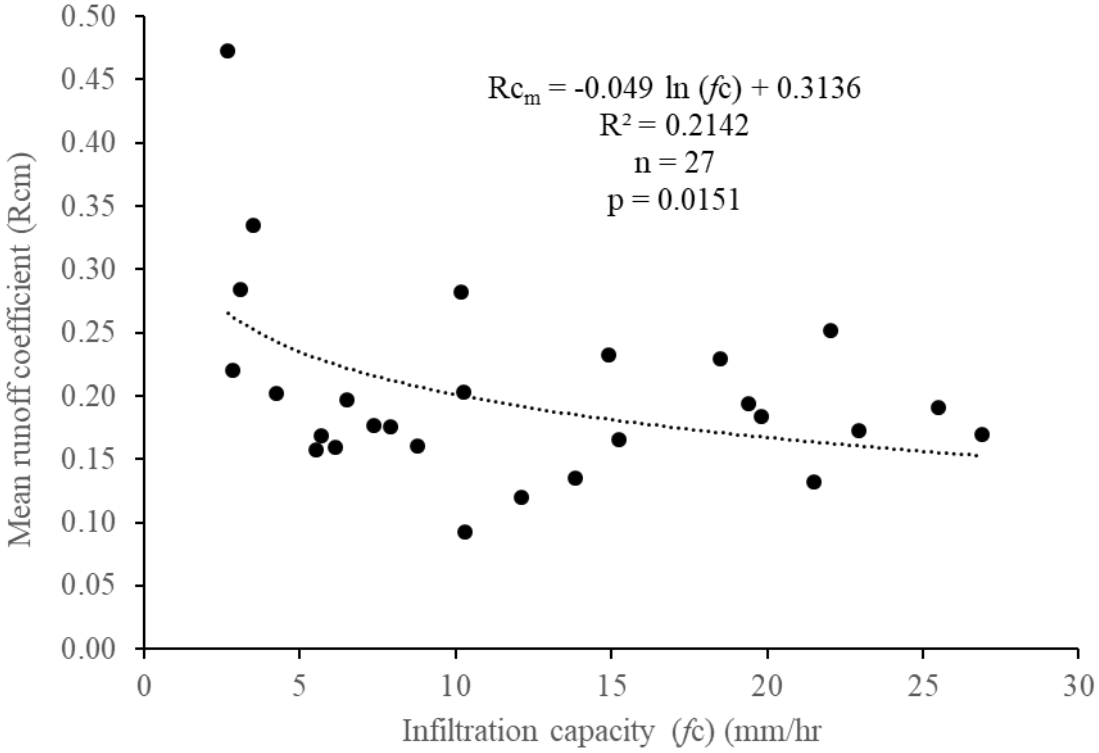

Figure 7.2 Relationship of mean runoff coefficient (Rc_m) with Infiltration capacity (*f*c) of soil for all 27 agricultural plots data (i.e. plots 1-27 of Table 3.1).

The effect of land use, *f*c, and slope on event-wise CNs was also studied using similar analysis (or tests) as discussed above for Rc. Here, standard SCS Equations 4.8 and 4.9 were employed for estimating the event wise CNs from observed P-Q event. As seen from Table 7.1, land uses did not show any significant difference in CNs except sugarcane which produced significantly ($p < 0.05$) higher CNs than black gram and fallow land uses. Furthermore, slope also did not show any effect on CNs as all three groups (i.e. 5, 3, and 1%) of slope were statistically insignificant. In the present study, CNs are seen to be influenced by *f*c of soil because all three groups of soil (i.e. A, B and C) exhibited significantly different CNs.

As already analyzed that *f*c is the main explanatory variable for Q-production in the study plots. The graphical representation of relationship of plot representative CN (at AMC-2) with *f*c is shown in Figure 7.3. In this Figure, the plots representative CN (AMC-2) was calculated employing least square fit technique i.e. Equation 5.1. As seen, an inverse relationship between CN and *f*c for all 27 study plots was detected with significant correlation ($R^2 = 0.461$, $p<0.01$). The results from this analysis support the applicability of NEH-4 tables where CNs decline with *f*c (or HSG).

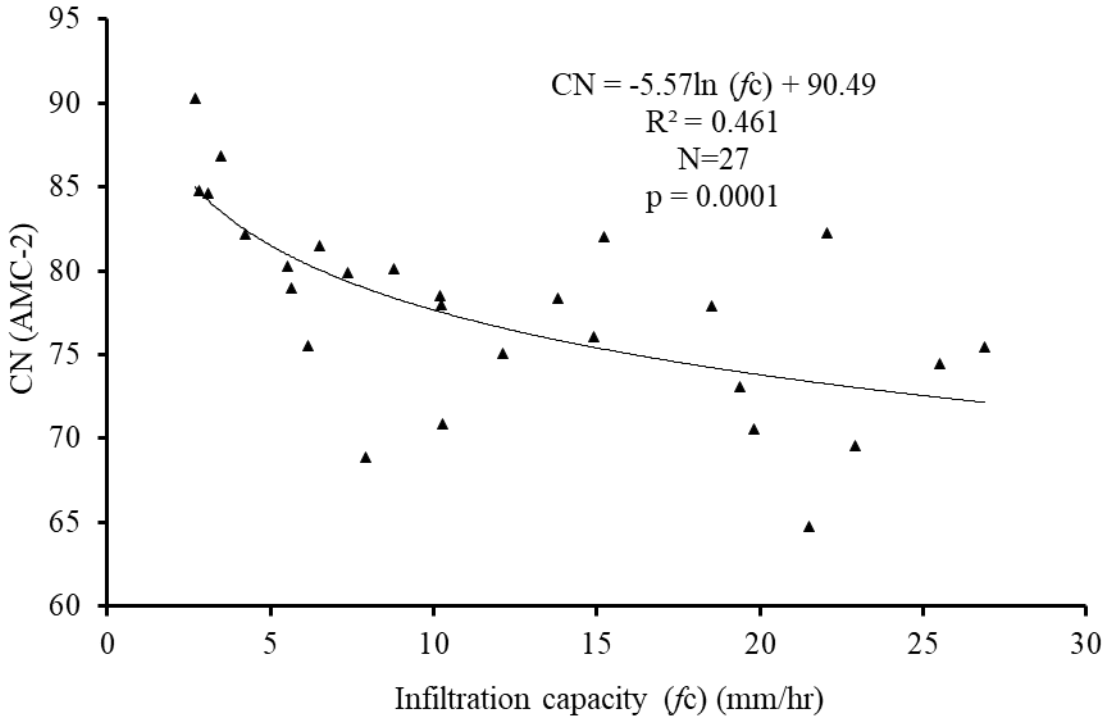

Figure 7.3 Relationship of Curve Number (CN) with Infiltration capacity (*f*c) of soil for all 27 agricultural plots data

Table 7.1 Mean event runoff coefficient (Rc) and CNs for the groups of different land uses, HSGs and slopes

Land uses group				HSG group				Slope group			
Land use type	Rc	CN	n	HSG*	Rc	CN	n	Slope (%)	Rc	CN	n
Sugarcane	0.245 a	83.66 a	126	A	0.178 a	80.26 a	210	5	0.200 a	81.99 a	115
Black gram	0.170 bc	80.99 bc	72	B	0.179 a	82.99 b	87	3	0.194 a	81.88 a	113
Maize	0.200 bca	82.40 bca	72	C	0.323 b	88.00 c	46	1	0.195 a	82.09 a	115
Fallow	0.151c	79.67 c	73								

Within one group, variables with no letter (alphabet, a, b, c) in common have significantly different Rc or CN at the 0.05 significance level (based on the Kruskal–Wallis test).

* HSGs are mainly determined by infiltration capacity: A > 7.26 mm/hr; 3.81 mm/hr < B < 7.26 mm/hr; 1.27 mm/hr < C < 3.81 mm/hr; D < 1.27 mm/hr.

Further, mean runoff coefficient of plot was derived as in Equation 3.10:

$$\text{Mean runoff coefficient } (Rc_m) = \frac{\sum_{i}^{n} \frac{Q_i}{P_i}}{n} \quad (7.1)$$

where Q_i is the direct surface runoff for event i, P_i is the rainfall amount for event i, and n is the total number of events.

As can be seen from Table 7.2, the mean runoff coefficient (Rc_m) as calculated by Equation 7.1 was higher for the plots having HSGs C followed by B and A. This pattern for Rc_m was followed by nearly all the plots with few exceptions (i.e. plots 12 and 21). Rc_m of the plots ranged from 0.093 to 0.473.

Runoff coefficients (Rc) for individual rainfall events also varied considerably from less than 0.005 to over 0.60, depending on the nature of the event and plot type. The Kolmogorov–Smirnov test revealed event wise Rc for all the individual plots not to be normally distributed. The non-parametric Kruskal–Wallis test (Kruskal and Wallis, 1952) revealed statistical significance difference between events Rc of all 27 study plots.

7.1.2 Utilizing P-Q data monitored during phase 2

This section discusses the effects of plot slope, land use/land cover and antecedent soil moisture on runoff generation and hence CN using the observed data from experimental plot nos. 10-18 from Table 3.2 (i.e. P-Q data monitored during phase 2). The CN were derived using standard SCS Equations. 4.8 and 4.9, and results are shown in Tables 7.3-7.5.

(a) Effect of plot Slope on Runoff and Curve Number

The graphs were drawn between observed rainfall and runoff for Maize crop, Finger millet crop and fallow land having slope 8%, 12% and 16% as shown in Figures 7.4, 7.5 and 7.6, respectively. The plotting of rainfall against runoff for maize, finger millet and fallow land for 8%, 12% and 16% slope shows that as the slope is increasing, the runoff is also increasing for a given HSG and crop type.

The event wise derived Curve number for each land use are given in Tables 7.3-7.5. The plots representative CN (i.e. AMC-II) were also calculated following Hjelmfelt et al. (1981) criterion, and results are given in Table 7.6. As can be seen from Figure 7.7, that 16% slope generated more runoff (or CN) than other slopes for given land use and soil.

Table 7.2 Coefficients of determination (R^2) of daily runoff (Q) (mm) and runoff coefficients (Rc) with previous day soil moisture (θ) (%), along with mean runoff coefficient (Rc_m) for each plot

Plot No.	n	Runoff (Q) depth		Runoff coefficient (Rc)		Rc_m
		P	θ	P	θ	
1	18	0.722*	0.075	0.415*	0.066	0.177
2	18	0.680*	0.056	0.431*	0.057	0.161
3	18	0.727*	0.048	0.438*	0.056	0.197
4	12	0.729*	0.028	0.552*	0.097	0.120
5	12	0.692*	0.187	0.409**	0.120	0.159
6	12	0.719*	0.188	0.483**	0.031	0.093
7	13	0.940*	0.152	0.519*	0.029	0.202
8	13	0.980*	0.115	0.742*	0.035	0.157
9	13	0.922*	0.208	0.606*	0.218	0.220
10	13	0.805*	0.035	0.646*	0.064	0.166
11	13	0.843*	0.070	0.593*	0.055	0.135
12	13	0.786*	0.153	0.375**	0.078	0.169
13	13	0.814*	0.034	0.140	0.346	0.191
14	13	0.558*	0.219	0.185	0.167	0.282
15	13	0.600*	0.080	0.148	0.228	0.232
16	11	0.737*	0.090	0.460**	0.344	0.203
17	11	0.820*	0.055	0.342	0.295	0.170
18	11	0.769*	0.093	0.451**	0.322	0.252
19	11	0.621*	0.079	0.313	0.284	0.132
20	11	0.639*	0.113	0.261	0.458	0.194
21	11	0.641*	0.037	0.359	0.231	0.229
22	13	0.435**	0.061	0.079	0.136	0.173
23	11	0.411**	0.124	0.364**	0.365	0.176
24	13	0.516*	0.391	0.381**	0.395	0.184
25	11	0.828*	0.071	0.605*	0.318	0.473
26	11	0.812*	0.053	0.688*	0.219	0.335
27	11	0.722*	0.387	0.616*	0.518	0.284

(* significant at 0.01 level; ** significant at 0.05 level)

Table 7.3 Computation of CN for plot nos. 10-12 of phase 2.

Event No.	Date	Rainfall (mm)	Runoff (Q) mm			Potential Max. Retention (S)			Curve Number (CN)		
			8%	12%	16%	8%	12%	16%	8%	12%	16%
			plot-12	plot-11	plot-10	plot-12	plot-11	plot-10	plot-12	plot-11	plot-10
1	19-Jun-17	44.00	14.21	30.12	31.92	48.49	14.87	12.47	83.97	94.47	95.32
2	26-Jun-17	34.20	13.40	26.45	24.78	30.71	7.67	9.72	89.21	97.07	96.31
3	28-Jun-17	75.20	48.66	50.94	64.03	29.43	26.14	10.39	89.62	90.67	96.07
4	29-Jun-17	17.70	6.39	10.56	9.17	17.41	8.32	10.80	93.59	96.83	95.92
5	30-Jun-17	15.00	7.06	9.83	13.03	10.62	5.68	1.81	95.99	97.81	99.29
6	6-Jul-17	36.40	19.12	28.68	27.23	21.70	7.56	9.28	92.13	97.11	96.48
7	24-Jul-17	14.00	0.67	4.14	5.53	41.83	16.75	12.45	85.86	93.82	95.33
8	2-Aug-17	79.50	33.20	42.51	44.31	66.06	45.98	42.68	79.36	84.67	85.61
9	3-Aug-17	9.60	1.96	3.35	4.57	15.28	9.79	6.68	94.33	96.29	97.44
10	7-Aug-17	27.40	18.86	20.94	25.11	9.12	6.45	2.03	96.54	97.52	99.21
11	10-Aug-17	43.40	19.93	26.87	35.90	31.80	18.82	7.11	88.87	93.10	97.28
12	19-Aug-17	22.30	2.94	9.19	9.89	45.69	18.83	17.14	84.75	93.10	93.68
13	22-Aug-17	58.10	28.95	30.90	43.40	37.72	33.92	14.89	87.07	88.22	94.46
14	23-Aug-17	15.50	2.32	2.54	6.71	29.75	28.29	12.31	89.51	89.98	95.38
15	25-Aug-17	61.80	32.28	36.59	49.78	37.19	29.51	11.59	87.23	89.59	95.64
16	1-Sep-17	44.00	14.98	20.53	34.42	46.04	31.52	9.42	84.66	88.96	96.43
17	1-Sep-17	23.00	14.65	18.81	20.90	9.35	4.00	1.87	96.45	98.45	99.27
18	2-Sep-17	61.10	26.27	33.22	24.89	48.91	34.32	52.37	83.85	88.10	82.91
19	3-Sep-17	26.00	19.06	13.51	17.68	7.11	15.78	8.95	97.28	94.15	96.60

Table 7.4 Computation of CN for plot nos. 13-15 of phase 2.

Event No.	Date	Rainfall (mm)	Runoff (Q) mm			Potential Max. Retention (S)			Curve Number (CN)		
			8%	12%	16%	8%	12%	16%	8%	12%	16%
			plot-15	plot-14	plot-13	plot-15	plot-14	plot-13	plot-15	plot-14	plot-13
1	19-Jun-17	44.00	13.03	17.75	27.20	52.56	38.14	19.16	82.85	86.94	92.99
2	26-Jun-17	34.20	11.59	15.06	26.17	35.94	26.53	8.00	87.60	90.54	96.95
3	28-Jun-17	75.20	49.82	54.61	68.35	27.73	21.24	6.09	90.16	92.28	97.66
4	29-Jun-17	17.70	10.56	7.78	13.34	8.32	13.77	4.40	96.83	94.86	98.30
5	30-Jun-17	15.00	6.78	9.14	12.33	11.24	6.74	2.54	95.76	97.41	99.01
6	6-Jul-17	36.40	13.34	24.29	30.01	35.22	13.17	6.07	87.82	95.07	97.67
7	24-Jul-17	14.00	2.75	2.75	2.75	22.87	22.87	22.87	91.74	91.74	91.74
8	2-Aug-17	79.50	24.17	34.87	41.53	92.74	62.02	47.82	73.25	80.37	84.15
9	3-Aug-17	9.60	0.57	4.74	6.13	26.88	6.32	3.88	90.43	97.57	98.50
10	7-Aug-17	27.40	17.47	20.25	25.80	11.11	7.30	1.39	95.81	97.21	99.46
11	10-Aug-17	43.40	22.01	26.18	33.12	27.40	19.93	10.27	90.26	92.72	96.12
12	19-Aug-17	22.30	1.55	5.72	10.44	59.40	30.07	15.89	81.05	89.41	94.11
13	22-Aug-17	58.10	16.31	25.34	35.06	72.73	45.66	26.65	77.74	84.76	90.50
14	23-Aug-17	15.50	2.54	3.15	3.93	28.29	24.77	21.10	89.98	91.12	92.33
15	25-Aug-17	61.80	28.42	38.67	50.47	45.19	26.18	10.82	84.89	90.66	95.91
16	1-Sep-17	44.00	10.81	18.98	17.75	61.38	35.09	38.14	80.54	87.86	86.94
17	1-Sep-17	23.00	12.56	16.04	16.73	12.81	7.37	6.46	95.20	97.18	97.52
18	2-Sep-17	61.10	29.05	24.05	42.94	42.59	54.54	19.12	85.64	82.32	93.00
19	3-Sep-17	26.00	6.56	9.34	20.45	35.51	25.71	5.43	87.73	90.81	97.91

Table 7.5 Computation of CN for plot nos. 16-18 of phase 2.

Event No.	Date	Rainfall (mm)	Runoff (Q) mm			Potential Max. Retention (S)			Curve Number (CN)		
			8%	12%	16%	8%	12%	16%	8%	12%	16%
			plot-18	plot-17	plot-16	plot-18	plot-17	plot-16	plot-18	plot-17	plot-16
1	19-Jun-17	44.00	12.31	20.39	29.56	55.25	31.83	15.64	82.13	88.86	94.20
2	26-Jun-17	34.20	8.12	18.12	20.62	48.97	20.09	15.72	83.84	92.67	94.17
3	28-Jun-17	75.20	45.98	56.87	64.92	33.53	18.42	9.47	88.34	93.24	96.41
4	29-Jun-17	17.70	5.00	13.34	14.72	22.03	4.40	2.81	92.02	98.30	98.91
5	30-Jun-17	15.00	5.39	10.17	10.94	14.84	5.21	4.17	94.48	97.99	98.38
6	6-Jul-17	36.40	17.79	26.07	32.29	24.35	10.75	3.72	91.25	95.94	98.56
7	24-Jul-17	14.00	1.36	2.75	4.14	32.92	22.87	16.75	88.52	91.74	93.82
8	2-Aug-17	79.50	22.09	38.20	40.14	100.41	54.56	50.55	71.67	82.32	83.40
9	3-Aug-17	9.60	0.57	3.35	5.71	26.88	9.79	4.53	90.43	96.29	98.25
10	7-Aug-17	27.40	16.00	13.30	20.25	13.45	18.52	7.30	94.97	93.20	97.21
11	10-Aug-17	43.40	20.07	19.93	34.65	31.49	31.80	8.49	88.97	88.87	96.77
12	19-Aug-17	22.30	4.61	6.42	14.94	35.22	27.33	7.99	87.82	90.28	96.95
13	22-Aug-17	58.10	23.26	33.67	35.90	50.85	28.95	25.32	83.32	89.77	90.93
14	23-Aug-17	15.50	2.54	5.32	4.54	28.29	16.09	18.70	89.98	94.04	93.14
15	25-Aug-17	61.80	38.67	31.45	45.61	26.18	38.82	16.52	90.66	86.74	93.89
16	1-Sep-17	44.00	12.20	17.75	30.70	55.68	38.14	14.07	82.02	86.94	94.75
17	1-Sep-17	23.00	14.65	13.81	20.90	9.35	10.66	1.87	96.45	95.97	99.27
18	2-Sep-17	61.10	33.22	25.72	48.50	34.32	50.27	12.27	88.10	83.48	95.39
19	3-Sep-17	26.00	13.51	10.68	19.06	15.78	22.07	7.11	94.15	92.01	97.28

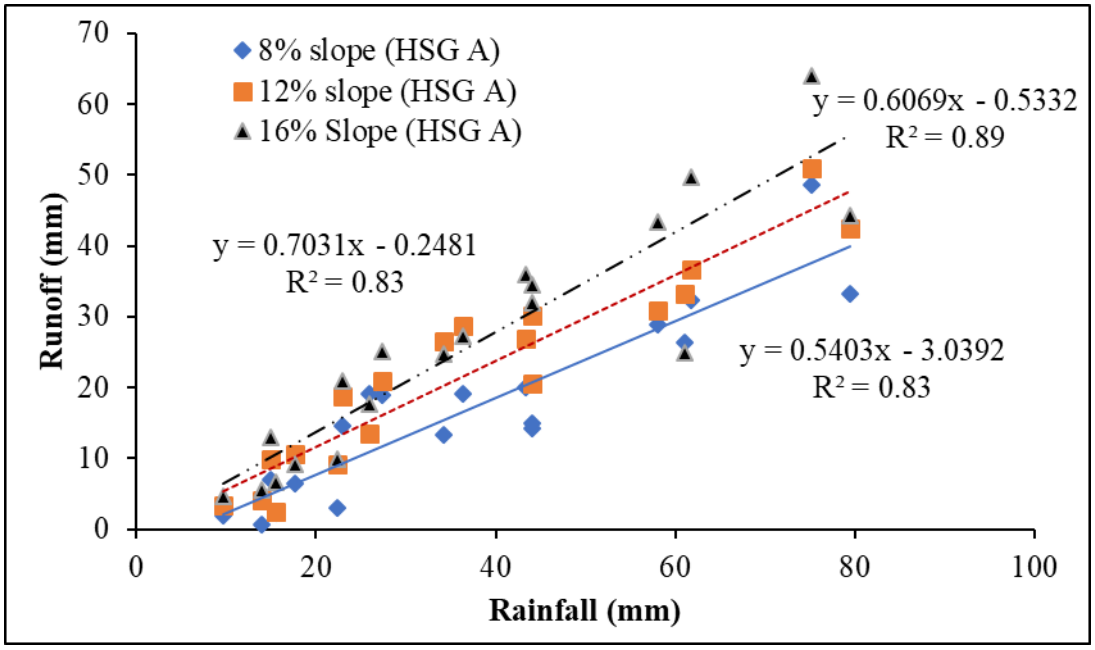

Figure 7.4 Rainfall vs runoff graph for Maize crop

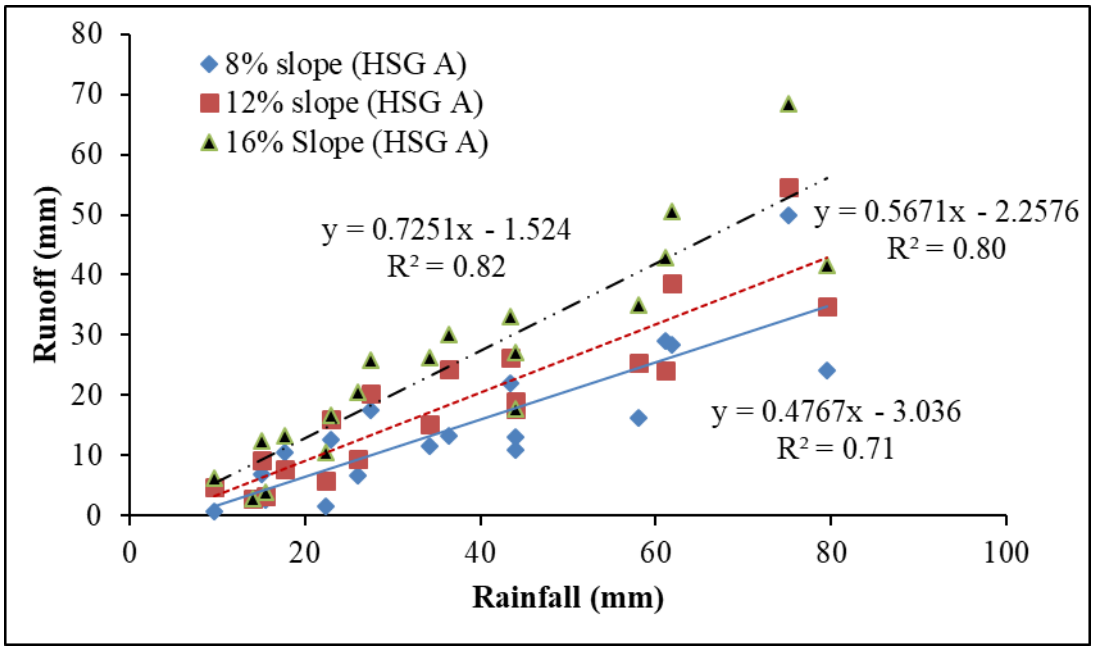

Figure 7.5 Rainfall vs runoff graph for Finger millet crop

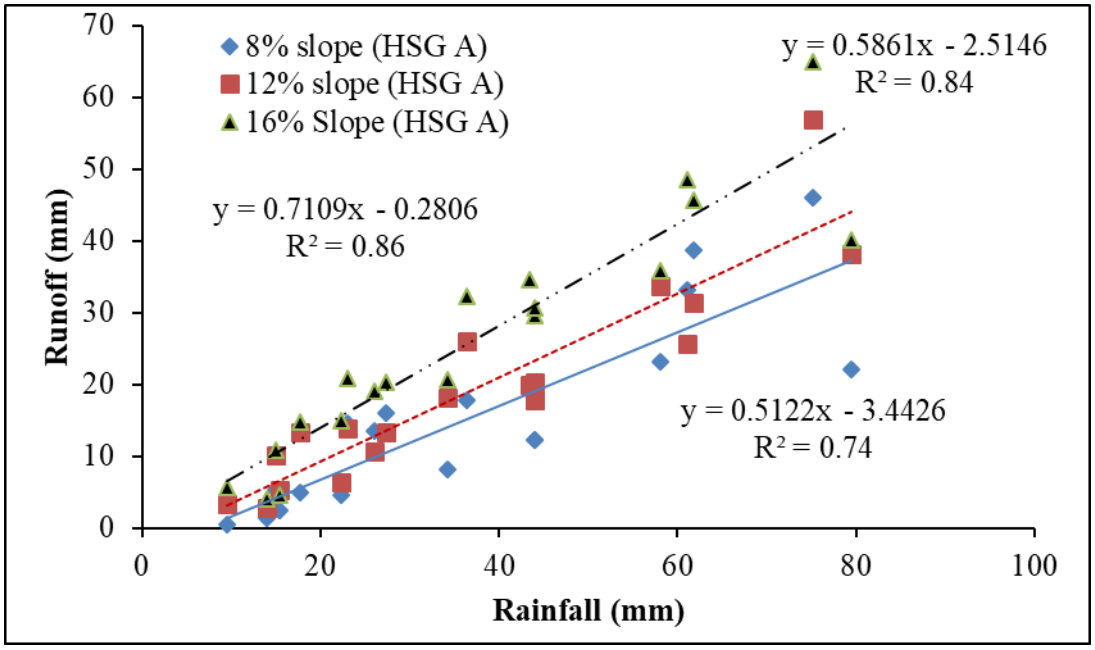

Figure 7.6 Rainfall vs runoff graph for Fallow land

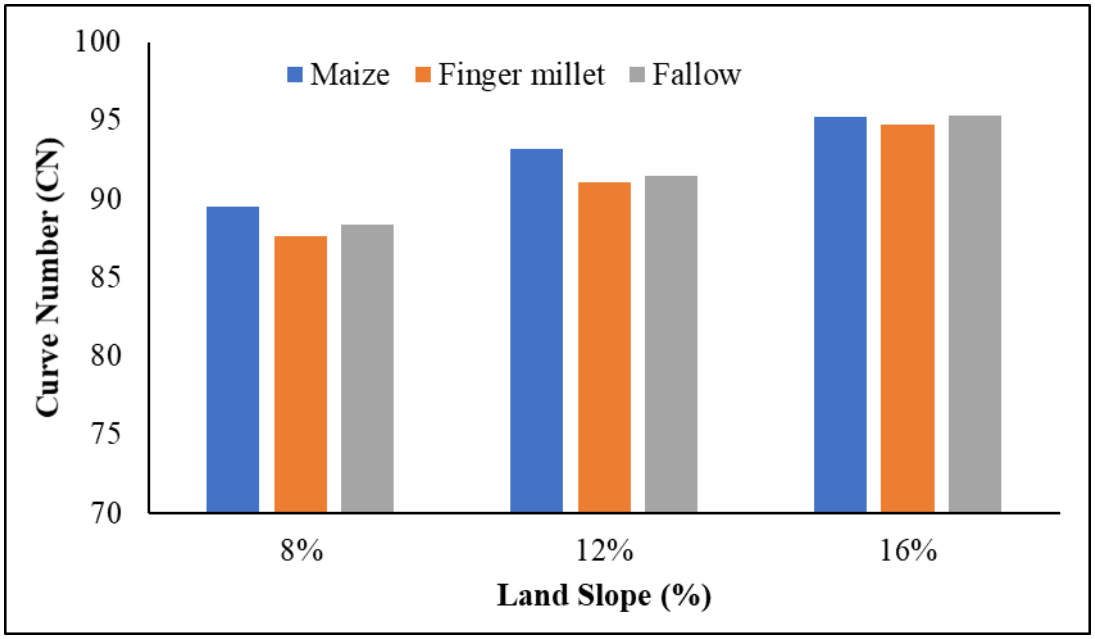

Figure 7.7 Effect of slope on Curve Number

The relation between curve number and slope (%) at different AMC condition of different crop viz. maize, Finger millet and Fallow land are also shown in Figures 7.8, 7.9 and 7.10, respectively. It can be easily inferred from these Figures that higher slope shows higher curve number and higher AMC value also shows higher curve number and vice versa.

Table 7.6 Different AMCs CN calculation following Hjelmfelt et al. (1981) criterion

Rank (m)	Descending Order CNs value for different Slope and having different crops									Probability of Exceedence = m/(n+1)*100	AMC
	Plot @8%			Plot @12%			Plot @16%				
	Plot no:12	Plot no:15	Plot no:18	Plot no:11	Plot no:14	Plot no:17	Plot no:10	Plot no:13	Plot no:16		
	Maize	Finger Millet	Fallow Land	Maize	Finger Millet	Fallow Land	Maize	Finger Millet	Fallow Land		
1	97.28	96.83	96.45	98.45	97.57	98.30	99.29	99.46	99.27	5.0	
2	96.54	95.81	94.48	97.81	97.41	97.99	99.27	99.01	98.91	10.0	III
3	96.45	95.76	94.15	97.52	97.21	92.01	99.21	98.50	98.38	15.0	
4	95.99	95.20	92.02	96.83	97.18	96.29	97.28	98.30	98.25	20.0	
5	94.33	91.74	90.66	96.29	94.86	95.97	96.60	97.91	96.41	25.0	
6	89.51	90.43	90.43	94.15	95.07	95.94	96.48	97.67	97.28	30.0	
7	93.59	90.26	89.98	93.82	92.72	83.48	96.43	97.52	97.21	35.0	
8	92.13	89.98	88.34	97.11	91.74	94.04	96.31	96.95	96.77	40.0	
9	87.23	87.82	88.52	93.10	90.81	93.20	95.92	96.12	95.39	45.0	
10	89.21	87.73	94.97	93.10	90.66	93.24	95.64	95.91	94.20	50.0	II
11	88.87	87.60	88.10	97.07	90.54	86.74	95.38	94.11	94.17	55.0	
12	87.07	90.16	87.82	90.67	89.41	91.74	95.33	97.66	93.89	60.0	
13	89.62	84.89	88.97	89.98	92.28	90.28	95.32	93.00	93.82	65.0	
14	85.86	85.64	83.84	89.59	86.94	89.77	94.46	92.99	98.56	70.0	
15	84.75	82.85	83.32	88.96	91.12	88.87	96.07	92.33	96.95	75.0	
16	84.66	81.05	82.02	94.47	82.32	86.94	93.68	91.74	94.75	80.0	
17	83.97	80.54	91.25	88.22	84.76	88.86	97.44	90.50	93.14	85.0	
18	83.85	77.74	82.13	88.10	87.86	92.67	85.61	86.94	90.93	90.0	I
19	79.36	73.25	71.67	84.67	80.37	82.32	82.91	84.15	83.40	95.0	
CNIII	96.54	95.81	94.48	97.81	97.41	97.99	99.27	99.01	98.91		
CNII	88.87	87.60	88.10	97.07	90.54	86.74	95.38	94.11	94.17		
CNI	83.85	77.74	82.13	88.10	87.86	92.67	85.61	86.94	90.93		

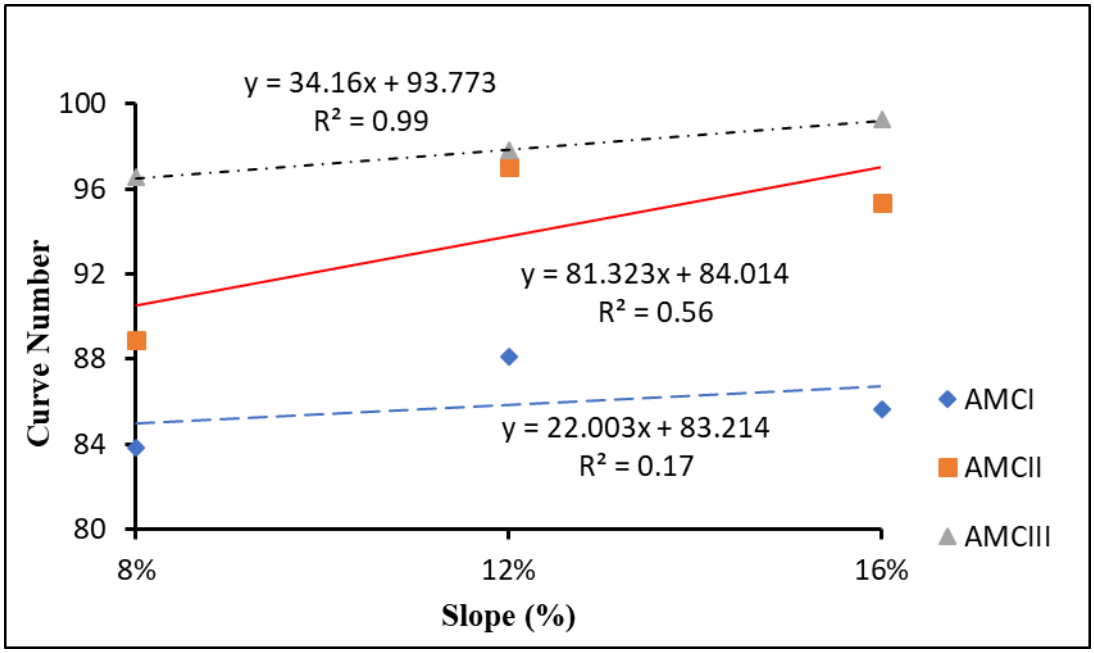

Figure 7.8 Effect of slope on Curve number at AMC condition of Maize

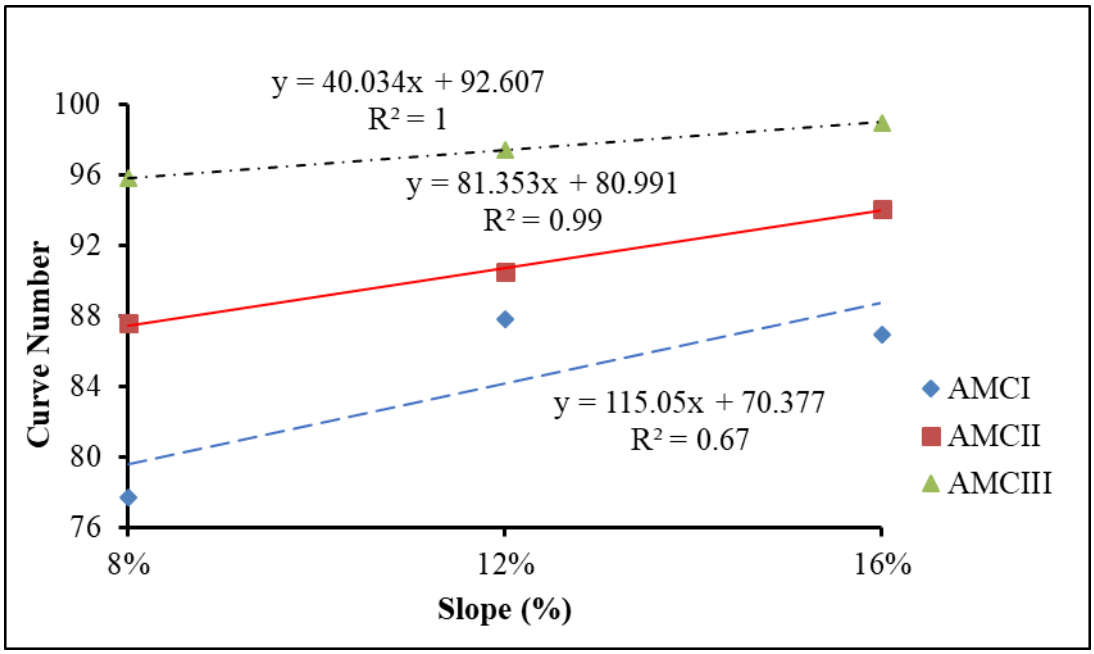

Figure 7.9 Effect of slope on Curve number at AMC condition of Finger millet

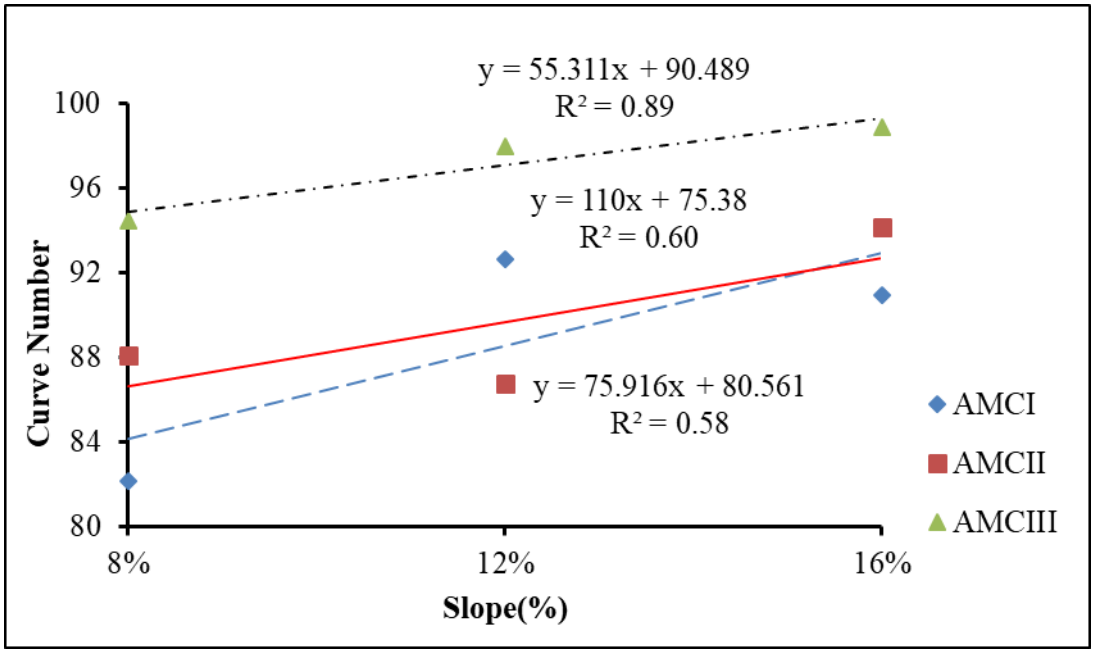

Figure 7.10 Effect of slope on Curve number at AMC condition of the Fallow land

(b) Effect of land use on Curve Number

The relation between Curve Number and land use at different slopes is shown in Figure 7.11. As seen, Maize Crop generates more runoff than Finger millet crops and fallow land for same slope and soil. In this study, for the slope of 16%, Maize land had the highest runoff and CN. It was seen that fallow land produced almost equal runoff and, in turn, CN and Finger millet relatively low runoff and CN as well because of a dense canopy.

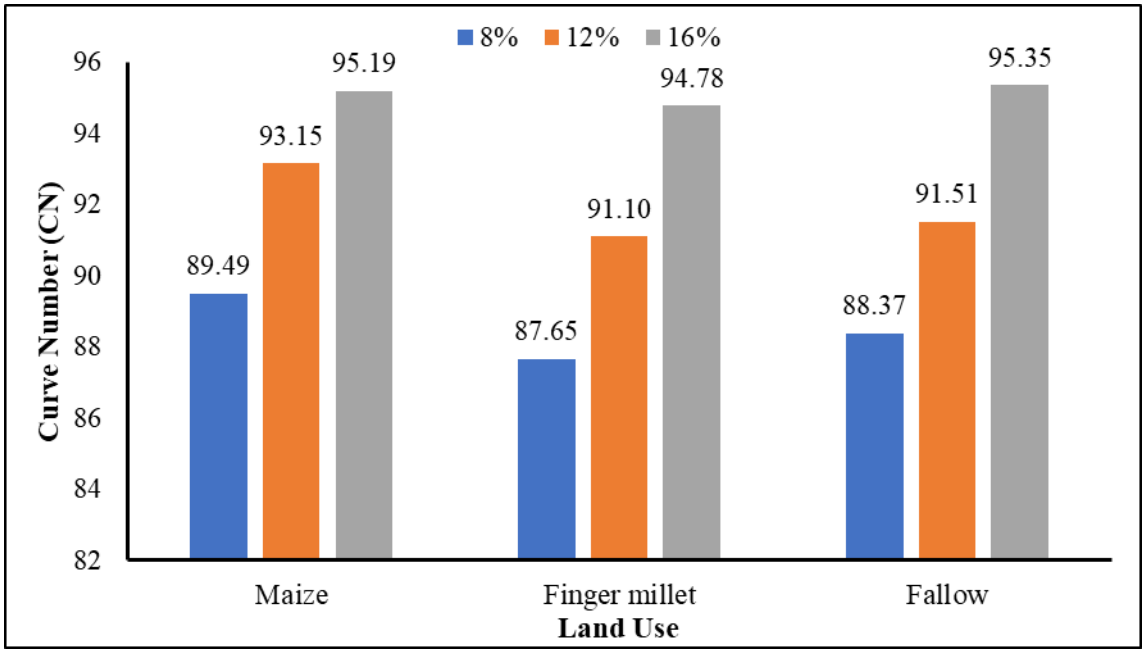

Figure 7.11 Effect of land use on Curve Number

(c) Relation between Curve Number (CN) and AMC (θ_0%)

As discussed in Chapter 3, the antecedent soil moisture content (θ_0%) was observed prior to rainfall event using TDR300. Table 7.6 indicates the values of CN of three different grades i.e. 8%, 12% and 16% of the experimental farm under three AMC conditions of different land uses; and these are plotted in Figures 7.12, 713 and 7.14 for Maize, Finger millet and Fallow land use respectively.

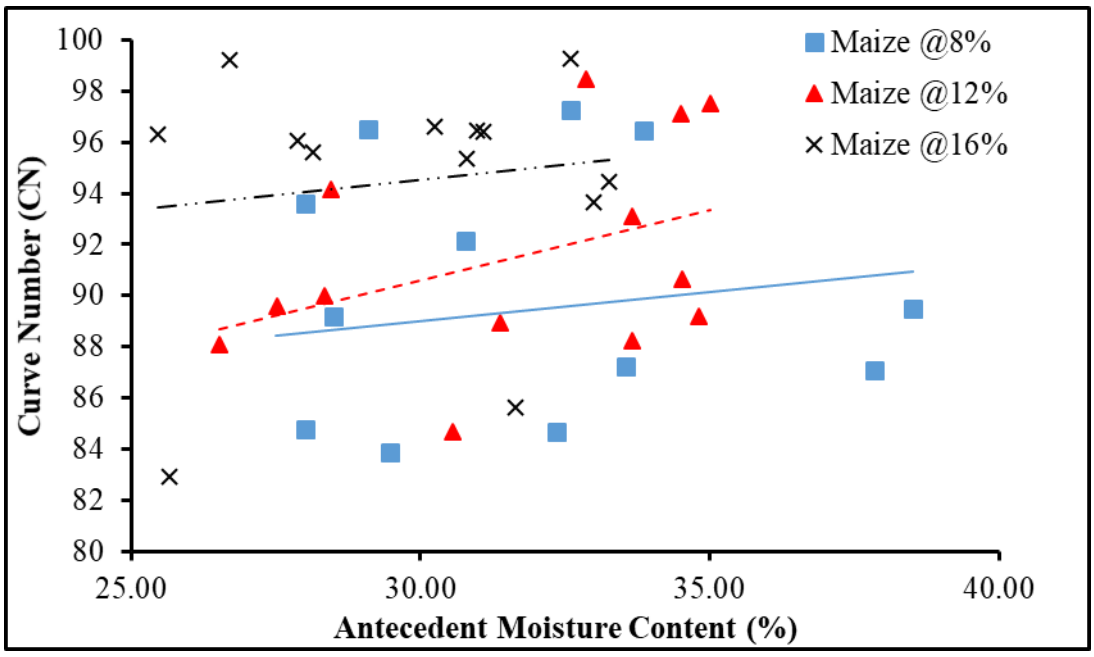

Figure 7.12 Relation between Curve number and AMC Maize Crops

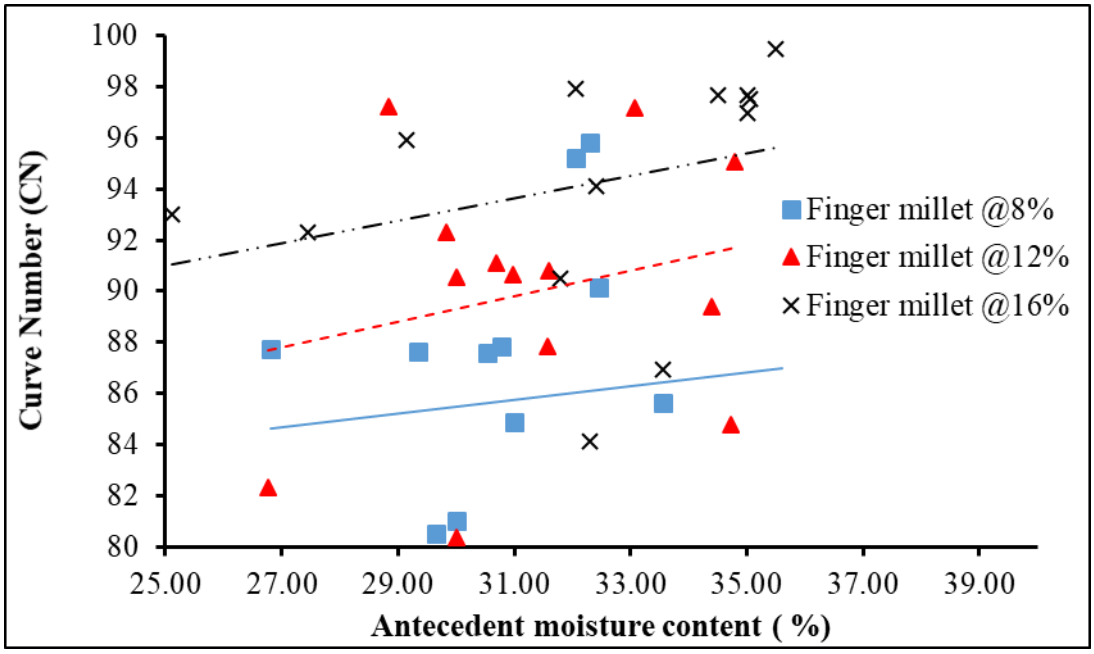

Figure 7.13 Relation between Curve Number and AMC Finger millet Crop

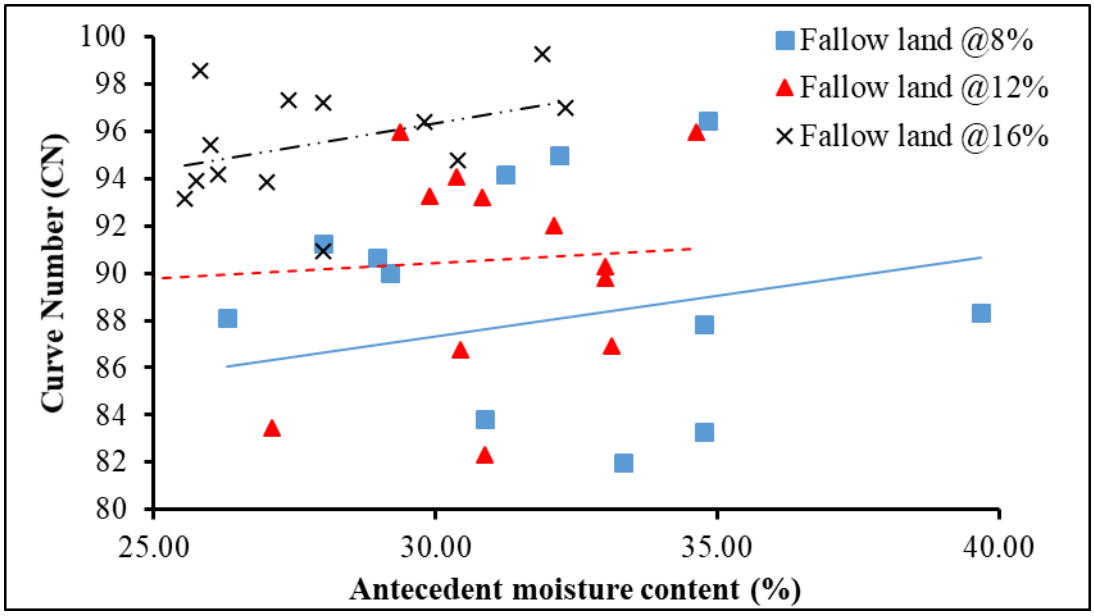

Figure 7.14 Relation between Curve Number and AMC fallow land

7.2 EVALUATION OF EXISTING SLOPE-BASED CN FORMULAE

7.2.1 Existing Slope-adjusted CN ($CN_{II\alpha}$) Models

This section briefly discusses the model based on watershed slope using CN concept as:

(a) Ajmal et al. Model:

Considering the effect of land slope and initial abstraction coefficient 'λ', Ajmal et al (2016) developed the following model. Here it is named as model 4 (M4).

$$CN_{II\alpha} = CN_{II}\left[\frac{2.2291+1.9274(\alpha-0.05)}{(\alpha-0.05)+2.2291}\right] \quad (7.2)$$

(b) Sharpley and Williams Model

Sharpley and Williams (1990) proposed a slope-adjusted CN model for estimating runoff from sloped watersheds. Here it is named as Model 5 (M5).

$$CN_{II\alpha} = 1/3\,(CN_{III} - CN_{II})\,(1 - 2\,e^{-13.86\,\alpha}) + CN_{II} \quad (7.3)$$

where, $CN_{II\alpha}$ = CN considering slope in normal conditions, CNII & CNIII are tabulated CNs with respect to normal as well as wet conditions respectively, and A= watershed average slope in m/m.

(c) Huang et al. Model

Huang et al. (2006) proposed a very simplified model for determining $CN_{II\alpha}$ basing on slopes which could range between 0.14 and 1.40.

The developed model is named here as M6.

$$CN_{II\alpha} = CN_{II}\,\frac{322.79+15.63\alpha}{\alpha+323.52} \quad (7.4)$$

In all the above cases the CN_{II} values were assumed to correspond to a 5% slope.

7.2.2 Development of slope and Ia-Based CN ($CN_{II\alpha}$) Models

This section discusses briefly the development of mathematical models for CN estimation considering watershed slope and initial abstraction. Three different models have been proposed in this study. Notably, no Slope and Ia-Based CN-conversion method exists in literature which considers the initial abstractions in their formulation whereas it also plays a major role in rainfall-runoff process.

7.2.2.1 Parameterization of the Proposed Models:

It can be observed from the existing slope adjusted $CN_{II\alpha}$ models (i.e., Ajmal et al., Sharpley and Williams, and Huang et al.) that they have different model architecture but use CNII and watershed slope (α). Here, it has been tried to develop $CNII_{(\alpha,\lambda)}$ models considering different architectures using CNII, watershed slope and initial abstraction as follows.

(a) Model No.1 (M1):

$$CN_{II(\alpha,\lambda)} = aCN_{II} + (\alpha - b\lambda)) \tag{7.5}$$

where a and b are the parameters, α = slope of the watershed (%) and λ = initial abstraction coefficient. The parameters a and b can be estimated using suitable optimization technique.

(b) Model No.2 (M2):

Model 2 (M2) was developed considering different model architecture as:

$$CN_{II(\alpha,\lambda)} = CN_{II} + (a\alpha - b\lambda)) \tag{7.6}$$

where a and b are the parameters, α = slope of the watershed (%) and λ = initial abstraction coefficient. Similar to the model M1, parameters a and b can be estimated using suitable optimization technique.

(c) Model No.3 (M3):

Finally, Model 3 (M3) was developed considering different model architecture as:

$$CN_{II\alpha} = CN_{II}\left[\frac{a + b(\alpha - \lambda)}{a + \alpha - b\lambda}\right] \tag{7.7}$$

where a and b are the parameters, α = slope of the watershed (%) and λ = initial abstraction coefficient. The parameters a and b can be estimated using suitable optimization technique.

Overall, 3 models have been developed as above at Equations 7.5, 7.6 and 7.7 considering watershed slope and initial abstraction for estimating adjusted $CNII_{(\alpha,\lambda)}$ and their efficacy is tested with those of Ajmal et al (2016) (M4), Sharpley and Williams (1990) (M5) and Huang et al. (2006) (M6).

For the conversion of $S_{0.2}$ (mm) to $S_{0.05}$ (mm) we can use the following formula,

$$S_{0.05} = 0.8187 S_{0.2}^{1.15} \tag{7.8}$$

Similarly, $CN_{0.05}$ can be computed using $CN_{0.2}$ as below:

$$CN_{0.05} = \frac{53.23}{[(100/CN_{0.2}) - 1]^{1.15} + 0.5323} \quad (7.9)$$

7.2.3 Application of $CNII_{(\alpha,\lambda)}$ Models for runoff Estimation Using NRCS-CN Method

The effect of the slope and initial abstractions on runoff estimation has been studied using naturally observed 26 (19 runoff generated + 7 non-runoff generated events) rainfall-runoff events with Maize, Finger millet and Fallow type land uses. The slope-adjusted CN equations of Ajmal et al. (2016) (Model 4), Sharpley and Williams (1990) (Model 5), and Huang et al. (2006) (Model 6) were analysed with the observed rainfall-runoff data and three new proposed models (M1-M3) as mentioned in previous section. The optimized values of the parameters a&b for all the models have been estimated by using Goal-seek as well as solver programmes in MS excel. The final expressions of the models M1-M3 along with optimized parameters values are given in Table 7.7.

Table 7.7 Proposed Models (M1-M3) with Optimized parameters

Proposed Models	Mathematical Expression	Optimized Parameter Values
Model 1 (M1)	$CN_{II\alpha} = CN_{II}\, a + (\alpha - b\lambda))$	a = 0.9863, b = 5.248
Model 2 (M2)	$CN_{II\alpha} = CN_{II} + (a\alpha - b\lambda))$	a = 0.9874, b = 5.345
Model 3 (M3)	$CN_{II\alpha} = CN_{II}\left[\frac{a + b(\alpha - \lambda)}{a + \alpha - b\lambda}\right]$	a = 4.975, b =1.0075

In application of the models, the values of slope 'α' have been taken as 8%, 12% and 16% as per the experimental field. The values of initial abstraction coefficient 'λ' are 0.05, 0.1, 0.2 & 0.3. Here, 0.3 has been considered for Indian condition. The types of land uses are Maize, Raagi (Finger Millet) and Fallow land. A total of 36 combinations considering watershed slope (α), initial abstraction (λ) and type of land use were formulated for evaluating the comparative performance of all the six models (3 proposed and 3 existing).

Tables 7.8 through 7.18 show the relative performance of all the six models M1, M2, M3, M4, M5 & M6, in which M1-M3 are the proposed models incorporating watershed slope and initial abstraction, whereas, the models M4-M6 are the existing models of Ajmal et al., Sharpley and Williams and Huang et al. based on only watershed slope. The performance was evaluated in terms of RMSE, R^2 & E. The evaluation process involved the observed data corresponding to the slope of 8%, 12% & 16% sloped plots with land uses of Maize, Raagi & Fallow land and initial abstraction ratios of 0.05, 0.1, 0.2 and 0.3.

Table 7.8 Performance Evaluation of the Six Models for Slope 16%, λ= 0.3 and 3 land uses (Fallow, Raagi and Maize)

Model	Fallow	Raagi	Maize	Fallow	Raagi	Maize	Fallow	Raagi	Maize
	RMSE			R^2			E		
M1	5.8596	5.5327	5.7460	0.9977	0.9977	0.9975	0.9668	0.9694	0.9692
M2	3.3036	3.1317	3.2400	0.9995	0.9995	0.9994	0.9894	0.9902	0.9902
M3	0.0578	0.0546	0.0564	1.0000	1.0000	1.0000	1.0000	1.0000	1.0000
M4	54.8996	18.1254	18.9869	0.3650	0.8161	0.8160	-1.9159	0.6718	0.6637
M5	0.6633	0.6779	0.6454	0.9998	0.9999	0.9999	0.9996	0.9995	0.9996
M6	1.4878	1.4414	1.3681	0.9985	0.9985	0.9987	0.9979	0.9979	0.9983

Table 7.9 Performance Evaluation of the Six Models for Slope 8%, λ= 0.3 and 3 land uses (Fallow, Raagi and Maize)

Model	Fallow	Raagi	Maize	Fallow	Raagi	Maize	Fallow	Raagi	Maize
	RMSE			R^2			E		
M1	5.5345	5.4725	5.3712	0.9974	0.9978	0.9976	0.9717	0.9741	0.9742
M2	3.1954	3.1648	3.0961	0.9993	0.9994	0.9994	0.9906	0.9913	0.9914
M3	0.0268	0.0265	0.0254	1.0000	1.0000	1.0000	1.0000	1.0000	1.0000
M4	8.5316	4.3822	3.2133	0.9470	0.9900	0.9950	0.9329	0.9834	0.9908
M5	0.6451	0.6075	0.6243	0.9998	0.9999	0.9999	0.9996	0.9997	0.9997
M6	1.3808	1.2420	1.2780	0.9991	0.9993	0.9994	0.9982	0.9987	0.9985

Table 7.10 Performance Evaluation of the Six Models for Slope 16%, λ= 0.2 and 3 land uses (Fallow, Raagi and Maize)

Model	Fallow	Raagi	Maize	Fallow	Raagi	Maize	Fallow	Raagi	Maize
	RMSE			R^2			E		
M1	4.315	4.040	4.224	0.999	0.999	0.999	0.982	0.984	0.983
M2	1.912	1.801	1.872	1.000	1.000	1.000	0.996	0.997	0.997
M3	0.050	0.047	0.049	1.000	1.000	1.000	1.000	1.000	1.000
M4	19.991	13.421	14.489	0.802	0.920	0.914	0.613	0.820	0.804
M5	1.928	2.011	1.821	0.999	0.999	0.999	0.996	0.996	0.997
M6	1.198	1.132	1.160	1.000	1.000	1.000	0.999	0.999	0.999

Table 7.11 Performance Evaluation of the Six Models for Slope 12%, λ= 0.2 and 3 land uses (Fallow, Raagi and Maize)

Model	Fallow	Raagi	Maize	Fallow	Raagi	Maize	Fallow	Raagi	Maize
	RMSE			R^2			E		
M1	4.1266	4.1503	4.1152	0.9989	0.9988	0.9985	0.9849	0.9870	0.9854
M2	1.8778	1.8714	1.8641	0.9998	0.9998	0.9998	0.9969	0.9973	0.9970
M3	0.0357	0.0354	0.0352	1.0000	1.0000	1.0000	1.0000	1.0000	1.0000
M4	22.7296	11.7405	8.4436	0.7120	0.9293	0.9655	0.5409	0.8957	0.9385
M5	1.3893	1.1184	1.3458	0.9995	0.9997	0.9996	0.9983	0.9991	0.9984
M6	0.6921	0.6851	0.6811	1.0000	1.0000	1.0000	0.9996	0.9996	0.9996

Table 7.12 Performance Evaluation of the Six Models for Slope 8%, λ= 0.2 and 3 land uses (Fallow, Raagi and Maize)

Model	Fallow	Raagi	Maize	Fallow	Raagi	Maize	Fallow	Raagi	Maize
	RMSE			R^2			E		
M1	4.0622	4.0061	3.9143	0.9985	0.9988	0.9987	0.9848	0.9861	0.9863
M2	1.8885	1.8648	1.8134	0.9998	0.9998	0.9998	0.9967	0.9970	0.9971
M3	0.0230	0.0227	0.0216	1.0000	1.0000	1.0000	1.0000	1.0000	1.0000
M4	37.1384	6.7717	3.9387	0.4284	0.9746	0.9946	-0.2722	0.9603	0.9861
M5	0.8222	0.7541	0.7788	0.9998	0.9999	0.9999	0.9994	0.9995	0.9995
M6	0.2763	0.2715	0.2579	1.0000	1.0000	1.0000	0.9999	0.9999	0.9999

Table 7.13 Performance Evaluation of the Six Models for Slope 16%, λ= 0.1 and 3 land uses (Fallow, Raagi and Maize)

Model	Fallow	Raagi	Maize	Fallow	Raagi	Maize	Fallow	Raagi	Maize
	RMSE			R^2			E		
M1	2.9472	2.7262	2.8780	0.9993	0.9993	0.9992	0.9916	0.9926	0.9923
M2	0.7174	0.6701	0.7003	1.0000	1.0000	1.0000	0.9995	0.9996	0.9995
M3	0.0427	0.0396	0.0415	1.0000	1.0000	1.0000	1.0000	1.0000	1.0000
M4	46.8885	12.6256	13.7641	0.3062	0.9491	0.9408	-1.1270	0.8408	0.8233
M5	3.2083	3.3790	3.0415	0.9961	0.9965	0.9972	0.9900	0.9886	0.9914
M6	2.1969	2.2838	2.1398	0.9993	0.9994	0.9995	0.9953	0.9948	0.9957

Table 7.14 Performance Evaluation of the Six Models for Slope 12%, λ= 0.1 and 3 land uses (Fallow, Raagi and Maize)

Model	Fallow	Raagi	Maize	Fallow	Raagi	Maize	Fallow	Raagi	Maize
	RMSE			R^2			E		
M1	2.8025	2.8318	2.8038	0.9994	0.9993	0.9992	0.9930	0.9939	0.9932
M2	0.7393	0.7374	0.7357	1.0000	1.0000	1.0000	0.9995	0.9996	0.9995
M3	0.0301	0.0300	0.0299	1.0000	1.0000	1.0000	1.0000	1.0000	1.0000
M4	33.8755	8.0260	7.4398	0.5996	0.9784	0.9839	-0.0199	0.9512	0.9522
M5	2.5905	2.1173	2.5405	0.9983	0.9989	0.9983	0.9940	0.9966	0.9944
M6	1.7857	1.5793	1.7677	0.9996	0.9998	0.9996	0.9972	0.9981	0.9973

Table 7.15 Performance Evaluation of the Six Models for Slope 8%, λ= 0.1 and 3 land uses (Fallow, Raagi and Maize)

Model	Fallow	Raagi	Maize	Fallow	Raagi	Maize	Fallow	Raagi	Maize
	RMSE			R^2			E		
M1	2.7670	2.7157	2.6353	0.9992	0.9994	0.9993	0.9929	0.9936	0.9938
M2	0.7801	0.7658	0.7371	0.9999	1.0000	1.0000	0.9994	0.9995	0.9995
M3	0.0194	0.0190	0.0180	1.0000	1.0000	1.0000	1.0000	1.0000	1.0000
M4	6.9808	38.0488	6.2347	0.9682	0.5291	0.9827	0.9550	-0.2536	0.9652
M5	2.2643	2.0826	2.1472	0.9984	0.9989	0.9990	0.9953	0.9962	0.9959
M6	1.6914	1.5822	1.6246	0.9993	0.9995	0.9995	0.9974	0.9978	0.9976

Table 7.16 Performance Evaluation of the Six Models for Slope 16%, λ= 0.05 and 3 land uses (Fallow, Raagi and Maize)

Model	Fallow	Raagi	Maize	Fallow	Raagi	Maize	Fallow	Raagi	Maize
	RMSE			R^2			E		
M1	2.3964	2.1441	2.2781	0.9995	0.9995	0.9995	0.9944	0.9954	0.9952
M2	0.1976	0.1838	0.1924	1.0000	1.0000	1.0000	1.0000	1.0000	1.0000
M3	0.0391	0.0360	0.0379	1.0000	1.0000	1.0000	1.0000	1.0000	1.0000
M4	13.2256	12.6393	13.8100	0.9208	0.9552	0.9458	0.8308	0.8404	0.8221
M5	1.8141	4.0669	3.6567	0.9987	0.9950	0.9960	0.9968	0.9835	0.9875
M6	0.9625	2.9972	2.7621	0.9999	0.9985	0.9988	0.9991	0.9910	0.9929

Table 7.17 Performance Evaluation of the Six Models for Slope 12%, λ= 0.05 and 3 land uses (Fallow, Raagi and Maize)

Model	Fallow	Raagi	Maize	Fallow	Raagi	Maize	Fallow	Raagi	Maize
	RMSE			R^2			E		
M1	2.2147	2.2460	2.2216	0.9996	0.9995	0.9994	0.9956	0.9962	0.9957
M2	0.2496	0.2490	0.2489	1.0000	1.0000	1.0000	0.9999	1.0000	0.9999
M3	0.0273	0.0274	0.0273	1.0000	1.0000	1.0000	1.0000	1.0000	1.0000
M4	20.2613	7.6355	7.3949	0.7871	0.9849	0.9877	0.6352	0.9559	0.9528
M5	1.3112	2.6243	3.1461	0.9996	0.9983	0.9974	0.9985	0.9948	0.9915
M6	0.5467	2.1010	2.4038	1.0000	0.9994	0.9990	0.9997	0.9967	0.9950

Table 7.18 Performance Evaluation of Six Models for Slope 8%, λ= 0.05 and 3 land uses (Fallow, Raagi and Maize)

Model	Fallow	Raagi	Maize	Fallow	Raagi	Maize	Fallow	Raagi	Maize
	RMSE			R^2			E		
M1	2.1937	2.1446	2.0708	0.9994	0.9995	0.9995	0.9956	0.9960	0.9962
M2	0.3042	0.2970	0.2836	1.0000	1.0000	1.0000	0.9999	0.9999	0.9999
M3	0.0177	0.0172	0.0162	1.0000	1.0000	1.0000	1.0000	1.0000	1.0000
M4	6.9015	10.5868	11.4047	0.9643	0.9273	0.9199	0.9561	0.9029	0.8836
M5	0.7682	2.7562	2.8412	0.9998	0.9981	0.9982	0.9995	0.9934	0.9928
M6	0.2189	2.2858	2.3508	1.0000	0.9989	0.9989	1.0000	0.9955	0.9951

It was a very extensive process for evaluating the models. It is seen that M3 Model performs best in all 36 combinations of watershed slope, initial abstraction and land uses followed by models M6 and M2. The proposed mathematical model, i.e., M1, M2 and M3 for CNII ($CNII_{(\alpha, \lambda)}$) were found to have lower values of RMSE and higher values of R^2 and ENS for all the combinations of watershed slope, initial abstraction and land use as compared to the existing models. The most striking feature of this finding is that the models M5 & M6 though also have performed well still these models are not capable of coping with initial abstraction ratio more than 0.2 and slope of 5%. Model M4 has failed to perform well in all the cases. Even in some cases, model M4, the values of RMSE and E were found to be negative.

Overall, the results found here show that the proposed models have versatility in applications and can be successfully applied for the land slope of more than 8% and for a

variable range of initial abstraction from 0.05 to 0.3. Notably, the existing models fail to perform beyond 5% slope and initial abstraction of 0.2. The statistical analysis further shows that all the three models proposed here performs better than the model of Ajmal et al. (2016). Hence, all the three models can be used in place of Ajmal et al. model for runoff estimation for a wide range of watershed slope and varying initial abstraction.

A comparison was also made between observed and computed runoff for all the six models with 36 combinations of land slope, initial abstraction and landuse. Figure 7.15, Figures 7.16 and Figures 7.17 show the best fit line drawn between observed runoff and estimated runoff for all the 6 models considering the three types of land uses and 8%, 12% and 16% slope for initial abstraction ($\lambda = 0.3$; Indian condition). It is evident from these graphs that the data of M3 follow the best fit line perfectly followed by M6 and M2 models.

To show the effect of the watershed slope and land use on models' runoff predictability, a comparison was also made between the models M1, M2 & M3 while keeping the value of initial abstraction constant ($\lambda = 0.3$). The results are shown in Figures 7.18, 7.19 and 7.20. Though calculations have been carried out for λ= 0.05, 0.1, 0.2 & 0.3, here only for 0.3 results have been shown as 0.3 is suitable as per Indian condition. It can be observed from these figures, that the watershed slope is one of the important factors followed by and Model 3 (M3) has enhanced predictability as compared to the models M1 and M2.

Figures 7.21, 7.22 and 7.23 show the bar charts of runoff estimated considering all the three types of land uses and slopes of 8%, 12% and 16% employing λ= 0.05, 0.1, 0.2 & 0.3. From the charts, it is construed that whenever initial abstraction ratio is increasing the estimated runoff is decreasing and vice-versa. Further model M3 has enhanced predictability than the models M2 and M1.

Figures 7.24 show the variation of observed CNII considering all the three types of land uses and slopes of 8%, 12% and 16%. Overall, it has been seen that the more is slope of the land, more is the value of CNII for all land use/land cover.

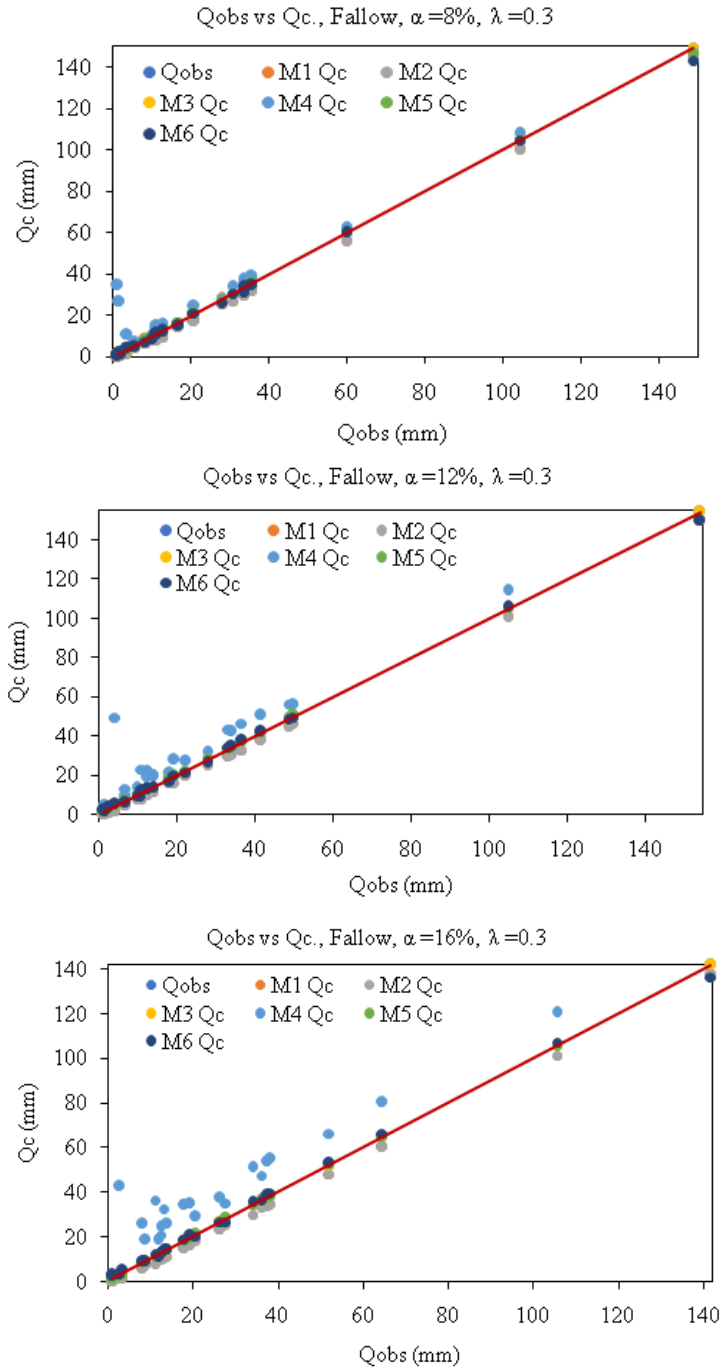

Figures 7.15 Comparison between Observed versus Computed runoff for Fallow land

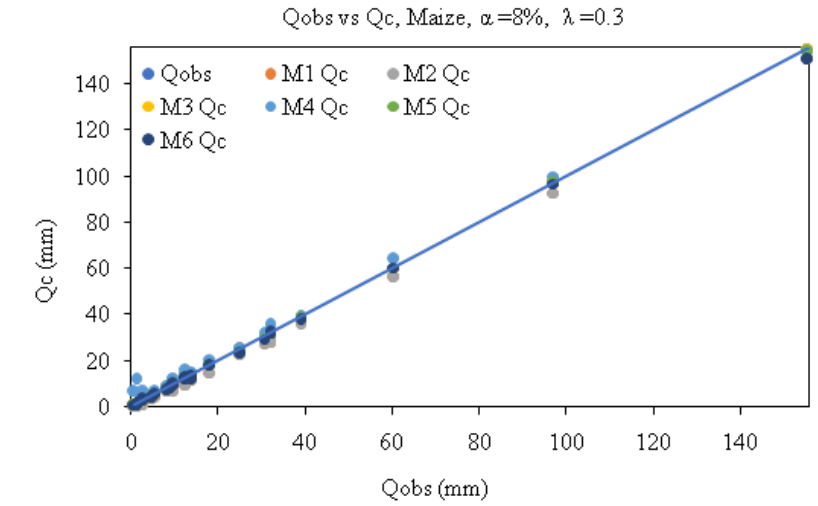

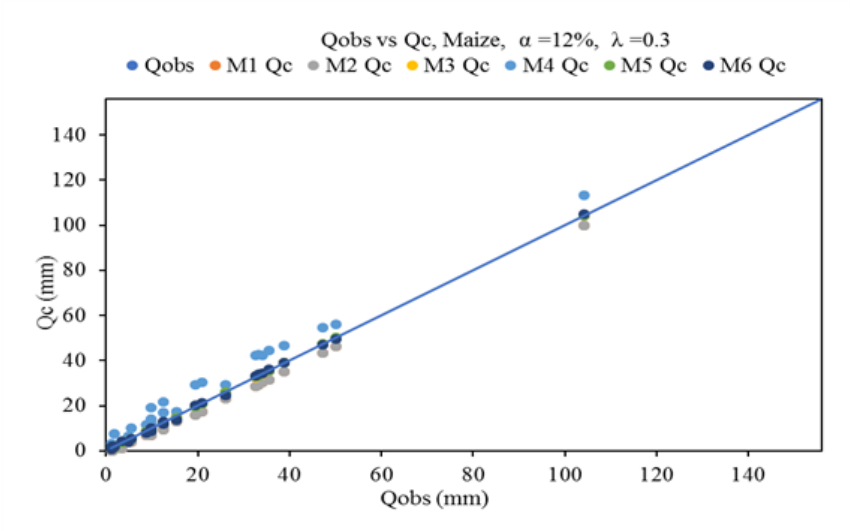

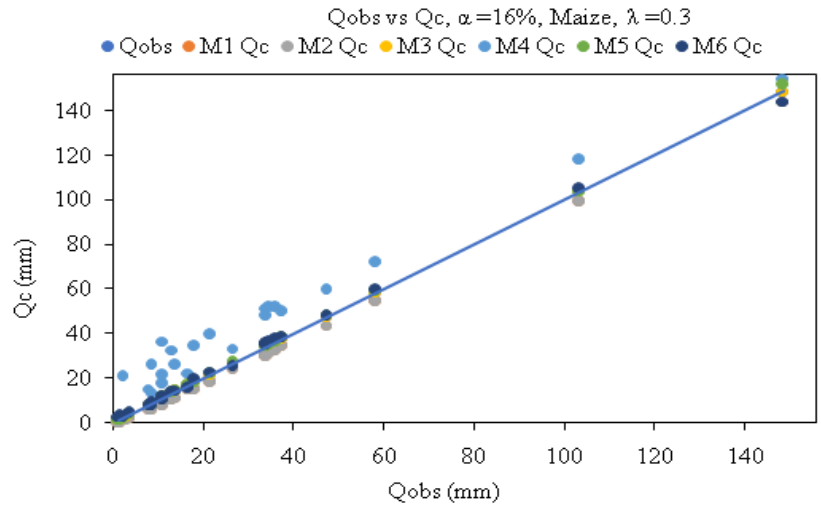

Figures 7.16 Comparison between Observed versus Computed runoff for Maize

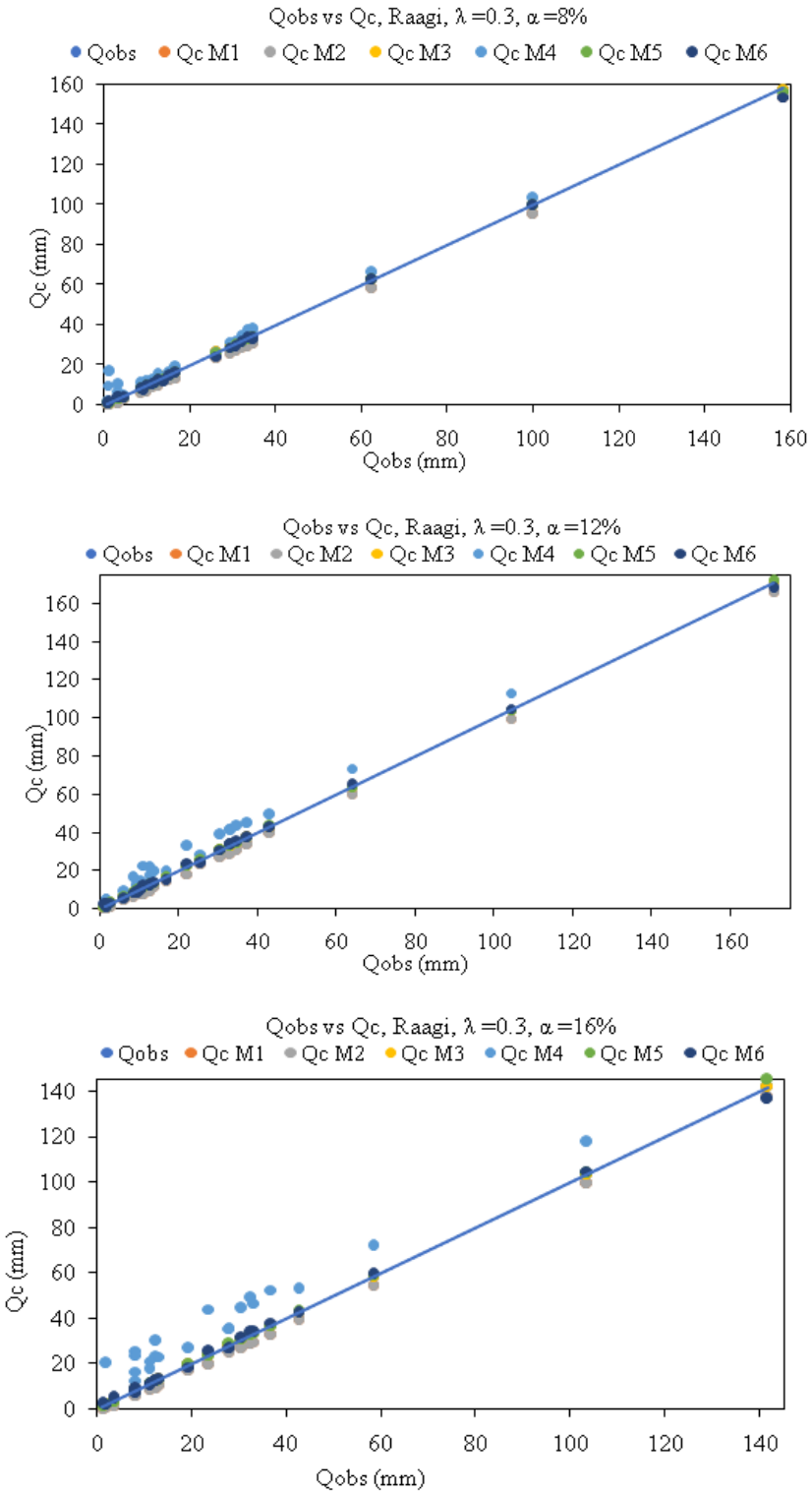

Figures 7.17 Comparison between Observed versus Computed runoff for Raagi

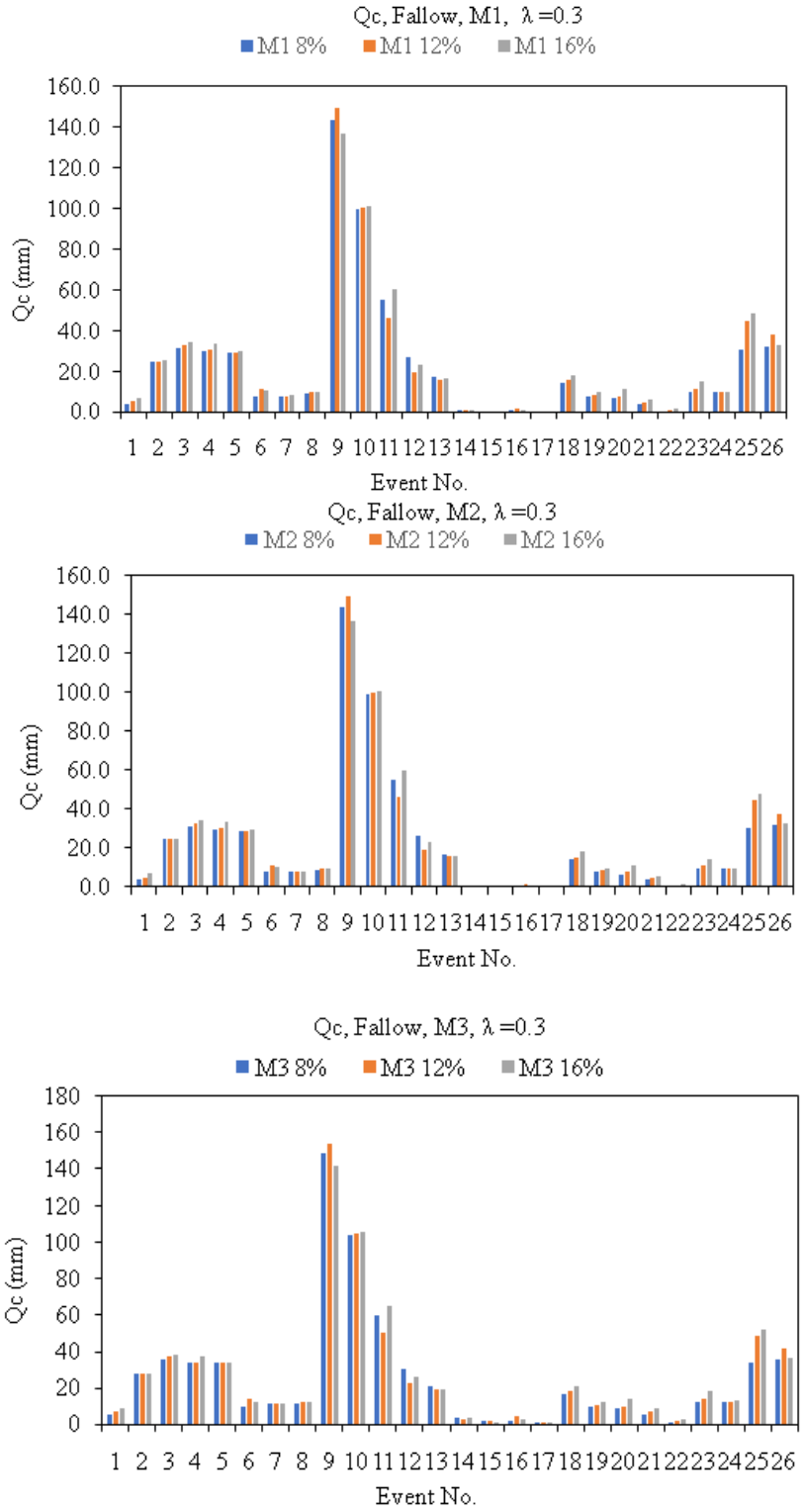

Figures 7.18 Inter-comparison of Models M1-M3 for a constant value of λ = 0.3 for Fallow land

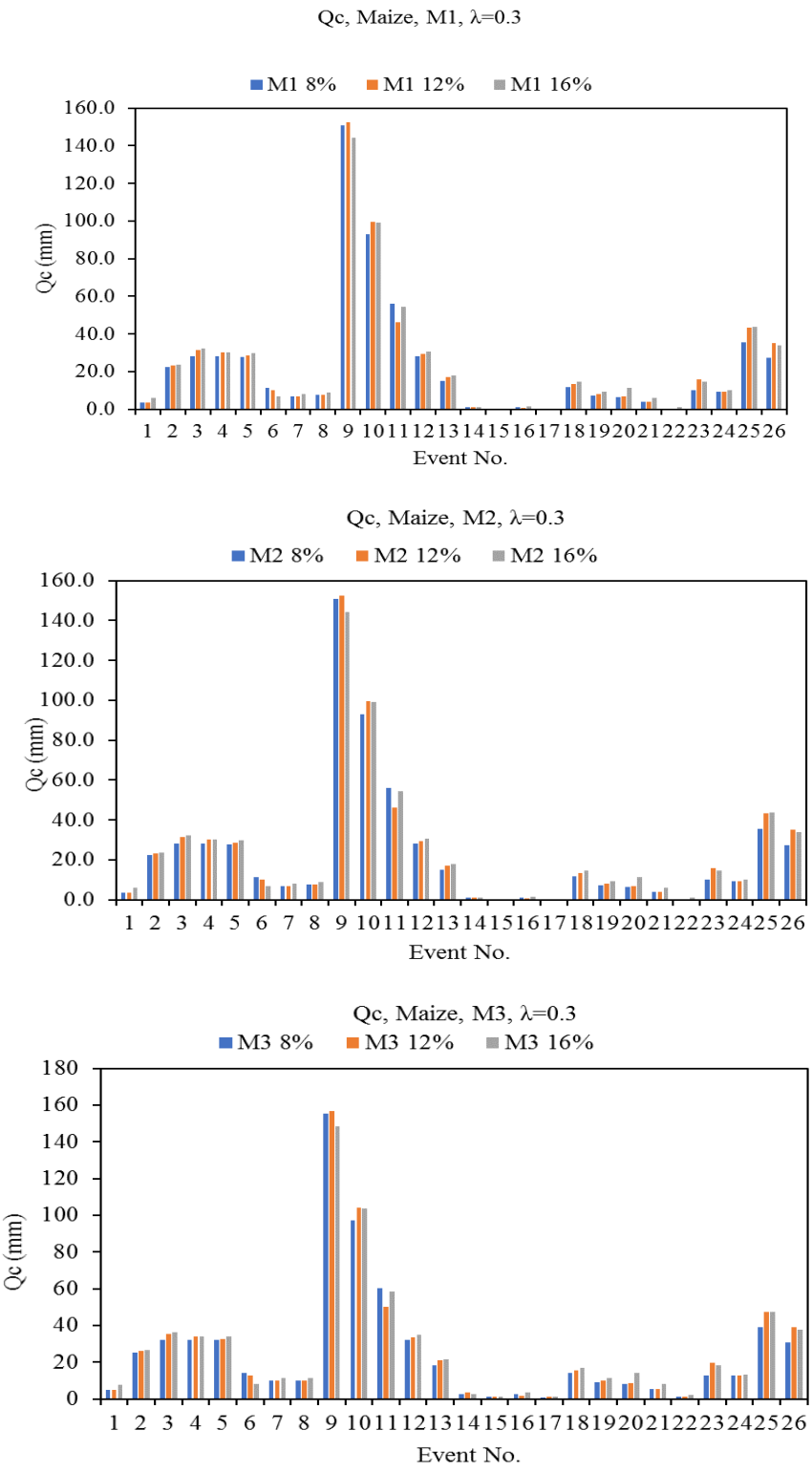

Figures 7.19 Inter-comparison of Models M1-M3 for a constant value of λ = 0.3 for Maize

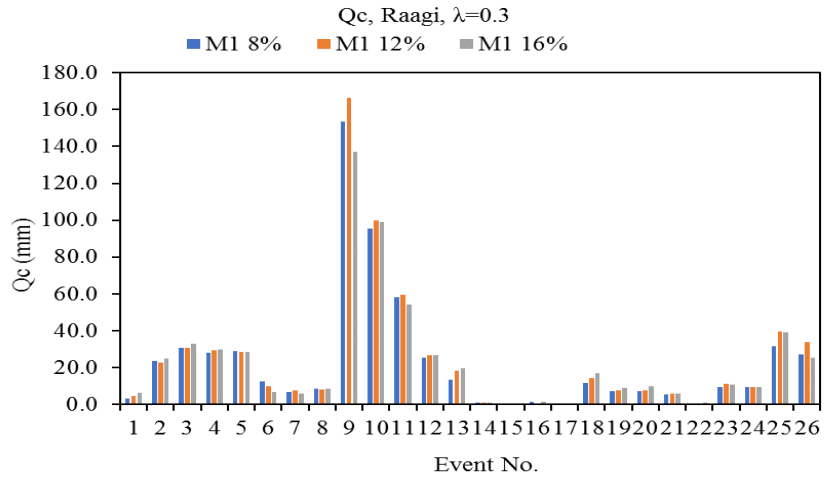

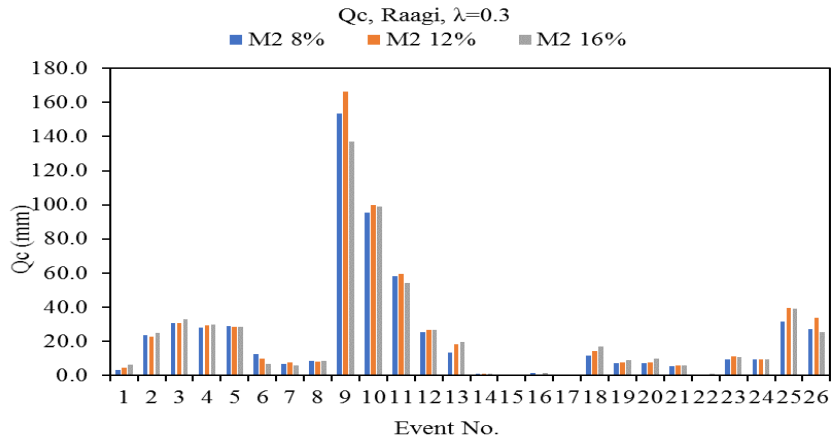

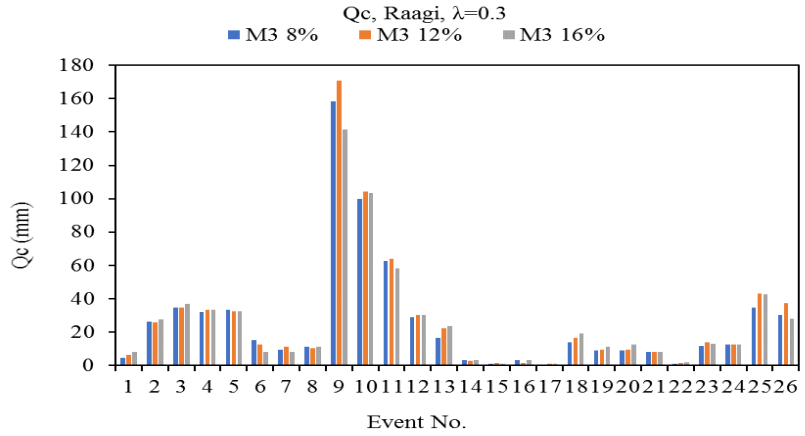

Figures 7.20 Inter-comparison of Models M1-M3 for a constant value of λ = 0.3 for Raagi

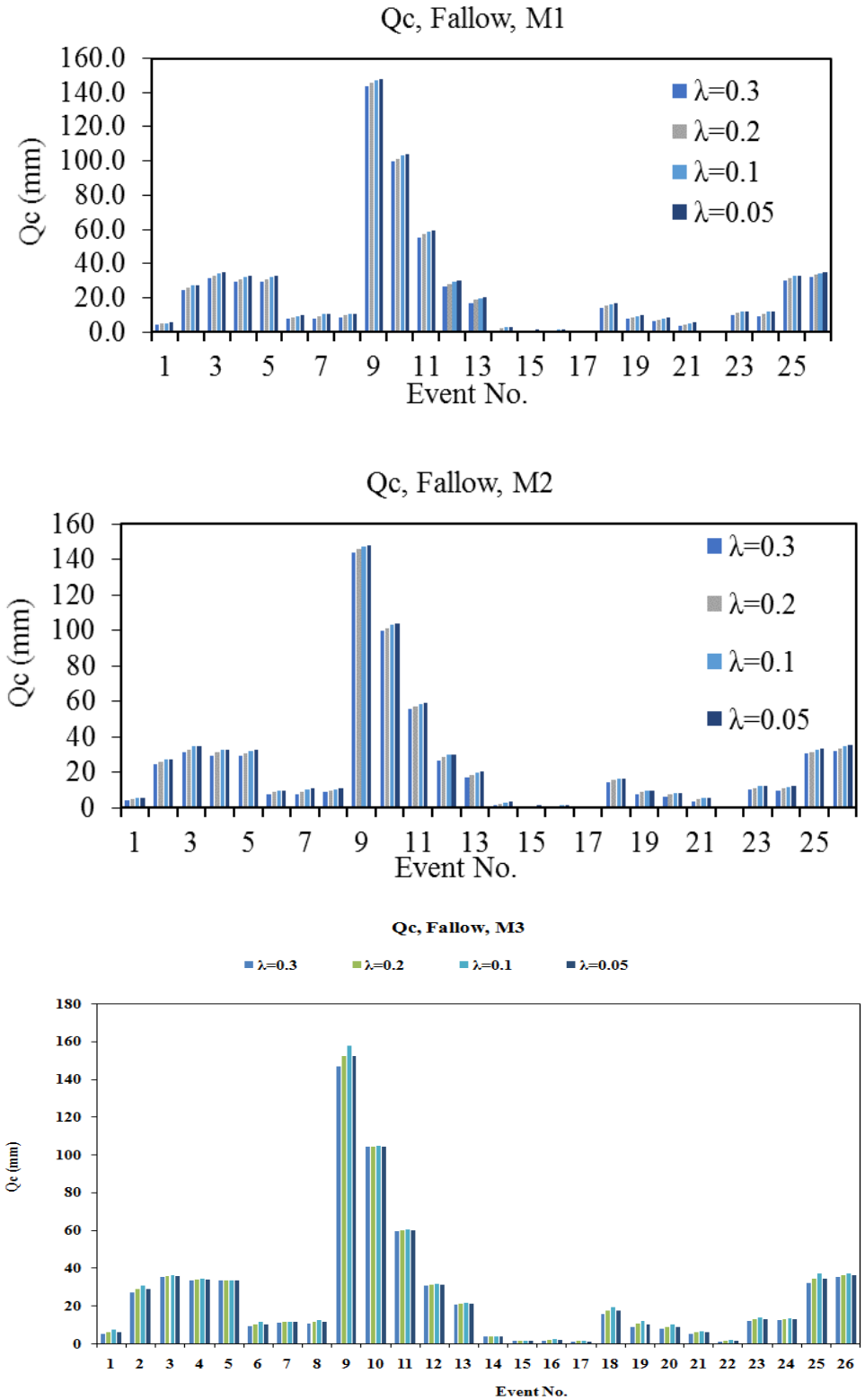

Figures 7.21 Inter-comparison of Models M1-M3 for varying λ for 8% watershed slope for Fallow Land

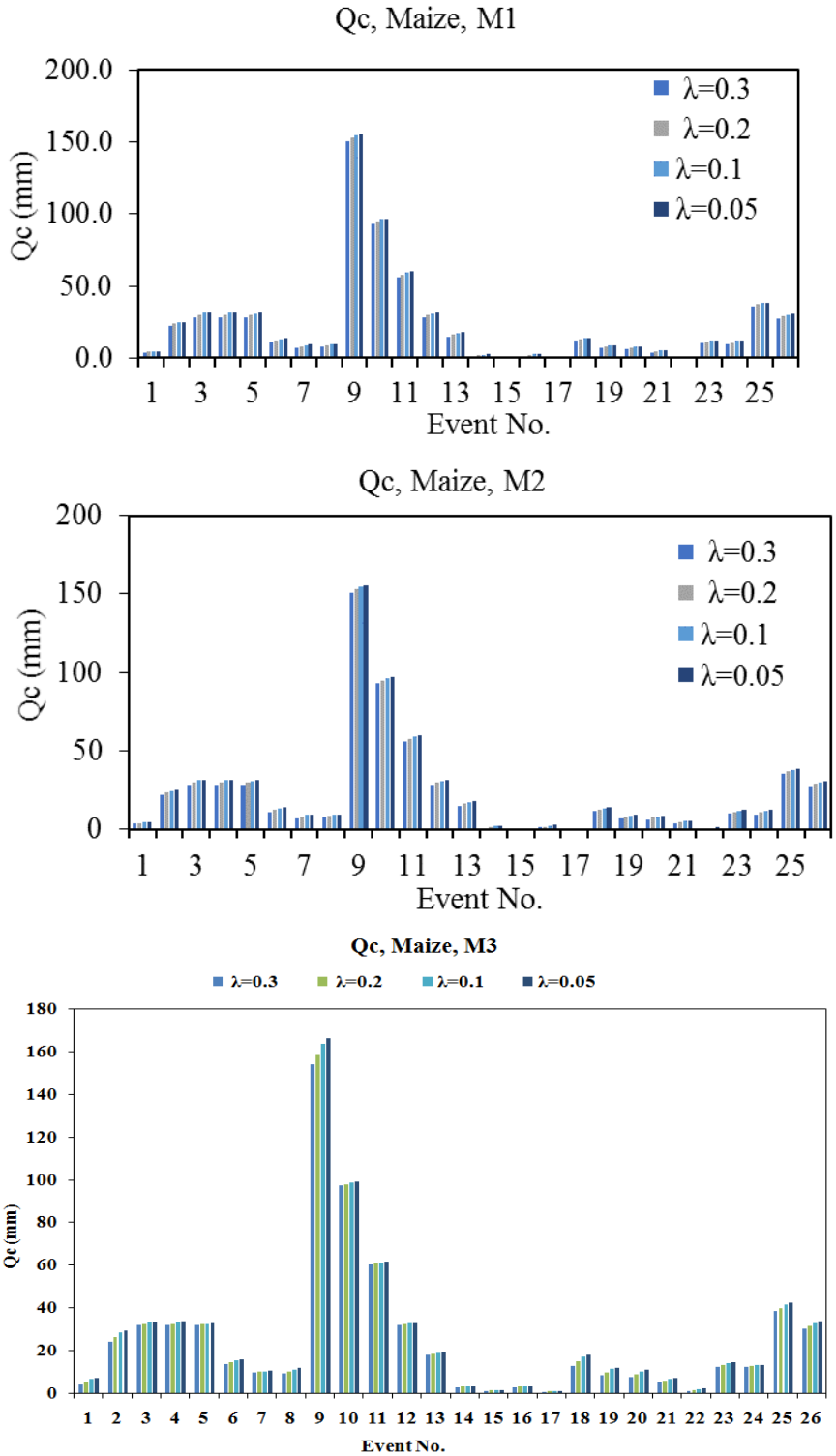

Figures 7.22 Inter-comparison of Models M1-M3 for varying λ for 8% watershed slope for Maize Land

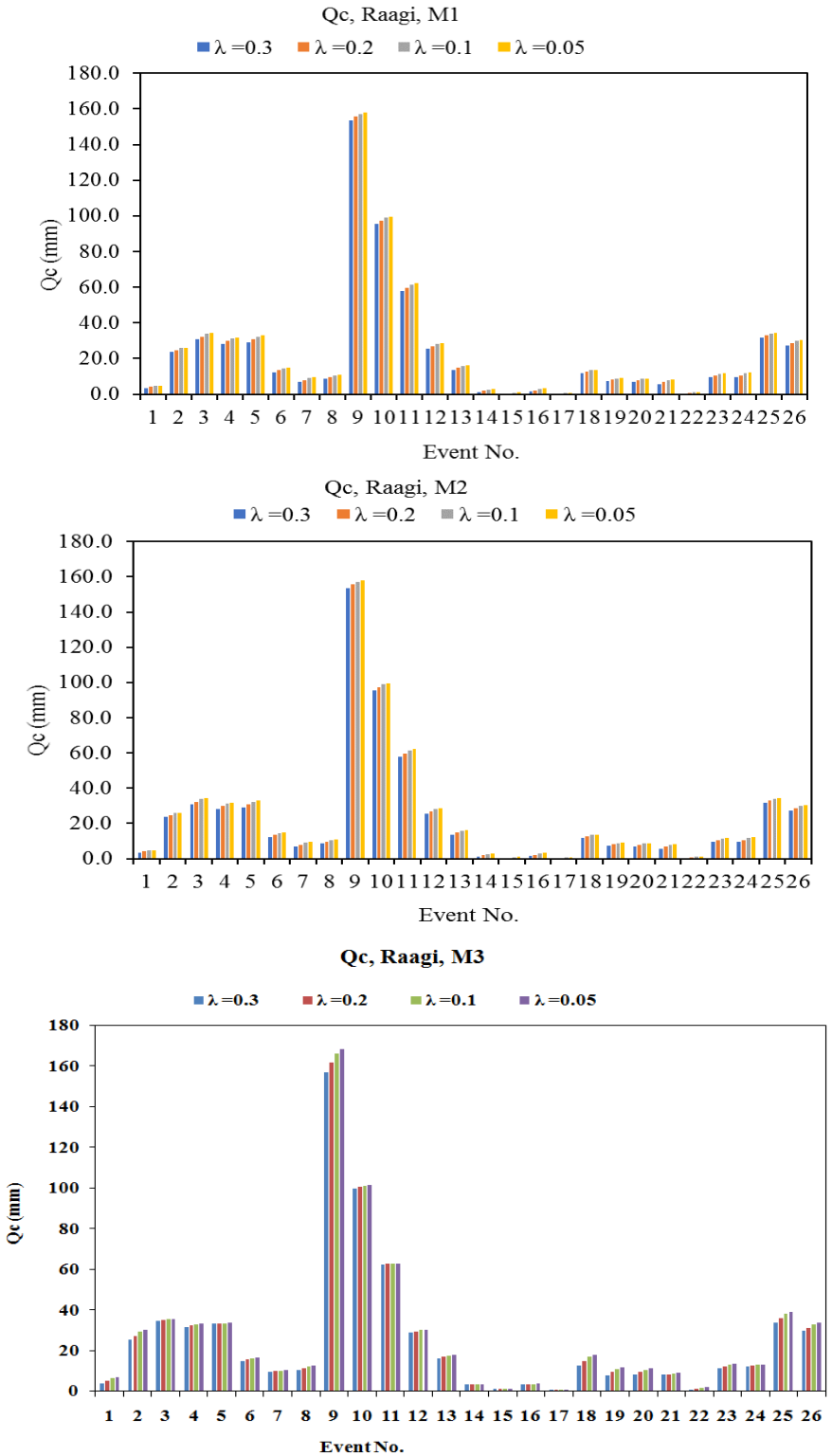

Figures 7.23 Inter-comparison of Models M1-M3 for varying λ for 8% watershed slope for Raagi

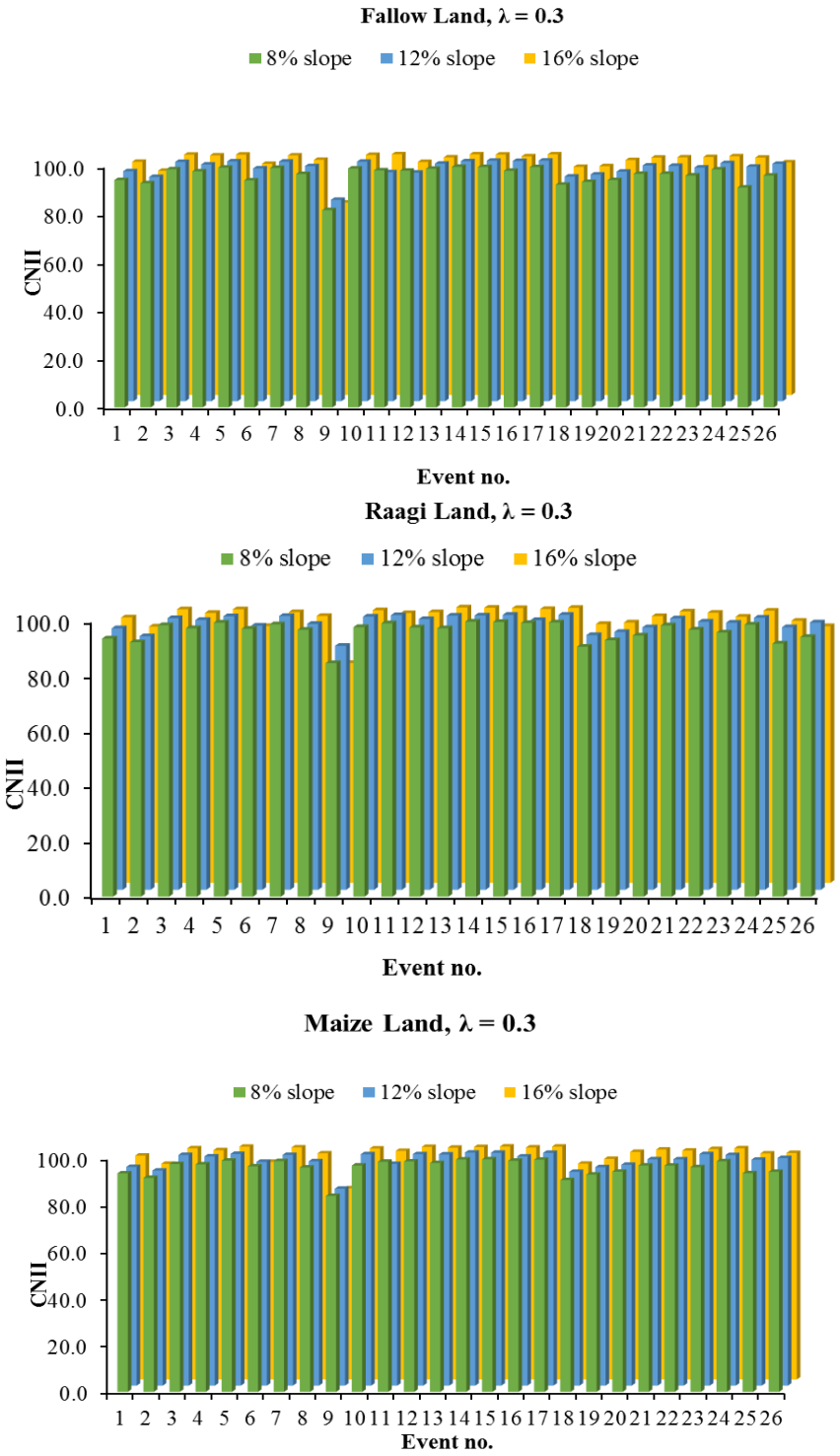

Figures 7.24 Observed CNII variation with varying slope and landuse for λ = 0.3

7.2.4 Comparison Between Observed CNII and Computed CNIIα/CNII(α,λ)

A comparison was made between the observed and computed CNIIα/$CNII_{(\alpha,\lambda)}$ to show the impact of watershed slope and initial abstraction. CNIIα represents CNII value estimated using watershed slope for the models M4-M6, whereas, $CNII_{(\alpha,\lambda)}$ represents CNII value with watershed slope and initial abstraction for the models M1-M3. Figures 7.25, Figures 7.26 & 7.27 show the best fitted line between CNII and CNIIα/$CNII_{(\alpha,\lambda)}$ for all the 26 storm events taken in this study.These figures have been prepared for three landuse, i.e., Fallow, Raagi and Maize and three land slopes, i.e., 16%, 12% and 8% for initial abstraction of 0.3. It is observed that $CNII_{(\alpha,\lambda)}$ computed using model M3 are closest to the best fit line followed by M6 model (CNIIα). The model M4 developed by Ajmal et al. (2016) is far away from the best fitted line. In case of M4 model, for few no. of storm events, the value of CNIIα was found to be more than 100, which is not realistic.

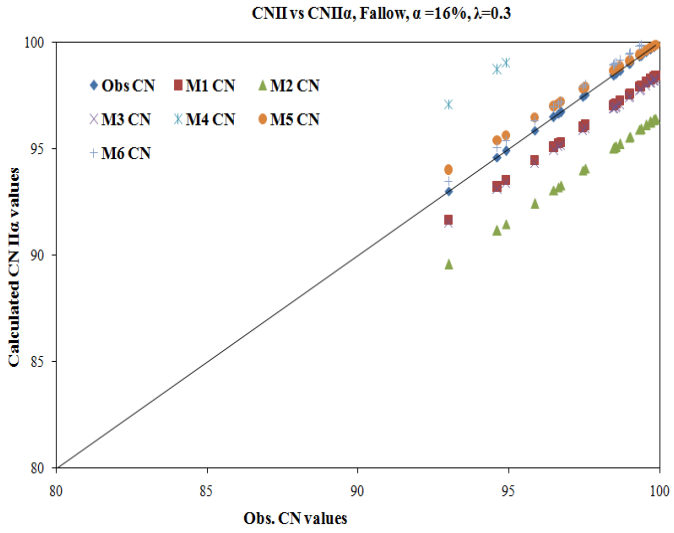

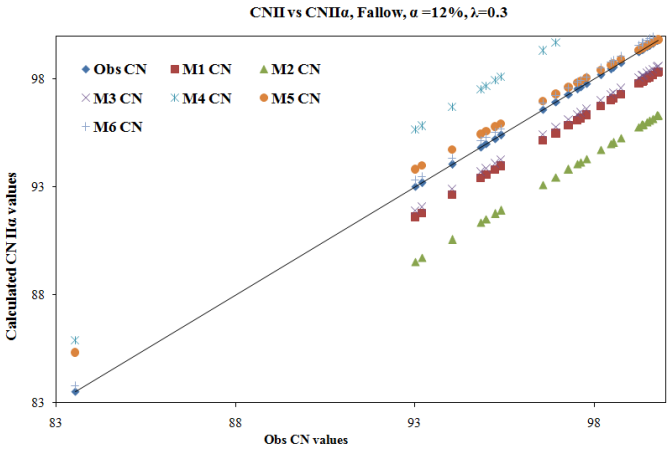

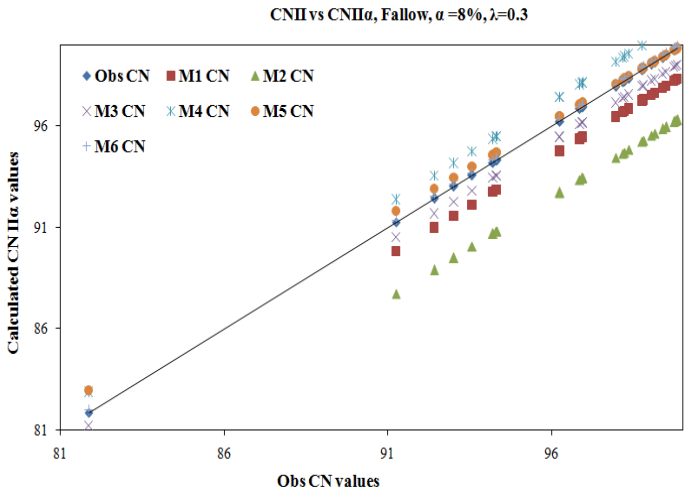

Figure 7.25 Comparison of CNII versus $CNII_{\alpha}$/$CNII_{(\alpha, \lambda)}$ for Fallow land with λ=0.3

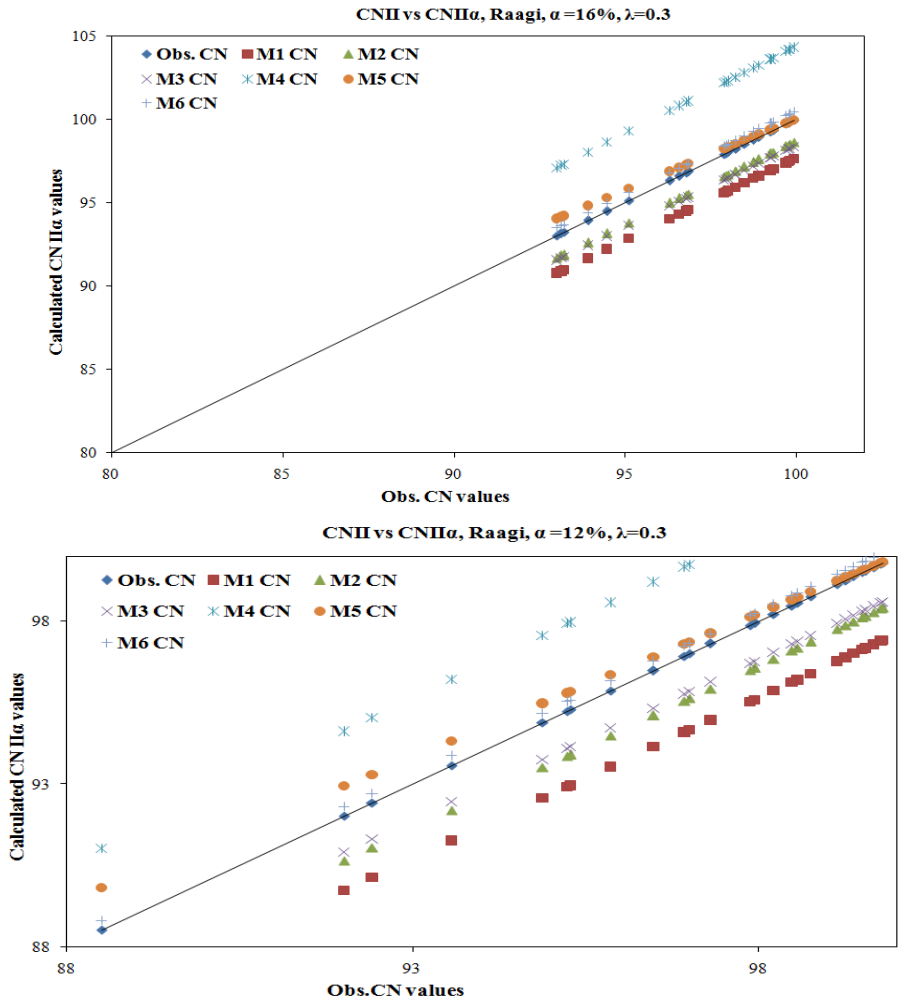

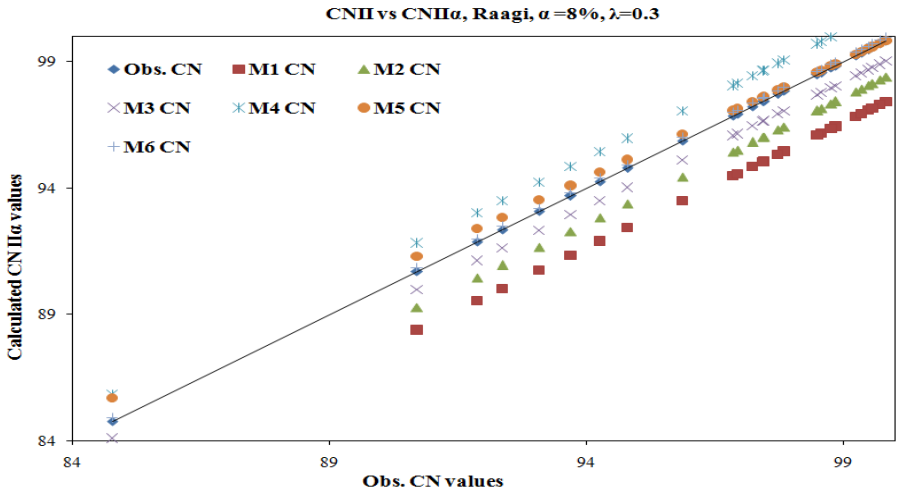

Figures 7.26 Comparison of CNII versus $CNII_{\alpha}$/$CNII_{(\alpha, \lambda)}$ for Raagi with λ=0.3

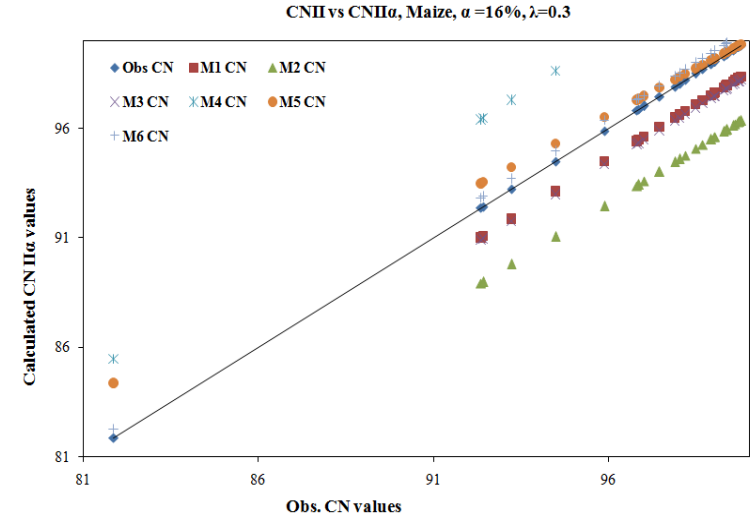

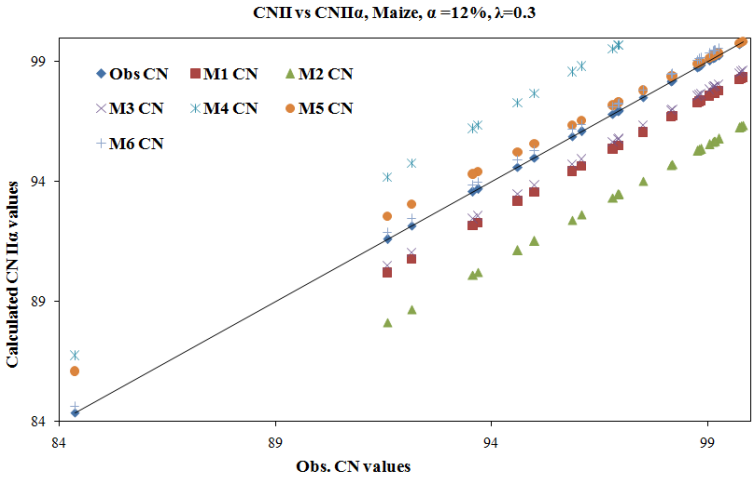

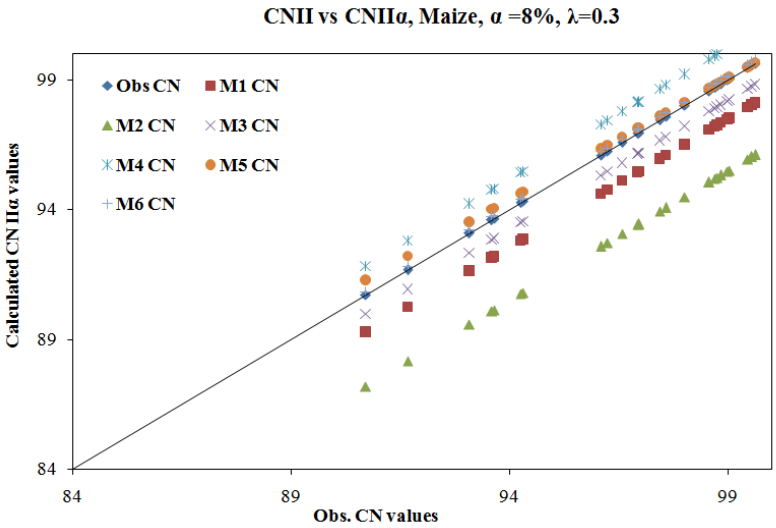

Figures 7.27 Comparison of CNII versus $CNII_{\alpha}$/$CNII_{(\alpha, \lambda)}$ for Maize with λ=0.3

7.3 RELATIONSHIP BETWEEN CN AND ANTECEDENT WETNESS CONDITION

It is of common experience that CN is a function of Antecedent Wetness Condition (AWC) AWC of the watershed, which may refer to the soil moisture prior to rainfall event. Expressed mathematically,

$$CN = f(AWC) \quad (7.10)$$

where AWC is a soil moisture index which can be described as 1–day antecedent soil moisture (θ_{o1}), 3–day average antecedent soil moisture (θ_{o3}), 5–day average antecedent soil moisture (θ_{o5}), 5–day antecedent rainfall (P_5), and so on. To evaluate the effect of AWC on CN (or S), regressions between CN derived from P–Q dataset and corresponding observed antecedent soil moisture indices such as θ_{o1}, θ_{o3}, θ_{o5}, and P_5 were developed, and their dependency on predicted runoff analyzed. The regression analysis used three forms, viz. linear, exponential, and logarithmic to fit the experimental data as follows:

$$CN = x + y\theta \quad (7.11)$$

$$CN = x \exp^{y\theta} \quad (7.12)$$

$$CN = x + y \ln(\theta) \quad (7.13)$$

where θ is the antecedent soil moisture index, CN is the curve number, ln is the natural logarithm operator, x and y are two regression coefficients to be estimated. The Standard SCS-CN equations 4.8 and 4.9 were employed for estimating the even wise CNs. The above relations lead to infer that as antecedent soil moisture increases, CN increases or S decreases, and vice versa. To validate the existence of such a relation, the randomized series of the total collected events were generated to represent fair coverage of all wetness situations. Thus, the 60% percent of events were used for calibration, and the remaining 40% percent for validation.

Here notably point is that data monitored during phase 1 were utilizing for validation of such relations.

Table 7.19 compares the performance of four soil moisture indices with three different regression models for improved runoff estimation. As seen, the exponential regression of CN with θ_{o1} (i.e. $CN=69.905exp^{0.0077\theta o}$) performed the best of all in both calibration and validation. However, the existing index based on 5-day antecedent rainfall (P_5) exhibited a poor performance in comparison to one day antecedent moisture (θ_{o1}), consistent with the results reported elsewhere (Brocca et al. 2008, 2009; Beck et al. 2009). To check the accuracy of developed relationships of CN with θ_{o1} (i.e. $CN=69.905exp^{0.0077\theta o1}$) and P_5 (i.e. $CN=79.82exp^{0.0011P5}$) in estimation of runoff, runoff was estimated by using both the relationships, for the data of three plots (plot nos. 1-3 of Table 4.1). As seen from Table 7.20, the $CN=69.905exp^{0.0077\theta o1}$ was found to produce better runoff estimates as compare to $CN=79.82exp^{0.0011P5}$ for all the three plots.

Table 7.20 Performance statistic for runoff estimation using CN relationship with θ_{o1} and P_5

Plot	$CN=69.905exp^{0.0077\theta o1}$		$CN=79.82exp^{0.0011P5}$	
No.	R^2	E	R^2	E
1	0.812	0.796	0.710	0.699
2	0.722	0.678	0.675	0.673
3	0.807	0.702	0.694	0.677

Table 7.19 Performance of various relations between CN and AWC indices

	1-day antecedent soil moisture (θ_{o1})				3-day average antecedent soil moisture (θ_{o3})				5-day average antecedent soil moisture (θ_{o5})				5-day antecedent rainfall (P_5)			
	Re (%)	R^2	E	Bias (e)	Re (%)	R^2	E	Bias (e)	Re (%)	R^2	E	Bias (e)	Re (%)	R^2	E	Bias (e)
Linear regression model (Equation 7.11)																
Calibration	8.58	0.737	0.610	0.51	14.68	0.722	0.493	0.87	14.34	0.704	0.460	0.85	9.51	0.708	0.511	0.56
Validation	16.15	0.835	0.726	0.96	21.31	0.830	0.676	1.26	23.13	0.829	0.649	1.37	17.90	0.816	0.699	1.06
Exponential regression model (Equation 7.12)																
	$CN=69.905\exp^{0.0077\theta o1}$				$CN=73.284\exp^{0.0058\theta o3}$				$CN=74.617\exp^{0.005\theta o5}$				$CN=79.82\exp^{0.0011P5}$			
Calibration	6.71	0.736	0.620	0.39	11.93	0.730	0.512	0.71	12.02	0.709	0.476	0.71	6.06	0.709	0.532	0.36
Validation	13.91	0.837	0.737	0.83	18.43	0.829	0.693	1.09	19.00	0.829	0.674	1.13	14.23	0.817	0.716	0.84
Logarithmic regression model (Equation 7.13)																
Calibration	12.48	0.730	0.560	0.74	15.74	0.718	0.473	0.93	15.28	0.703	0.451	0.90	14.01	0.708	0.441	0.83
Validation	21.21	0.830	0.686	1.26	23.43	0.830	0.652	1.39	23.26	0.829	0.640	1.38	25.94	0.816	0.632	1.54

CHAPTER 8

COMPARISON OF SCS-CN INSPIRED MODELS

8.1 Evaluation and comparison of SCS-CN inspired models

8.1.1 Model description and its parameterization

(a) Original SCS-CN method

The original SCS-CN method is given chapter 4 consisting Equations 4.6 and 4.8.

(b) Woodward et al. (2004) model

Using a model fitting technique with the iterative least squares procedure, Woodward et al. (2004) recognized $\lambda = 0.05$ as the best fit value and suggested it for field applications. For $\lambda=0.05$, Eq. 3.5 becomes:

$$Q = \frac{(P - 0.05S)^2}{(P + 0.95S)} \text{ for } P>0.05S; \text{ else } Q = 0 \quad (8.1)$$

Nevertheless, a new set of CNs must be developed for λ values other than 0.2, because the CNs with $\lambda = 0.05$ are not the same as those used in estimating direct runoff with $\lambda = 0.2$. The relationship adjusted for the conversion of $CN_{0.2}$ to $CN_{0.05}$:

$$CN_{0.05} = 53.23/ [\{(100/CN_{0.2})-1\}^{1.15}+0.5323] \quad (8.2)$$

The CN determined by above two methods (i.e. (a) & (b)) represents the CN_{II} (AMC-II) of the plots/ watersheds. Furthermore, in order to get the required AMC (i.e. I and III) level based on 5-day antecedent rainfall (P_5), CNs were converted by using Hawkins (1985) formula as given in Equations 5.2 and 5.3.

(c) Ajmal et al. (2015a) model

Considering the high dependency of runoff on rainfall event distribution, Ajmal et al. (2015a) found that the initial abstraction as 2% of the total rainfall amount ($I_a=0.02P$) is a better option to the originally assumed $I_a = 0.2S$. Using this interpretation for direct runoff estimation, original SCS Equation 4.5 becomes:

$$Q = \frac{(P - 0.02P)^2}{(S + 0.98P)} = \frac{0.9604P^2}{S + 0.98P} \quad (8.3)$$

(d) Mishra and Singh (2002)

Using the C = Sr concept, where C is the runoff coefficient (=Q/(P-Ia)) and Sr = degree of saturation, Mishra and Singh (2002) modified the original SCS-CN method (Equation 4.4) incorporating antecedent moisture (M) into it as:

$$Q = \frac{(P - I_a)(P - I_a + M)}{P - I_a + M + S} \quad (8.4)$$

Here, I_a is the same as in Equation 4.4.

In the above Eq. 8.4, M is computed as:

$$M = \frac{S_I(P_5 - \lambda S_I)}{P_5 + (1+\lambda)S_I} \quad (8.5)$$

Where P_5 is the 5-day antecedent precipitation amount and S_I is the potential maximum retention corresponding to AMC I, and λ is the initial abstraction ratio.

In Equation 8.5, S_I be treated as absolute maximum retention capacity, then

$$S_I = S + M \quad (8.6)$$

Where, S is the maximum potential retention.

Further the coupling of Equations 8.5 and 8.6 amplifies it as

$$M = 0.5[-(1+\lambda) S + \sqrt{((1-\lambda)^2 S^2 + 4P_5 S)}] \quad (8.7)$$

Here + sign before the square root is retained for $M \geq 0$, and $P_5 \geq \lambda S$.

(e) Mishra and Singh Model (2003)

Using similar concept given by Mishra and Singh (2002), Mishra and Singh (2003) further amended the modified SCS-CN method for antecedent moisture M as

$$M = \alpha P_5 \quad (8.8)$$

where α is proportionality coefficient. In this model, Equation 8.4 developed by Mishra and Singh (2002) is utilized for runoff computation.

(f) Mishra et al. (2006b) model

Mishra et al. (2006b) recommended an improved SCS-CN model incorporating antecedent moisture (M) in initial abstraction (I_a). The modified nonlinear relation between I_a and S incorporating antecedent moisture M is expressed as:

$$I_a = \frac{\lambda S^2}{(S + M)} \quad (8.9)$$

In above Equation 8.9, for M = 0 or a completely dry condition, it becomes $I_a = \lambda S$, which is the same as original SCS-CN equation (i.e. Equation 4.4). Thus, Equation 4.4 is specialized form of Equation 8.9.

The other relationships for determining the M developed by Mishra et al. (2006b) is expressed as:

$$Mc = \alpha\sqrt{(P_5 S)} \quad (8.10)$$

$$Mc = 0.72\sqrt{(P_5 S)} \quad (8.11)$$

(g) Jain et al. (2006) model

Based on the mathematical consideration by Mishra and Singh (1999) and Mishra et al. (2003), Jain et al. (2006) found that λ is perfectly correlated with S and P, rather than S alone. Therefore, they proposed a non-linear relation between I_a and S expressed as

$$\mathbf{Ia} = \lambda \mathbf{S}\left(\frac{\mathbf{P}}{\mathbf{P}+\mathbf{S}}\right)^{\alpha} \tag{8.12}$$

For α = 0, Equation 8.12 becomes an Equation 4.4, which shows that the former is a generalized form of the latter.

In order to evaluate the SCS inspired models, the P-Q data monitored on 12 plots (i.e. plot nos. 13-24 of Table 3.1) and two watersheds (Kalu and Hemavati) were selected. Kalu River which is a tributary of River Ulhas, is located in Maharashtra. The location of catchment (224 km^2) is situated between latitudes 19° 17' N to 19° 26' N and longitudes 73° 36' E to 73° 49' E. The average annual rainfall in the catchment is about 2450 mm; and situated at 1200 meters above mean sea level with hilly topography. Land use pattern of the watershed is forest 50% and agriculture 50%. The seventeen P-Q events were selected for study which was monitored during the year 1990-1993.

Hemavati is a tributary of River Cauvery in Karnataka. The watershed having area 600 km^2 is situated between latitudes 12° 55' N to 13° 11' N and longitudes 75° 29' E to 75° 5' E and its elevation ranges from 890 to 1240 m above mean sea level. The average annual rainfall in the catchment is 2972 mm and topography of watershed is low land, partly hill. Forest 12 %, agriculture 59 % and coffee plantation 29 % are land use pattern of the watershed. Thirteen natural P-Q events are selected for study which was monitored during the year 1990-1992. Detail characteristics of these plots/catchments are presented in Table 8.1.

8.1.2 Model parameter description

The total eleven measured rainfall and runoff events for experimental plots having size 22 m × 5 m were selected for this study. On the other hand, seventeen rainfall-runoff events for Kalu and thirteen events for Hemawati were utilized for the study. The performance of eight (8) different models, including the original SCS-CN was evaluated for better runoff estimation. The details of each model are described in Table 8.2.

Table 8.1 Characteristics of study plots and watersheds used in evaluation of SCS inspired models

S.N.	Description	Watersheds/Plots		
		Hemawati	Kalu	Plots 13-24 of Table 3.1
1	River	Cauveri	Ulhas	Solani river catchment
2	State	Karnataka	Maharahstra	Uttarakhand
3	Topography	Low land, partly hilly	Hilly	Slopes 5%, 3% and 1%.
4	Area (km^2)	600	224	Size 22 m × 5 m per plot
5	Longitude	75° 29’ E to 75° 51’ E	73° 36’ E to 73° 49’ E	77° 55’ 21” E
6	Latitude	12° 55’ N to 13°11’ N	19° 17’ N to 19° 26’ N	29° 50’ 9” N
7	Soil	Red loamy and red sandy soil	Silty loam and sandy loam	Hydrologic Soil Group (HSG) A
8	Land use	Forest 12%, agriculture 59% and coffee plantation 29%	Forest 50% and agriculture 50%	Sugarcane, maize, black gram and fallow land
9	Climate	Hot seasonally, dry tropical savanna	Hot and humid	Semi humid and subtropical
10	Average annual rainfall (mm)	2972	2450	1200-1500
11	Elevation (m) above MSL	890-1240	1200	226

8.1.3 Model parameter estimation

The stepwise procedure for determining the parameters mentioned in various models is as follows:

i. Employing Equations 4.8 and 4.9, the CN values for Models M1 and M2 were calculated from observed P-Q events based on procedures mentioned in the National Engineering Handbook, Section-4 (NEH-4), and results are presented in Table 8.3.

ii. The parameter for models M3 to M8 was determined using least square fitting (optimization) employing MS-Excel (Solver) software. In optimization, the CN was allowed to vary in the range (1-100) with keeping the initial estimate as 50. The λ was allowed to vary in the range (0-1) with keeping the initial estimate as 0.05. Similarly, the parameter α in Equation 8.12 was permitted to vary in the range (0.01, 2) with its initial value equal to 0.1. In model M8, range of parameters λ, ϒ and α were selected as 0 to 100, 0 to 10, and -10 to 10 with initial estimate values as 1, 0 and 1 respectively. The computed values of the model parameters are presented in Table 3.9.

Table 8.2 SCS inspired models and their parameter description.

Model ID	Parameters					Model expression	Remarks
	λ	α	ϒ	α	CN		
M1	0.2	-	-	-	Median	Original SCS CN	Eq. 4.5
M2	0.05	-	-	-	Median	Woodward et al. (2004)	Eq. 8.1
M3	0.02	-	-	-	Constrained Least square	Ajmal et al. (2015a)	Eq. 4.6
M4	Varying	-	-	-	do	Original SCS CN	Eq. 4.5
M5	Varying	-	-	-	do	MS Model (2002)	Eqs. 8.4, 8.7
M6	Varying	-	-	-	do	MS Model (2002)	Eqs. 8.4, 8.7 & 8.9
M7	Varying	Varying	-	-	do	MS Model (2006b)	Eqs. 8.4, 8.10 & 8.12
M8	Varying	-	Varying	Varying	do	MS Model (2003)	Eqs. 8.4, 8.8 & 8.12

Note: do means similar as above, MS model stands for Mishra and Singh model.

Table 8.3 SCS inspired models estimated parameters

Watersheds		Sugar 5%	Sugar 3%	Sugar 1%	Maize 5%	Maize 3%	Maize 1%	Fallow 5%	Fallow 3%	Fallow 1%	BG 5%	BG 3%	BG 1%	Kalu	Hemawati
Models		13	14	15	16	17	18	22	23	24	19	20	21	W1	W2
M1	CN_c	79.833	83.651	84.481	81.519	80.017	82.471	83.066	81.663	81.424	79.440	81.721	79.649	72.401	45.493
M2	CN_c	69.110	77.898	73.656	71.220	65.752	70.786	71.680	67.516	72.111	63.927	65.856	62.961	67.272	37.615
M3	CN_c	58.567	64.653	59.899	63.535	58.806	72.006	47.339	46.940	48.279	39.778	55.344	63.079	67.906	31.166
	'λ'	0.020	0.020	0.020	0.020	0.020	0.020	0.020	0.020	0.020	0.020	0.020	0.020	0.020	0.020
	R^2	0.690	0.423	0.536	0.627	0.813	0.663	0.368	0.132	0.196	0.298	0.523	0.461	0.943	0.763
M4	CN_c	50.000	50.000	50.000	50.000	50.000	50.000	49.541	45.799	50.000	42.889	50.000	50.000	65.051	29.802
	'λ'	0.000	0.000	0.000	0.000	0.000	0.000	0.000	0.000	0.000	0.000	0.000	0.000	0.000	0.000
	R^2	0.811	0.416	0.533	0.620	0.812	0.650	0.369	0.131	0.198	0.300	0.521	0.455	0.943	0.762
M5	CN_c	46.428	50.000	50.000	50.000	60.636	50.000	39.315	41.847	41.707	34.108	47.665	50.000	62.250	28.655
	'λ'	0.000	0.000	0.000	0.000	0.047	0.000	0.000	0.000	0.000	0.000	0.000	0.000	0.000	0.000

	R^2	0.717	0.586	0.635	0.824	0.854	0.889	0.410	0.284	0.405	0.584	0.607	0.603	0.945	0.749
M6	CN_c	46.851	50.000	50.000	50.000	56.221	50.000	41.474	41.575	50.000	33.995	48.903	50.000	62.250	28.905
	'λ'	0.000	0.000	0.000	0.000	0.027	0.000	0.000	0.000	0.000	0.000	0.001	0.000	0.000	0.001
	R^2	0.718	0.586	0.635	0.824	0.843	0.889	0.411	0.285	0.392	0.585	0.608	0.603	0.945	0.750
M7	CN_c	52.125	48.578	46.758	69.559	50.104	81.624	38.661	39.068	36.680	26.018	48.437	50.000	55.068	29.701
	'λ'	0.000	0.000	0.000	0.249	0.001	0.538	0.000	0.001	0.001	0.000	0.001	0.000	0.000	0.000
	α	0.132	0.684	0.484	1.220	0.283	1.263	0.276	0.424	0.496	0.552	0.321	0.594	2.000	0.093
	R^2	0.811	0.550	0.628	0.905	0.878	0.926	0.387	0.228	0.363	0.653	0.599	0.599	0.948	0.761
M8	CN_c	96.159	83.553	90.707	52.883	53.757	60.496	79.288	61.476	63.495	51.841	86.796	81.514	45.370	35.920
	'λ'	8.704	2.651	3.768	0.000	0.000	0.000	3.762	36.459	100.000	6.921	2.996	1.692	0.001	20.110
	α	4.755	2.592	2.695	2.637	2.615	2.633	2.810	4.411	5.465	2.759	2.423	1.906	-2.934	10.000
	ϒ	0.323	0.743	0.932	1.082	0.369	1.321	0.125	0.556	0.334	0.692	0.487	0.972	10.000	0.000
	R^2	0.867	0.617	0.654	0.825	0.869	0.902	0.450	0.409	0.517	0.689	0.648	0.642	0.911	0.782

8.2 EVALUATION AND COMPARISON OF SCS-CN INSPIRED MODELS

8.2.1 Analysis based on individual plot datasets

The performance of the SCS-CN inspired models was evaluated using three indices, RMSE and E. The comparative performance based on RMSE is shown in Table 8.4. As seen, the modified model M2 with $\lambda = 0.05$ performed better than model M1 ($\lambda = 0.2$) in all watersheds except plot having maize with 1% slope. Models M3, M5, M6, and M7 performed better (for lower RMSE reason) in all 14 watersheds than M1 followed by M2, M4, and M8, which also performed well on 13 watersheds. M8 performed better for in 11 out of 14 watersheds followed by M7.

Table 8.4 Comparison of RMSE (mm) in all watersheds.

Plot/ Watersheds	Models							
	M1	M2	M3	M4	M5	M6	M7	M8
13	8.39	6.69	5.25	3.06	2.94	2.94	2.44	2.00
14	7.59	6.55	6.13	7.35	4.99	4.99	4.70	4.18
15	8.57	6.67	4.69	5.30	3.74	3.74	3.70	3.49
16	6.64	6.04	5.01	6.10	3.87	3.87	2.52	3.55
17	5.26	5.02	2.86	3.51	2.53	2.62	2.46	2.43
18	7.83	8.34	6.14	9.12	6.39	6.39	2.88	3.97
22	9.59	7.37	3.97	4.05	3.48	3.60	3.49	2.98
23	7.55	5.88	6.14	6.14	5.13	5.12	5.33	4.51
24	7.54	6.30	5.40	5.42	4.16	4.97	4.26	3.60
19	7.19	4.98	3.52	3.62	2.40	2.39	2.08	1.94
20	7.94	6.30	4.31	4.44	3.58	3.62	3.59	3.25
21	8.36	8.00	6.09	6.93	5.12	5.12	4.94	4.72
W1	62.04	58.61	52.36	52.67	51.23	51.23	49.61	68.51
W2	118.19	110.49	75.52	75.81	76.82	76.94	75.69	69.44

The comparative performance based on higher n(t) is shown in Table 8.5. Models M3, M5, M6 performed better (higher n(t)) in all 14 watersheds than M1 followed by M2, M4, M7, and M8, which performed well on 13 watersheds. Model M8 performed better in 11 watersheds followed by M7.

Table 8.5 Comparison of n (t) in all watersheds.

Plot/Watersheds	Models							
	M1	M2	M3	M4	M5	M6	M7	M8
13	-0.33	-0.15	0.08	0.85	0.93	0.92	1.32	1.84
14	-0.07	0.07	0.15	-0.04	0.41	0.41	0.50	0.68
15	-0.28	-0.07	0.32	0.16	0.65	0.65	0.67	0.77
16	0.28	0.41	0.70	0.39	1.19	1.19	2.37	1.39
17	0.31	0.38	1.41	0.97	1.74	1.64	1.81	1.85
18	0.41	0.33	0.80	0.22	0.73	0.73	2.85	1.79
22	-0.56	-0.43	0.05	0.03	0.20	0.16	0.20	0.40
23	-0.19	0.04	0.00	0.00	0.19	0.19	0.15	0.36
24	0.68	0.04	0.97	1.13	0.80	0.80	0.67	1.38
19	-0.49	-0.27	0.03	0.01	0.52	0.52	0.75	0.88
20	-0.28	-0.09	0.32	0.29	0.60	0.57	0.59	0.76
21	-0.02	0.02	0.34	0.18	0.60	0.60	0.66	0.73
W1	2.61	2.82	3.28	3.25	3.37	3.37	3.51	2.27
W2	0.31	0.40	1.05	1.04	1.01	1.01	1.04	1.23

The comparative performance based on higher E is shown in Table 8.6. As shown in this table, the performance based on E revealed that Models M3, M5, M6, and M7 performed better (higher E) in 13 out of 14 watersheds than M1 followed by M2, M4, and M8, which performed well in 12 watersheds. Based on RMSE and E, Model M8 performed better in 10 out of 14 watersheds followed by M7, which performed well in 3 watersheds.

Table 8.6 Comparison of E (%) in all watersheds.

Plot/Watersheds	Models							
	M1	M2	M3	M4	M5	M6	M7	M8
13	-138.06	-51.30	6.84	68.41	70.80	70.68	79.89	86.53
14	-2.34	23.87	33.23	4.00	55.81	55.81	60.86	68.96
15	-97.27	-19.43	41.00	24.53	62.38	62.38	63.21	67.32
16	33.28	44.80	62.01	43.56	77.31	77.31	90.39	80.86
17	37.17	42.80	81.35	71.96	85.50	84.45	86.27	86.64
18	49.31	42.47	68.78	31.26	66.27	66.27	93.16	86.95
22	-417.42	-206.07	11.28	7.55	31.72	27.21	31.24	50.02
23	-57.08	4.68	-3.96	-4.07	27.37	27.56	21.67	43.95
24	79.44	63.93	39.78	42.89	34.11	34.00	26.02	51.84
19	-138.85	-14.60	42.68	39.65	73.48	73.55	80.03	82.61
20	-111.57	-33.29	37.70	33.90	57.05	55.92	56.88	64.66
21	-11.75	-2.30	40.71	23.20	58.07	58.07	60.93	64.36
W1	97.48	97.75	98.20	98.18	98.28	98.28	98.39	96.92
W2	75.90	78.93	90.16	90.08	89.82	89.79	90.12	91.68

Figure 8.1 compares the observed and calculated runoff for Hemawati watershed. On this watershed data, M8 performed better than all other models and showed higher coefficient of determination (R^2).

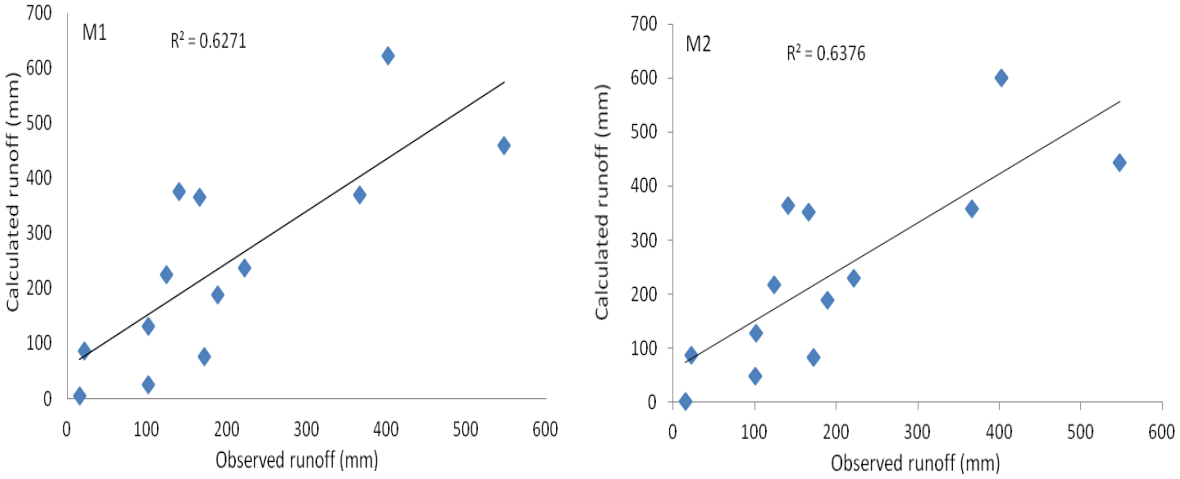

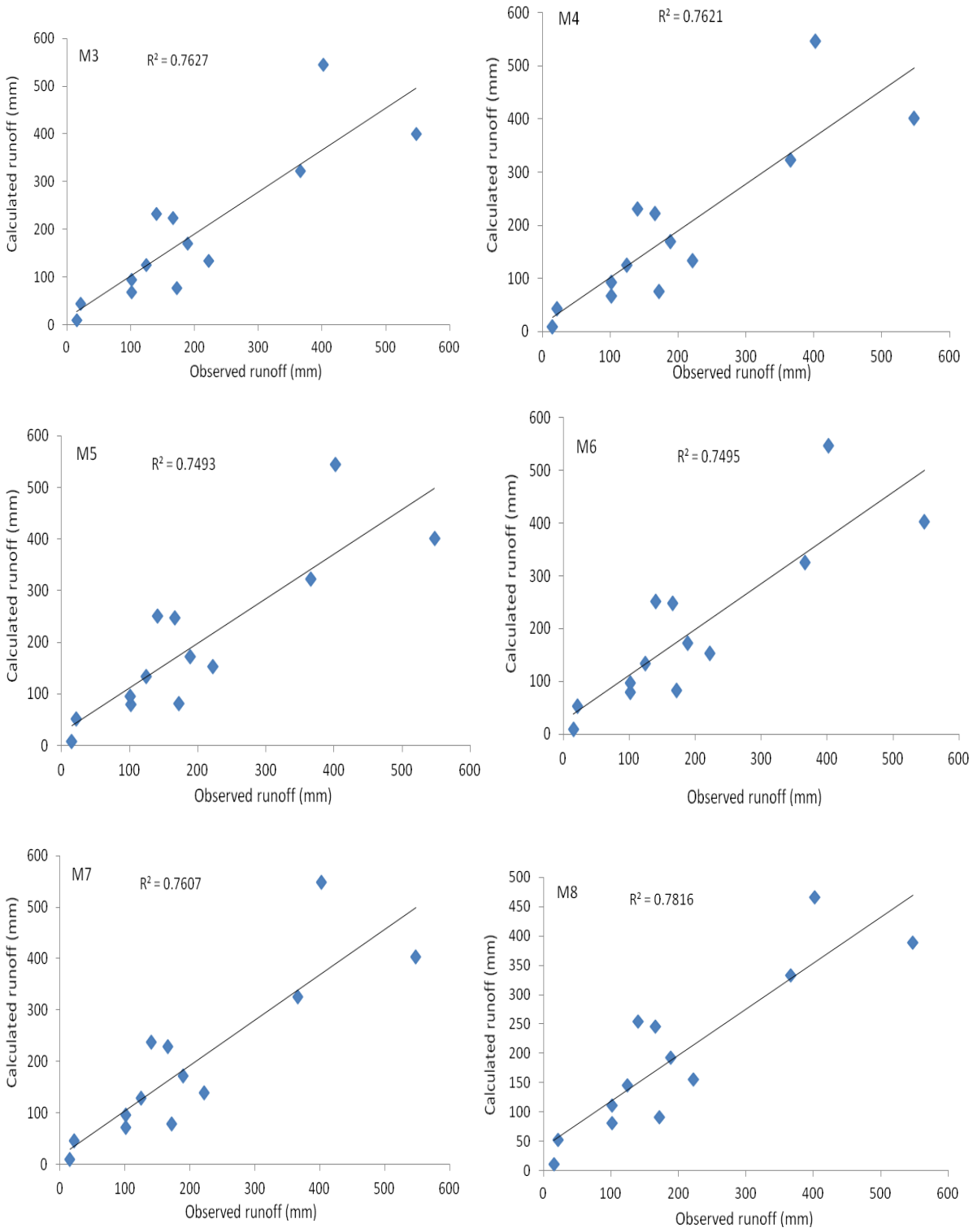

Figure 8.1 Observed runoff versus calculated runoff for models M1 to M8 in Hemawati watershed.

8.2.2 Performance based on the results of all watersheds data

For the overall performance of the models in runoff prediction, the models were ranked based on cumulative mean RMSE, NSE, and n(t) statistics derived from the data of all 14 watersheds. Ranks of 1-8 were assigned from the lowest to the highest for the mean RMSE, and from the highest to the lowest for both the mean n(t) and mean NSE. The score of 16 to 2 was assigned to each model with 2 score for each rank based on performance of RMSE, NSE, and n(t). The highest score (16) was assigned to the method which had highest NSE, and n (t) (or lowest RMSE). Similarly, lowest score (2) was assigned to the method which has lowest NSE, and n (t) (or highest RMSE). Table 8.7 shows the ranking and scoring of the models' cumulative mean values of all three performance indices. Based on the ranks and scores of each individual model for each performance index, model M7 performed the best followed by M8, M5, M6, M3, M4 and M2; and M1 the poorest.

Table 8.7 Performance evaluation of models based on cumulative means values and rank score.

Model (ID)	RMSE (mm)	Score	Rank	n(t)	Score	Rank	E (%)	Score	Rank	Total Score	Overall rank
M1	19.48	2	8	0.17	2	8	-42.98	2	8	6	8
M2	17.66	4	7	0.25	4	7	5.16	4	7	12	7
M3	13.39	8	5	0.68	8	5	46.41	8	5	24	5
M4	13.82	6	6	0.60	6	6	41.08	6	6	18	6
M5	12.60	14	2	0.92	12	3	63.43	12	3	38	3
M6	12.68	12	3	0.91	10	4	62.95	10	4	32	4
M7	**11.98**	**16**	**1**	**1.22**	**14**	**2**	**67.07**	**14**	**2**	**44**	**1**
M8	12.75	10	4	1.17	16	1	73.09	16	1	42	2

CHAPTER 9

EVALUATION OF CURVE NUMBER-BASED SEDIMENT YIELD MODELS

9.1 EVALUATION OF SCS-CN BASED SEDIMENT YIELD MODEL

9.1.1 Description of model

Using the concept of C = Sr = DR, where C is runoff coefficient, Sr = the degree of saturation and DR = delivery ratio, Mishra et al. (2006a) developed SCS-CN based sediment yield model by coupling the SCS-CN method with USLE for computing event sediment yield.

For $I_a = 0$, the runoff coefficient (C) and degree of saturation (Sr) can be defined as

$$C = \frac{Q}{P} \tag{9.1}$$

$$S_r = \frac{F}{S} = \frac{P}{P+S} \tag{9.2}$$

Where, F =cumulative infiltration amount (mm)

The sediment delivery ratio (DR) is a ratio of sediment yield (Y) to the potential soil erosion (A) and expressed as

$$DR = \frac{Y}{A} \tag{9.3}$$

Based on above hypothesis, Equations (9.1), (9.2) and (9.3) can be coupled as follows:

$$\frac{Q}{P} = \frac{F}{S} = \frac{P}{P+S} = \frac{Y}{A} \tag{9.4}$$

The equation (9.5) defines Y as

$$Y = \frac{AP}{P+S} \tag{9.5}$$

Equation 3.24 is a simplified form of the sediment yield model for $I_a = 0$. Furthermore, Mishra et al. (2006a) incorporated various hydrological elements and watershed characteristics such as initial abstraction (I_a), initial soil moisture (M) in the sediment yield model, and different formulated forms are shown in Table 9.1. In this table, S1 is the simplified form of the model and excludes initial abstraction (I_a) and antecedent moisture (M) component. Model S2 incorporates initial abstraction with $\lambda = 0.2$ whereas in model S3, λ is allowed to vary. Models S4 and S5 incorporate both I_a and M. In S4, values of λ are taken as 0.2 whereas in S5 it was allowed to vary.

Table 9.1 Different forms of SCS-CN based sediment yield model

Model No.	Sediment Yield Model	Remarks
S1	$Y = \frac{AP}{P+S}$	For Ia=0, M=0
S2	$Y = \frac{A(P-0.2S)}{P+0.8S}$	For Ia=0.2S, M=0
S3	$Y = \frac{A(P-\lambda S)}{P+(1-\lambda)S}$	For Ia=λS, M=0
S4	$Y = \frac{A(P-0.2S+M)}{P+0.8S+M}$	For Ia=0.2S, M≠0
S5	$Y = \frac{A(P-\lambda S+M)}{P+(1-\lambda)S+M}$	For Ia=λS, M≠0

9.1.2 Parameter estimation (or optimization)

The iterative least squares fitting (or best fit) procedure of statistical analysis was employed to estimate model parameter A (potential maximum soil erosion) and S (potential maximum retention) using sediment data of plots 13-24 of Tables 3.1 (i.e. Data monitored during phase 1). The objective of fitting is to find values of A and S such that the following is minimum (Equation 9.6).

$$\sum_{i=1}^{N}(Y_o - Y_c)_i = \left(Y_o - \frac{A(P-\lambda S+M)}{P+(1-\lambda)S+M}\right)_i = minimum \qquad (9.6)$$

where Y_o = observed sediment yield (t/ha), Y_c = computed sediment yield (t/ha), P= rainfall depth (mm), M= Antecedent moisture content (mm), i = individual rainfall event, N= total number of the rainfall event. The antecedent moisture content (M) was calculated from the measured volumetric water content (θ_o) prior to each rainfall event.

9.2 MODEL PERFORMANCE EVALUATION USING PLOT DATA

Since the sediment yield model S2 (Table 9.1) is corresponding to the original SCS-CN rainfall-runoff model (Equation 4.4) with Ia= 0.2S, it was therefore applied to the plot-wise datasets to evaluate its performance. Out of eleven runoff and sediment generated rainfall events, six randomly selected events were used for the calibration of model parameters whereas remaining five events were used for validation purpose. The estimated value of model parameters (in calibration phase) and corresponding performance in validation phase for all twelve plots (i.e. plot nos. 13-24 of Table 3.1) is presented in Table 9.2. As shown in this

Table, estimated value of potential soil erosion (A) varies from 0.25 t/ha for plot no 24 (fallow land with 1% slope) to 0.93 t/ha for the plot no 13 and 17 (Sugarcane with 5% and 3% slope). The estimated parameter S for the model S2 ranges from the 59.90 mm for plot no. 21 (Sugarcane with 1% slope) to 93.13 mm for plot no 23 (blackgram with 1% slope). The estimated values of S seem to be lower for sugarcane plots as compared to others land uses plots, which indicates sugarcane plots to be high runoff productive than other land uses plots, consistent with results of CN calculation where higher median CNs were observed for sugarcane plots. The resulting E and R^2 of sediment yield computation vary respectively, from 57.26% and 0.63, to 93.13% and 0.95 indicating satisfactory performance of the model.

Table 9.2 Results of application of sediment yield model (S2) for plot wise data sets

Model no	Plot no	Land Use	Parameter of Sediment yield model		Model Performance	
			S (mm)	A (t/ha)	E (%)	R^2
S2	13	Sugarcane	74.38	0.93	62.77	0.64
	14	Maize	78.10	0.73	83.33	0.87
	15	Blackgram	84.86	0.55	63.35	0.64
	16	Fallow	77.12	0.33	57.26	0.63
	14	Sugarcane	65.76	0.93	60.38	0.69
	18	Maize	93.05	0.50	84.85	0.89
	19	Blackgram	81.69	0.66	65.86	0.67
	20	Fallow	80.48	0.54	93.13	0.95
	21	Sugarcane	59.90	0.71	86.75	0.94
	22	Maize	88.40	0.63	82.76	0.89
	23	Blackgram	93.13	0.61	71.93	0.73
	24	Fallow	74.64	0.25	71.44	0.82
Mean			79.29	0.61	73.65	0.78
Maximum			93.13	0.93	93.13	0.95
Minimum			59.90	0.25	57.26	0.63

The estimated values of S by sediment yield model S2 were also converted into CN (using Equation 4.9); and thus, compared with the CNs estimated from SCS-CN method as given in Table 4.15. It is seen that CN values estimated from sediment yield model (S2) are slightly lower than the CNs derived from SCS-CN method. The reason for the underestimation of the CN by sediment yield model is due to sediment deposition (Mishra et al. 2006a).

Table 9.3 CN values derived from runoff model and sediment yield model (S2)

Plot No.	Runoff Model	Sediment Model
13	82.78	77.35
14	81.52	76.48
15	79.44	74.96
16	83.42	76.71
17	86.28	79.43
18	80.02	73.19
19	81.72	75.66
20	81.66	75.94
21	85.58	80.92
22	82.48	74.18
23	79.65	73.17
24	82.68	77.29

The CNs estimated from sediment yield model for all plots were correlated with the median CNs derived from observed rainfall and runoff data sets. The plotting (Figure 9.1) of median CNs for all plots against CNs obtained from sediment yield model shows the quadratic relationship as shown in Equation 9.1. The coefficient of determination R^2= 0.78 indicates the satisfactory fitting of the CNs derived from entirely two different approaches and supports the analytical approach of coupling of the SCS-CN method with USLE.

$$y = 0.026x^2 - 3.236x + 175.77 \quad (9.1)$$

However, the estimation of A and S from the above models excludes the observed runoff. In practice, sediment yield from upland area is better correlated with observed runoff than rainfall (Mishra et al., 2006a). The underestimation of CN from sediment yield model is also seen from Figure 9.1.

Therefore, it is necessary to transform the S (or CN) values obtained from the sediment yield model (S2) using Equation 9.1 to those values corresponding to rainfall-runoff data. The performance of runoff computation using the S (or CN) value from sediment yield model with and without transformation is presented in Table 9.4 which shows slight improvement in coefficient of determination (R^2) between computed and observed runoff. It indicates satisfactory model performance and supports S (or CN) transformation for runoff computation.

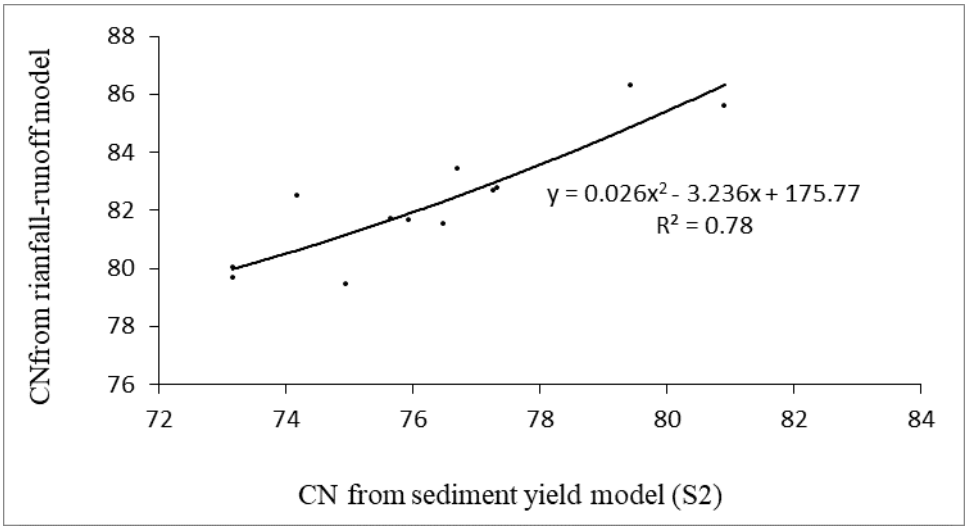

Figure 9.1 Relationship between CNs derived from sediment yield model and existing SCS-CN model (using rainfall-runoff data)

Table 9.4 Comparison of runoff computation using S value from Sediment yield model

Plot No.	Runoff computation efficiency (R^2)	
	Without S transformation	With S transformation
1	0.87	0.87
2	0.61	0.62
3	0.28	0.30
4	0.39	0.40
5	0.51	0.52
6	0.80	0.81
7	0.50	0.51
8	0.12	0.13
9	0.67	0.68
10	0.62	0.64
11	0.42	0.44
12	0.18	0.20

9.3 PERFORMANCE EVALUATION FOR OVERALL PLOTS DATASET

The model parameters and performance efficiencies were also estimated by mixing 12 plots data sets and considering the experimental plot as a unit of the representative watershed in the region of the study. Out of the observed data sets for all plots, seventy percent data sets were randomly selected for the calibration of model parameters and remaining thirty percent data sets were used for validation purpose. The results obtained from the application of the data sets

on various forms of sediment yield models (designated as per Table 9.1) are shown in the Table 9.5. For the sediment yield model S3 and S5, the value of λ was taken as 0.01, 0.1, 0.15 and 0.25 and the effect of variability of λ on sediment yield estimation was evaluated.

S1 is the simplest form of all the five models resulting low efficiency of 59.02%. Incorporation of the initial abstraction (Ia=0.2S) in model S2, the model efficiency was improved to 65.97%. Similarly, incorporation of antecedent moisture content (M), as in model S4, further improved the efficiency to 66.16%.

The estimate of both parameters A and S are found to be affected by variation of λ value (Table 9.5). Notably, it is seen from the Table 9.5, an increase in λ value decreases both S and A, and vice-versa. The computed sediment yield was plotted against observed value for visual comparison (Figures 9.2, 9.3, 9.4). The closeness of data points to the line of perfect fits indicates the satisfactory performance of the model and further supports the applicability of the model on the agricultural watershed of the study area region.

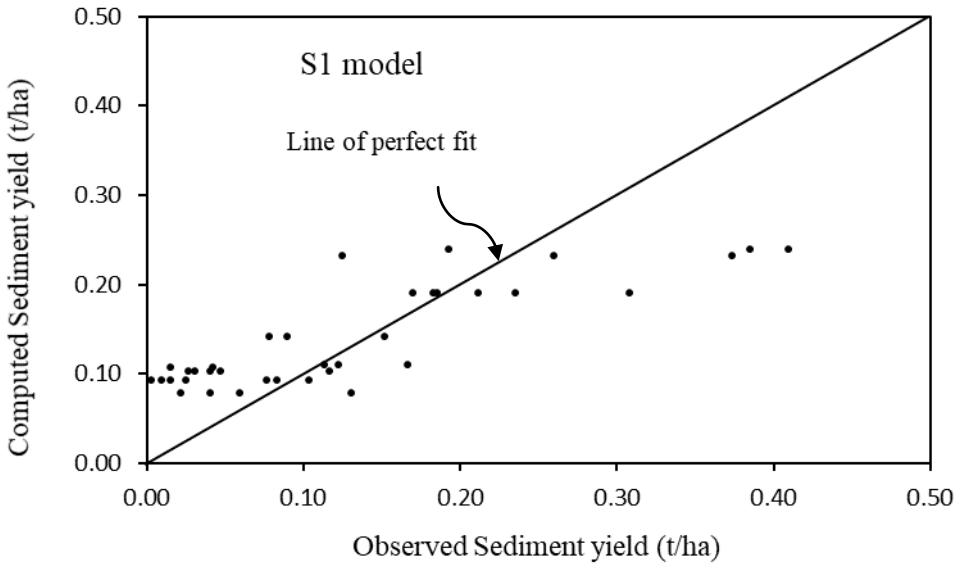

Figure 9.2 Comparison between observed and computed sediment yield using model S1

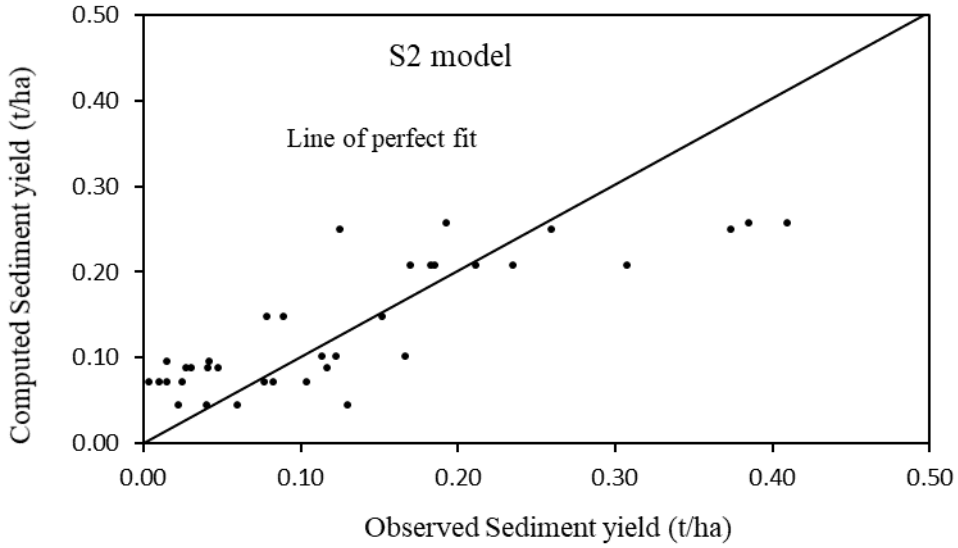

Figure 9.3 Comparison between observed and computed sediment yield using model S2

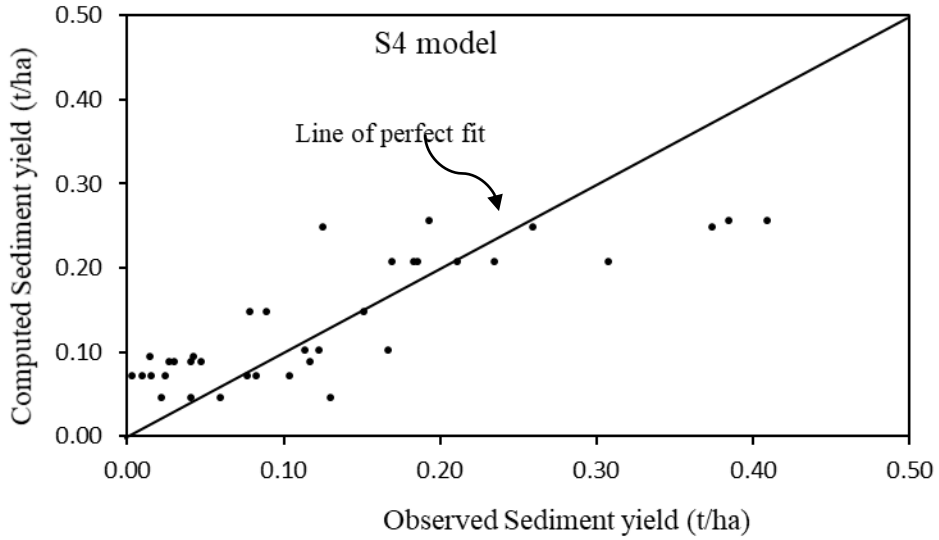

Figure 9.4 Comparison between observed and computed sediment yield using model S4

Table 9.5 Results of various model applications to data sets of overall plots

Model	Parameter of Sediment yield model			Model Performance	
	Λ	S (mm)	A (t/ha)	NSE (%)	R^2
S1	0	311.45	1.29	59.02	0.70
S2	0.2	70.47	0.57	65.97	0.69
S4	0.2	81.35	0.62	66.16	0.68
S3 for λ =0.05	0.05	190.33	1.05	66.23	0.70
S3 for λ =0.10	0.1	116.50	0.76	66.21	0.70
S3 for λ =0.15	0.15	87.03	0.64	66.11	0.69

S3 for λ =0.25	0.25	59.65	0.53	65.78	0.68
S5 for λ =0.05	0.05	288.26	1.48	66.83	0.70
S5 for λ =0.10	0.10	151.32	0.91	66.61	0.69
S5 for λ =0.15	0.15	105.07	0.72	66.39	0.69
S5 for λ =0.25	0.25	66.73	0.56	65.92	0.68

9.4 DEVELOPMENT OF SEDIMENT-DISCHARGE RELATIONSHIPS

The relationship between runoff and sediment yield was established using the observed runoff-sediment data monitored on plots 10-18 of Table 3.2 (i.e. Data monitored during phase 2). The observed runoff and sediment data for (i.e. plot nos. 10-18) maize, finger millet and fallow landuse are given in Tables 9.6, 9.7 and 9.8, respectively. The sediment rating curves were also drawn between the observed sediment and discharge for all nine plots, and results are shown in Figures 9.5 to 9.13. These rating curves can be used for estimation of sediment for a given discharge. It can also be inferred from Table 9.6 to 9.8 that higher density and higher canopy crop (Finger millet) has the lowers turn off and sediment yield. The coefficient of determination R^2 of maize crops in 8 %, 12% and 16% slopes are 0.55, 0.55 and 0.60, respectively. For Finger millet crops in 8 %, 12% and 16% slopes, R^2-values are 0.54, 0.42 and 0.56, respectively. Similarly, the Fallow land yielded R^2 values as 0.5, 0.58 and 0.52, respectively.

Table 9.6 Observed runoff and sediment yield for Maize crop (or plot nos. 10-12)

Event No.	Date	Rainfall (mm)	Runoff (m^3) Maize crops			Sediment Yield (kg)		
			Plot12	Plot 11	Plot 10	Plot12	Plot 11	Plot 10
1	19-Jun-17	44.00	0.51	1.08	1.15	3.03	10.12	23.01
2	26-Jun-17	34.20	0.48	0.95	0.89	2.65	8.29	13.88
3	28-Jun-17	75.20	1.75	1.83	2.31	20.76	27.23	40.17
4	29-Jun-17	17.70	0.23	0.38	0.33	0.76	2.28	4.42
5	30-Jun-17	15.00	0.25	0.35	0.47	0.35	0.56	2.62
6	6-Jul-17	36.40	0.69	1.03	0.98	2.62	8.98	14.04
7	24-Jul-17	14.00	0.02	0.15	0.20	0.05	0.54	0.30
8	2-Aug-17	79.50	1.20	1.53	1.60	4.98	10.87	25.61
9	3-Aug-17	9.60	0.07	0.12	0.16	0.03	0.07	0.02
10	7-Aug-17	27.40	0.68	0.75	0.90	0.32	0.83	1.64
11	10-Aug-17	43.40	0.72	0.97	1.29	0.77	2.56	4.53

12	19-Aug-17	22.30	0.11	0.33	0.36	0.07	0.21	1.13
13	22-Aug-17	58.10	1.04	1.11	1.56	0.56	1.26	5.40
14	23-Aug-17	15.50	0.08	0.09	0.24	0.04	0.10	0.36
15	25-Aug-17	61.80	1.16	1.32	1.79	0.55	0.93	2.51
16	1-Sep-17	44.00	0.54	0.74	1.24	0.22	0.80	2.18
17	1-Sep-17	23.00	0.53	0.68	0.75	0.12	0.12	1.50
18	2-Sep-17	61.10	0.95	1.20	0.90	1.00	1.43	1.62
19	3-Sep-17	26.00	0.69	0.49	0.64	0.16	0.24	0.51
Total			11.70	15.11	17.76	39.04	77.45	145.45

Table 9.7 Observed runoff and sediment yield for Finger millet (or plot nos. 13-15)

Event No.	Date	Rainfall (mm)	Runoff (m^3) Maize crops			Sediment Yield (kg)		
			Plot15	Plot 14	Plot 13	Plot15	Plot 14	Plot 13
1	19-Jun-17	44	0.47	0.64	0.98	1.66	14.31	25.19
2	26-Jun-17	34.2	0.42	0.54	0.94	1.32	9.19	14.59
3	28-Jun-17	75.2	1.79	1.97	2.46	16.18	25.00	37.82
4	29-Jun-17	17.7	0.38	0.28	0.48	0.80	1.54	5.70
5	30-Jun-17	15	0.24	0.33	0.44	0.48	0.68	1.71
6	6-Jul-17	36.4	0.48	0.87	1.08	2.16	13.18	14.23
7	24-Jul-17	14	0.10	0.10	0.10	0.12	0.43	0.32
8	2-Aug-17	79.5	0.87	1.26	1.50	2.67	9.92	22.96
9	3-Aug-17	9.6	0.02	0.17	0.22	0.01	0.17	0.28
10	7-Aug-17	27.4	0.63	0.73	0.93	0.18	0.64	1.82
11	10-Aug-17	43.4	0.79	0.94	1.19	0.25	3.26	2.87
12	19-Aug-17	22.3	0.06	0.21	0.38	0.04	0.18	1.19
13	22-Aug-17	58.1	0.59	0.91	1.26	0.07	0.82	5.40
14	23-Aug-17	15.5	0.09	0.11	0.14	0.03	0.08	0.07
15	25-Aug-17	61.8	1.02	1.39	1.82	0.55	0.79	1.80
16	1-Sep-17	44	0.39	0.68	0.64	0.17	0.96	1.42
17	1-Sep-17	23	0.45	0.58	0.60	0.16	0.10	1.13
18	2-Sep-17	61.1	1.05	0.87	1.55	0.38	0.89	1.82
19	3-Sep-17	26	0.24	0.34	0.74	0.03	0.24	0.42
Total			10.08	12.91	17.44	27.26	90.58	140.74

Table 9.8 Observed runoff and sediment yield for Fallow land (or plot nos. 16-18)

Event No.	Date	Rainfall (mm)	Runoff (m^3) Maize crops			Sediment Yield (kg)		
			Plot18	Plot 17	Plot 16	Plot18	Plot 17	Plot 16
1	19-Jun-17	44	0.44	0.73	1.06	2.24	10.14	22.03
2	26-Jun-17	34.2	0.29	0.65	0.74	1.66	5.06	12.77
3	28-Jun-17	75.2	1.66	1.46	2.34	16.87	31.82	44.06
4	29-Jun-17	17.7	0.18	0.48	0.53	0.78	2.77	7.51
5	30-Jun-17	15	0.19	0.37	0.39	0.20	0.44	3.55
6	6-Jul-17	36.4	0.64	0.94	1.16	5.50	10.59	15.70
7	24-Jul-17	14	0.05	0.10	0.15	0.04	0.20	0.65
8	2-Aug-17	79.5	0.80	1.38	1.45	3.80	11.74	21.50
9	3-Aug-17	9.6	0.02	0.12	0.21	0.01	0.05	0.12
10	7-Aug-17	27.4	0.58	0.48	0.73	0.14	1.16	1.62
11	10-Aug-17	43.4	0.72	0.72	1.25	0.24	3.94	5.43
12	19-Aug-17	22.3	0.17	0.23	0.54	0.26	0.52	1.48
13	22-Aug-17	58.1	0.84	1.21	1.29	0.44	1.39	6.93
14	23-Aug-17	15.5	0.09	0.19	0.16	0.08	0.18	0.13
15	25-Aug-17	61.8	1.39	1.13	1.64	0.41	0.48	1.39
16	1-Sep-17	44	0.44	0.64	1.11	0.15	1.32	1.80
17	1-Sep-17	23	0.53	0.50	0.75	0.16	0.17	1.38
18	2-Sep-17	61.1	1.20	0.93	1.75	1.33	1.88	3.38
19	3-Sep-17	26	0.49	0.38	0.69	0.14	0.17	0.59
Total			10.70	12.64	17.93	34.44	84.02	152.03

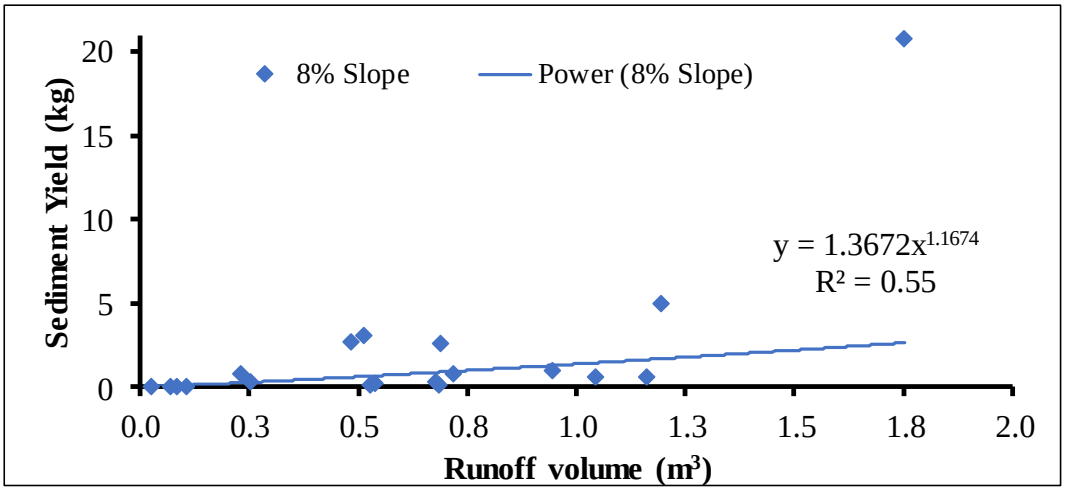

Figure 9.5 Sediment rating curve of Maize Crops 8% slope (Plot 12)

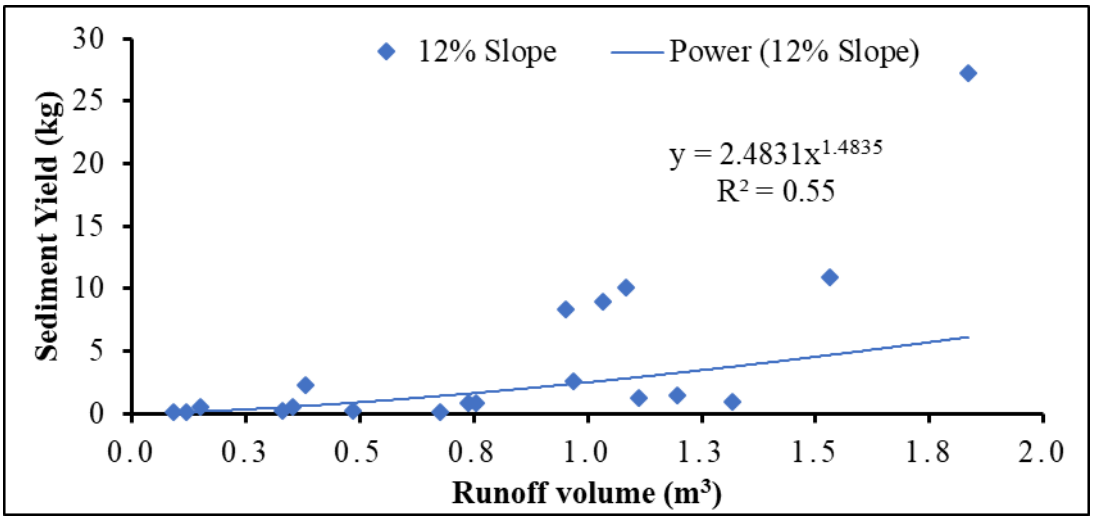

Figure 9.6 Sediment rating curve of Maize Crops 12% slope (Plot 11)

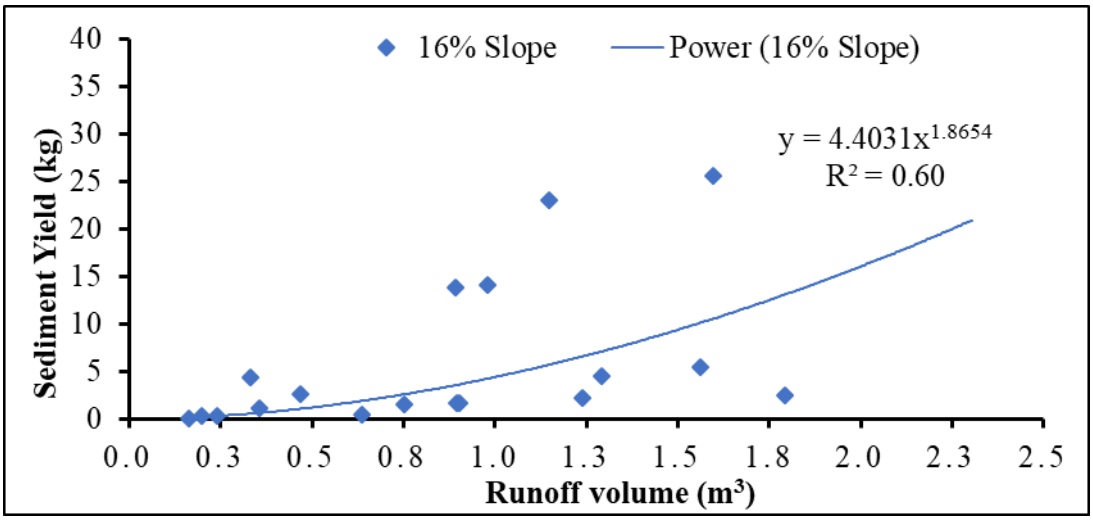

Figure 9.7 Sediment rating curve of Maize Crops 16% slope (Plot 10)

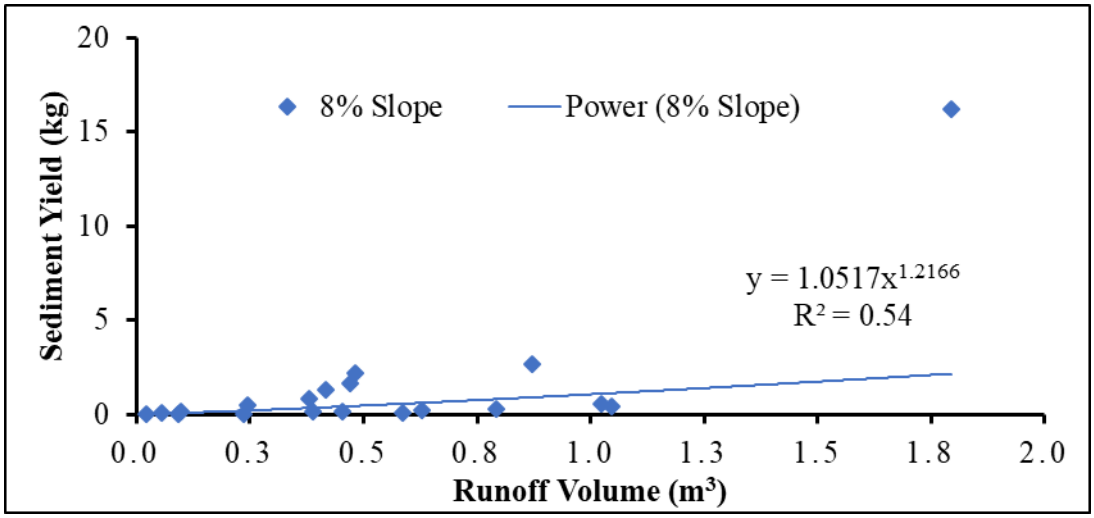

Figure 9.8 Sediment rating curve of Finger Millet 8% slope (Plot 15)

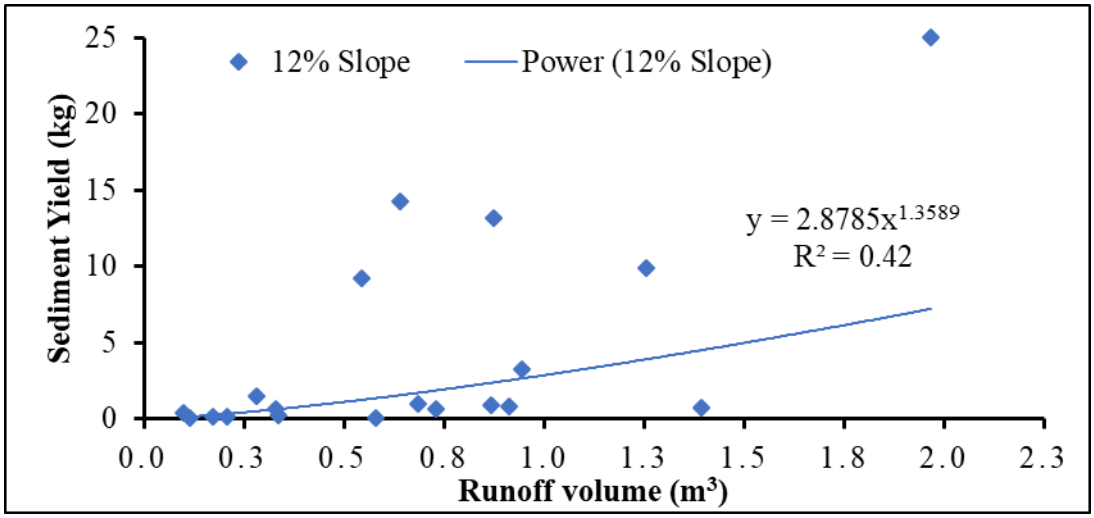

Figure 9.9 Sediment rating curve of Finger Millet 12% slope (Plot 14)

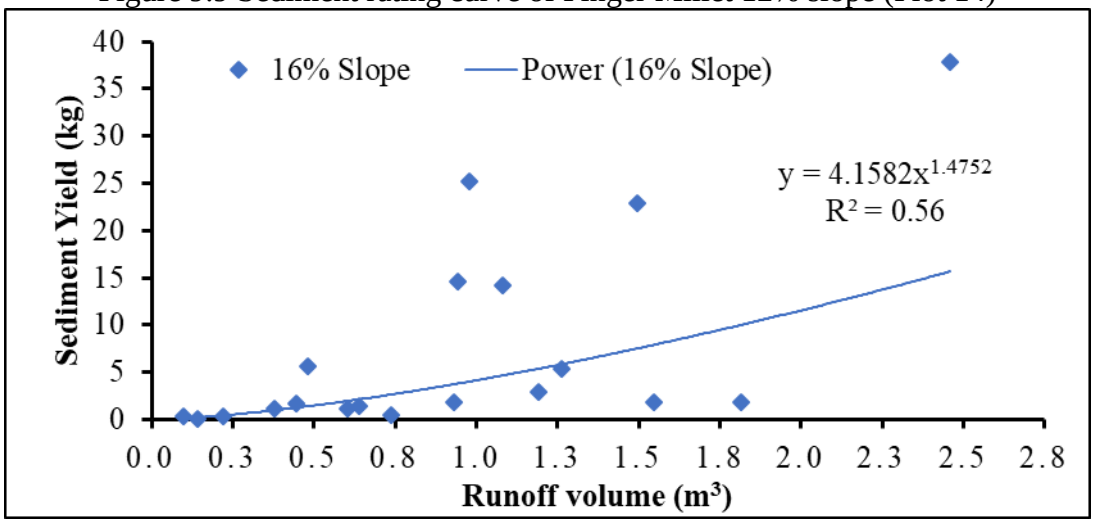

Figure 9.10 Sediment rating curve of Finger Millet 16% slope (Plot 13)

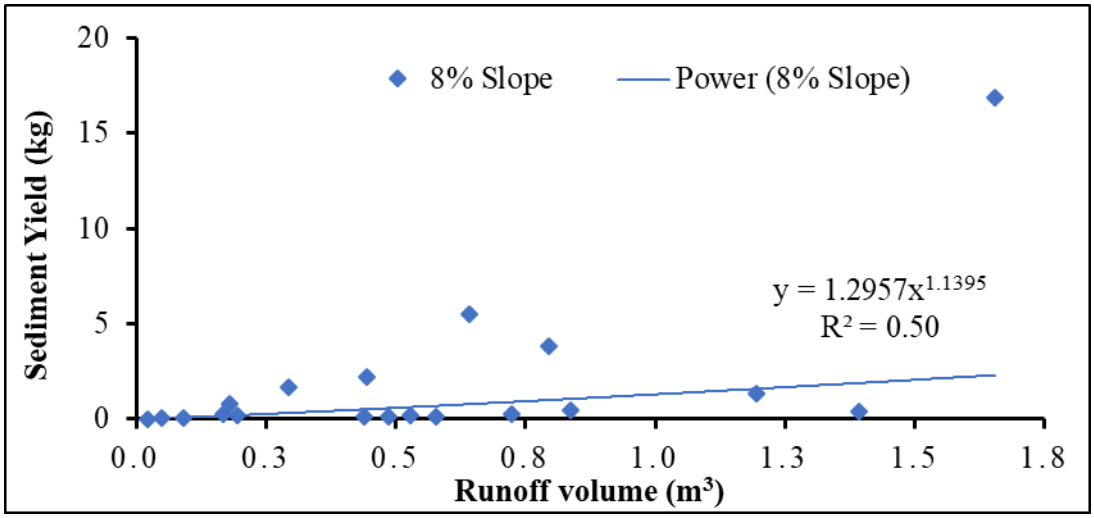

Figure 9.11 Sediment rating curve of Fallow land 8% slope (Plot 18)

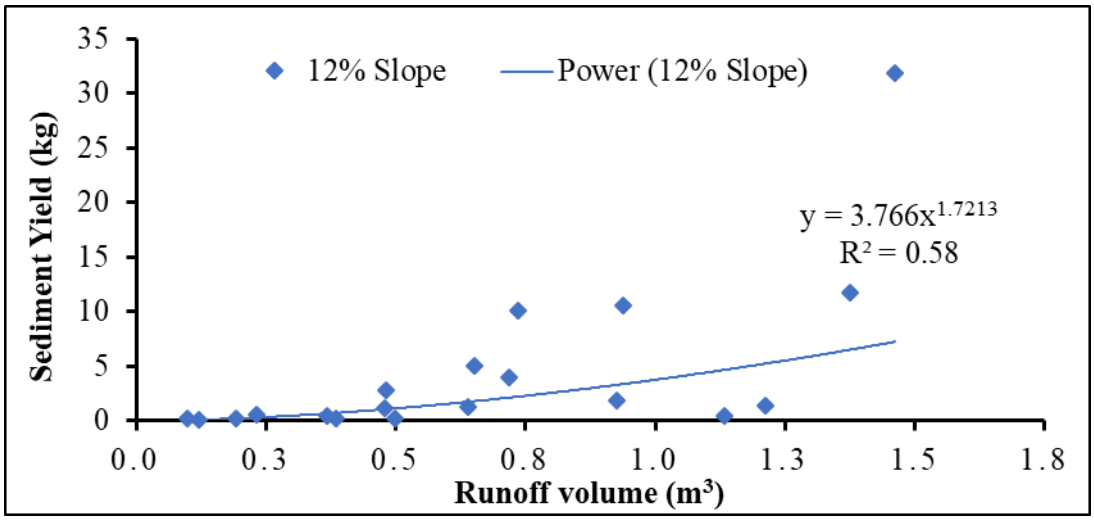

Figure 9.12 Sediment rating curve of Fallow land 12% slope (Plot 17)

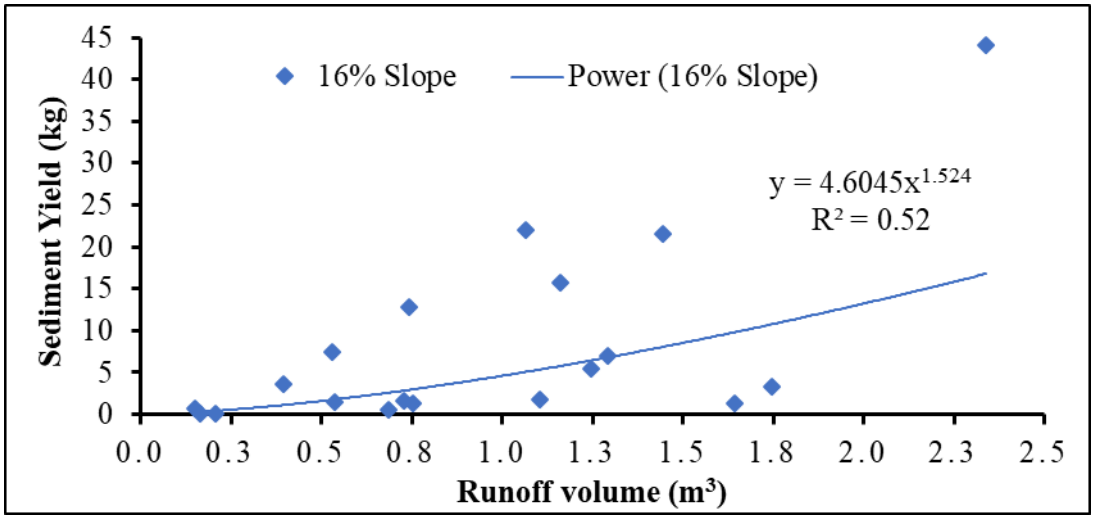

Figure 9.13 Sediment rating curve of Fallow land 16% slope (Plot 16)

CHAPTER 10
SUMMARY AND CONCLUSSIONS

The Soil Conservation Service curve number (SCS-CN) presently known as Natural Resources Conservation Service curve number (NRCS–CN) is widely used for predicting surface runoff from small agricultural watersheds, primarily because of its simplicity and the requirement of only two parameters for runoff prediction, which are the initial abstraction ratio (λ) and the potential maximum retention (S) expressed in terms of curve number (CN). In practice, for ungauged watersheds, CNs are derived from the well–known National Engineering Handbook chapter–4 (NEH–4) tables using watershed characteristics. The empirical evidences however show that the use of NEH–4 tables CN values normally over-design the hydrological systems, and therefore, use of CN values based on observed rainfall (P)–runoff (Q) data is recommended. Thus, there is need of such regional studies for analyzing the accuracy of various parameters like CN determination methods, initial abstraction ratio, relative accuracy of existing AMC formulae and relationship between CN (or S) and AWC etc. in runoff prediction using locally measured P–Q data. The accuracy of curve number method for Indian watersheds is rarely been examined due to lack of observed P–Q data from agricultural watershed.

To accomplish the objective of the present research study, agricultural plots of 20m x 5 m of different land uses, soils, and land uses were prepared in a demonstration farm located nearby Roorkee (Uttarakhand). Arrangements were made for collection of runoff generated at the outlet of each plot due to both natural and artificial rain events. The rainfall-runoff-sediment yield data were collected during the period 2013-2018. The analysis was carried out in perspective of the Soil Conservation Service Curve Number (SCS-CN) methodology and the results are summarized in the following text.

10.1 RAINFALL−RUNOFF BEHAVIOR STUDY

Initially, rainfall−runoff behaviour pattern was analysed for study plots. Regression analysis was performed to investigate relationships of runoff (Q)–depth with P-depth for each plot separately. The concluding remarks of rainfall−runoff behavior, and effect of soil type, land use and slope on runoff and Curve number are as follows:

- The P–Q relationship was statistically significant ($p<0.05$) for all the tested runoff plots. The mean runoff coefficient (Rc_m) was higher for the plots having HSGs C followed by B and A.

- The non-parametric Kruskal–Wallis test revealed that land uses did not show any significant difference in Rc except sugarcane which produced significantly ($p < 0.05$) higher Rc than blackgram and fallow land uses. The HSG C had significantly higher Rc than did B and A, but the last ones did not differ from each other. Notably, slope did not show any effect on Rc as all three groups of slopes were insignificantly different from each other. An inverse relationship between CN and fc for all 27 study plots was detected with significant correlation ($R^2 = 0.461$, $p<0.01$). Compared to land use and slope, infiltration capacity (fc) was the main explanatory variable for runoff (or CN) production in the study plots. The results from this analysis support the applicability of NEH-4 tables where CNs decline with fc (or HSG).

10.2 CN-DETERMINATION METHODS

The relative accuracy of different CNs determination methods was analyzed to find the best method for the study region. In order to check the suitability of Handbook table CNs for study region, the observed P-Q data-based Curve number were compared with Handbook table CNs and the results are as follows:

- P-Q data-based curve number estimation analysis showed that, in general, the CNs estimated by Geometric-mean method were usually larger (17 of 36 plots) followed by S-probability (15 of 36 plots). Based on the Kruskal–Wallis test analysis, mix results were obtained. There was no single method which produced significantly higher (or lower) CNs than other. Geometric-mean produced significantly ($p < 0.05$) higher CNs than M2 and M4, but it was statistically insignificant with others. The S-probability method proves to be best among all methods followed by geometric mean method. Based on overall score the methods performance can be described as follows: S-probability > geometric mean > storm event mean > rank order median > rank order mean > least square fit > storm event median > log normal frequency. CN values derived from ordered data (CN_{LSo}) are higher than CN values derived from natural data (CN_{LSn}).

- The derived CN values from observed P–Q data were considerably different from conventional NEH-4 table values. P–Q derived CNs are higher than those from NEH-4

tables. However, these are closer for higher CN values, consistent with the general notion that the existing SCS-CN method performs better for high P-Q (or CN) events. The group of CN_{HT} lower than 75 shows a higher PBIAS (=-12.84%) than the group of CN_{HT} higher than 75 (=1.03%). Overall, pair–wise comparison showed a significant difference ($p<0.05$) to exist between CN_{HT} and CN_{LSn} means.

10.3 INVESTIGATION FOR INITIAL ABSTRACTION RATIO (λ)

In order to find the suitable (representative) initial abstraction ratio (λ) value for study region, λ–values were derived for both natural and ordered P-Q data sets of 27 plots employing least square fit method. The concluding remarks are as follows:

- The optimized λ–values derived for both natural (ranging from 0 to 0.208) and ordered (ranging from 0 to 0.659) P–Q datasets varied widely from plot to plot with 0 as the most frequent value. The cumulative frequency distribution of λ-values for both datasets shows that λ values were larger for ordered data, the distribution was skewed, and most λ-values (out of 27, 26 for natural and 21 for ordered P–Q datasets) were less than the standard λ=0.2 value. The mean and median λ-values are 0.030 & 0 for natural, and 0.108 & 0 for ordered data, were quite different from standard λ = 0.20, but consistent with the results of other studies carried out elsewhere
- Runoff estimation improved as λ decreased; for 26 out of 27 plots by changing λ-value from 0.2 to 0.03. A relationship between $CN_{0.20}$ (λ = 0.20) and $CN_{0.03}$ (λ = 0.03), useful for CN conversion for field application was also developed.
- In contrast to the existing notion, I_a when plotted against S exhibited no correlation for both natural and ordered datasets, consistent with the findings of Jiang (2001). The study also indicated that the existing SCS-CN method is primarily a 2-parameter model and the parameters are Ia and S, which are independent of each other. Correlating Ia with S through Initial Abstraction Ratio (λ) is fundamental to all the problems/confusions associated with the description of the behaviour of SCS-CN model.

10.4 INVESTIGATION FOR ANTECEDENT MOISTURE CONDITION (AMC)

The existence of a relationship between CN (or S) and AMC was explored to improve the runoff prediction using regression models between CN derived from P-Q dataset and corresponding observed antecedent soil moisture indices such as θ_{o1}, θ_{o3}, θ_{o5}, and P_5. The exponential regression of CN with θ_{o1} performed the best of all in both calibration and

validation. However, the existing index based on 5-day antecedent rainfall (P_5) exhibited a poor performance in comparison to one day antecedent moisture (θ_{o1}), consistent with the results reported elsewhere (Brocca et al. 2008, 2009; Beck et al. 2009; Pfister et al. 2003).

10.5 COMPARATIVE EVALUATION OF SCS-CN-INSPIRED MODELS

The eight different SCS-CN inspired models including the existing SCS-CN method were comparison using the rainfall-runoff data measured from plot scale agricultural watersheds in India. The following conclusions can be derived from the study:

- The SCS model with λ=0.05 performed better than the original SCS-CN model with λ=0.2
- Model M8 performed the best of all followed by M7 with lower RMSE, higher n(t), higher NSE, and based on the performance rating and model efficiency limitation criteria.
- Based on the ranks and scores of each individual model for each performance index, the model M7 performed the best followed by M8, M5, M6, M3, M4, and M2 whereas M1 performed the poorest of all.

10.6 EFFECT OF SLOPE ON CURVE NUMBER (CN)

Improved models of CN_{II} estimation incorporating both the watershed slope and initial abstraction in their formulation (rather than incorporating λ = 0.3) in the existing NRCS-CN method were developed for Indian conditions. The developed CNII estimation models were applied to a range of watershed slope, initial abstraction coefficient and land use. The effect of the slope and initial abstractions on runoff estimation was studied using carefully observed 26 rainfall-runoff events with Maize, Raagi and Fallow type land uses. The slope adjusted CN equations of Ajmal et al (2016) (Model 4), Sharpley and Williams (1990) (Model 5), and Huang et al. (2006) (Model 6) were compared with the three proposed new models (M1-M3). A total of 36 combinations considering watershed slope (α), initial abstraction (λ) and type of land use were formulated for evaluating the comparative performance of all the six models. The following conclusions were drawn from this analysis.

- The proposed mathematical model, i.e., M1, M2 and M3 for CNII ($CNII_{(\alpha, \lambda)}$) were found to have lower values of RMSE and higher values of R^2 and ENS for all the combinations of watershed slope, initial abstraction and land use as compared to the existing models. The performance of M3 model was best followed by M5 and M2 and M1 models. The model M4 found to least performing model in all the 36 combinations.

- The most striking finding was that though the models M5 & M6 performed well still these models were not able to cope with initial abstraction ratio more than 0.2 and slope of 5%. Even in some cases, model M4, the values of RMSE and NSE were found to be negative. The proposed models exhibited versatility in applications and could be successfully applied for the land slope of more than 8% and for a variable range of initial abstraction from 0.05 to 0.3. With an increase in initial abstraction ratio the estimated runoff decreased, and vice-versa. Further model M3 showed enhanced predictability than the models M2 and M1.
- The observed CNII and computed CNII(α,λ) for model M3 were closest to the best fit line followed by M6 model (CNIIα). On the other hand, the CNIIα values computed by model M4 (Ajmal et al., 2016) were far away from the best fitted line. Model M4 showed unrealistic CNIIα values even more than 100.

10.7 CN-BASED SEDIMENT YIELD MODELLING

The SCS-CN based sediment yield models were tested to the datasets of rainfall-runoff-sediment yield observed from the experimental plots of different land uses, infiltration capacities and slopes. The concluding remarks are as follows:

- CN values estimated from sediment yield model (S2) were slightly lower than the CNs derived from SCS-CN method. The existence of a relationship between CNs derived from these two different approaches supports the coupling of the SCS-CN method with USLE.
- In application to plot wise rainfall-runoff-sediment yield data sets, the model S2 estimated sediment yield with efficiency varying from 57.26% to 93.13% with 73.65% as average value. Similarly, in application to rainfall-runoff-sediment yield data sets of overall plots in the region of the study, the models S2 and S4 respectively computed the sediment yield with an efficiency of 65.97% and 66.16% indicating satisfactory performance of the model in study area.
- The incorporation of the antecedent moisture content (M) in the sediment yield model improved the model performance. Further, an increase in initial abstraction ratio (λ) led to decrease both S and A parameters of the sediment yield models, and vice versa. The results from the present study supported the application of SCS coupled model for predicting the event-based sediment yield.

CHAPTER 11
RESEARCH ACCOMPLISHMENTS AND ACHIEVEMENTS

11.1 ACCOMPLISHMENT OF THE RESEARCH OBJECTIVES

The objectives of the present project report and their accomplishments, as envisaged at the stage of proposal formulation, are as follows:

a) Physical significance of Curve Number (CN)

The literature review showed that the Curve Number (CN) has a physical significance and is correlated with the soil's physical characteristics relating to retention and permeability. It has been shown in the present study that the CN values derived from P-Q data very well correlate with the infiltration capacity of the soil. Notably, infiltration fully relies on the retention capacity and permeability of the soil. In general, the NEH-4 Curve Numbers were seen to be applicable universally when tested using the field data.

b) Development of a new computational procedure

In the present study, several CN determination methods were compared and the best one identified which could be employed for runoff prediction. More appropriate value of the initial abstraction ratio was identified and recommended for field application. The effect of slope, land use, and soil type was evaluated and procedures were suggested. A SCS-CN-based sediment yield has been proposed and suggested.

c) Investigation of the behaviour of a natural process

The present study explored the SCS-CN methodology and investigated for its various components. Study found that the method is basically a two-parameter model and these are Ia and S, rather than initial abstraction ratio and S. The existing Ia-S relationship is a forced relationship wrongly embedded into the fabric of SCS-CN formulation and the fundamental to all associated problems/confusions.

d) Contribution to Water Resources Development

The present study correlated the P-Q derived CN values with the infiltration capacity of the soil derived physically from observations, and thus, verified that the Curve Number (CN) had a physical significance and is correlated with the soil's physical retention and permeability characteristics. Several CN determination methods were compared, and the best one identified for runoff more accurate prediction. More appropriate value of the initial abstraction ratio was identified and recommended for field application. The effect of slope, land use, and soil type was evaluated and procedures were suggested. A SCS-CN-based

sediment yield has been proposed and suggested. Since the SCS-CN methodology is the most popular rainfall-runoff method and is a part of a number of globally available commercial softwares, the presented enhanced understanding shall prove to be a mile-stone in its application world-wide. It is obviously a significant contribution to the field of water resources planning, development, and management.

e) Putting the Research to Use

The outcome of the research shall be disseminated through digital and physical media of communication. The report shall be sent to various academic, state irrigation departments, and other institutions dealing with water and soil conservation. A training workshop is also planned at an appropriate place for dissemination of the results of the study.

11.2 RESEARCH ACHIEVEMENTS

11.2.1 Research Publications

(A) International Journals (SCI journals)

1. Mishra, S. K., Chaudhary, A., Shrestha, R. K., Pandey, A. and Lal, M. (2014) "Experimental verification of the effect of slope and land use on SCS runoff curve number". Water Resources Management 28(11), 3407–3416
2. Lal, M., Mishra, S. K., Pandey, A. (2015). "Physical verification of the effect of land features and antecedent moisture on runoff curve number. Catena 133:318–327
3. Lal, M., Mishra, S. K., Pandey, A., Pandey, R. P., Meena, P. K., Chaudhary, A., Jha, R. K., Shreevastava, A. K. and Kumar, Y. (2017). "Evaluation of the Soil Conservation Service curve number methodology using data from agricultural plots" Hydrogeology Journal, 25(1):151-167.
4. **Lal, M.**, Mishra, S. K. and Kumar, M. (2019). Reverification of antecedent moisture condition dependent runoff curve number formulae using experimental data of Indian watersheds. Catena 173:48–58.

(B) National Journals (NAAS rated journals)

1. Lal, M. and Mishra, S. K. (2015). "Characterization of Surface Runoff, Soil Erosion, Nutrient Loss and their Relationship for Agricultural Plots in India." Current World Environment, 10(2), 593–601.
2. Karn, A.L., Lal, M., Mishra, S.K., Chaube, U.C. and Pandey, A. (2016) "Evaluation of SCS-CN inspired models and their comparison". Journal of Indian Water Resource Society, 36(3), 19-27.

3. Lal, M., Mishra, S. K., Pandey, A. (2017). "Empirical evaluation of Soil Conservation Service Curve Number inspired sediment yield model." Journal of Soil and Water Conservation India, 16(2): 142-150
4. Lal, M., Mishra, S. K., Pandey, A. (2017) Plot Scale Assessment of Effect of Watershed Features on Runoff and Sediment Generation in Uttarakhand, India, Indian Journal of Dryland Agricultural Research and Development, 32(2): 50-55
5. Jha, R.K., Mishra, S.K., and Pandey, A., 2014. Experimental verification of effect of slope, soil, and AMC of a fallow land on runoff curve number. Journal of Indian Water Resources Society, 34 (2), 40–47
6. Chaudhary, A., Mishra, S.K., and Pandey, A., 2013. Experimental verification of effect of slope on runoff and curve numbers. Journal of Indian Water Resources Society, 33 (1), 40–46.
7. Shrestha, R.K., Mishra, S.K., and Pandey, A., 2013. Curve number affected by slope of experimental plot having maize crop. Journal of Indian Water Resources Society, 33 (2), 42–50.
8. Lal, M., Mishra, S. K., Pandey, A., Jha, R.K. (2013). Watershed features vis-à-vis SCS curve number, frontiers of science, A Journal of Multiple Sciences ISSN: 0974-5297, Vol: VII, (7)

(C) Conference papers

1. Lal, M., Mishra, S. K., Pandey, A. (2015) Curve number derivation for experimental plots of different slopes, hydrologic soil groups and land uses. Paper presented at 20th International Conference on Hydraulics, Water Resources and River Engineering, 17-19 December, 2015, at IIT Roorkee, India, Volume: HYDRO 2015 INTERNATIONAL
2. Lal, M., Mishra, S. K., Pandey, A., Kumar, Y., (2016) Runoff Curve Number for 36 Small Agricultural Plots at Two Different Climatic Conditions in India. Paper presented at national conference WRHP (Water Resource & Hydropower) held during 16-18th June, 2016, Dehradun.
3. Lal, M., Mishra, S. K., Pandey, A., Kumar, Y., (2018). A Revisit to Antecedent Moisture Content Based Curve Number Formulae. Paper presented at International Conference on Sustainable Technologies for Intelligent Water Management (STIWM-2018) during February 16-19, 2018 at IIT Roorkee.

(D) Book Chapter

Lal, M., Mishra, S. K., Pandey, A., Kumar, Y. Runoff Curve Number for 36 Small Agricultural Plots at Two Different Climatic Conditions in India. In book:

Development of Water Resources in India, Edition: vol 75, Chapter: 22, Publisher: Water Science and Technology Library, Springer, Cham, Editors: Garg V., Singh V., Raj V. (eds)

11.2.2 Ph.D and MTech Degrees Awarded

(A) Ph.D. Theses

Sl. No.	Name of student	Thesis Title	Year
1.	Mohan Lal	Investigation of SCS-CN Methodology on Experimental Plot and Catchment Scales	2019
2.	Shailendra Kumar Kumre	SCS-CN-inspired rainfall-runoff, sediment yield, and environmental flow modelling	2019

(B) M.Tech Dissertations

Sl. No.	Name	Topic	Year
1	Anubhav Chaudhary	Determination of runoff curve number and sediment yield in monsoon season for sugarcane grown on a soil with different grades	2013
2	Raj Kaji Shreshtha	Determination of runoff curve number and sediment yield in non-monsoon season for sugarcane grown on a soil with different grades	2013
3	Ranjit Kumar Jha	Effect of soil, land use, antecedent moisture condition (AMC), and slope on runoff curve number	2014
4	Rajendra Prasad Deo	Effect of soil, land use, antecedent moisture condition (AMC), and slope on sediment yield	2014
5	Lek Nath Subedi	Effect of soil, land use, AMC, and slope on nutrition loss of soil	2014
6	Dinesh Poudel	Relationship among runoff curve number, sediment yield and nutrition loss	2014
7	Santosh Kumar Choaudhary	Universal soil loss equation (USLE) based plot scale study on soil erosion	2014
8	Ajeet Kumar Srivastava	Effect of land use, soil type, and antecedent moisture condition (AMC) on runoff curve number	2015
10	Shree Prasad Sah	Effect of soil type, land use, and antecedent moisture condition (AMC) on sediment yield	2015
11	Binaya Paudel	Relationship among rainfall, runoff curve number and sediment yield	2015
12	Arun Lal Karn	Evaluation of SCS-CN inspired method	2016
13	Mohit Tomar	An advanced NRCS-CN model for runoff estimation using GIS and Remote Sensing	2017
14	Srinivasulu Pasila	Development of SCS-CN model for runoff estimation using soil moisture proxies	2017

REFERENCES

1. Ajmal, M., Moon, G., Ahn, J. and Kim, T (2015a). Investigation of SCS and its inspired modified models for runoff estimation in South Korean watersheds. J. Hydro. Environ. Res., 9(4):592-603.
2. Ajmal, M., Moon, G., Ahn, J. and Kim, T. (2015b). Quantifying excess storm water using SCS-CN–based rainfall runoff models and different curve number determination methods. J. Irrig. Drain. Eng. 141(3): 04014058
3. Ajmal, M., Waseem, M., Ahn, J. and Kim, T. (2015c). Improved runoff estimation using event-based rainfall-runoff models. Water Resour. Manage., 29:1995-2010
4. Ajmal, M., Waseem, M., Ahn, J. and Kim, T. (2016). Runoff estimation using the NRCS slope-adjusted curve number in mountainous watershes. J. Irrig. Drain. Eng. 142(4): 04016002
5. Ali, S. and Sharda, V. N. (2008). A comparison of curve number-based methods for runoff estimation from small watersheds in a semi-arid region of India. Hydrol. Res., 39(3):191-200
6. Baltas, E. A., Dervos, N. A., Mimikou, M. A. (2007). Determination of the SCS initial abstraction ratio in an experimental watershed in Greece. Hydrol. Earth Syst. Sci., 11:1825-1829.
7. Beck, H. E., Jeu, R. A. M., Schellekens. J., Van Dijk, A. I. J. M. and Bruijnzeel, L. A. (2009). Improving curve number-based storm runoff estimation using soil moisture indices. IEEE, Journal of selected topics in applied earth observations and remote sensing 2(4), 250-259.
8. Bonta, J. V. (1997). Determination of watershed curve number using derived distributions. J. Irrig. Drain. Div., 123(1): 28–36.
9. Brocca, L. Melone, F. and Moramarco, T. (2008). On the estimation of antecedent wetness conditions in rainfall–runoff modeling. Hydrol. Process., 22, 629–642.
10. Brocca, L., Melone, F., Moramarco, T. and Singh, V.P. (2009). Assimilation of observed soil moisture data in storm rainfall–runoff modelling. J. Hydrol. Eng., 14 (2): 153–165.
11. Central Unit for Soil Conservation (Hydrology and Sedimentation) (1972). Handbook of Hydrology, Soil Conservation Division, Ministry of Agriculture, Govt. of India.
12. D'Asaro, F. and Grillone, G. (2012). Empirical investigation of curve number method parameters in the Mediterranean area. J. Hydrol. Eng., 17, 1141-1152

13. D'Asaro, F., Grillone, G. and Hawkins, R. H. (2014). Curve number: empirical evaluation and comparison with curve number handbook tables in Sicily. J. Hydrol. Eng., 19(12): 04014035 (1-13).
14. Elhakeem, M. and Papanicolaou, A. N. (2009). Estimation of the runoff curve number via direct rainfall simulator measurements in the state of Iowa, USA. Water Resour. Manag. 23(12): 2455-2473.
15. Fennessey, L. A. (2000). The effect of inflection angle, soil proximity and location on runoff. Ph.D. dissertation, Pennsylvania State University, State College, PA
16. Feyereisen, G. W., Strickland, T. C., Bosch, D. D., Truman, C. C., Sheridan, J. M. and Potter, T. L. (2008). Curve number estimates for conventional and conservation tillages in the southeast Coastal Plain. J. Soil and Water Conserv., 63(3): 120-128.
17. Fu, S., Zhang, G., Wang, N. and Luo, L. (2011). Initial abstraction ratio in the SCS-CN method in the Loess Plateau of China. Trans ASABE, 54(1):163–169.
18. Garg, V., Nikarn, B. R., Thakur, P. K., Aggarwal, S. P. (2013). Assessment of the effect of slope on runoff potential of a watershed using NRCS-CN method. Int. J. Hydro. Sci. Tech. 3(2): l41-159.
19. Hauser, V. L. and Jones, O. R. (1991). Runoff curve numbers for the southern great plains. Trans. Am. Soc. Agricul. Engi., 34(1): (Jan-Feb 1991), 142- 148.
20. Hawkins, R. H. (1973). Improved prediction of storm runoff in mountain watershed. J. Irrig. Drain. Div. ASCE, 99, 519-523.
21. Hawkins, R. H. (1984). A comparison of predicted and observed runoff curve numbers. Symposium, Proceeding, Water Today and Tomorrow, ASCE, Reston, VA, 702-709
22. Hawkins, R. H. (1993). Asymptotic determination of runoff curve numbers from data. J. Irrig. Drain. Eng., 119(2): 334-345.
23. Hawkins, R. H. and Ward, T. J. (1998). Site and cover effects on event runoff, Jornada experimental range, New Mexico. Symp. Proc., Conf. on Rangeland Management and Water Resources, American Water Resources Associations, Middleburg, VA, 361-370
24. Hawkins, R. H., Hjelmfelt, A. T. and Zevenbergen, A. W. (1985). Runoff probability, storm depth, and curve numbers. J. Irrig. Drain. Eng., 111(4): 330–340.
25. Hawkins, R. H., Jiang, R., Woodward, D. E., Hjelmfelt, A. T., Van Mulle, J. A. and Quan, Q. D. (2002). Runoff curve number method: Examination of the initial abstraction ratio, in Proceedings of the Second Federal Interagency Hydrologic Modeling Conference, ASCE Publications: Las Vegas

26. Hawkins, R. H., Ward, T. J., Woodward, D. E. and Van Mullem, J. A. (2009). Curve number hydrology: state of practice. ASCE, Reston, VA, 15 pp.
27. Hjelmfelt, A. T. (1980). Empirical-investigation of curve number techniques. J. Hydraul. Eng. Div. 106(9):1471–1476.
28. Hjelmfelt, A. T. Jr. (1991). Investigation of curve number procedure. J. Hydraul. Eng. 117, 725–737.
29. Huang, M., Jacgues, G., Wang, Z., Monique, G. (2006). A modification to the Soil Conservation Service curve number method for steep slopes in the Loess plateau of China. Hydrol. Process., 20(3), 579-589.
30. Jain, M.K., Mishra, S. K., Suresh Babu, P., Venugopal, K., and Singh, V. P. (2006). Enhanced runoff curve number model incorporating storm duration and a nonlinear Ia-S relation. Journal of Hydraulic. Engineering.11 (6): 631–635.
31. Jiang, R. (2001). Investigation of Runoff Curve Number Initial Abstraction Ratio. MS Thesis Watershed Management, University of Arizona. pp.120
32. Kostka, Z. and Holko, L. (2003). Analysis of rainfall-runoff events in a mountain catchment. Interdisciplinary approaches in small catchment hydrology: Monitoring and research, L. Holko and P. Miklanek, eds., IHP-VI Technical Documents in Hydrology No. 67, UNESCO, Paris, 19–25.
33. Kruskal, W. H. and Wallis, W. A. (1952). Use of ranks in one-criterion variance analysis. J. Am. Stat. Assoc., 47(260): 583–621.
34. Kumar, K., Hari Prasad, K. S and Arora, M. K. (2012). Estimation of water cloud model vegetation parameters using a genetic algorithm. Hydrol. Sci. J., 57(4): 776-789.
35. Lal, M., Mishra, S. K. and Pandey, A. (2015). Physical verification of the effect of land features and antecedent moisture on runoff curve number. Catena 133:318–327
36. Lal, M., Mishra, S. K., Pandey, A., Pandey, R. P., Meena, P. K., Chaudhary, A., Jha, R. K., Shreevastava, A. K. and Kumar, Y. (2017). Evaluation of the Soil Conservation Service curve number methodology using data from agricultural plots. Hydrogeol. J., 25(1):151-167.
37. Legates, D. R. and McCabe Jr., G. J. (1999). Evaluating the use of "goodness-of-fit" measures in hydrologic and hydroclimatic model validation, Water Resour. Res., 35(1): 233–241
38. Massari, C., Brocca, L., Barbetta, S., Papathanasiou, C., Mimikou, M., Moramarco, T. (2014). Using globally available soil moisture indicators for flood modelling in mediterranean catchments. Hydrol Earth Syst. Sci., 10(8): 10997–1033.

39. Mays, L. W. (2005). Water resources engineering, 2nd edn. Willey, Arizona, ISBN: 978-0-470-46064-1.
40. Menberu, M. W., Haghighi, A. T., Ronkanen, A. K., Kværner, J. and Kløve, B. (2015). Runoff curve numbers for peat-dominated watersheds. J. Hydraul. Eng., 20(4): 04014058
41. Mishra, S. K. and Singh, V. P. (2003). Soil Conservation Service Curve Number (SCS-CN) Methodology. Kluwer Academic Publishers, Dordrecht.
42. Mishra, S. K., Tyagi, J. V., Singh, V. P., & Singh, R. (2006a). SCS-CN-based modeling of sediment yield. Journal of Hydrology, 324 (1-4), 301–322.
43. Mishra, S.K. and Singh, V.P. (2002). SCS-CN method: Part-I: Derivation of SCS-CN based models. Acta Geophysica Polonica 50(3):457-477.
44. Mishra, S.K., Sahu, R.K., Eldho, T.I. and Jain, M.K. (2006b). An improved Ia-S relation incorporating antecedent moisture in SCS-CN methodology. Journal of Water Resource. Management. 20:643-660.
45. Moriasi, D. N., Arnold, J. G., Van Liew, M. W., Bingner, R. L., Harmel, R. D and Veith, T. L. (2007). Model evaluation guidelines for systematic quantification of accuracy in watershed simulations. Transactions of the ASABE 50(3):885–900.
46. Motovilov, Y. G., Gottschalk, L., England, K. and Rodhe, A. (1999). Validation of a distributed hydrological model against spatial observations. Agric Forest Meteorol 98(99): 257–277.
47. Nadal-Romero, E., Latron, J., Lana-Renault, N., Serrano-Muela, P., Martí-Bono, C. and David Regüés, D. (2008). Temporal variability in hydrological response within a small catchment with badland areas, central Pyrenees. Hydrol. Sci. J., 53: 629–639.
48. Nash, J. E. and Sutcliffe, J. V. (1970). River flow forecasting through conceptual models, Part I - A discussion of principles. J. Hydrol., 10, 282–290.
49. NRCS (2001). 'Hydrology' national engineering handbook, supplement A, Section 4, Soil Conservation Service, USDA, Washington, DC
50. Parajuli, P. B., Mankin, K. R. and Barnes, P. L. (2009). Source specific fecal bacteria modeling using soil and water assessment tool model. Bio. Resour. Tech., 100(2): 953–963.
51. Ritter, A. and Muñoz-Carpena, R. (2013). Performance evaluation of hydrological models: Statistical significance for reducing subjectivity in goodness-of-fit assessments. J. Hydrol., 480, 33-45.

52. Rodríguez-Blanco, M. L., Taboada-Castro, M. M. and Taboada-Castro, M. T. (2012). Rainfall–runoff response and event-based runoff coefficients in a humid area (northwest Spain). Hydrolog. Sci. J., 57(3): 445-459.
53. Sahu, R. K., Mishra, S. K., Eldho, T. I. and Jain, M. K. (2007). An advanced soil moisture accounting procedure for SCS curve number method. J. Hydrol. Process., 21(21): 2872–2881.
54. Schneider, L. E. and McCuen, R. H. (2005). Statistical guidelines for curve number generation. J. Irrig. Drain. Eng., 131(3): 282-290.
55. SCS (1956, 1964, 1971, 1972, 1985). 'Hydrology' national engineering handbook, supplement A, Section 4, Soil Conservation Service, USDA, Washington, DC.
56. Senbeta, D. A., Shamseldin, A. Y. and O'Connor, K. M. (1999). Modification of the probability-distributed interacting storage capacity model. J. Hydrol., 224:149-168.
57. Sharpley, A. N. and Williams, J. R. (1990). EPIC-Erosion/Productivity Impact Calculator: 1. Model determination, US Department of Agriculture. Technical Bulletin, No. 1768.
58. Soulis, K. X. and Valiantzas, J. D. (2013). Identification of the SCS-CN parameter spatial distribution using rainfall-runoff data in heterogeneous watersheds. Water Resour Manag 27(6):1737–1749.
59. Stewart, D., Canfield, E. and Hawkins, R. H. (2012). Curve number determination methods and uncertainty in hydrologic soil groups from semiarid watershed data. J. Hydrol. Eng., 17, 1180-1187.
60. Taguas, E., Yuan, Y., Licciardello, F. and Gómez, J. (2015). Curve numbers for olive orchard catchments: case study in southern Spain. J. Irrig. Drain. Eng., DOI: 10.1061/(ASCE)IR.1943-4774.0000892.
61. Tedela, N. H., McCutcheon, S. C., Rasmussen, T. C. and Tollner, E. W. (2008). Evaluation and improvement of the curve number method of hydrological analysis on selected forested watersheds of Georgia. Project report submitted to Georgia Water Resources Institute, Supported by the U.S. Geological Survey. pp.40
62. Tedela, N. H., McCutcheon, S. C., Rasmussen, T. C., Hawkins, R. H., Swank, W. T., Campbell, J. L., Adams, M. B., Jackson, C. R and Tollner, E. W. (2012). Runoff Curve Numbers for 10 Small forested watersheds in the mountains of the eastern United States. J. Hydrol. Eng., 17(11):1188-1198.
63. Titmarsh, G. W., Cordery, I. and Pilgrim, D. H. (1995). Calibration procedures for rational and USSCS design hydrographs. J. Hydraul. Eng., 121(1): 61–70.

64. Titmarsh, G. W., Cordery, I. and Pilgrim, D. H. (1996). Closure of calibration procedures for rational and USSCS design flood methods. J. Hydraul. Eng., 122(3):177.
65. Titmarsh, G. W., Pilgrim, D. H., Cordery, I. and Hossein, A. A. (1989). An examination of design flood estimations using the U.S. soil conservation services method. Hydrology and water resources symposium, Institution of Engineers, Barton, ACT, Australia
66. Woodward, D. E., Hawkins, R. H., Jiang, R., Hjelmfelt, A. T., Van Mullem, J. A. and Quan, Q. D. (2004). Runoff Curve Number Method: Examination of the initial abstraction ratio in proceedings of the world water and environmental resources congress and related symposis. ASCE Publications: Philadelphia, PA
67. Yuan, Y., Nie, J., McCutcheon, S. C. and Taguas, E. V. (2014). Initial abstraction and curve numbers for semiarid watersheds in south eastern Arizona. Hydrol. Process., (28):774–783.
68. Zhang, Y., Wei, H. and Nearing, M. A. (2011). Effects of antecedent soil moisture on runoff modeling in small semiarid watersheds of southeastern Arizona. Hydrol. Earth Syst. Sci., 15, 3171–3179.
69. Zhou, S.M. and Lei, T.W., (2011). Calibration of SCS-CN Initial Abstraction Ratio of a typical small watershed in the Loess Hilly-Gully region. China Agric. Sci. 44, 4240–4247.

APPENDIX A

Table A1 Observed rainfall, runoff and previous day soil moisture data for experimental plot nos. 1, 2 and 3

Event No.	Date	Rainfall(P) mm	Runoff(Q) mm			Previous day soil moisture (%)		
			Plot 1	Plot 2	Plot 3	Plot 1	Plot 2	Plot 3
1	16-Jun-13	73.00	44.77	49.84	43.76	22.70	24.27	30.87
2	28-Jun-13	32.00	11.61	11.47	15.18	26.57	23.87	29.33
3	20-Jul-13	88.50	28.14	29.42	31.51	17.70	21.77	25.33
4	29-Jul-13	46.50	18.93	20.02	20.70	22.50	21.70	23.33
5	05-Aug-13	16.80	0.37	0.04	0.38	25.73	20.93	26.57
6	13-Aug-13	17.00	1.95	4.37	2.16	21.30	23.50	24.07
7	22-Aug-13	42.00	3.90	1.85	7.85	17.43	18.47	19.80
8	28-Aug-13	16.00	0.08	0.15	0.15	20.73	22.07	22.70
9	30-Aug-13	27.40	3.74	2.19	12.28	23.97	24.47	24.17
10	11-Oct-13	18.40	0.68	0.50	0.70	11.80	8.40	5.40
11	18-Jan-14	53.9	5.72	3.57	4.78	19.50	21.20	22.60
12	23-Jan-14	35.2	5.42	4.94	4.52	21.50	26.20	26.50
13	14-Feb-14	24.8	0.64	0.45	0.02	19.10	20.50	22.50
14	15-Feb-14	39	14.32	8.20	18.02	27.30	30.90	30.40
15	12-03-2014	22	1.849	1.728	0.228	19.3	23.7	30.1

Table A2 Observed rainfall, runoff and previous day soil moisture data for experimental plot nos. 4, 5 and 6

Event No.	Date	Rainfall (mm)	Runoff(Q) mm			Previous day soil moisture (%)		
			Plot 4	Plot 5	Plot 6	Plot 4	Plot 5	Plot 6
1	16-Jun-13	73.00	38.20	39.59	30.61	27.3	22.3	19.7
2	28-Jun-13	32.00	3.43	5.05	0.49	18.77	25.40	21.37
3	20-Jul-13	88.50	20.14	16.73	17.32	17.60	19.53	16.23
4	29-Jul-13	46.50	6.65	11.02	1.97	19.73	19.83	19.73
5	05-Aug-13	16.80	0.37	0.09	0.48	21.10	22.23	22.20
6	13-Aug-13	17.00	2.39	2.47	0.35	22.60	23.33	24.93
7								
8	28-Aug-13	16.00	0.23	0.04	0.08	20.37	19.63	21.30
9	30-Aug-13	27.40	1.33	9.56	1.53	24.10	23.73	23.27
10	11-Oct-13	18.40	0.23	0.12	0.20	8.3	7.7	5.7

Table A3 Observed rainfall, runoff and previous day soil moisture data for experimental plot nos. 7, 8 and 9

Event No.	Date	Rainfall (mm)	Runoff(Q) mm			Previous day soil moisture (%)		
			Plot 7	Plot 8	Plot 9	Plot 7	Plot 8	Plot 9
1	16-Jun-13	73.00	30.29	27.53	45.56	20.67	28.30	26.80
2	28-Jun-13	32.00	11.43	8.31	15.84	28.47	24.07	22.13
3	20-Jul-13	88.50	43.37	44.51	43.87	17.10	13.73	22.97
4	29-Jul-13	46.50	20.34	10.97	13.24	22.53	24.10	26.57
5	05-Aug-13	16.80	0.18	0.06	0.10	20.47	26.13	27.40
6	13-Aug-13	17.00	0.68	1.12	0.92	22.17	24.07	25.87
7	22-Aug-13	42.00	5.35	4.58	9.72	17.70	18.77	19.33
8	28-Aug-13	16.00	0.02	0.20	0.24	22.67	23.33	24.67
9	30-Aug-13	27.40	10.01	5.65	8.60	23.73	23.90	26.67
10	11-Oct-13	18.40	0.30	0.11	0.18	10.30	11.20	11.60

Table A4 Observed rainfall, runoff and previous day soil moisture data for experimental plot nos. 10, 11 and 12

Event No.	Date	Rainfall (mm)	Runoff(Q) mm			Previous day soil moisture (%)		
			Plot 10	Plot 11	Plot 12	Plot 10	Plot 11	Plot 12
1	16-Jun-13	73.00	48.95	37.09	39.17	25.40	25.25	26.05
2	28-Jun-13	32.00	13.67	13.20	15.35	20.67	23.17	21.37
3	20-Jul-13	88.50	33.46	31.19	29.23	14.33	14.90	19.73
4	29-Jul-13	46.50	10.56	7.74	12.84	20.27	22.97	22.07
5	05-Aug-13	16.80	0.10	0.26	0.19	18.30	23.13	26.03
6	13-Aug-13	17.00	0.83	0.28	1.77	24.10	23.70	25.00
7	22-Aug-13	42.00	4.44	1.81	0.53	15.77	20.20	18.80
8	28-Aug-13	16.00	0.24	0.38	0.31	21.50	23.07	24.73
9	30-Aug-13	27.40	3.56	2.10	0.87	23.37	24.77	26.43
10	11-Oct-13	18.40	0.30	0.20	0.28	8.90	12.50	12.70

Table A5 Observed rainfall, runoff and previous day soil moisture data for experimental plot nos. 13, 14 and 15

Event No.	Date	Rainfall (mm)	Runoff(Q) mm			Previous day soil moisture (%)		
			Plot 13	Plot 14	Plot 15	Plot 13	Plot 14	Plot 15
1	01-Jul-14	71.50	19.66	21.19	16.61	12.30	16.10	13.45
2	02-Jul-14	29.40	8.95	14.90	8.33	28.70	31.53	31.88
3	14-Jul-14	20.20	1.80	1.72	2.05	10.83	10.57	12.70
4	15-Jul-14	24.20	6.44	6.08	4.18	29.07	31.67	29.83
5	16-Jul-14	38.80	7.48	19.18	17.41	24.90	23.93	28.90
6	18-Jul-14	54.20	10.96	20.87	17.55	20.60	21.17	22.00
7	29-Jul-14	24.20	3.35	5.26	5.82	16.73	18.93	19.40
8	05-Aug-14	27.00	3.90	12.47	8.14	14.37	14.70	17.37
9	29-Aug-14	29.10	0.57	0.55	0.78	15.70	17.20	16.77
10	06-Sep-14	68.60	17.88	16.18	19.41	19.00	20.77	21.10
11	08-Sep-14	28.20	6.50	6.69	7.77	28.83	29.07	29.03
12	02-Mar-15	62.40	9.83	9.80	8.26	20.00	19.30	20.53
13	04-Apr-15	45.40	9.12	14.22	8.85	21.73	25.33	23.77

Table A6 Observed rainfall, runoff and previous day soil moisture data for experimental plot nos. 16, 17 and 18

Event No.	Date	Rainfall (mm)	Runoff(Q) mm			Previous day soil moisture (%)		
			Plot 16	Plot 17	Plot 18	Plot 16	Plot 17	Plot 18
1	01-Jul-14	71.50	12.20	16.04	18.79	9.00	14.00	14.00
2	02-Jul-14	29.40	11.25	9.63	18.40	26.40	31.33	29.70
3	14-Jul-14	20.20	1.16	0.80	0.30	9.70	10.20	9.73
4	15-Jul-14	24.20	2.99	1.90	1.82	26.55	22.97	26.50
5	16-Jul-14	38.80	12.51	4.86	10.94	19.90	21.77	23.60
6	18-Jul-14	54.20	18.17	13.16	27.03	20.67	17.17	21.33
7	29-Jul-14	24.20	0.91	2.06	0.84	15.53	15.67	19.57
8	05-Aug-14	27.00	2.09	4.76	3.74	16.43	14.27	24.37
9	29-Aug-14	29.10	0.24	0.05	0.78	16.73	16.57	15.80
10	06-Sep-14	68.60	26.94	21.38	30.88	21.83	20.20	23.27
11	08-Sep-14	28.20	9.03	7.19	10.19	29.80	29.83	28.83

Table A7 Observed rainfall, runoff and previous day soil moisture data for experimental plot nos. 19, 20 and 21

Event No.	Date	Rainfall (mm)	Runoff(Q) mm			Previous day soil moisture (%)		
			Plot 19	Plot 20	Plot 21	Plot 19	Plot 20	Plot 21
1	01-Jul-14	71.5	6.20	15.96	18.64	9.30	15.10	12.45
2	02-Jul-14	29.4	8.86	12.13	16.67	25.47	32.13	28.13
3	14-Jul-14	20.2	1.28	1.19	0.36	10.43	10.90	14.77
4	15-Jul-14	24.2	2.88	3.03	1.68	26.23	24.73	27.80
5	16-Jul-14	38.8	10.33	15.16	21.50	17.40	23.43	24.07
6	18-Jul-14	54.2	8.24	9.39	12.64	18.33	17.20	19.06
7	29-Jul-14	24.2	1.08	2.08	1.65	18.47	15.57	22.67
8	05-Aug-14	27	2.41	5.79	4.09	15.27	14.17	13.37
9	29-Aug-14	29.1	0.43	0.69	0.57	15.10	17.63	15.43
10	06-Sep-14	68.6	9.01	13.18	17.54	19.07	19.00	22.37
11	08-Sep-14	28.2	5.22	6.74	9.00	29.73	26.83	28.57

Table A8 Observed rainfall, runoff and previous day soil moisture data for experimental plot nos. 22, 23 and 24

Event No.	Date	Rainfall (mm)	Runoff(Q) mm			Previous day soil moisture (%)		
			Plot 22	Plot 23	Plot 24	Plot 22	Plot 23	Plot 24
1	01-Jul-14	71.5	14.99	15.37	13.86	11.75	14.00	15.70
2	02-Jul-14	29.4	7.87	11.27	4.89	33.67	34.27	28.00
3	14-Jul-14	20.2	2.67	1.17	1.11	10.27	10.93	8.70
4	15-Jul-14	24.2	3.82	2.17	4.68	26.13	23.43	21.23
5	16-Jul-14	38.8	13.24	15.75	15.47	23.53	23.70	17.23
6	18-Jul-14	54.2	10.26	13.58	16.87	18.83	17.37	18.47
7	29-Jul-14	24.2	3.08	3.06	4.08	17.47	15.53	19.70
8	05-Aug-14	27	7.61	5.23	6.65	13.50	13.23	14.70
9	29-Aug-14	29.1	0.34	0.58	1.04	10.07	10.27	9.43
10	06-Sep-14	68.6	6.60	0.15	2.38	18.60	17.60	14.10
11	08-Sep-14	28.2	4.57	5.25	5.69	29.70	29.13	29.33
12	02-Mar-15	62.40	7.63	N.A.	9.03	20.13	N.A.	19.47
13	04-Apr-15	45.40	7.03	N.A.	10.83	22.8	N.A.	21.73

Table A9 Observed rainfall, runoff and previous day soil moisture data for experimental plot nos. 25, 26 and 27

Event No.	Date	Rainfall (mm)	Previous day soil moisture (%)			Runoff (mm)		
			Plot 25	Plot 26	Plot 27	Plot 25	Plot 26	Plot 27
1	13-Sep-12	22.2	32.7	30.7	30.1	14.73	6.69	5.35
2	14-Sep-12	30.2	32.5	27.4	27.6	14.74	11.49	9.18
3	17-Sep-12	42.1	34.5	32	31	24.38	22.30	21.17
4	18-Sep-12	29.1	34.8	32.1	31.84	23.05	18.18	16.45
5	18-Jan-13	56.2	28.4	27.6	26.8	19.46	18.75	15.05
6	05-Feb-13	48.2	29.8	27.9	26.6	20.14	13.82	9.87
7	06-Feb-13	22.4	29.3	29.1	26.9	8.25	4.84	3.51
8	16-Feb-13	43.2	28.6	25.6	24.4	25.32	17.68	16.35
9	17-Feb-13	53.8	32.4	29.8	27.6	30.85	25.83	23.09
10	23-Feb-13	10.2	31.15	31.43	30.93	2.85	0.68	0.35

Table A10 Observed rainfall and runoff data for experimental plot nos. 28, 29 and 30

Event No.	Date	Rainfall (mm)	Runoff(Q) mm		
			Plot 28	Plot 29	Plot 30
1	13-Sep-12	22.20	15.46	8.73	3.64
2	14-Sep-12	30.20	19.00	18.79	15.88
3	17-Sep-12	42.10	25.56	22.30	16.16
4	18-Sep-12	29.10	20.65	18.18	8.75

Table A11 Observed rainfall and runoff data for experimental plot nos. 31 and 32

Event No.	Date	Rainfall (mm)	Runoff(Q) mm	
			Plot 31	Plot 32
1	18-01-2014	53.90	3.04	2.75
2	23-01-2014	35.20	12.34	5.06
3	14-02-2014	24.80	0.79	0.02
4	15-02-2014	39.00	11.44	14.58
5	12-03-2014	22.00	1.14	0.32

Table A12 Observed rainfall and runoff data for experimental plot nos. 33, 34 and 35

Event No.	Date	Rainfall (mm)	Runoff(Q) mm		
			Plot 33	Plot 34	Plot 35
1	18-01-2014	53.90	1.54	0.02	0.27
2	23-01-2014	35.20	5.63	1.45	8.10
3	14-02-2014	24.80	0.49	0.27	0.06
4	15-02-2014	39.00	4.56	4.80	9.80
5	12-03-2014	22.00	3.152	1.652	1.334

Appendix B

List of tables for data collected during phase 1

Table B1 Observed rainfall and runoff data for experimental plot nos. 1 to 9.

Event No.	Date	Rainfall (mm)	Runoff (mm)								
			plot 1	plot 2	plot 3	plot 4	plot 5	plot 6	plot 7	plot 8	plot 9
1	15-Jun-16	17	10.66	4.86	1.28	9.86	9.27	5.35	11.77	7.88	2.68
2	16-Jun-16	46.5	35.50	27.10	22.24	32.65	21.82	24.49	36.82	30.92	18.17
3	22-Jun-16	39.2	27.23	21.53	14.31	24.03	19.87	15.70	31.67	20.98	16.26
4	7-Feb-16	35	26.75	18.41	17.72	21.89	19.80	19.11	18.41	12.16	16.33
5	3-Jul-16	22.8	11.20	9.81	7.04	12.59	9.81	5.65	9.81	11.20	5.65
6	6-Jul-16	13	8.27	8.41	4.28	7.23	8.62	7.06	9.32	6.71	8.45
7	16-Jul-16	19.1	8.97	6.88	3.41	7.30	7.58	6.88	4.80	6.88	6.61
8	22-Jul-16	65	49.43	45.82	40.61	51.62	47.66	40.61	53.11	49.99	45.89
9	23-Jul-16	36	30.07	25.90	16.18	25.21	25.21	21.74	27.29	17.57	24.51
10	25-Jul-16	23.8	18.28	15.50	11.06	20.78	13.83	12.45	16.61	16.61	9.67
11	6-Aug-16	24	5.47	4.08	0.75	4.08	6.86	2.00	5.47	2.69	1.30
12	8-Aug-16	20.8	11.64	6.36	3.16	12.19	5.66	2.19	10.94	5.39	9.97
13	11-Aug-16	12.4	0.89	1.59	0.20	1.59	0.89	0.20	2.97	0.89	0.89
14	14-Aug-16	22	15.49	14.10	9.93	10.63	11.32	9.93	15.49	11.32	11.32
15	14-Aug-16	12	5.81	4.42	0.95	7.20	3.03	3.03	5.81	3.03	1.64
16	29-Aug-16	46.5	31.27	25.02	16.13	28.77	28.49	27.79	29.88	29.18	24.32
17	22-Sep-16	20	9.11	7.45	4.81	8.84	5.78	5.36	7.45	3.28	4.95

Table B2 Observed daily rainfall, runoff and previous day soil moisture data for experimental plot nos. 10-12.

Event No.	Date	Rainfall (mm)	Runoff(Q) mm			Previous day soil moisture (%)		
			Plot 10	Plot 11	Plot 12	Plot 10	Plot 11	Plot 12
1	19-Jun-17	44.0	34.29	27.12	14.21	12.30	10.50	13.80
2	26-Jun-17	34.2	26.63	26.45	13.40	25.47	25.87	28.50
3	28-Jun-17	75.2	66.07	50.94	48.66	29.10	27.60	30.40
4	29-Jun-17	17.7	10.99	10.56	6.39	29.80	29.50	30.40
5	30-Jun-17	15.0	13.39	9.83	7.06	29.45	28.55	30.40
6	6-Jul-17	36.4	29.01	28.68	19.12	23.00	18.00	20.00
7	24-Jul-17	14.0	7.41	4.14	0.67	18.00	23.40	20.90
8	2-Aug-17	79.5	51.73	42.51	33.20	17.80	24.00	15.90
9	3-Aug-17	9.6	5.66	3.35	1.96	31.65	30.57	34.30
10	7-Aug-17	27.4	25.51	20.94	18.86	25.70	23.40	31.80
11	10-Aug-17	43.4	37.29	26.87	19.93	26.70	24.10	29.10
12	19-Aug-17	22.3	12.61	9.19	2.94	NA	NA	NA
13	22-Aug-17	58.1	46.25	30.90	28.95	24.00	24.00	25.70
14	23-Aug-17	15.5	8.64	2.54	2.32	33.40	33.30	37.80
15	25-Aug-17	61.8	52.04	36.59	32.28	27.70	26.40	31.00
16	1-Sep-17	44.0	36.24	20.53	14.98	25.85	25.20	28.35
17	1-Sep-17	23.0	21.27	18.81	14.65	32.60	32.87	33.85
18	2-Sep-17	61.1	32.90	33.22	26.27	25.67	26.53	29.47
19	3-Sep-17	26.0	19.34	13.51	9.06	30.25	28.45	32.60

Table B3 Observed daily rainfall, runoff and previous day soil moisture data for experimental plot nos. 13-15.

Event No.	Date	Rainfall (mm)	Runoff(Q) mm			Previous day soil moisture (%)		
			Plot 13	Plot 14	Plot 15	Plot 13	Plot 14	Plot 15
1	19-Jun-17	44.0	27.20	17.75	13.03	14.20	12.00	11.30
2	26-Jun-17	34.2	26.17	15.06	11.59	26.87	25.53	30.53
3	28-Jun-17	75.2	68.35	54.61	49.82	31.50	30.60	32.10
4	29-Jun-17	17.7	13.34	7.78	10.56	34.30	35.10	37.60
5	30-Jun-17	15.0	12.33	9.14	6.78	32.90	32.85	34.85
6	6-Jul-17	36.4	30.01	24.29	13.34	21.00	21.00	20.20
7	24-Jul-17	14.0	2.75	2.75	2.75	24.50	25.40	19.80
8	2-Aug-17	79.5	41.53	34.87	24.17	23.70	21.50	22.00
9	3-Aug-17	9.6	6.13	4.74	0.57	32.30	32.23	35.25
10	7-Aug-17	27.4	25.80	20.25	17.47	26.20	25.90	24.50
11	10-Aug-17	43.4	33.12	26.18	22.01	26.03	28.83	32.30
12	19-Aug-17	22.3	10.44	5.72	1.55	NA	NA	NA
13	22-Aug-17	58.1	35.06	25.34	16.31	23.00	26.20	29.00
14	23-Aug-17	15.5	3.93	3.15	2.54	30.30	25.60	35.30
15	25-Aug-17	61.8	50.47	38.67	28.42	25.60	28.90	28.00
16	1-Sep-17	44.0	17.75	18.98	10.81	24.30	27.55	28.50
17	1-Sep-17	23.0	16.73	16.04	12.56	35.05	33.07	33.55
18	2-Sep-17	61.1	42.94	24.05	29.05	25.10	26.77	26.80
19	3-Sep-17	26.0	20.45	9.34	6.56	32.05	31.60	29.33

Table B4 Observed daily rainfall, runoff and previous day soil moisture data for experimental plot nos. 16-18.

Event No.	Date	Rainfall (mm)	Runoff(Q) mm			Previous day soil moisture (%)		
			Plot 16	Plot 17	Plot 18	Plot 16	Plot 17	Plot 18
1	19-Jun-17	44.0	29.56	20.39	12.31	10.10	7.30	10.50
2	26-Jun-17	34.2	20.62	18.12	8.12	26.13	23.90	30.87
3	28-Jun-17	75.2	64.92	56.87	45.98	24.00	24.90	28.70
4	29-Jun-17	17.7	14.72	13.34	5.00	39.00	30.70	37.00
5	30-Jun-17	15.0	10.94	10.17	5.39	31.50	27.80	32.85
6	6-Jul-17	36.4	32.29	26.07	17.79	16.00	19.00	22.00
7	24-Jul-17	14.0	4.14	2.75	1.36	18.30	18.40	19.00
8	2-Aug-17	79.5	40.14	38.20	22.09	17.00	24.50	20.50
9	3-Aug-17	9.6	5.71	3.35	0.57	33.00	30.87	35.67
10	7-Aug-17	27.4	20.25	13.30	16.00	25.40	29.00	30.20
11	10-Aug-17	43.4	34.65	19.93	20.07	28.00	30.83	32.20
12	19-Aug-17	22.3	14.94	6.42	4.61	NA	NA	NA
13	22-Aug-17	58.1	35.90	33.67	23.26	22.50	29.20	31.20
14	23-Aug-17	15.5	4.54	5.32	2.54	32.80	32.80	35.60
15	25-Aug-17	61.8	45.61	31.45	38.67	24.40	28.10	26.20
16	1-Sep-17	44.0	30.70	17.75	12.20	23.45	28.65	28.70
17	1-Sep-17	23.0	20.90	13.81	14.65	31.90	34.63	34.83
18	2-Sep-17	61.1	48.50	25.72	33.22	24.10	27.10	26.30
19	3-Sep-17	26.0	19.06	10.68	13.51	27.40	32.10	31.23

Table B5 Observed daily rainfall, runoff and previous day soil moisture data for experimental plot nos. 19-21.

Event No.	Date	Rainfall (mm)	Runoff(Q) mm			Previous day soil moisture (%)		
			Plot 19	Plot 20	Plot 21	Plot 19	Plot 20	Plot 21
1	3-Jul-18	57	44.07	25.32	16.11	13.1	11.96	16.03
2	4-Jul-18	11	8.34	5	3.2	18.25	23.55	22.55
3	27-Jul-18	57	45.46	15.6	11.85	10.86	14.9	13.86
4	28-Jul-18	129.4	70.46	63.66	46.71	18.13	20.16	24.63
5	29-Jul-18	35	17.25	16.56	10.31	16.46	18.3	22.36
6	1-Aug-18	19	14.92	12.14	9.36	8.34	9.28	11.34
7	5-Aug-18	13	12.79	12.65	11.27	12.51	12.7	13.13
8	6-Aug-18	20.5	7.67	6.28	4.2	15.06	15.29	15.8
9	12-Aug-18	7.3	3.11	2.97	1.86	14.15	16.8	14.7
10	25-Aug-18	11.5	2.82	2.54	1.15	11.45	12.8	13.7
11	26-Aug-18	17.2	15.7	12.64	6.95	18.8	16.85	17.8
12	31-Aug-18	117.8	79.6	73.91	73.22	17.5	13.5	17
13	2-Sep-18	29.6	20.98	16.26	10.84	22.1	16.9	17.8
14	3-Sep-18	29	14.71	10.54	8.74	20.3	16.7	23.05
15	7-Sep-18	17.2	11.81	5.14	4.31	13.92	13.92	16.52
16	23-Sep-18	15.6	0.88	0.74	0.6	8	9.6	6.4
17	24-Sep-18	43.7	6.06	4.25	3.28	14.2	15.48	12.92
18	25-Sep-18	22.2	1.22	0.8	0.52	19.88	21.68	18.09

Table B6 Observed daily rainfall, runoff and previous day soil moisture data for experimental plot nos. 22-24.

Event No.	Date	Rainfall (mm)	Runoff(Q) mm			Previous day soil moisture (%)		
			Plot 22	Plot 23	Plot 24	Plot 22	Plot 23	Plot 24
1	3-Jul-18	57	55.18	12.13	4.49	11.63	17.33	17.1
2	4-Jul-18	11	7.09	4.45	2.09	16.7	27.15	22.3
3	27-Jul-18	57	22.13	11.29	9.49	13.93	17.96	18
4	28-Jul-18	129.4	56.57	50.05	38.8	18.96	26.1	23.8
5	29-Jul-18	35	5.45	3.78	2.39	17.21	23.7	21.61
6	1-Aug-18	19	14.92	6.17	5.2	8.73	12.01	10.96
7	5-Aug-18	13	8.49	4.32	2.24	12.59	13.27	13.05
8	6-Aug-18	20.5	3.09	2.05	1.98	15.16	15.97	15.71
9	12-Aug-18	7.3	1.44	1.3	0.89	17.5	14.55	15.05
10	25-Aug-18	11.5	2.12	1.15	1.01	12.67	13.25	15.35
11	26-Aug-18	17.2	8.75	1.95	0.56	19.65	19.2	21.05
12	31-Aug-18	117.8	57.52	45.16	39.47	17.5	18.5	21.6
13	2-Sep-18	29.6	18.06	10.01	9.17	17.75	18.85	22.3
14	3-Sep-18	29	15.27	9.29	7.63	20.3	22.1	24.25
15	7-Sep-18	17.2	6.11	4.59	0.98	15.76	16.88	16.24
16	23-Sep-18	15.6	1.71	0.33	0.19	8.16	6.8	8.4
17	24-Sep-18	43.7	3.83	3.56	1.06	14.32	13.24	14.52
18	25-Sep-18	22.2	1.64	0.66	0.39	20.06	18.54	20.33

Table B7 Observed daily rainfall, runoff and previous day soil moisture data for experimental plot nos. 25-27.

Event No.	Date	Rainfall (mm)	Runoff(Q) mm			Previous day soil moisture (%)		
			Plot 16	Plot 17	Plot 18	Plot 16	Plot 17	Plot 18
37	3-Jul-18	57	19.77	16.15	7.27	10.96	14.86	13.4
38	4-Jul-18	11	5.84	3.61	2.64	19.15	27.15	23.9
39	27-Jul-18	57	25.04	9.07	4.07	10.76	17.5	16.2
40	28-Jul-18	129.4	55.46	35.88	36.16	22.23	25.3	28.46
41	29-Jul-18	35	4.75	2.81	2.25	20.18	22.97	25.84
42	1-Aug-18	19	7.28	5.75	4.36	10.23	11.65	13.1
43	5-Aug-18	13	5.02	6.68	5.71	12.9	13.19	13.49
44	6-Aug-18	20.5	4.06	2.12	1.7	15.53	15.88	16.24
45	12-Aug-18	7.3	2.97	2.27	1.3	15.82	22.65	20.85
46	25-Aug-18	11.5	2.82	1.71	0.46	12.06	16.75	13.9
47	26-Aug-18	17.2	5	3.06	2.09	19.22	14.2	20.5
48	31-Aug-18	117.8	53.77	49.6	45.02	17.5	21.55	17.5
49	2-Sep-18	29.6	19.45	17.78	8.48	23.7	23.6	17.75
50	3-Sep-18	29	19.43	6.24	4.29	17.8	21.9	17.8
51	7-Sep-18	17.2	5.7	3.34	1.11	18.12	18.2	14.36
52	23-Sep-18	15.6	3.66	2.83	2.41	6.8	8.4	9.44
53	24-Sep-18	43.7	6.19	4.81	1.19	13.24	14.52	15.35
54	25-Sep-18	22.2	2.05	1.77	0.94	18.54	20.33	21.5

APPENDIX C

Table C1 Infiltration test data for experimental plot no. 1

Plot 1 (Date of test: 04/02/2014)					
Time	Time Interval (min.)	Cumulative Time (min.)	Volume of Water Added ml (cm^3)	Infiltration Depth (mm)	Infiltration Capacity (mm/hr.)
12:25 PM	0	Start = 0			
12:26 PM	1	1	250	3.54	212.21
12:27 PM	1	2	110	1.56	93.37
12:28 PM	1	3	100	1.41	84.88
12:30 PM	2	5	135	1.91	57.30
12:32 PM	2	7	115	1.63	48.81
12:34 PM	2	9	110	1.56	46.69
12:40 PM	6	15	310	4.39	43.86
12:45 PM	5	20	225	3.18	38.20
12:50 PM	5	25	220	3.11	37.35
1::00 PM	10	35	400	5.66	33.95
1:10 PM	10	45	380	5.38	32.26
1:25 PM	15	60	540	7.64	30.56
1:40 PM	15	75	500	7.07	28.29
2:00 PM	20	95	650	9.20	27.59
2:20 PM	20	115	550	7.78	23.34
2:40 PM	20	135	550	7.78	23.34
3:05 PM	25	160	650	9.20	22.07
3:30 PM	25	185	450	6.37	15.28
4:00 PM	30	215	500	7.07	14.15
4:30 PM	30	245	400	5.66	11.32
5:00 PM	30	275	345	4.88	9.76
5:30 PM	30	305	260	3.68	7.36
6:00 PM	30	335	260	3.68	7.36

Table C2 Infiltration test data for experimental plot no. 2

Plot 2 (Date of test: 04/02/2014)					
Time (Hr: Min)	Time interval(min)	Cumulative time (min)	Volume of water added (ml)	Infiltration depth (mm)	Infiltration Capacity (mm/hr)
12:32	Start	0	0	0	0
12:33	1	1	250	3.54	212.21
12:34	1	2	190	2.69	161.28
12:37	3	5	35	0.50	9.90
12:40	3	8	50	0.71	14.15
12:45	5	13	125	1.77	21.22
12:50	5	18	130	1.84	22.07
12:55	5	23	140	1.98	11.88
1:05	10	33	115	1.63	9.76
1:15	10	43	180	2.55	15.28
1:25	10	53	170	2.41	9.62
1:40	15	68	225	3.18	12.73
1:55	15	83	210	2.97	11.88
2:10	15	98	155	2.19	6.58
2:30	20	118	190	2.69	8.06
2:50	20	138	220	3.11	9.34
3:10	20	158	170	2.41	4.81
3:40	30	188	275	3.89	7.78
4:10	30	218	310	4.39	8.77
4:40	30	248	310	4.39	8.77

Table C3 Infiltration test data for experimental plot no. 3

Plot 3 (Date of test: 03/02/2014)					
Time	Time Interval (min.)	Cumulative Time (min.)	Volume of Water Added ml (cm^3)	Infiltration Depth (mm)	Infiltration Capacity (mm/hr.)
12:14 PM	0	Start = 0			
12:15 PM	1	1	90	1.27	76.39
12:16 PM	1	2	80	1.13	67.91
12:18 PM	2	4	95	1.34	40.32
12:20 PM	2	6	50	0.71	21.22
12:22 PM	2	8	60	0.85	25.46
12:27 PM	5	13	50	0.71	8.49
12:32 PM	5	18	130	1.84	22.07
12:37 PM	5	23	140	1.98	23.77
12:42 PM	5	28	125	1.77	21.22
12:52 PM	10	38	135	1.91	11.46
1:02 PM	10	48	275	3.89	23.34
1:12 PM	10	58	180	2.55	15.28
1:27 PM	15	73	220	3.11	12.45
1:42 PM	15	88	320	4.53	18.11
1:57 PM	15	103	290	4.10	16.41
2:17 PM	20	123	290	4.10	12.31
2:37 PM	20	143	400	5.66	16.98
2:57 PM	20	163	400	5.66	16.98
3:27 PM	30	193	340	4.81	9.62
3:57 PM	30	223	250	3.54	7.07
4:27 PM	30	253	250	3.54	7.07
4:57 PM	30	283	240	3.40	6.79
5:27 PM	30	313	230	3.25	6.51
5:57 PM	30	343	230	3.25	6.51

Table C4 Infiltration test data for experimental plot no. 4

Plot 4 (Date of test: 05/09/2013)					
Watch time	Time Elapsed(t) min.	Cumulative time(min)	Reading on Scale(cm)	Real Dropdown, d (cm)	Rate of infiltration (cm/hr)
11:00	0	0	5.6	0	0
11:01	1	1	5.8	0.2	12
11:02	1	2	5.9	0.1	6
11:05	3	5	6	0.1	2
11:10	5	10	6.2	0.2	2.4
11:15	5	15	6.4	0.2	2.4
11:20	5	20	6.5	0.1	1.2
11:25	5	25	6.7	0.2	2.4
11:30	5	30	6.8	0.1	1.2
11:35	5	35	7	0.2	2.4
11:40	5	40	7.2	0.2	2.4
11:45	5	45	7.4	0.2	2.4
11:50	5	50	7.6	0.2	2.4
11:55	5	55	7.8	0.2	2.4
12:00	5	60	8	0.2	2.4
12:10	10	70	8.2	0.2	1.2
12:20	10	80	8.5	0.3	1.8
12:30	10	90	8.7	0.2	1.2
12:40	10	100	9	0.3	1.8
12:50	10	110	9.2	0.2	1.2
13:00	10	120	9.6	0.4	2.4
13:10	10	130	9.8	0.2	1.2
13:20	10	140	10	0.2	1.2
13:35	15	155	10.2	0.2	0.8
13:50	15	170	10.5	0.3	1.2
14:05	15	185	10.8	0.3	1.2
14:20	15	200	11.1	0.3	1.2
14:35	15	215	11.4	0.3	1.2
14:50	15	230	11.7	0.3	1.2
15:05	15	245	12	0.3	1.2
15:20	15	260	12.3	0.3	1.2
15:40	20	280	12.8	0.5	1.5
16:00	20	300	13.2	0.4	1.2
16:20	20	320	13.5	0.3	0.9
16:40	20	340	13.9	0.4	1.21

Table C5 Infiltration test data for experimental plot no. 5

Plot 5 (Date of test: 07/09/2013)					
Watch time	Time Elapsed(t) min.	Cumulative time(min)	Reading on Scale(cm)	Real Dropdown (cm)	Rate of infiltration (cm/hr)
10:06	0	0	19.2	0	0
10:07	1	1	19	0.2	12
10:08	1	2	18.8	0.2	12
10:13	5	7	18.7	0.1	1.2
10:18	5	12	18.5	0.2	2.4
10:23	5	17	18.4	0.1	1.2
10:33	5	22	18.3	0.1	1.2
10:43	10	32	18.2	0.1	0.6
10:53	10	42	18.1	0.1	0.6
11:03	10	52	17.9	0.2	1.2
11:13	10	62	17.7	0.2	1.2
11:23	10	72	17.6	0.1	0.6
11:38	15	87	17.4	0.2	0.8
11:53	15	102	17.3	0.1	0.4
12:08	15	117	17.2	0.1	0.4
12:23	15	132	17	0.2	0.8
12:38	15	147	16.9	0.1	0.4
12:58	20	167	16.8	0.1	0.3
13:18	20	187	16.6	0.2	0.6
13:38	20	207	16.4	0.2	0.6
13:58	20	227	16.3	0.1	0.3
14:28	30	257	16	0.3	0.6
14:58	30	287	15.7	0.3	0.6
15:28	30	317	15.4	0.3	0.6
15:58	30	347	15.1	0.3	0.615

Table C6 Infiltration test data for experimental plot no. 6

Plot 6 Date of test: 07/09/2013					
Watch time	Time Elapsed(t) min.	Cumulative time(min)	Reading on Scale(cm)	Real Dropdown (cm)	Rate of infiltration (cm/hr)
10:22	0	0	9.4	0	0
10:23	1	1	9.5	0.1	6
10:24	1	2	9.6	0.1	6
10:25	1	3	9.7	0.1	6
10:26	1	4	9.8	0.1	6
10:27	1	5	9.9	0.1	6
10:32	5	10	10.0	0.1	1.2
10:37	5	15	10.1	0.1	1.2
10:42	5	20	10.3	0.2	2.4
10:47	5	25	10.5	0.2	2.4
10:52	5	30	10.6	0.1	1.2
10:57	5	35	10.7	0.1	1.2
11:02	5	40	10.8	0.1	1.2
11:07	5	45	10.9	0.1	1.2
11:17	10	55	11.3	0.4	2.4
11:27	10	65	11.5	0.2	1.2
11:37	10	75	11.7	0.2	1.2
11:47	10	85	11.9	0.2	1.2
11:57	10	95	12.2	0.3	1.8
12:07	10	105	12.4	0.2	1.2
12:22	15	120	12.7	0.3	1.2
12:37	15	135	12.9	0.2	0.8
12:52	15	150	13.1	0.2	0.8
13:07	15	165	13.3	0.2	0.8
13:22	15	180	13.5	0.2	0.8
13:42	20	200	13.8	0.3	0.9
14:02	20	220	14.0	0.2	0.6
14:32	30	250	14.5	0.5	1.22
15:02	30	280	15.0	0.5	1.22
15:32	30	310	15.5	0.5	1.21
16:02	30	340	16.0	0.5	1.21

Table C7 Infiltration test data for experimental plot no. 7

Plot 7 (Date of test: 01/02/2014)					
Time (Hr:Min)	Time interval(min)	Cumulative time(min)	Volume of water added(ml)	Infiltration depth(mm)	Infiltration Capacity(mm/hr)
12:15	start	0	0	0	0
12:16	1	1	150	2.12	127.33
12:17	1	2	100	1.41	84.88
12:18	1	3	50	0.71	42.44
12:20	2	5	50	0.71	21.22
12:22	2	7	50	0.71	21.22
12:24	2	9	55	0.78	9.34
12:29	5	14	25	0.35	4.24
12:34	5	19	35	0.50	2.97
12:44	10	29	100	1.41	8.49
12:54	10	39	55	0.78	4.67
1:04	10	49	125	1.77	10.61
1:14	10	59	120	1.70	5.09
1:34	20	79	60	0.85	2.55
1:54	20	99	65	0.92	2.76
2:14	20	119	100	1.41	4.24
2:34	20	139	100	1.41	2.83
3:04	30	169	135	1.91	3.82
3:34	30	199	140	1.98	3.96
4:04	30	229	150	2.12	4.24
4:34	30	259	150	2.12	4.24

Table C8 Infiltration test data for experimental plot no. 8

Plot 8 (Date of test: 01/02/2014)					
Time (Hr:Min)	Time interval(min)	Cumulative time(min)	Volume of water added(ml)	Infiltration depth(mm)	Infiltration Capacity(mm/hr)
12:33	Start	0	0	0	0
12:34	1	1	80	1.13	67.91
12:36	2	3	35	0.50	14.85
12:48	12	15	120	1.70	8.49
12:53	5	20	70	0.99	11.88
12:58	5	25	35	0.50	5.94
1:08	10	35	305	4.31	25.89
1:18	10	45	50	0.71	4.24
1:28	10	55	60	0.85	5.09
1:38	10	65	165	2.33	9.34
1:53	15	80	90	1.27	3.82
2:13	20	100	190	2.69	8.06
2:33	20	120	95	1.34	4.03
2:53	20	140	230	3.25	6.51
3:23	30	170	205	2.90	5.80
3:53	30	200	195	2.76	5.52
4:23	30	230	195	2.76	5.52

Table C9 Infiltration test data for experimental plot no. 9

Plot 12 (Date of test: 31/12/2014)					
Time (Hr:Min)	Time interval(min)	Cumulative time(min)	Volume of water added(ml)	Infiltration depth(mm)	Infiltration Capacity(mm/hr)
12:37	start	0	0	0	0
12:39	2	2	255	3.61	108.23
12:41	2	4	85	1.20	36.08
12:43	2	6	55	0.78	23.34
12:48	5	11	195	2.76	33.10
12:53	5	16	25	0.35	4.24
1:03	5	21	150	2.12	12.73
1:13	10	31	140	1.98	11.88
1:23	10	41	145	2.05	12.31
1:33	10	51	60	0.85	5.09
1:43	10	61	130	1.84	7.36
1:58	15	76	155	2.19	8.77
2:13	15	91	170	2.41	9.62
2:28	15	106	65	0.92	2.76
2:48	20	126	225	3.18	9.55
3:08	20	146	185	2.62	7.85
3:28	20	166	160	2.26	4.53
3:58	30	196	200	2.83	5.66
4:28	30	226	200	2.83	5.66

Appendix D

Infiltration test data for experimental plot of Phase 2

Plot 8 (Date of test: 31/12/2014)				Plot 9 (Date of test: 31/12/2014)				Plot 1 (Date of test: 31/12/2014)			
Time interval (min)	Cumulative time (min)	Infiltration depth (mm)	Infiltration Capacity (mm/hr)	Time interval (min)	Cumulative time (min)	Infiltration depth (mm)	Infiltration Capacity (mm/hr)	Time interval (min)	Cumulative time (min)	Infiltration depth (mm)	Infiltration Capacity (mm/hr)
start	0	0	0	start	0	0	0	start	0	0	0
1	1	3	180	1	1	5	300	1	1	5	300
1	2	2	120	1	2	4	240	1	2	4	240
1	3	3	180	1	3	3	180	1	3	2	120
1	4	3	180	1	4	2.1	126	1	4	5	300
1	5	6	360	1	5	2	120	1	5	4	240
1	6	4	240	1	6	1.9	114	1	6	4	240
1	7	4	240	1	7	2	120	1	7	2	120
1	8	6	360	1	8	1.5	90	1	8	3	180
1	9	3	180	1	9	1.3	78	1	9	2	120
1	10	3	180	1	10	1.2	72	1	10	2	120
10	20	11	66	10	20	7	42	10	20	7	42
10	30	9	54	10	30	8	48	10	30	5	30
10	40	10	60	10	40	9	54	10	40	5	30
10	50	4	24	10	50	8	48	10	50	8	48
30	80	11	22	30	80	16	32	10	60	6	36
30	110	9	18	10	90	6	36	30	90	16	32

60	140	12	12	30	120	9	18	30	120	12	24
60	200	12	12	30	150	10	20	30	150	13	26
60	260	8	8	30	180	11	22	30	180	15	30
60	320	9	9					30	210	15	30

Plot 10 (Date of test: 19/09/2017)				Plot 11 (Date of test: 18/09/2017)				Plot 12 (Date of test: 14/09/2017)			
Time interval (min)	Cumulative time (min)	Infiltration depth (mm)	Infiltration Capacity (mm/hr)	Time interval (min)	Cumulative time (min)	Infiltration depth (mm)	Infiltration Capacity (mm/hr)	Time interval (min)	Cumulative time (min)	Infiltration depth (mm)	Infiltration Capacity (mm/hr)
start	0	0	0	start	0	0	0	start	0	0	0
1	1	10	600	1	1	5	300	1	1	5.0	300.0
1	2	5	300	1	2	9	510	1	2	9.0	540.0
1	3	5	300	1	3	3	210	1	3	3.0	180.0
1	4	5	300	1	4	4	240	1	4	4.0	240.0
1	5	5	300	1	5	3	180	1	5	3.0	180.0
1	6	5	300	1	6	3	180	1	6	4.0	240.0
1	7	2	120	1	7	2	120	1	7	1.0	60.0
1	8	3	180	1	8	2	120	1	8	2.0	120.0
1	9	5	300	1	9	3	180	1	9	3.0	180.0
1	10	3	180	1	10	2	120	1	10	2.0	120.0
2	12	2	60	2	12	2	60	2	12	2.0	60.0
2	14	4	120	2	14	3	90	2	14	3.0	90.0
2	16	9	270	2	16	5	150	2	16	5.0	150.0
2	18	3	90	2	18	2	60	2	18	2.0	60.0
2	20	7	210	2	20	5	150	2	20	5.0	150.0

10	30	17	102	10	30	10	60	10	30	10.0	60.0
10	40	22	132	10	40	8	48	10	40	8.0	48.0
10	50	18	108	10	50	4	24	10	50	4.0	24.0
10	60	20	120	10	60	5	30	10	60	5.0	30.0
30	90	45	90	30	90	5	10	30	90	5.0	10.0
30	120	45	90	30	120	15	30	30	120	15.0	30.0
30	150	40	80	30	150	13	26	30	150	25.0	50.0
30	180	40	80	30	180	11	22	30	180	10.0	20.0
30	210	40	80	30	210	11	22	30	210	10.0	20.0
30	240	40	80	30	240	11	22	30	240	10.0	20.0
30	270	11	22	30	270	11	22	30	270	10.0	20.0
30	300	11	22								
30	330	11	22								

Plot 13 (Date of test: 02/11/2017)				Plot 14 (Date of test: 10/09/2017)				Plot 15 (Date of test: 16/07/2017)			
Time interval (min)	Cumulative time (min)	Infiltration depth (mm)	Infiltration Capacity (mm/hr)	Time interval (min)	Cumulative time (min)	Infiltration depth (mm)	Infiltration Capacity (mm/hr)	Time interval (min)	Cumulative time (min)	Infiltration depth (mm)	Infiltration Capacity (mm/hr)
start	0	0.0	0	start	0	0.0	0	start	0	0.0	0
1	1	6.0	360	1	1	8.0	480	1	1	4.0	240
1	2	3.0	180	1	2	3.0	180	1	2	3.0	180
1	3	2.0	120	1	3	2.0	120	1	3	2.5	150
1	4	1.0	60	1	4	1.0	60	1	4	2.0	120
1	5	1.0	60	1	5	1.0	60	1	5	1.5	90
1	6	2.0	120	1	6	2.0	120	1	6	1.0	60

1	7	3.0	180	1	7	3.0	180	1	7	1.5	90
1	8	2.0	120	1	8	0.5	30	1	8	1.1	66
1	9	1.0	60	1	9	0.5	30	1	9	1.4	84
1	10	1.0	60	1	10	1.0	60	1	10	1.0	60
2	12	1.0	30	2	12	2.0	60	2	12	1.9	57
2	14	1.0	30	2	14	1.0	30	2	14	0.9	27
2	16	1.0	30	2	16	2.0	60	2	16	2.2	66
2	18	2.0	60	2	18	2.0	60	2	18	1.5	45
2	20	1.0	30	2	20	1.0	30	2	20	1.0	30
10	30	9.0	54	10	30	4.0	24	10	30	4.5	27
10	40	9.0	54	10	40	5.0	30	10	40	4.5	27
10	50	10.0	60	10	50	4.0	24	10	50	4.5	27
10	60	10.0	60	10	60	5.0	30	10	60	5.0	30
30	90	10.0	20	30	90	5.0	10	30	90	5.0	10
30	120	27.0	54	30	120	12.0	24	30	120	22.0	44
30	150	20.0	40	30	150	20.0	40	30	150	20.0	40
30	180	30.0	60	30	180	13.0	26	30	180	20.0	40
30	210	30.0	60	30	210	13.0	26	30	210	20.0	40
30	240	30.0	60	30	240	13.0	26	30	240	20.0	40
30	270	30.0	60	30	270	13.0	26	30	270	20.0	40

Plot 16 (Date of test: 05/11/2017)				Plot 17 (Date of test: 12/09/2017)				Plot 18 (Date of test: 13/09/2017)			
Time interval (min)	Cumulative time (min)	Infiltration depth (mm)	Infiltration Capacity (mm/hr)	Time interval (min)	Cumulative time (min)	Infiltration depth (mm)	Infiltration Capacity (mm/hr)	Time interval (min)	Cumulative time (min)	Infiltration depth (mm)	Infiltration Capacity (mm/hr)
start	0	0	0	start	0	0.0	0	start	0	0	0
1	1	10	600	1	1	5.0	300	1	1	10	600
1	2	10	600	1	2	9.0	540	1	2	5	300
1	3	10	600	1	3	3.0	180	1	3	5	300
1	4	7	420	1	4	4.0	240	1	4	5	300
1	5	13	780	1	5	3.0	180	1	5	5	300
1	6	4	240	1	6	4.0	240	1	6	5	300
1	7	3	180	1	7	1.0	60	1	7	2	120
1	8	3	180	1	8	2.0	120	1	8	3	180
1	9	7	420	1	9	3.0	180	1	9	2	120
1	10	3	180	1	10	2.0	120	1	10	6	360
2	12	3	90	2	12	2.0	60	2	12	2	60
2	14	4	120	2	14	3.0	90	2	14	4	120
2	16	6	180	2	16	5.0	150	2	16	9	270
2	18	7	210	2	18	2.0	60	2	18	3	90
2	20	8	240	2	20	5.0	150	2	20	4	120
10	30	32	192	10	30	10.0	60	10	30	10	60
10	40	50	300	10	40	8.0	48	10	40	10	60
10	50	30	180	10	50	4.0	24	10	50	10	60
10	60	20	120	10	60	5.0	30	10	60	10	60
30	90	80	160	30	90	5.0	10	30	90	10	20

30	120	30	60	30	120	15.0	30	30	120	10	20
30	150	30	60	30	150	25.0	50	30	150	20	40
30	180	30	60	30	180	10.0	20	30	180	10	20
30	210	10	20	30	210	10.0	20	30	210	14	28
30	240	10	20	30	240	10.0	20	30	240	14	28
30	270	10	20	30	270	10.0	20	30	270	14	28
								30	300	14	28
								30	330	14	28

Plot 20 (Date of test: 15/11/2018)				Plot 23 (Date of test: 15/11/2018)				Plot 26 (Date of test: 16/11/2018)			
Time interval (min)	Cumulative time (min)	Infiltration depth (mm)	Infiltration Capacity (mm/hr)	Time interval (min)	Cumulative time (min)	Infiltration depth (mm)	Infiltration Capacity (mm/hr)	Time interval (min)	Cumulative time (min)	Infiltration depth (mm)	Infiltration Capacity (mm/hr)
start	0	0	0	start	0	0.0	0	start	0	0	0
1	1	3	180	1	1	2	120	1	1	5	300
1	2	2	120	1	2	2	120	1	2	3	180
1	3	3	180	1	3	1	60	1	3	3	180
1	4	2	120	1	4	1	60	1	4	2	120
1	5	1	60	1	5	1	60	1	5	2	120
1	6	1	60	1	6	1	60	1	6	2	120
1	7	2	120	1	7	1	60	1	7	2	120
1	8	1	30	1	8	1	60	1	8	1	60
1	9	1	30	1	9	1	60	1	9	1	60
1	10	1	60	1	10	1	60	1	10	1	60

10	20	8	48	10	20	8	48	10	20	13	78
10	30	6	36	10	30	6	36	10	30	9	54
10	40	3	18	10	40	5	30	10	40	8	48
30	70	10	20	30	70	16	32	30	70	25	50
30	100	9	18	30	100	12	24	30	100	23	46
30	130	8	16	30	130	11	22	30	130	21	42
60	190	14	14	60	190	22	22	60	190	40	40
60	250	15	15	60	250	24	24	60	250	39	39
60	310	15	15	60	310	20	20	60	310	35	35
60	370	15	15	60	370	20	20	60	370	34	34
60	430	15	15	60	430	10	10				

Plot 21 (Date of test: 15/11/2018)				Plot 24 (Date of test: 16/11/2018)				Plot 27 (Date of test: 16/11/2018)			
Time interval (min)	Cumulative time (min)	Infiltration depth (mm)	Infiltration Capacity (mm/hr)	Time interval (min)	Cumulative time (min)	Infiltration depth (mm)	Infiltration Capacity (mm/hr)	Time interval (min)	Cumulative time (min)	Infiltration depth (mm)	Infiltration Capacity (mm/hr)
start	0	0	0	start	0	0	0	start	0	0	0
2	2	10	300	1	1	3	180	2	2	8	240
2	4	4	120	1	2	3	180	2	4	5	150
2	6	4	120	1	3	2	120	2	6	3	90
2	8	3	90	1	4	2	120	2	8	3	90
2	10	4	120	1	5	1	60	2	10	2	60
10	20	16	96	1	6	1	60	10	20	6	36
10	30	14	84	1	7	1	60	10	30	5	30

10	40	13	78	1	8	1	60	10	40	4	24
30	70	35	70	1	9	1	60	30	70	13	26
30	100	35	70	1	10	1	90	30	100	6	12
30	130	33	66	10	20	11	63	30	130	5	10
60	190	62	62	10	30	6	36	60	190	10	10
60	250	58	58	10	40	6	36	60	250	7	7
60	310	57	57	30	70	11	22	60	310	7	7
60	370	51	51	30	100	10	20	60	370	7	7
				30	130	9	18				
				60	190	15	15				
				60	250	15	15				
				60	310	14	14				
				60	370	14	14				

Plot 19 (Date of test: 17/11/2018)				Plot 22 (Date of test: 17/11/2018)				Plot 25 (Date of test: 07/07/2018)			
Time interval (min)	Cumulative time (min)	Infiltration depth (mm)	Infiltration Capacity (mm/hr)	Time interval (min)	Cumulative time (min)	Infiltration depth (mm)	Infiltration Capacity (mm/hr)	Time interval (min)	Cumulative time (min)	Infiltration depth (mm)	Infiltration Capacity (mm/hr)
start	0	0.0	0	start	0	0	0	start	0	0.0	0
1	1	1.2	72	2	2	15	450	1	1	5.0	300
1	2	0.4	24	2	4	5	150	1	2	6.0	360
1	3	0.4	24	2	6	4	120	1	3	2.0	120
1	4	0.3	18	2	8	4	120	1	4	5.0	300
1	5	0.3	18	2	10	3	90	1	5	4.0	240

1	6	0.3	18	10	20	13	78	1	6	4.0	240
1	7	0.3	18	10	30	11	66	1	7	2.0	120
1	8	0.3	18	10	40	11	66	1	8	3.0	180
1	9	0.2	12	30	70	27	54	1	9	2.0	120
1	10	0.2	12	30	100	25	50	1	10	2.0	120
10	20	2.2	13	30	130	21	42	10	20	24.0	144
10	30	1.8	11	60	190	39	39	10	30	20.0	120
10	40	1.8	11	60	250	35	35	10	40	19.0	114
10	50	1.8	11	60	310	35	35	30	70	49.0	98
20	70	3.2	10	60	370	33	33	30	100	40.0	80
30	100	4.5	9					30	130	37.0	74
30	130	4.1	8					60	190	67.0	67
30	160	3.8	8					60	250	64.0	64
30	190	3.7	7					60	310	64.0	64
30	220	3.6	7					60	370	62.0	62
30	250	3.4	7								
30	280	3.2	6								
30	310	3.1	6								
30	340	3.1	6								
30	370	3.0	6								